BEST CASES

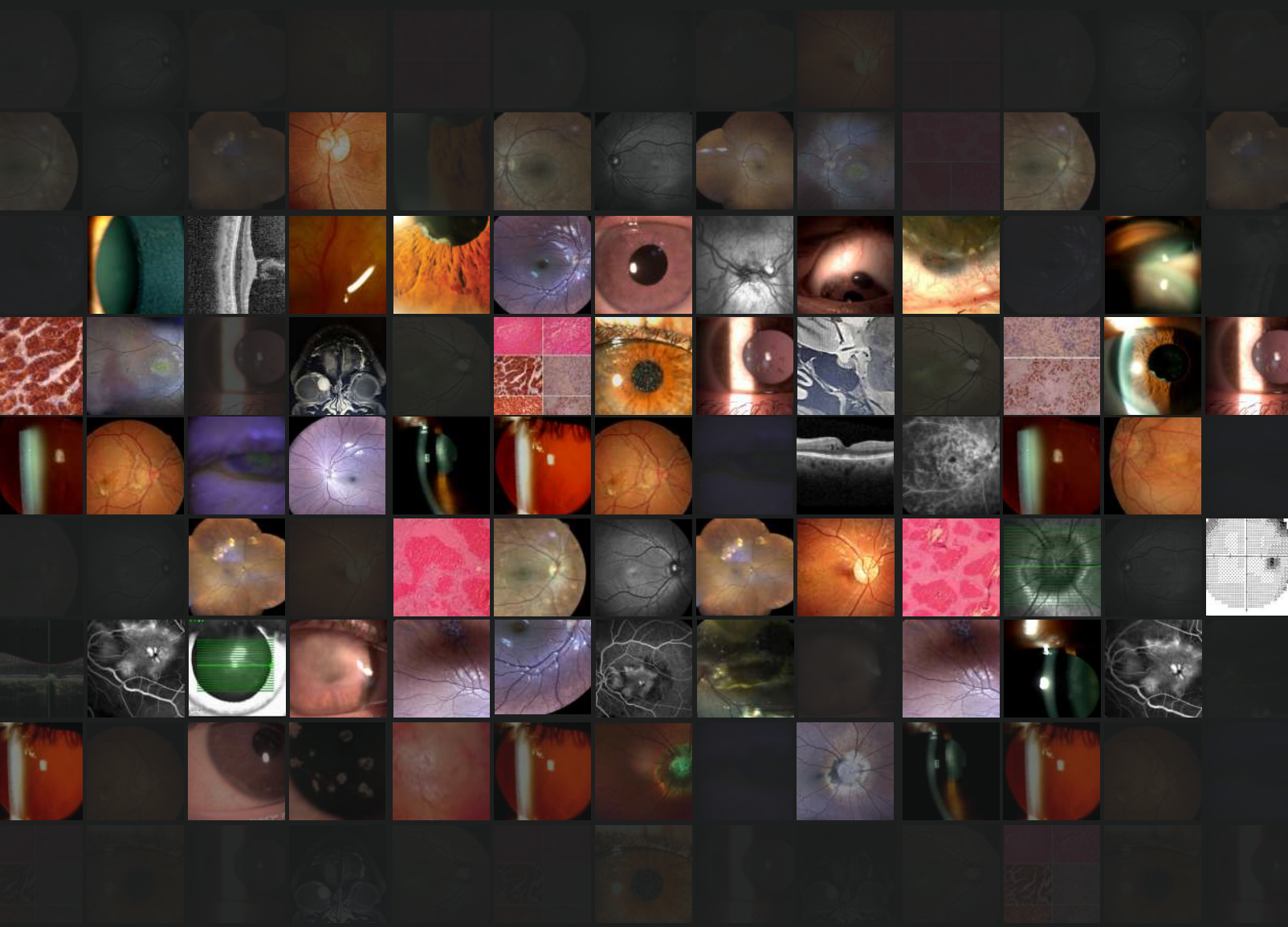

ophthalmica

Seeing is believing

Best Cases

ISBN 978-618-85557-2-3

© by Ophthalmocheirourgiki SA 2024

Introduction

In October 2020, just after the surge of the COVID-19 pandemic, a new chapter was added to the history of the Ophthalmica Institute of Ophthalmology & Microsurgery in Thessaloniki, Greece. The clinic started a series of publications featuring the most remarkable clinical cases encountered by its ten head physicians throughout the years.

Four years later, Ophthalmica's library of high-complexity cases has grown. Twenty-five highlights, selected from those previously shared with our external network of colleagues, were chosen to compose this **Ophthalmica's Best Cases** collection.

Case selection was based on predetermined criteria to make this work both interesting and educational to the reader. Characteristics such as the level of rarity, the quality of medical records, and the success in management and outcomes were considered. The primary goal of **Ophthalmica's Best Cases** is to contribute to the enlightenment and knowledge acquisition of our fellow ophthalmologists.

As a center of excellence that receives a significant volume of referred patients - not only from Northern Greece but also from neighboring Balkan countries - Ophthalmica is able to handle the most intriguing and challenging cases in ophthalmological practice. With world-class specialists and cutting-edge equipment comprising every imaging method for diagnosing and recording ocular disorders, the clinic provides the ideal conditions for documenting and sharing rich medical content.

This book is a compilation of the finest cases assisted by Ophthalmica's medical team over the last few years, in an initiative to thank you for being by our side in this journey towards healing and caring for our patients in the best possible way. We deeply appreciate your support and trust, and hope you enjoy the reading.

Penelope Burle de Politis, MD
Ophthalmologist
Main Editor

Periklis Markousis MSc
General Manager
Project Coordinator

Table of Contents

Case 1 - October 2020

IRIS VARICES

A 74-year-old well-controlled glaucomatous woman presented with spontaneously waning iris vessels in her right eye.

Presented by
Thanos Sousouras, MD, DO

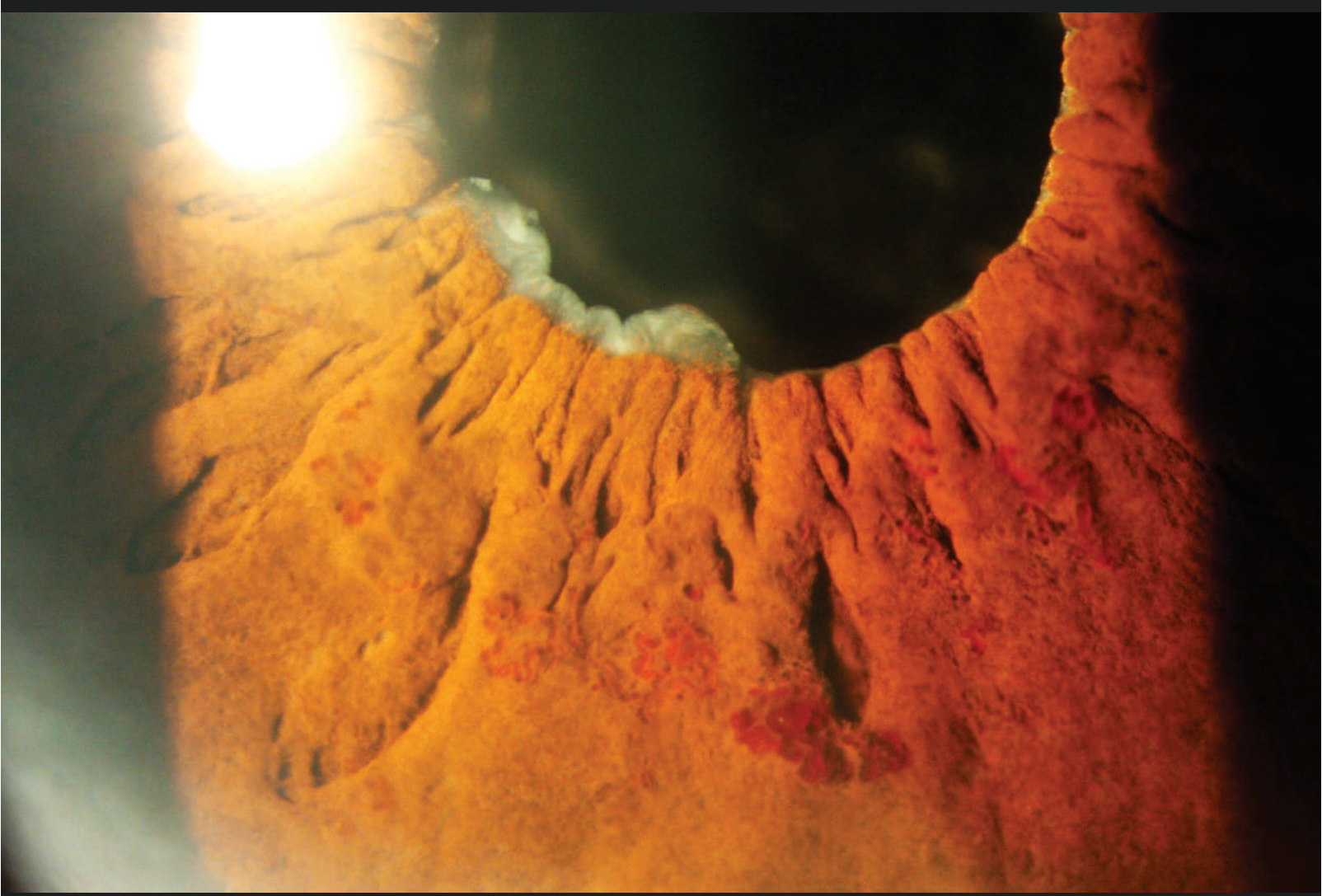

Edited by
Penelope Burle de Politis, MD

Case History

A 74-year-old Caucasian woman with well-controlled bilateral primary open-angle glaucoma was scheduled for YAG-laser capsulotomy due to post-cataract surgery blurred vision in the right eye (RE). Her best-corrected visual acuity (BCVA) was 7/10 in the RE and 9/10 in the left eye (LE). Intraocular pressure was respectively 12 and 14 mmHg. Slit-lamp examination of the RE revealed multiple vascular tufts in the middle third of the lower temporal iris surface, with no apparent blood leaking **(Figures 1 and 2)**. The lesions appeared as heterogeneous reddish threads of variable dimensions, disposed both radially and circumferentially. The surrounding iris architecture was normal, and the pupil was round and reactive. There were cells clumped on the adjacent iris margin but no hyphema. The eye was phakic, with moderate posterior capsule opacification. Gonioscopy showed an open angle with no vessels or deposits on the trabecular meshwork **(Figure 3)**. The left eye had no similar findings. A thorough screening for uveitis was requested and the patient was scheduled for iris optical coherence tomography angiography (OCT-A) within 3 weeks. Both steroid and non-steroid anti-inflammatory eye-drops were prescribed (dexamethasone and nepafenac). Upon return for the OCT scanning, the vessels were no longer present **(Figure 4)**. The patient's vision had returned to baseline and therapy was discontinued.

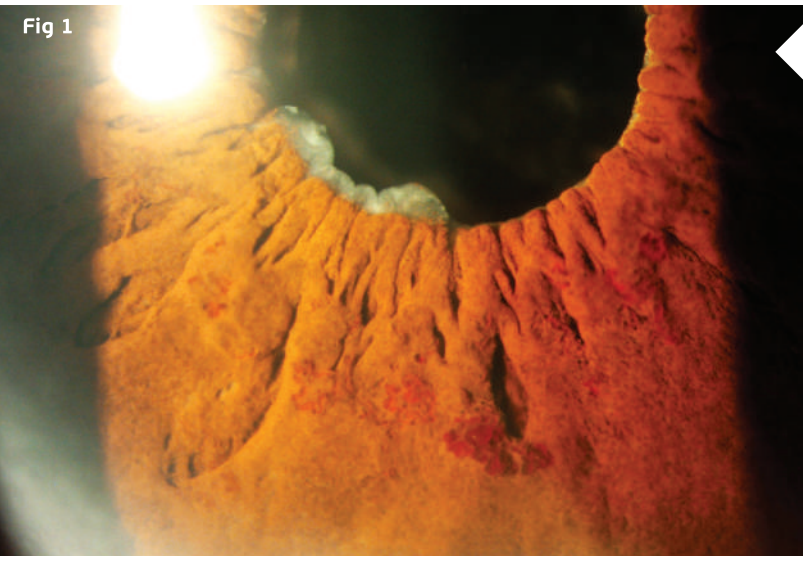

Figure 1: Slit-lamp photograph showing multiple vascular tufts at the inner half of the lower temporal iris surface.

Figure 2: Magnified slit-lamp photograph showing the heterogeneous morphological arrangement of the iris vascular tufts, varying from flat radial sinuous veins to multi-saccular circumferential clusters.

Additional History

The diagnosis of iris varices in this case was done by chance. The patient had been followed-up for bilateral glaucoma for about 9 years, lastly in use of latanoprost and a combination of dorzolamide and timolol, with IOP no higher than 17 mmHg on previous follow-up visits. Two years before the iridial manifestation, she presented with a lacrimal duct obstruction on the right and iridocyclitis with subsequent posterior synechiae on the left. Six months later, she underwent an uneventful lens extraction with IOL implantation on the RE. At 4 months postoperatively, posterior capsular opacification was noted, and the patient was advised to return for YAG-laser capsulotomy sometime in the following months — when the varices arose.

Differential Diagnosis of Abnormal Iris Vascular Formations

- iris varices
- iris melanoma
- vascular malformations (capillary hemangioma, cavernous hemangioma, micro-hemangioma)
- juvenile xanthogranuloma
- metastasis to the iris
- fibrovascular proliferative response following inflammation or hemorrhage

Basically, any vascular formations that are not normally observed in the iris may present as reddish tumors on the iris surface.

Figures 3: Gonioscopy of the right eye showing an open anterior chamber angle, with no vessels or deposits on the trabecular meshwork.

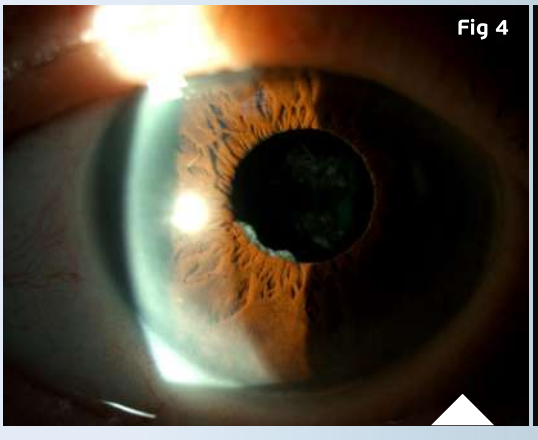

Figures 4 and 5: Slit-lamp photography on the day scheduled for OCT-A, showing total involution of the varicose vessels.

Discussion and Literature

The first reported case of iris varix as a primary vascular lesion was in 1975. In a 2019 retrospective study on 28 eyes of 26 patients diagnosed with iris varix over a 10-year period, a single varix was found in two thirds of eyes and multiple varices in one third, the inferotemporal iris quadrant being affected in 75%. No progression or associated morbidities were detected, and spontaneous waning occurred in only 3.6% of all cases.

In 1992, an iris varix causing hyphema was reported in a 76-year-old woman with pseudoexfoliation syndrome and showing complete spontaneous regression in the two-month follow-up. Cases of a primary iris varix requiring excision for recurrent hyphema, and of iris varix presenting recurrent hemorrhages into the anterior chamber, with intermittent blurring of vision by hyphema and secondary glaucoma, demanding lesion removal, have been described.

Varices of the iris are extremely rare. As a general vascular condition, varices are caused by structural alterations in the vein wall or venous obstruction by thrombosis or external compression.

Iris varix may be symptomatic or a random finding. Definitive diagnosis and exclusion of other infirmities is done by histopathological and immunohistochemical examination. Spontaneous regression may occur. Treatment, when required, is by excision or photocoagulation. Photocoagulation of the varix can stop bleeding and induce regression. Excision by iridectomy is both therapeutic and diagnostic, especially when the morphological aspect is unclear or history and physical findings point to other diseases.

Keep in mind

- ✓ Varix of the iris is a rare condition, and their spontaneous remission is ever rarer.
- ✓ Complications and differential diagnosis of iris varices must be excluded.
- ✓ Treatment of iris various veins is not always required but follow-up is necessary.

References

1 Andersen SR & Other A (1975). Varix of the iris. Archives of ophthalmology (Chicago, Ill.: 1960), 93(1), 32–33. https://doi.org/10.1001/archopht.1975.01010020036005

2 Jain P & Finger PT (2019). Iris varix: 10-year experience with 28 eyes. Indian journal of ophthalmology, 67(3), 350–357. https://doi.org/10.4103/ijo.IJO_1253_18

3 Küchle M & Naumann GO (1992). Varixknoten der Iris mit Spontan-Regression [Varix node of the iris with spontaneous regression]. Klinische Monatsblatter fur Augenheilkunde, 200(3), 233–236. https://-doi.org/10.1055/s-2008-1045745

4 Ang LP, Sim DH, Chiang GS & Yong VS (1997). Iris varix. Eye (London, England), 11 (Pt 5), 733–735. https://-doi.org/10.1038/eye.1997.187

5 Rohrbach JM, Eckstein A & Schuster I (1995). Varixknoten der Iris [Varicose vein of the iris]. Klinische Monatsblatter fur Augenheilkunde, 207(3), 206–207. https://doi.org/10.1055/s-2008-1035370

6 Broaddus E, Lystad LD, Schonfield L & Singh AD (2009). Iris varix: report of a case and review of iris vascular anomalies. Survey of ophthalmology, 54(1), 118–127. https://doi.org/10.1016/j.survophthal.2008.10.005

7 Matlach J, Kasper K, Kasper B & Klink T (2013). Successful argon and diode laser photocoagulation treatment of an iris varix with recurrent hemorrhage. European journal of ophthalmology, 23(3), 431–435. https://-doi.org/10.5301/ejo.5000242

Case 2 - December 2020

LASER POINTER-INDUCED MACULOPATHY

A 10-year-old otherwise healthy girl presented with sudden-onset painless visual loss in the right eye for a month.

Presented by
Paris Tranos, MD, PhD, ICOphth, FRCS

Edited by
Penelope Burle de Politis, MD

Case History

A 10-year-old girl with no previous ocular or systemic disorders noticed reduced visual acuity in her right eye. She confirmed the relatively low eyesight on the right by intuitively performing a self-cover test and reported the symptom to her parents. She was brought for examination after 6 weeks of unchanged blurred vision in the right eye. On examination, best-corrected visual acuity (BCVA) was 7/10 in the right eye and 10/10 in the left. Anterior segment and intraocular pressures were normal in both eyes. Fundoscopy revealed a round, well-defined deep yellowish-orange discoloration at the level of the retinal pigment epithelium (RPE) in the right foveola, with no evidence of fluid or retinal hemorrhage **(Figure 1)**. Structural and spectral-domain optical coherence tomography (SD-OCT) showed a hyperreflective lesion at the right fovea, with disruption of the overlying ellipsoid zone **(Figure 2)**.

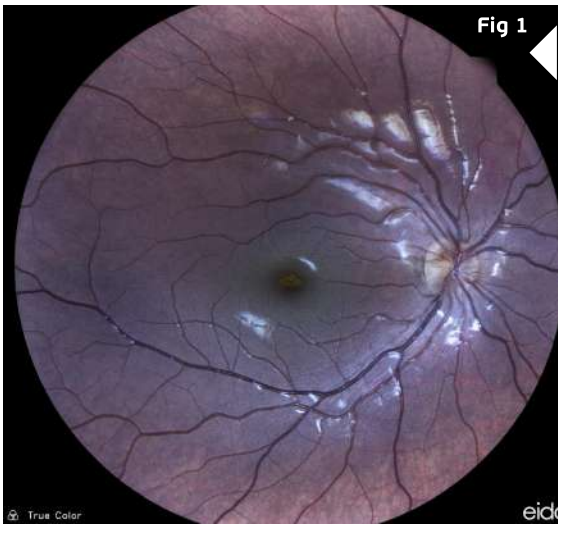

Figure 1: Fundus photograph of the right eye showing a round, well-defined deep yellowish-orange discoloration at the level of the retinal pigment epithelium in the foveola.

Figure 2: SD-OCT (Spectralis®) scan showing a hyperreflective lesion at the right fovea, with disruption of the overlying ellipsoid zone. Note the choroidal shadowing associated with the lesion.

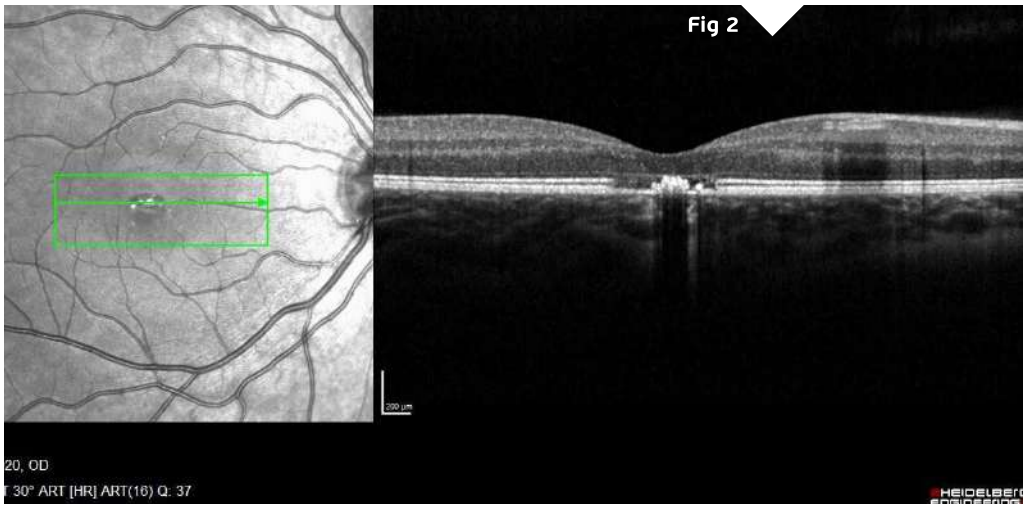

Fundus autofluorescence and fundus fluorescein angiography were unremarkable. Optical coherence tomography angiography (OCT-A) revealed a hypointense lesion in correspondence with the focal hyperreflectivity detected on structural OCT, suggesting rarefaction of the choriocapillaris **(Figure 3)**.

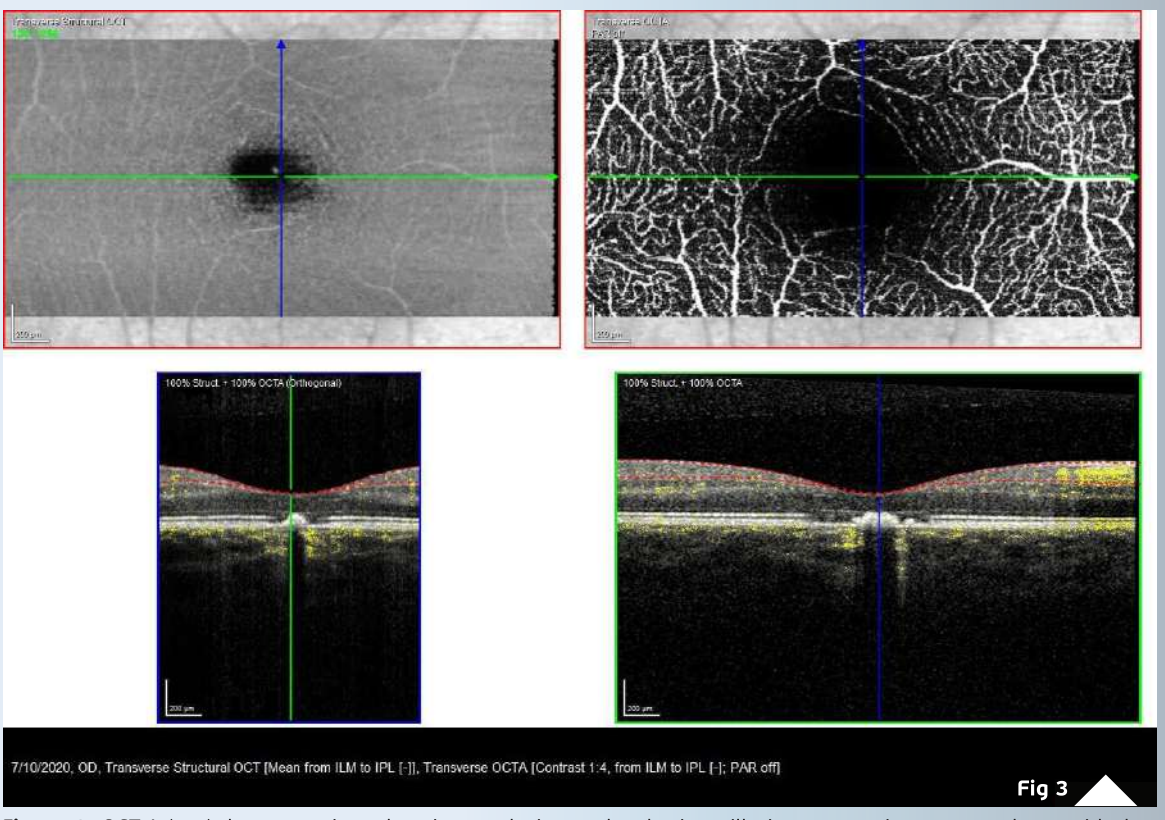

Figure 3: OCT-A (**top**) demonstrating a hypointense lesion at the choriocapillaris segment, in correspondence with the focal hyperreflectivity detected on structural OCT (**bottom**), suggesting rarefaction of the choriocapillaris (Spectralis®).

Four weeks later, the patient presented with subjective improvement, reporting scotoma size reduction. Visual acuity had improved to 8/10 and structural OCT showed partial restoration of the ellipsoid zone disruption **(Figures 4 and 5)**.

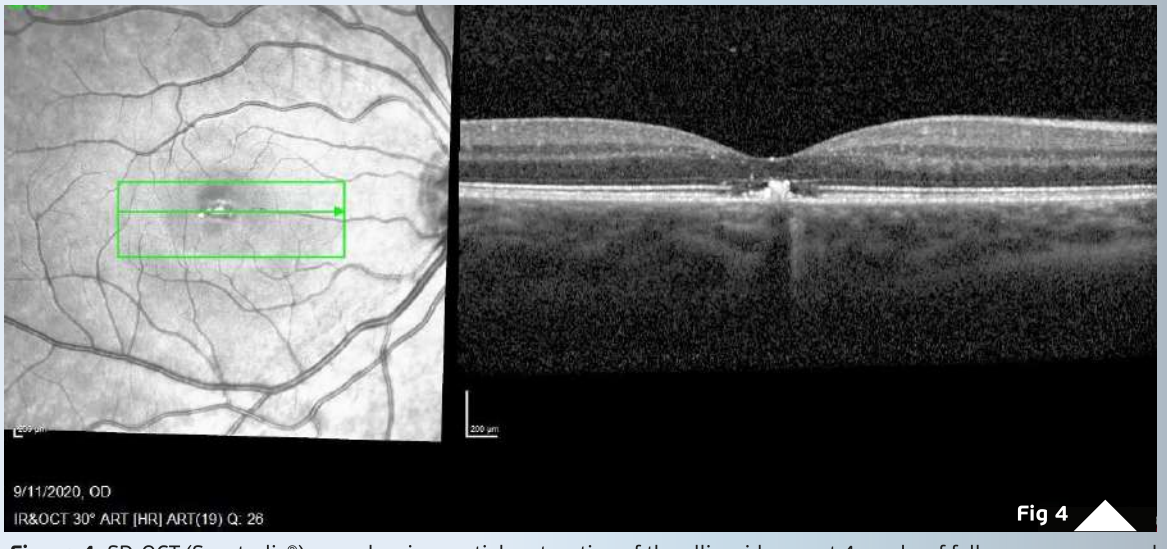

Figure 4: SD-OCT (Spectralis®) scan showing partial restoration of the ellipsoid zone at 4-weeks of follow-up, as opposed to baseline OCT scan.

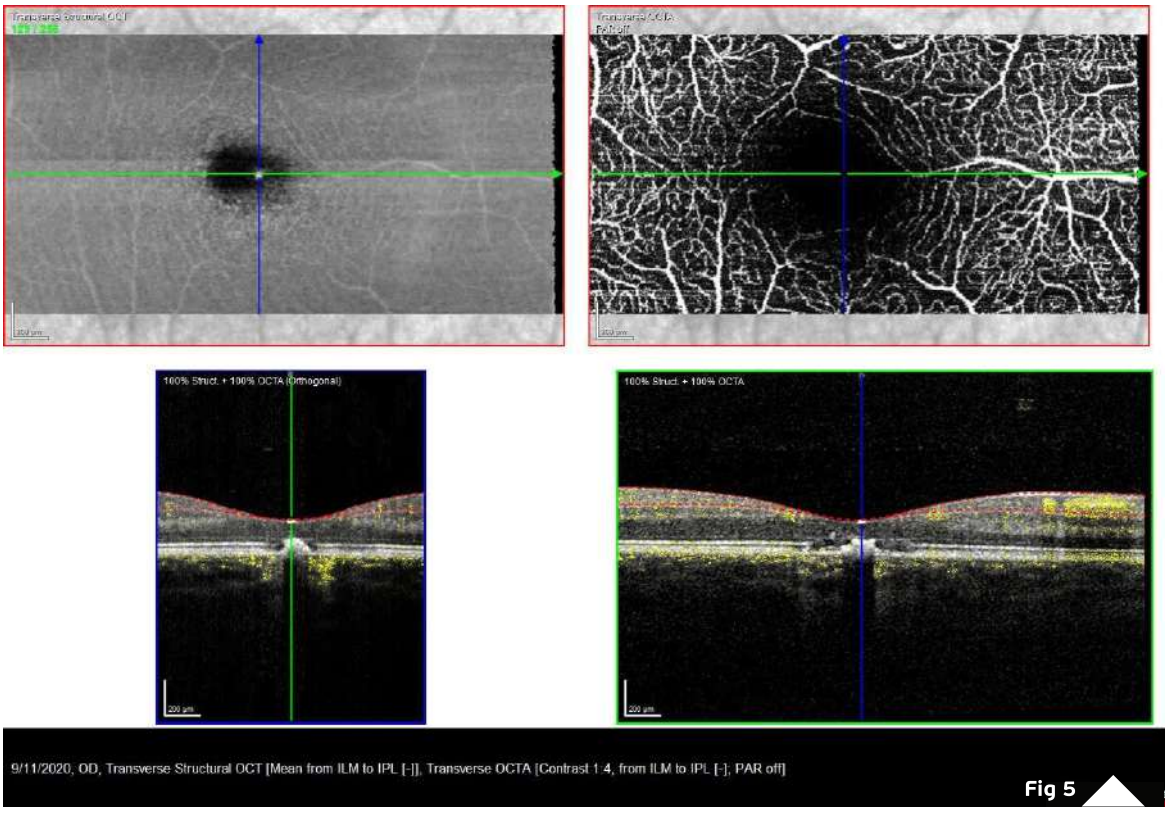

Figures 5: Correspondent OCT-A and structural OCT at 4-weeks of follow-up.

Additional History

Upon further questioning, the patient admitted having played with a laser pointer and directing the aiming beam to her eyes. Though no immediate visual disturbance was perceived, the following morning she noticed a slight blurriness in central vision on the right.

Differential Diagnosis of Abnormal Iris Vascular Formations

- Acute pigment epitheliitis
- Vitelliform macular dystrophy
- Resolved pigment epithelial detachment
- Central serous retinopathy
- Laser pointer-induced maculopathy
- Macular microhole

Possible differential diagnoses of laser pointer injuries include retinal dystrophies, as well as inflammatory and ischemic retinopathies. Even in the case of insufficient patient history, laser pointer injuries can be differentiated from genetic retinal diseases using multimodal imaging. Laser pointer injury findings remain stable following acute damage, whereas genetic retinal diseases are characterized by bilaterality and slow progression. Electrophysiological investigation can elucidate doubtful diagnosis.

Discussion and Literature

Depending on wavelength, radiation power, exposure time, localization, and spot size, laser pointers can cause photothermal injury to the eye and lead to permanent blindness. The natural protective mechanisms of the eye – such as the blink reflex or looking away – are ineffective against lasers with an output power greater than 5 milliwatts, and severe retinal damage may occur, even after momentary exposure.

The hallmark symptom of laser pointer-induced ocular injury is a central or paracentral scotoma. BCVA at presentation may range from very low to 20/20. Typical retinal finding is a round, well-defined deep yellowish-orange discoloration at the level of the RPE in the foveola, but may be as severe as cystoid macular edema, macular subhyaloid hemorrhage and full-thickness macular hole. Spectral domain optical coherence tomography (SD-OCT) is the preferred imaging method, demonstrating disruption of the photoreceptor inner segment/outer segment junction (ellipsoid zone band), extended towards the inner aspect of the RPE band and ranging from focal interruption to extensive full-thickness macular hole.

Treatment and visual prognosis of these lesions depend on the morphology of retinal damage. While spontaneous healing is possible, some cases require surgery and for others there is no treatment. Clinical management of mild cases is limited to systemic steroids though there is no properly established data on the efficacy of corticosteroid administration.

Devices and toys containing lasers become increasingly popular and readily available to ordinary people. Misclassification of laser power and lack of proper warning on devices and packaging pose serious risk not only for users but also for the ones around them. Reports and propositions regarding the danger of indiscriminate laser pointer usage date back to the late 90s. After a series of market publications claiming that such devices were not that harmful, attention was called to the need to inform the general population of the safety measures for using laser pointers, recommending usage control and that these devices should be kept away from children. A study released in 2013 by the journal of the American Academy of Ophthalmology warns that the wide availability of these devices, often marketed as toys, could lead to an epidemic of eye injuries. Ineffective control of laser pointers circulating for importation and purchase is per se a world public health hazard and should be taken accordingly.

Keep in mind

- ✓ Laser pointers can cause permanent retinal damage.
- ✓ Users must be warned to never aim or shine a laser pointer at anyone, especially towards the eye.
- ✓ Do not regard laser pointers as toys. Keep them away from children.

References

1. Birtel J, Harmening WM, Krohne TU, Holz FG, Charbel Issa P & Herrmann P (2017). Retinal Injury Following Laser Pointer Exposure. Deutsches Arzteblatt international, 114(49), 831–837. https://doi.org/10.3238/arztebl.2017.0831
2. https://www.aao.org/eye-health/news/laser-pointer-eye-injury
3. Mtanes K, Mimouni M & Zayit-Soudry S (2018). Laser Pointer-Induced Maculopathy: More Than Meets the Eye. Journal of pediatric ophthalmology and strabismus, 55(5), 312–318. https://doi.org/10.3928/01913913-20180405-01
4. Zubicoa Enériz A, Tabuenca Del Barrio L, Mozo Cuadrado M, Plaza Ramos P, & Gonzalvo Ibañez FJ (2019). Retinopatía por puntero láser: presentación de dos casos [Handheld laser maculopathy: two case reports]. Archivos argentinos de pediatria, 117(6), e640–e643. https://doi.org/10.5546/aap.2019.e640
5. Bartsch DU, Muftuoglu IK & Freeman WR (2016). Laser Pointers Revisited. Retina (Philadelphia, Pa.), 36(9), 1611–1613. https://doi.org/10.1097/IAE.0000000000001253
6. Thanos S, Böhm MR, Meyer zu Hörste M & Schmidt PF (2015). Retinal damage induced by mirror-reflected light from a laser pointer. BMJ case reports, 2015, bcr2015210311. https://doi.org/10.1136/bcr-2015-210311
7. Zamir E, Kaiserman I & Chowers I (1999). Laser pointer maculopathy. American journal of ophthalmology, 127(6), 728–729. https://doi.org/10.1016/s0002-9394(99)00017-3
8. Luttrull JK & Hallisey J (1999). Laser pointer-induced macular injury. American journal of ophthalmology, 127(1), 95–96. https://doi.org/10.1016/s0002-9394(98)00254-2
9. Israeli D, Hod Y & Geyer O (2000). Laser pointers: not to be taken lightly. The British journal of ophthalmology, 84(5), 555–556. https://doi.org/10.1136/bjo.84.5.554d
10. Alsulaiman SM, Alrushood AA, Almasaud J, Alzaaidi S, Alzahrani Y, Arevalo JF, Ghazi NG, Abboud EB, Nowilaty SR, Al-Amry M, Al-Rashaed S & King Khaled Eye Specialist Hospital Collaborative Retina Study Group (2014). High-power handheld blue laser-induced maculopathy: the results of the King Khaled Eye Specialist Hospital Collaborative Retina Study Group. Ophthalmology, 121(2), 566–72.e1. https://doi.org/10.1016/j.ophtha.2013.09.006

Case 3 - December 2020

TERRIEN'S MARGINAL DEGENERATION

A 4-year-old boy presented with a brown engorgement at the upper temporal corneal periphery on the left eye, noticed by his parents a week before.

Presented by
Miltos Balidis, MD, PhD, FEBOphth, ICOphth

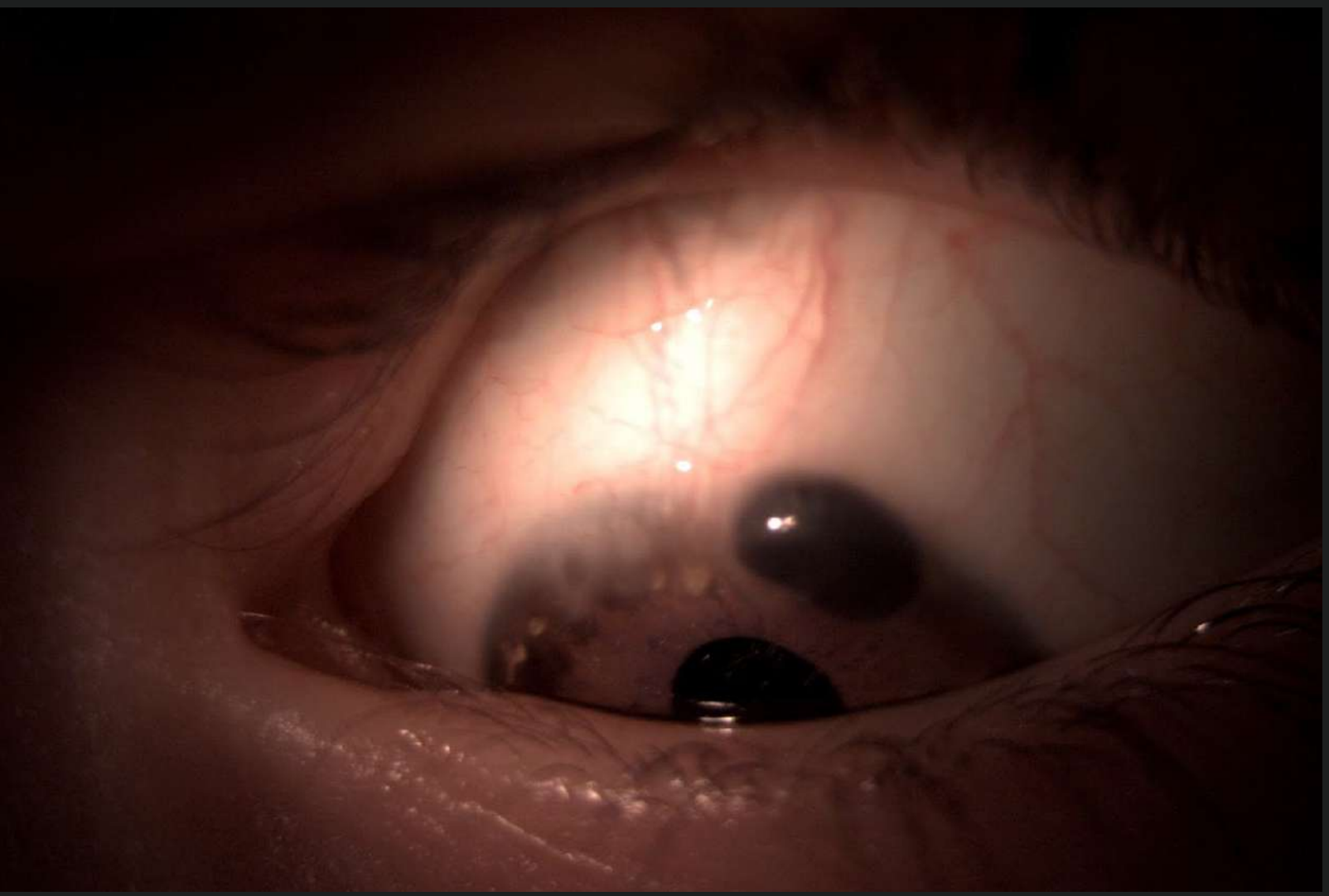

Edited by
Penelope Burle de Politis, MD

Case History

A 4-year-old boy with no previous ocular or systemic disorders presented a sudden brown engorgement at the upper temporal corneal periphery on the left eye, noticed by his parents for 1 week (**Figure 1**). On examination, best-corrected visual acuity (BCVA) on the left was 5/10 with a refractive error of +1.00 -2.75@70⁰. Biomicroscopy revealed a protruding band of iris tissue at 12 to 2 hours of peripheral cornea, through an area of thinning and guttering, surrounded by neovascularization and lipid deposits (**Figure 2**). The right eye was emmetrope with 10/10 vision and presented an area of corneal thinning at the lower temporal periphery (**Figure 3**). Anterior spectral-domain optical coherence tomography (SD-OCT) scan was attempted, but difficult to perform due to photophobia and low age.

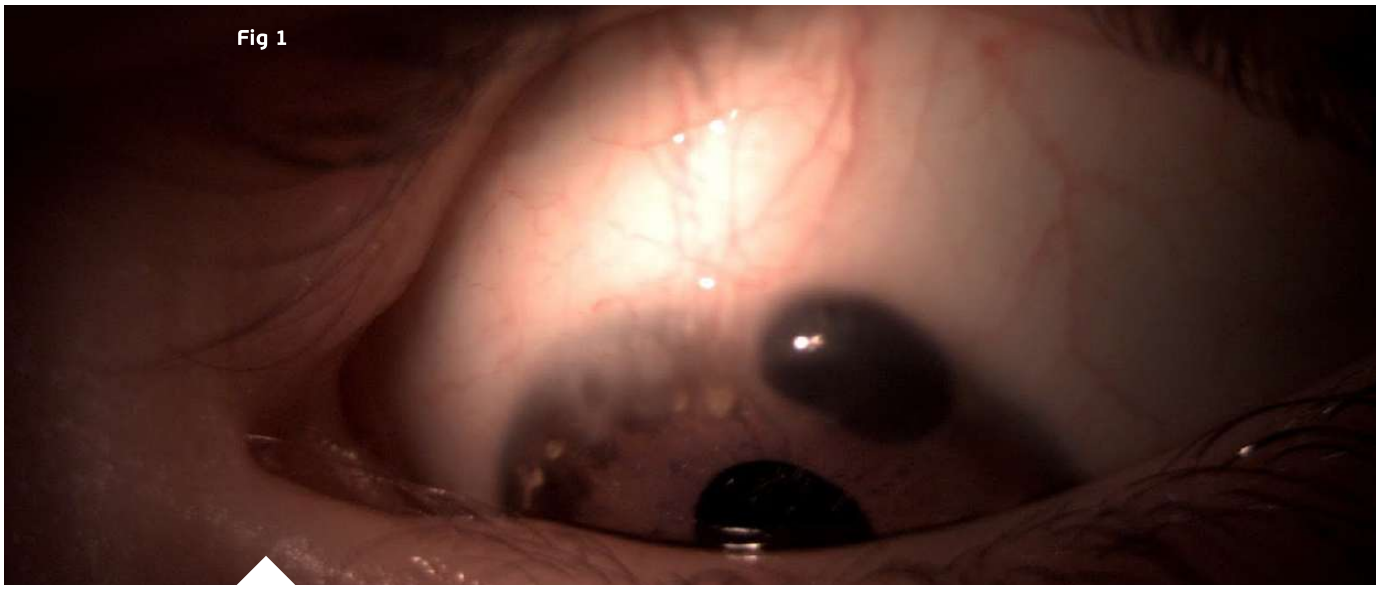

Figure 1: Slit lamp photography of the reported lesion

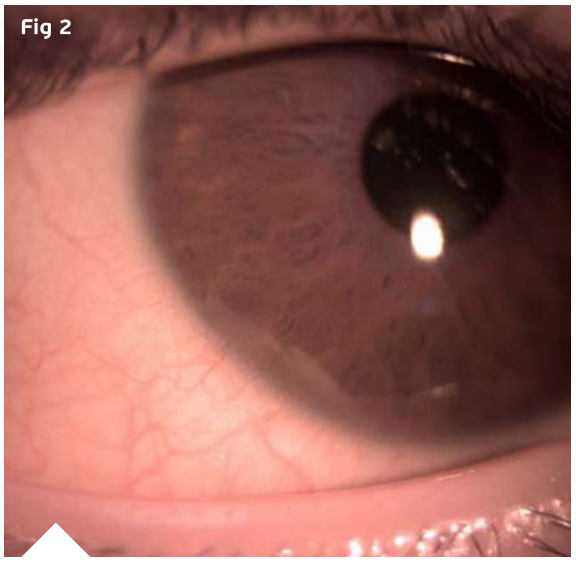

Figure 2: SD-OCT (Spectralis®) scan showing a hyperreflective lesion at the right fovea, with disruption of the overlying ellipsoid zone. Note the choroidal shadowing associated with the lesion.

Figure 3: Slit lamp photography of the right eye revealing an asymptomatic area of corneal thinning at the lower temporal periphery.

Two weeks later, the patient underwent surgical reduction of the herniated iris segment and mechanical tamponade of the affected area with double amniotic membrane graft as a preventive measure for corneal rupture (**Figure 4**).

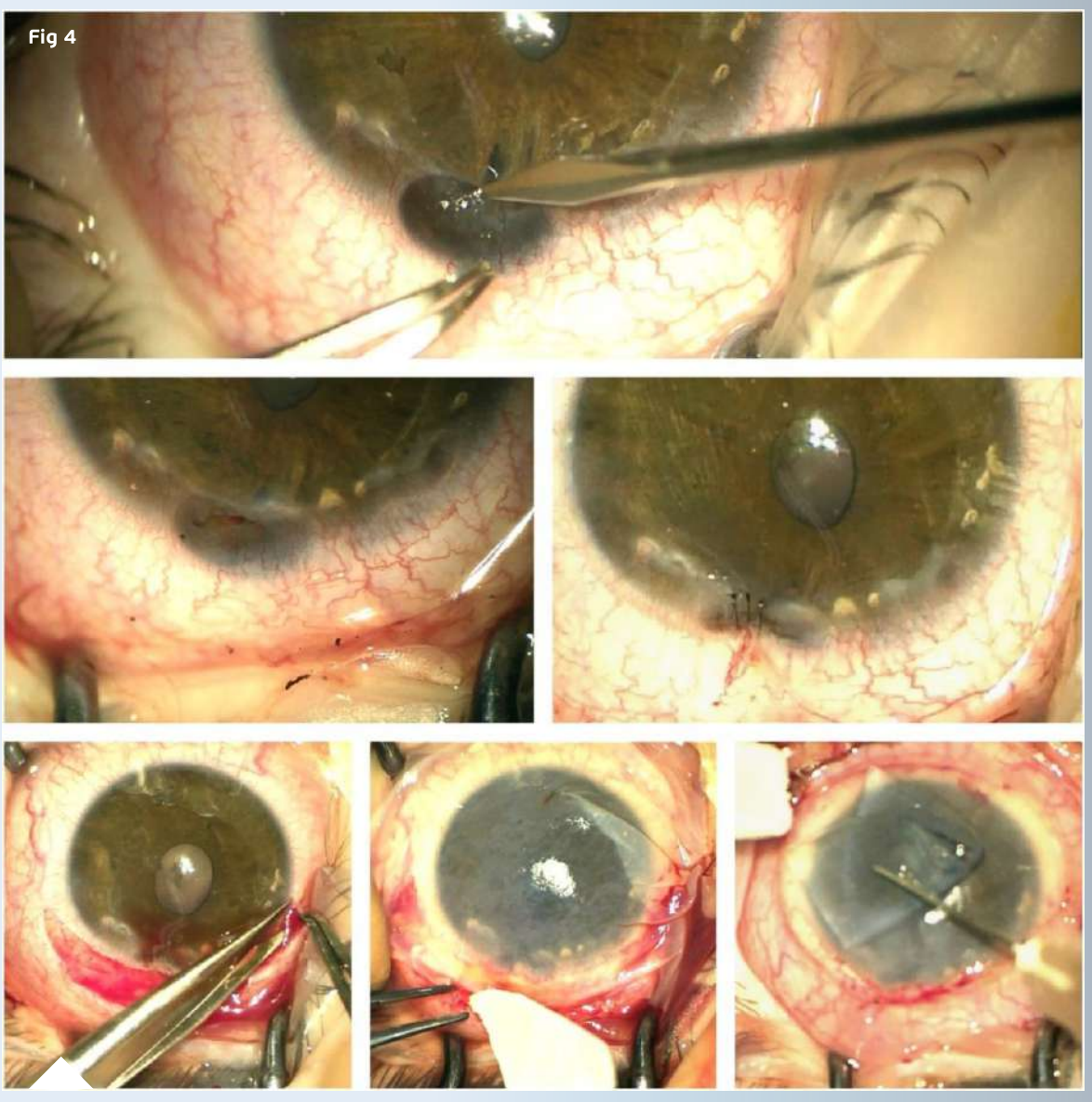

Figures 4: OCT-A (**top**) demonstrating a hypointense lesion at the choriocapillaris segment, in correspondence with the focal hyperreflectivity detected on structural OCT (**bottom**), suggesting rarefaction of the choriocapillaris (Spectralis®).

Additional History

Upon further questioning, the parents mentioned that the child had recently suffered an accidental fall, hitting his forehead just above the affected eye. Though no immediate ocular disturbance was noticed, observation on the next following days revealed the described finding.

Differential Diagnosis

- Marginal furrow (Terrien's) degeneration
- Dellen
- Collagen vascular disease
- Pellucid marginal degeneration
- Sclerokeratitis
- Keratoconjunctivitis sicca
- Staphylococcal marginal keratitis
- Infectious corneal ulcer

Terrien's marginal degeneration may be differentiated from other peripheral corneal thinning disorders by the lack of inflammation, presence of superficial vascularization, advancing linear deposition of lipid, lack of epithelial defect and slow progressive course.

Discussion and Literature

Terrien's marginal degeneration is a rare (Terrien himself saw only 3 cases in 30 years of practice), bilateral condition, of unclear etiology, compromising corneal periphery. The upper corneal half is more commonly and severely involved. Opacity, vascularization and yellowish discoloration of peripheral cornea due to lipid deposition at the advancing edge are the earliest signs. There is progressive thinning of Bowman's membrane and anterior layers of the stroma, so that a gutter is formed, allowing for bulging of intraocular structures. As the disease progresses, peripheral thinning may be so pronounced that perforation and extrusion of eye contents may happen under minor trauma, such as rubbing, or even spontaneously.

Terrien's marginal degeneration is also referred to as furrow keratitis. Although an inflammatory form may exist, inflammation being reported as attacks of pain or redness, the condition is mostly degenerative, with a slow-course structural weakening of the peripheral corneal stroma. The disease is usually asymmetric and symptoms in the fellow eye may be delayed as long as 25 years. Depending on the extent and depth of compromised peripheral thickness, marginal corneal ectasia may be asymptomatic and go unnoticed until late in life, or be diagnosed at a young age in the event of a complication, as in the reported case.

The peripheral corneal weakness induced by Terrien's marginal degeneration reduces both mechanical and optical corneal power. In fact, the hallmark symptom of uncomplicated furrow corneal degeneration is decreased visual acuity from high corneal astigmatism due to flattening of the involved meridian. Though rare, presentation in young children must be approached soon enough to restore visual acuity and prevent amblyopia from inadequate optic stimulation. In addition, proper advice regarding ocular protection (e.g. with glasses) and avoidance of direct pressure applied to the eye is of ultimate importance, especially during school years.

Ineffective ophthalmic screening in childhood may conceal different types of ocular disorders, many of them preventable or manageable. While small children are unlikely to complain of visual disturbances, their optical system must be offered full developmental potentials to ensure functional vision later in life. Anisometropic astigmatism in children should always be further investigated. Meticulous slit-lamp examination and computerized topographic analysis may grant early diagnosis of corneal pathologic conditions, especially in the presence of irregular astigmatism. Most corneal ectasia can be halted or treated by means of proper medical advice and timely indication of adequate therapy.

Compared to other forms of corneal ectasia, Terrien's marginal degeneration is mostly expected to be found in adults and older individuals. However, it is possible that the onset of peripheral corneal degeneration precedes clinical manifestation by many decades, leading to cases being overlooked or undiagnosed, due to the insidious nature of the disease. Earliest detection of new cases such as the one described in this report may contribute to better understanding and managing not only Terrien's corneal degeneration, but possibly other ectatic corneal conditions sharing similar features and whose pathogenesis have not yet been fully explained.

Keep in mind

- ✓ Corneal ectasia in young children must be approached soon enough to prevent amblyopia from high ametropia.
- ✓ Terrien's marginal degeneration is an uncommon form of peripheral corneal thinning, rarely presenting in childhood.
- ✓ Management of Terrien's marginal degeneration is focused on visual improvement and prevention of ocular rupture.

References

1 Khurana S, Gupta PC, Kumar A & Ram J (2020). Globe rupture following eye rubbing in a case of Terrien's marginal degeneration in a young male. Indian journal of ophthalmology, 68(11), 2493–2494. https://doi.org/10.4103/ijo.IJO_1858_19

2 Ding Y, Murri MS, Birdsong OC, Ronquillo Y & Moshirfar M (2019). Terrien marginal degeneration. Survey of ophthalmology, 64(2), 162–174. https://doi.org/10.1016/j.survophthal.2018.09.004

3 Chung J, Jin KH, Kang J & Kim TG (2017). Spontaneous corneal perforation in Terrien's marginal degeneration in childhood: A case report. Medicine, 96(49), e9095. https://doi.org/10.1097/MD.0000000000009095

4 Chan AT, Ulate R, Goldich Y, Rootman DS & Chan CC (2015). Terrien Marginal Degeneration: Clinical Characteristics and Outcomes. American journal of ophthalmology, 160(5), 867–872.e1. https://doi.org/10.1016/j.ajo.2015.07.031

5 Srinivasan S, Murphy CC, Fisher AC, Freeman LB & Kaye SB (2006). Terrien marginal degeneration presenting with spontaneous corneal perforation. Cornea, 25(8), 977–980. https://doi.org/10.1097/01.ico.0000226367.41925.ab

6 Pouliquen Y, Dhermy P, Renard G, Goichot-Bonnat L, Foster G & Savoldelli M (1989). Terrien's disease: clinical and ultrastructural studies, five case reports. Eye (London, England), 3 (Pt 6), 791–802. https://doi.org/10.1038/eye.1989.123

7 Beauchamp GR (1982). Terrien's marginal corneal degeneration. Journal of pediatric ophthalmology and strabismus, 19(2), 97–99.

8 Austin P & Brown S I (1981). Inflammatory Terrien's marginal corneal disease. American journal of ophthalmology, 92(2), 189–192. https://doi.org/10.1016/0002-9394(81)90768-6

9 Doggart JH (1930). MARGINAL DEGENERATION OF THE CORNEA. The British journal of ophthalmology, 14(10), 510–516. https://doi.org/10.1136/bjo.14.10.510

10 RICHARDS WW (1963). MARGINAL DEGENERATION OF THE CORNEA WITH PERFORATION. Archives of ophthalmology (Chicago, Ill.: 1960), 70, 610–615. https://doi.org/10.1001/archopht.1963.00960050612006

Case 4 - January 2021

PERIPAPILLARY PACHYCHOROID SYNDROME

A 46-year-old man presented with progressive bilateral visual loss for one year.

Presented by
Paris Tranos, MD, PhD, ICOphth, FRCS

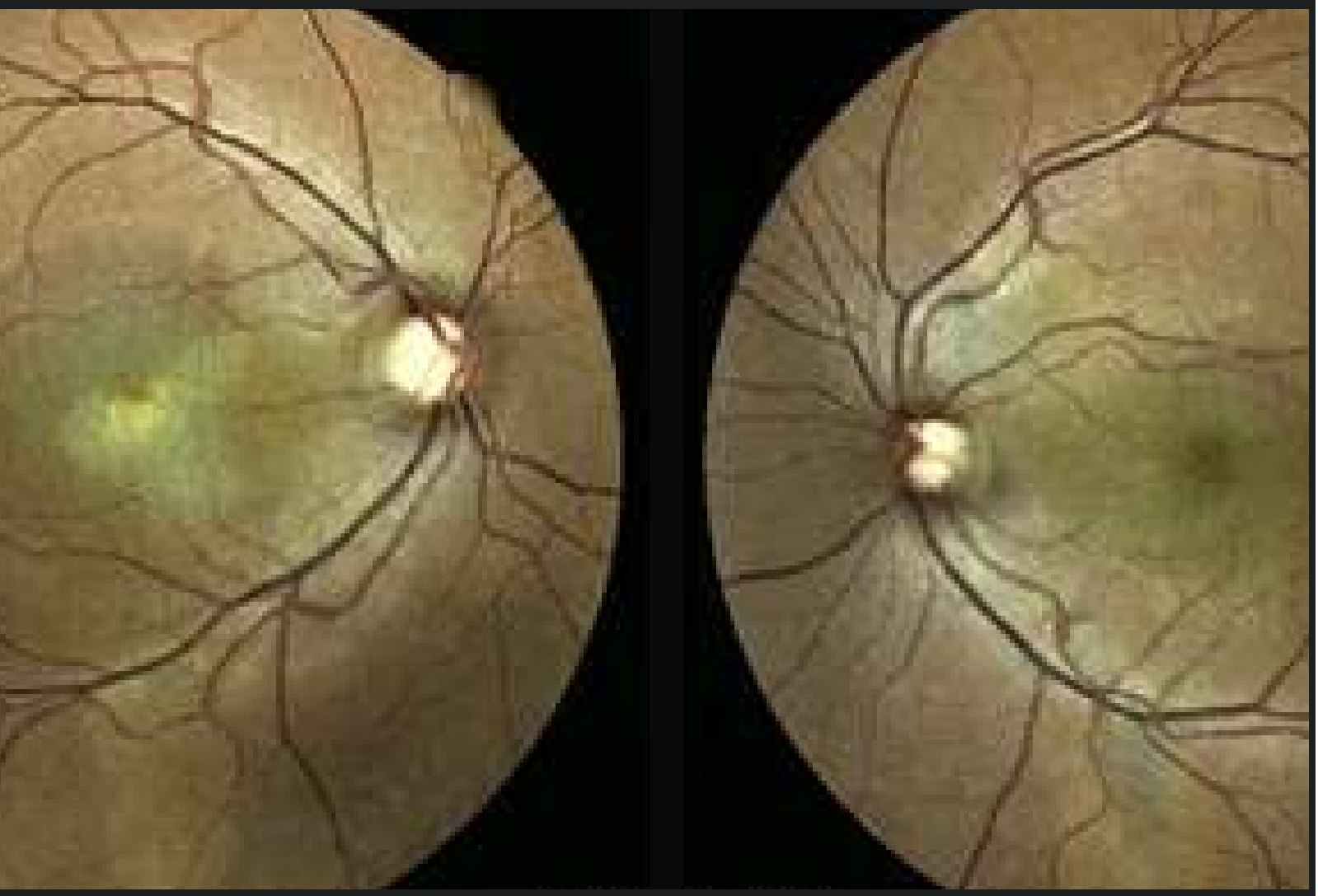

Edited by
Penelope Burle de Politis, MD

Case History

A 46-year-old Caucasian man presented with progressive bilateral visual loss for one year, with partial spontaneous improvement on the left but none on the right. Past medical and family history were unremarkable, and he was not on any medication. On examination, best-corrected visual acuity (BCVA) was reduced to counting fingers on the right and 5/10 on the left. Intraocular pressure was within normal limits and there was no sign of inflammation in the anterior or posterior segments. Fundoscopy revealed atrophic lesions and evidence of shallow subretinal fluid at the right and left macules, respectively (**Figure 1**).

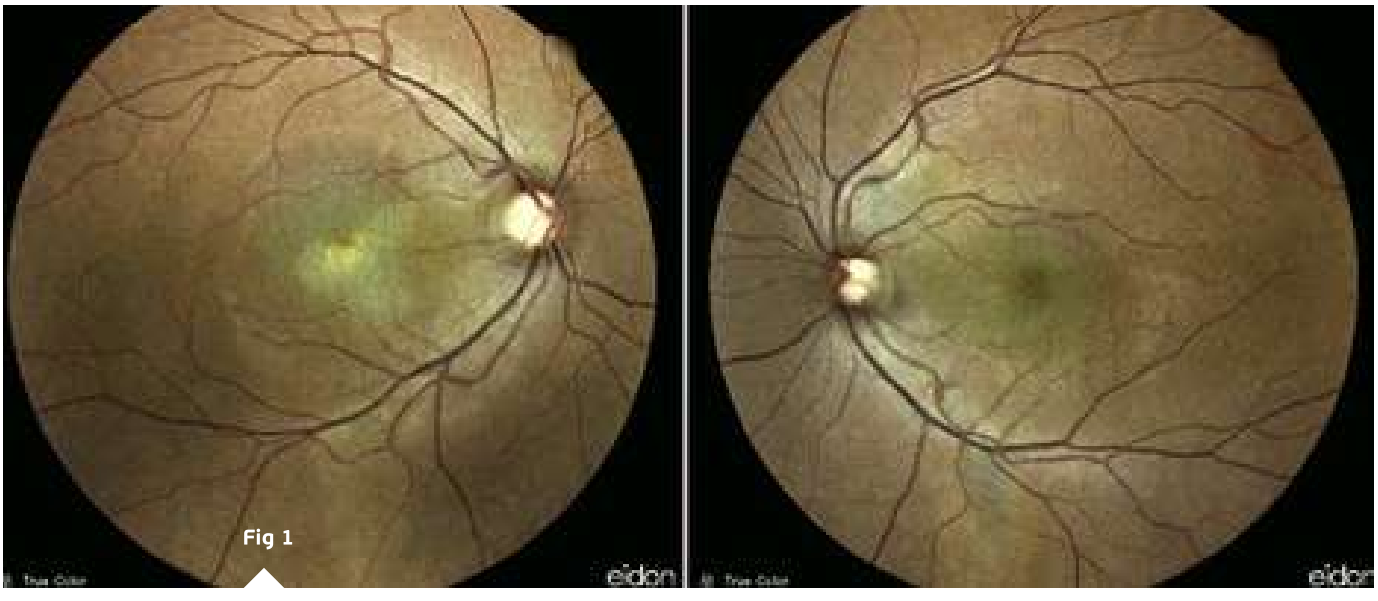

Figure 1: Fundus photographs of the right and left eye showing atrophic lesions at both macules.

Further investigation with multimodal imaging — autofluorescence (AF), fundus fluorescein angiography (FFA), optical coherence tomography (OCT) and indocyanine green (ICG) angiography — was carried on (**Figures 2 and 3**).

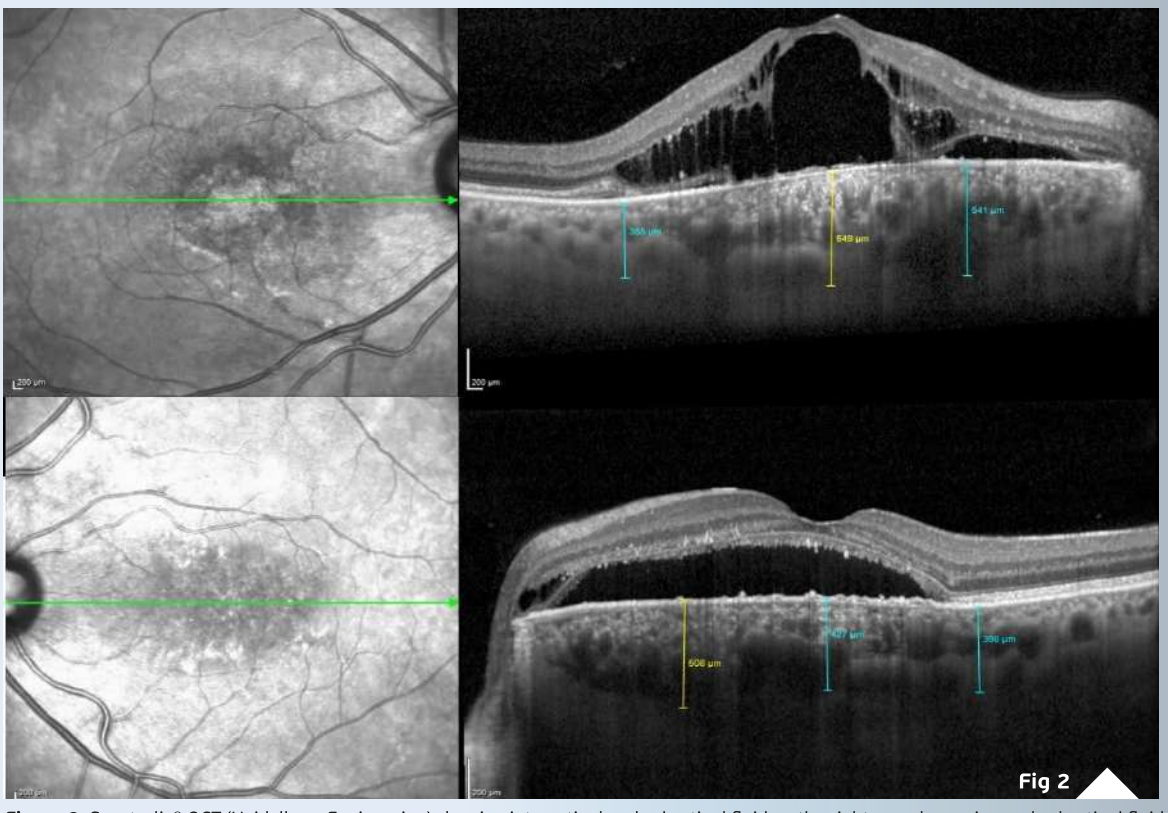

Figure 2: Spectralis® OCT (Heidelberg Engineering) showing intraretinal and subretinal fluid on the right macular region and subretinal fluid at the left macula, extending up to the optic disc. A small pocket of intraretinal fluid is noticeable adjacent to the left papilla. The choroid is significantly thickened in both eyes, with more pronounced thickening nasal to the macula on the left.

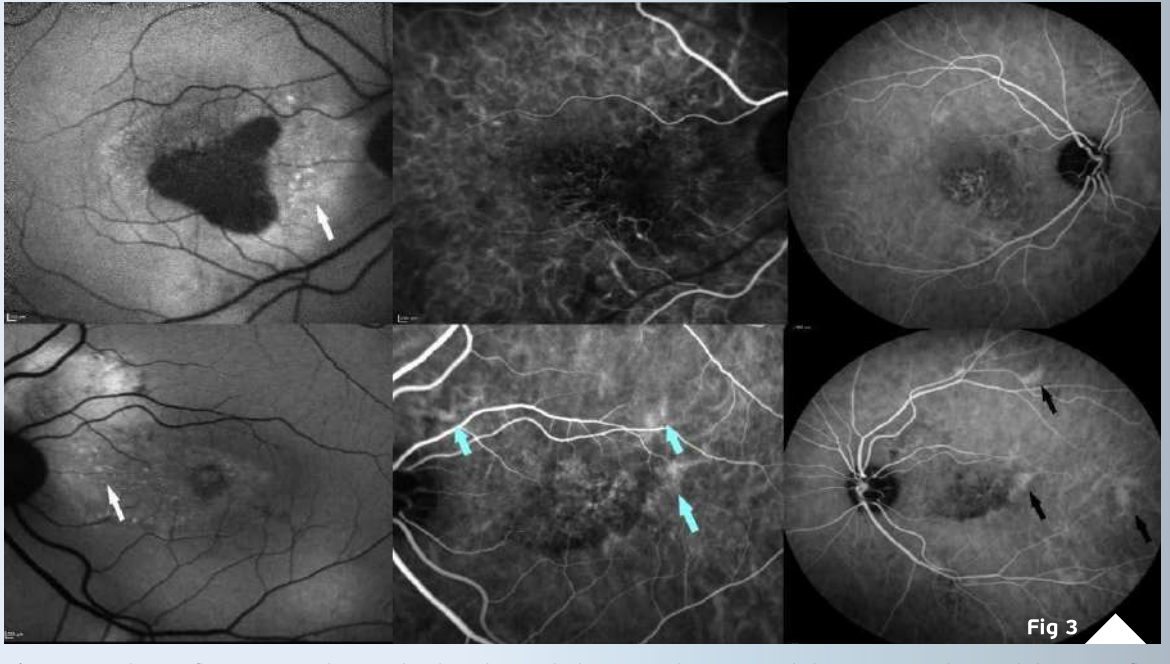

Figure 3: Fundus autofluorescence is decreased at the right macula due to retinal pigment epithelium (RPE) atrophy. Stipple hyper-autofluorescence is evident at the peripapillary area in both eyes (white arrows). Indocyanine green angiography shows pachyvessels (blue arrows) in early phase and multifocal hyperpermeability (black arrows) in midphase.

Additional History

Due to the severe atrophic changes at the macula, the right eye had poor visual prognosis and was managed with observation only. Half-dose photodynamic therapy was applied to the left eye, with complete resolution of subretinal and intraretinal fluid at both macular and peripapillary areas 2 months later (Figure 4). Nevertheless, BCVA change was minimal, improving only to 6/10 after fluid absorption on the left.

Differential Diagnosis

- Peripapillary pachychoroid syndrome
- Other causes of macular edema (diabetic retinopathy, retinal vein occlusion, etc.)
- Pachychoroid neovasculopathy
- Ocular tumors (circumscribed choroidal hemangioma, choroidal hamartoma)
- Cavitary optic disc anomalies (optic pit, advanced glaucoma, coloboma)
- Tractional maculopathy

The peripapillary disposition, associated with nasal choroidal thickening and peripapillary IRF point to the diagnosis of Peripapillary Pachychoroid Syndrome.

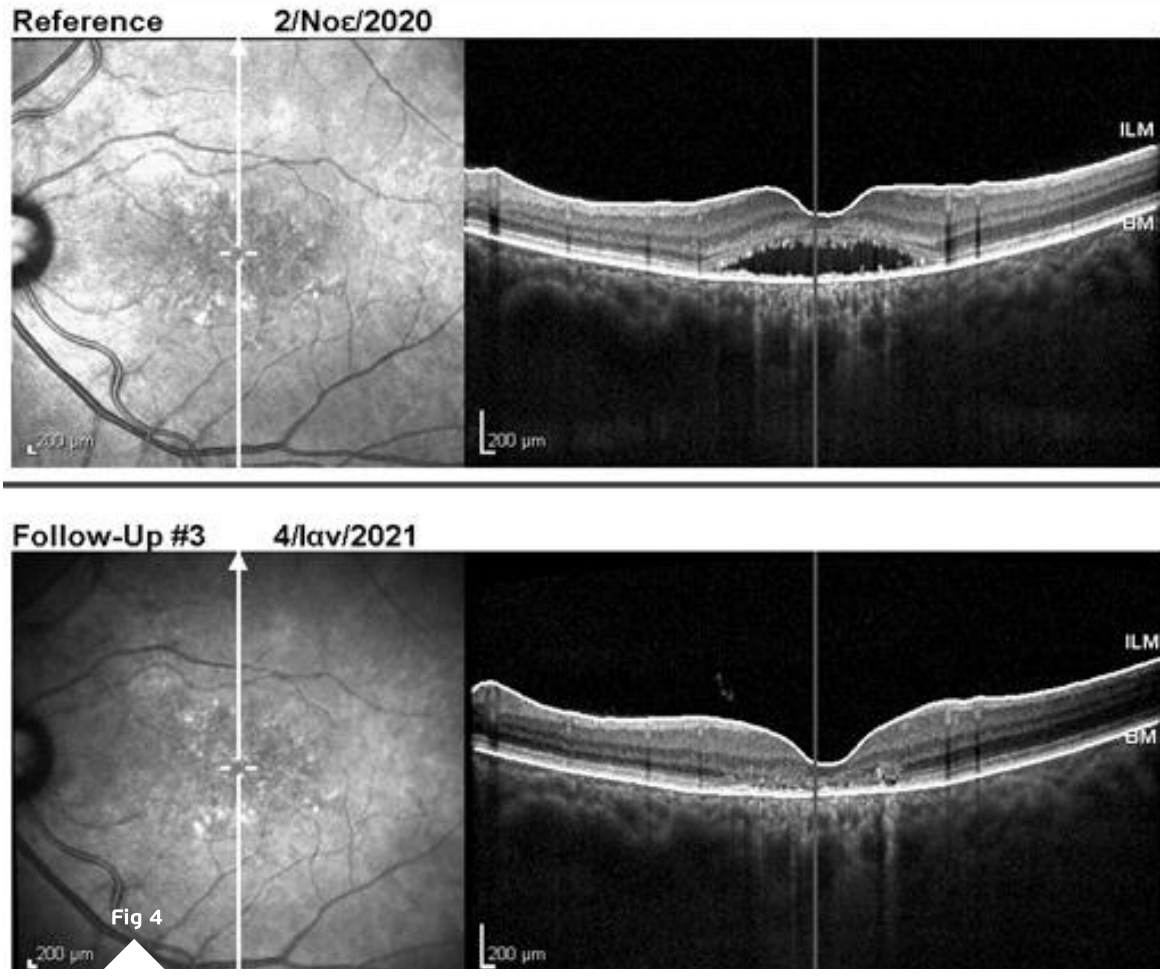

Figure 4: Serial OCT for comparison of pre- and post-treatment macular aspect.

Discussion and Literature

A structurally and functionally intact choroid tissue is vitally important for retinal function. While the central retinal artery supplies the internal 2 thirds of the retina, the choroidal vein network is responsible for the remaining external third. Abnormal choroidal blood flow leads to photoreceptor dysfunction and death. A wide range of choroidal diseases manifest with increased choroidal thickness, thus being referred to as Pachychoroid Spectrum Disorders, a relatively new concept in ophthalmology (2013), still evolving both in concept and in terminology.

Pachychoroid Spectrum Disorders (PSD) classification has been constantly revised and is presently divided in six disorders, sometimes coexisting in the same eye: Pachychoroid Pigment Epitheliopathy, Central Serous Chorioretinopathy (CSC), Pachychoroid Neovasculopathy, Polypoidal Choroidal Vasculopathy, Focal Choroidal Excavation and Peripapillary Pachychoroid Syndrome (PPS) — these two being the latest additions. They all share three basic characteristics: increased choroidal thickening, pathologically dilated veins in Haller's (outer choroid) layer — pachyvessels — and attenuation of the choriocapillaris and Sattler's (middle choroid) layer.

Peripapillary Pachychoroid Syndrome was introduced as a variant of CSC, but is now considered a separate syndrome, due to its particular features, notably the tendency to surround the optic nerve. Also, patients with PPS are mostly men but typically older than those with CSC. Cardinal findings are peripapillary intraretinal fluid (IRF) and/or subretinal fluid (SRF), extending to the nasal macula, with thickening of the nasal macular choroid — as opposed to temporal in CSC. Besides, IRF is more prevalent than SRF and appears earlier in the course of the disease than in CSC. Additional characteristics of PPS include choroidal folds, peripapillary RPE mottling and pachyvessels on ICG. A relatively short axial length and hyperopia are common associations with this disorder.

Peripapillary Pachychoroid Syndrome may go unnoticed until there is macular involvement, thus manifesting as marked reduction in visual acuity. The disease is bilateral, but involvement may be asymmetric. Diagnosis poses a challenge in identifying PPS among other forms of PDS, as they are believed to represent different manifestations of a common pathogenic process, with overlapping features and possible progression from one to another. Multimodal imaging is the recommended approach for distinguishing this new clinical entity, also from disorders such as posterior uveitis and neuro-ophthalmologic conditions sharing similar features, namely disk leakage and edema, both of which may ensue in complicated PPS.

Management of PPS may be conservative (observation) or include anti-vascular endothelial growth factor (anti-VEGF) injections and/or photodynamic therapy, the latter being suggested as the most effective treatment modality. Despite encouraging anatomical results, visual improvement is usually minimal to moderate. Advanced cases may be entirely refractory to treatment.

Keep in mind

- ✓ PPS is a distinct entity and one of the pachychoroid syndromes.
- ✓ It is important to exclude the presence of choroidal neovascular membrane, ocular tumors and optic disc cavitary lesions prior to establishing the diagnosis of PPS.
- ✓ Management of PPS is similar to that for CSC, PDT being the most effective treatment modality.

References

1. Akkaya S (2018). Spectrum of pachychoroid diseases. International ophthalmology, 38(5), 2239–2246. https://doi.org/10.1007/s10792-017-0666-4
2. Moraru AD, Costin D, Moraru RL, Costuleanu M & Brănișteanu DC (2020). Current diagnosis and management strategies in pachychoroid spectrum of diseases (Review). Experimental and therapeutic medicine, 20(4), 3528–3535. https://doi.org/10.3892/etm.2020.9094
3. Manayath GJ, Verghese S, Ranjan R & Narendran V (2020). Simultaneous multiple pachychoroid spectrum entities coexisting in the same eye. Indian journal of ophthalmology, 68(10), 2234–2235. https://doi.org/10.4103/ijo.IJO_931_20
4. Castro-Navarro V, Behar-Cohen F, Chang W, Joussen AM, Lai T, Navarro R, Pearce I, Yanagi Y & Okada AA (2020). Pachychoroid: current concepts on clinical features and pathogenesis. Graefe's archive for clinical and experimental ophthalmology = Albrecht von Graefes Archiv fur klinische und experimentelle Ophthalmologie, 10.1007/s00417-020-04940-0. https://doi.org/10.1007/s00417-020-04940-0
5. Cheung C, Lee WK, Koizumi H, Dansingani K, Lai T & Freund KB (2019). Pachychoroid disease. Eye (London, England), 33(1), 14–33. https://doi.org/10.1038/s41433-018-0158-4
6. Phasukkijwatana N, Freund KB, Dolz-Marco R, Al-Sheikh M, Keane PA, Egan CA, Randhawa S, Stewart JM, Liu Q, Hunyor AP et al. (2018). PERIPAPILLARY PACHYCHOROID SYNDROME. Retina (Philadelphia, Pa.), 38(9), 1652–1667. https://doi.org/10.1097/IAE.0000000000001907
7. Xu D, Garg E, Lee K, Sakurada Y, Amphornphruet A, Phasukkijwatana N, Liakopoulos S, Pautler SE, Kreiger AE, Yzer S et al. (2020). Long-term visual and anatomic outcomes of patients with peripapillary pachychoroid syndrome. The British journal of ophthalmology, bjophthalmol-2019-315550. Advance online publication. https://doi.org/10.1136/bjophthalmol-2019-315550
8. Alonso-Martín B, de-Lucas-Viejo B, Gimeno-Carrero M, Ferro-Osuna M & Sambricio J (2020). Diagnosis by multimodal imaging in peripapillary pachychoroid syndrome: A case report. Diagnóstico mediante imagen multimodal en síndrome paquicoroideo peripapilar: a propósito de un caso. Archivos de la Sociedad Española de Oftalmología, 95(5), 248–253. https://doi.org/10.1016/j.oftal.2020.01.013

Case 5 - March 2021

GRANULAR CORNEAL DYSTROPHY TYPE I

A 33-year-old woman presented asymptomatic corneal flecks in a routine eye exam.

Presented by
Presented by Giorgos Sidiropoulos, MD, FEBOphth

Edited by
Penelope Burle de Politis, MD

Case History

A 33-year-old Caucasian woman presented bilateral corneal opacities during routine ophthalmic examination. Her only complaint was asthenopia related to prolonged computer use. On examination, uncorrected visual acuity (UCVA) was 12/10 bilaterally. Objective refraction was -0,50@75 on the right and plano on the left. Intraocular pressure and fundoscopy were normal for both eyes. Biomicroscopy revealed calm eyes displaying whitish spiky granules at stroma level of both corneas, best evidentiated upon retroillumination through the pupillary area (**Figures 1 and 2**).

Figure 1: Microscope photograph under broad beam direct illumination showing multiple irregular corneal opacities in the pupillary area.

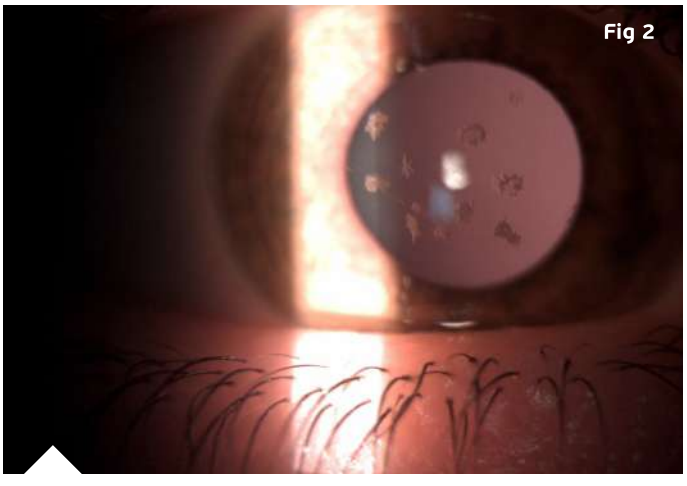

Figure 2: Slit-lamp photograph of the right eye showing whitish, irregularly-shaped, sharply-demarcated granules in the anterior corneal stroma, with clear intervening stroma and sparing corneal periphery.

Anterior segment optical coherence tomography (OCT) demonstrated multiple dense granules in the anterior stroma of both corneas, some of them underlining the epithelium on the right eye (**Figure 3**).

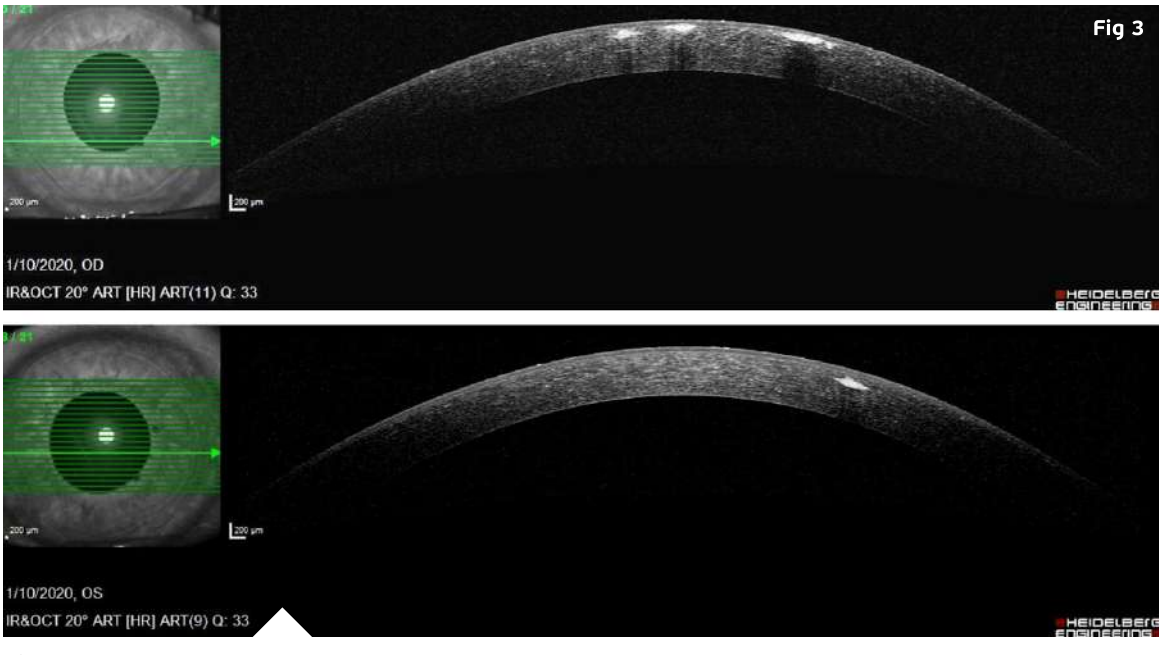

Figure 3: Anterior segment OCT (Heidelberg Engineering®) showing multiple hyperreflective dots in the anterior stroma, more numerous and anteriorly distributed on the right eye. Notice that corneal periphery is spared.

Additional History

The patient had undergone an ophthalmologic examination a couple of years before and was told about the corneal spots on that occasion. Her mother had been examined by the same doctor and was detected with an identical ocular aspect. Neither mother nor daughter suffered from any other ocular or systemic disorder.

Differential Diagnosis

- granular corneal dystrophy (GCD) type I
- other types of corneal dystrophy
- monoclonal gammopathies
- corneal degeneration
- recurrent corneal erosions
- infectious keratitis
- neurotrophic keratitis
- band keratopathy
- diseases of basement membrane (Alport and Usher syndromes)

The major distinction to be done for corneal dystrophies (CD) is with corneal degeneration. Generally, CDs have a bilateral, symmetric presentation, unrelated to environmental factors. Most often, though, CDs must be differentiated among one another, as clinical presentations may overlap. Biomicroscopy helps in identifying different types of CD. Genetic testing may aid in final differentiation. Specifically, lesions in GCD type I can resemble a lot those found in monoclonal gammopathies.

Discussion and Literature

Corneal dystrophy is a collection of rare hereditary, non-inflammatory disorders of abnormal depositions in the cornea. As proposed in 2015 by the International Classification of Corneal Dystrophies (IC3D), CD is subclassified by anatomic location: epithelial/-subepithelial, epithelial-stromal, stromal, and endothelial. There is no gender predilection. There seems to be a higher prevalence among Caucasian individuals. Clinical manifestation depends on the involved corneal layer(s). Based on the type and severity of CD, patients can be asymptomatic or experience any combination of visual loss, photophobia, dry eye, corneal edema, recurrent corneal erosions and pain. Symptoms can begin at any age and management ranges from simple observation to corneal transplantation. The IC3D lists 22 distinct forms of corneal dystrophy, but more than 30 forms have already been described. Inheritance is predominantly autosomal dominant, although autosomal recessive and X-chromosomal dominant patterns do exist.

Formerly called corneal dystrophy Groenouw type I or “classic”, GCD type I belongs to the TGFBI-associated CDs (corneal dystrophies associated with mutations in the transforming growth factor, ß-induced gene). Inheritance is autosomal dominant with complete penetrance. It has been well mapped, with MIM (Mendelian Inheritance in Man) #121900, genetic locus 5q31, predominant mutation Arg555Trp.

In light microscopy, GCD displays multiple stromal deposits, mostly distributed in the anterior stroma. Lesions are seen in transmission electron microscopy as dense rod-shaped bodies and, in confocal microscopy, as hyperreflective opacities in snowflake and trapezoidal shapes. In immunohistochemistry essays, the abnormal material reacts with antibodies to TGFBI protein (keratoepithelin).

Clinically, GCD type I may be noticeable from childhood, as early as 2 years of age. Glare and photophobia are initial symptoms. At slit-lamp examination, GCD I is characterized by opacities in the corneal stroma, in an irregular crumb- or flake-like fashion, slightly white. Deposits may be both discrete and confluent, but do not extend to the limbus. In children, a vortex pattern of brownish granules develops, superficial to the Bowman layer. As the patient ages, the size and number of granules increase, resulting in the typical glassy splinters, crushed bread crumbs or snowflakes appearance. Later in life, granules may coarsen and extend into the deeper stroma, approaching Descemet's membrane.

Management and prognosis of GCD type I depend on stage and manifestations. Homozygote cases have more severe symptoms and the type of mutation is an important phenotype determinant. As the disease progresses and the opacities become more confluent in the superficial cornea, reduction in visual acuity (VA) and recurrent erosions occur, requiring medical intervention. Although serial observation demonstrates that granule drop out after epithelial erosions may actually result in stromal clearing, some patients may need lamellar or penetrating keratoplasty (PKP) by the fifth decade. According to deposit size and distribution, an alternative treatment to improve VA and postpone corneal grafting is phototherapeutic keratectomy (PTK). However, recurrence-free survival is longer with PKP. Refractive corneal surgeries are contraindicated as they induce progression of the disease. Deep anterior lamellar keratoplasty (DALK) is a good therapeutic option, even if repeated procedures are required.

Keep in mind

- ✓ GCD type I is typically an anterior stromal form of CD, but may extend anterior and posteriorly as the disease progresses.
- ✓ Despite complete penetrance of the abnormal gene, phenotypic manifestation of GCD type I varies. Interventional therapy is reserved for symptomatic cases.
- ✓ Homozygosity in GCD type I is related to higher severity; therefore, parental counseling is advisable.

References

1 Moshirfar M, Bennett P & Ronquillo Y (2021). Corneal Dystrophy. In StatPearls. StatPearls Publishing.

2 Munier F & Schorderet D (2008) Classification of Corneal Dystrophies on a Molecular Genetic Basis. In: Reinhard T., Larkin F. (eds) Cornea and External Eye Disease. Essentials in Ophthalmology. Springer, Berlin, Heidelberg. https://doi.org/10.1007/978-3-540-33681-5_5

3 Lisch W & Weiss JS (2019). Clinical and genetic update of corneal dystrophies. Experimental eye research, 186, 107715. https://doi.org/10.1016/j.exer.2019.107715

4 Solari HP, Ventura MP, Perez AB, Sallum JM, Burnier MN Jr & Belfort R Jr (2007). TGFBI gene mutations in Brazilian patients with corneal dystrophy. Eye (London, England), 21(5), 587–590. https://doi.org/10.1038/sj.eye.6702264

5 Malkondu F, Arıkoğlu H, Erkoç Kaya D, Bozkurt B & Özkan F (2020). Investigation of TGFBI (transforming growth factor beta-induced) Gene Mutations in Families with Granular Corneal Dystrophy Type 1 in the Konya Region. Turkish journal of ophthalmology, 50(2), 64–70. https://doi.org/10.4274/tjo.galenos.2019.55770

6 Eiberg H, Møller HU, Berendt I et al. Assignment of Granular Corneal Dystrophy Groenouw Type I (CDGG1) to Chromosome 5q. Eur J Hum Genet 2, 132–138 (1994). https://doi.org/10.1159/000472353

7 Weiss JS, Møller HU, Aldave AJ, Seitz B, Bredrup C, Kivelä T, Munier FL, Rapuano CJ, Nischal KK, Kim EK, Sutphin J, Busin M, Labbé A, Kenyon KR, Kinoshita S & Lisch W (2015). IC3D classification of corneal dystrophies--edition 2. Cornea, 34(2), 117–159. https://doi.org/10.1097/ICO.0000000000000307

8 Lin ZN, Chen J & Cui HP (2016). Characteristics of corneal dystrophies: a review from clinical, histological and genetic perspectives. International journal of ophthalmology, 9(6), 904–913. https://doi.org/10.18240/ijo.2016.06.20

9 Møller HU (1989). Inter-familial variability and intra-familial similarities of granular corneal dystrophy Groenouw type I with respect to biomicroscopical appearance and symptomatology. Acta ophthalmologica, 67(6), 669–677. https://doi.org/10.1111/j.1755-3768.1989.tb04400.x

10 Seitz B, Behrens A, Fischer M, Langenbucher A & Naumann GO (2004). Morphometric analysis of deposits in granular and lattice corneal dystrophy: histopathologic implications for phototherapeutic keratectomy. Cornea, 23(4), 380–385. https://doi.org/10.1097/00003226-200405000-00013

11 Lewis DR, Price MO, Feng MT & Price FW Jr (2017). Recurrence of Granular Corneal Dystrophy Type 1 After Phototherapeutic Keratectomy, Lamellar Keratoplasty, and Penetrating Keratoplasty in a Single Population. Cornea, 36(10), 1227–1232. https://doi.org/10.1097/ICO.0000000000001303

12 Uit de Bosch LM, Ormonde S & Misra SL (2016). Visual Outcomes Following Deep Anterior Lamellar Keratoplasty in Granular Corneal Dystrophy Types 1 and 2. Korean journal of ophthalmology: KJO, 30(6), 481–482. https://doi.org/10.3341/kjo.2016.30.6.481

Case 6 - March 2021

ORBITAL SCHWANNOMA

A 36-year-old woman presented with a lump on the right upper eyelid for 3 months.

Presented by
Evaggelos Lokovitis, MD, FEBOphth

Edited by
Penelope Burle de Politis, MD

Case History

A 36-year-old Caucasian woman was referred for a progressively enlarging painless engorgement at the medial corner of the upper right lid for 3 months. She had sought an ophthalmologist 6 months before, for disturbances in bilateral vision, with no significant findings. On examination, uncorrected visual acuity (UCVA) was 10/10 on each eye, but the complaint of poor stereopsis persisted. Fundoscopy was bilaterally normal. Intraocular pressure was 19 mmHg on the right and 14 on the left eye. There were neither signs of inflammation, nor ulcers or scars. A slight lateral deviation was noticeable on the right eye. Exophthalmometry was negative, as was the flashlight test for relative afferent pupillary defect. Palpation of the eyelid denoted a soft, slightly mobile mass, painless on retropulsion, with no detectable pulse or bruit. Imaging investigation with MRI of the skull displayed an orbital mass of rather homogenous hyperintensity, superomedial to the ocular globe, not disrupting contiguous structures (**Figures 1 and 2**).

Figure 1: Color slit-lamp photograph of the right eye displaying pseudophakia and a slightly irregular pupil.

Figure 2: Color fundus photograph of the right eye (EIDON true-color confocal scanner®) showing a mild vitreous hemorrhage at the superotemporal retinal periphery.

Surgery for excisional biopsy was indicated and the surgical approach disclosed a well-circumscribed, encapsulated tumor, thoroughly resectable, not compromising adjacent structures. The lesion measured 2.7 X 1.7 cm and had a complete smooth, translucid capsule and slightly lobulated structure. Vascularization was prominent, but there was no evident bleeding nor macroscopic signs of necrosis (**Figure 3**).

Under microscopic examination, the neoplasm consisted predominantly of bundles of spindle cells (highly cellular, solid areas), with elongated, deep-colored nuclei, alternated with areas of modest cellularity without visible nuclei (non-pigmented), in an irregular arrangement over a substrate of loose myxoid connective tissue.

Figure 3: Macroscopic aspect of the resected mass, a cone-shaped tumor with a whitish-colored outline and elastic texture, measuring 2.7cm in the largest axis.

Additional History

The patient had delivered a child one year before. She also had a history of surgery for strabismus sometime during childhood. There were no other lumps in any part of her body and her remaining medical records were unremarkable.

Differential Diagnosis

- orbital schwannoma
- neurofibroma
- malignant peripheral nerve sheath tumors
- meningioma
- cavernous hemangioma
- lymphangioma
- fibrous histiocytoma
- lymphoma
- dermoid cyst
- hemangiopericytoma
- pleomorphic adenoma of the lacrimal gland

Definitive diagnosis of an orbital neoplasm requires biopsy. It is nearly impossible to differentiate between these tumors based on clinical exam alone. Cellular architecture alternating two distinct patterns — solid cellular areas and areas of loose microcystic tissue — is typical of schwannomas.

Discussion and Literature

Schwannoma, also called neurilemmoma, is a benign neoplasm, relatively rare, originating from the Schwann cells that form the myelin sheath around peripheral nerves. It may occur anywhere in the body, but the usual site of occurrence is the head or neck. In the ophthalmic area, it usually presents in the orbit. Schwannomas occur mainly in individuals aged between 20 and 50 years and account for only 1–2% of all orbital tumors. There is no side or gender predilection.

Orbital schwannomas most commonly arise from the supratrochlear or supraorbital branch of the trigeminal nerve, although identification of the nerve of origin is not always possible. Due to their indolent behavior, such masses may grow over the course of many years, until complications arise in the form of compression, dislocation or disruption of adjacent structures, usually manifesting by exophthalmos, optic neuropathy, diplopia, anterior orbital mass or sinusitis. Tumor with intracranial extension may give rise to neurologic repercussions.

Although computerized tomography and ultrasonography may be of aid, magnetic resonance imaging is the method of choice for suspected orbital schwannomas, because of its high sensitivity, especially when contrast is used for signal enhancement. In a large review of 62 confirmed cases over 7 years, the cone-shaped lesions were the most frequent, followed by dumbbell-shaped, oval and round lesions. The superior aspect of the orbit was the most common site, followed by the medial superior and the orbital apex.

Diagnostic certainty is attained through excision of the tumor and histopathologic analysis. Surgical resection must be performed through the most accessible, least invasive route, under general anesthesia. For lesions presenting anteriorly, a transconjunctival or transcutaneous approach is the access of choice. Schwannomas confined to the orbit can usually be entirely removed, with good outcomes. Larger masses extending out of the orbit need a multispecialty procedure. The microscopic arrangement of schwannomas typically displays two distinct patterns: a fibrillary, elongated, highly cellular tissue type, called “Antoni A”, and a soft mucinous background, known as “Antoni B”. Immunohistochemistry is a useful complement when pathology is doubtful, notably for the expression of protein S100.

In most cases, schwannoma usually manifests as a single neoplasm. The presence of multiple growths is usually indicative of neurofibromatosis type 1 or 2. Despite the unlikelihood of a schwannoma in the orbit, considering it in the differential diagnosis of well-circumscribed, slow-growing tumors is of ultimate importance, since total removal, with preservation of orbital anatomy, is possible even for long-standing disease. Radiotherapy is an option for cases not allowing full surgical elimination. The recurrence rate after complete excision is low and malignant transformation is extremely rare, but long-term follow-up is advised.

Keep in mind

- ✓ Any unilateral engorgement in the orbital area should be examined and managed by a qualified professional.
- ✓ Orbital tumors vary widely in nature. Proper investigation can allow early treatment and better prognosis.
- ✓ Schwannomas of the orbit may have aesthetic and/or functional implications, but surgical intervention can be curative in most cases.

References

1. Chen MH & Yan JH (2019). Imaging characteristics and surgical management of orbital neurilemmomas. International journal of ophthalmology, 12(7), 1108–1115. https://doi.org/10.18240/ijo.2019.07.09.
2. Konrad A & Thiel HJ (1984). Schwannoma of the orbit. Ophthalmologica. Journal international d'ophtalmologie. International journal of ophthalmology. Zeitschrift fur Augenheilkunde, 188(2), 118–127. https://doi.org/10.1159/000309352.
3. Rootman J, Goldberg C & Robertson W (1982). Primary orbital schwannomas. The British journal of ophthalmology, 66(3), 194–204. https://doi.org/10.1136/bjo.66.3.194.
4. Wang Y & Xiao LH (2008). Orbital schwannomas: findings from magnetic resonance imaging in 62 cases. Eye (London, England), 22(8), 1034–1039. https://doi.org/10.1038/sj.eye.6702832.
5. Yong KL, Beckman TJ, Cranstoun M & Sullivan TJ (2020). Orbital Schwannoma-Management and Clinical Outcomes. Ophthalmic plastic and reconstructive surgery, 36(6), 590–595. https://doi.org/10.1097/IOP.0000000000001657.
6. Kim KS, Jung JW, Yoon KC, Kwon YJ, Hwang JH & Lee SY (2015). Schwannoma of the Orbit. Archives of craniofacial surgery, 16(2), 67–72. https://doi.org/10.7181/acfs.2015.16.2.67.
7. Wippold FJ 2nd, Lubner M, Perrin RJ, Lämmle M & Perry A (2007). Neuropathology for the neuroradiologist: Antoni A and Antoni B tissue patterns. AJNR. American journal of neuroradiology, 28(9), 1633–1638. https://doi.org/10.3174/ajnr.A0682.
8. Bagagli SA, Meduri A, Inferrera L, Gennaro P, Gabriele G, Polito E, Fruschelli M, Lorusso N, Tarantello A & Mazzotta C (2020). Intraconal Retro-Orbital B-Type Antoni Neurinoma Causing Vision Loss. The Journal of craniofacial surgery, 31(6), e597–e599. https://doi.org/10.1097/SCS.0000000000006726.
9. Chang BY, Moriarty P, Cunniffe G, Barnes C & Kennedy S (2003). Accelerated growth of a primary orbital schwannoma during pregnancy. Eye (London, England), 17(7), 839–841. https://doi.org/10.1038/sj.eye.6700475.
10. Sweeney A, Burkat CN, Stewart K & Lee V. American Academy of Opthalmology. Orbital schwannoma. www.eyewiki.org/Orbital_schwannoma.

Case 7 - April 2021

ANGIOID STREAKS

A 44-year-old man presented with bilateral progressive visual loss for 6 months, gradually worsening on the right eye over the last 4 weeks.

Presented by
Presented by Solon Asteriades, MD, FRCS

Edited by
Penelope Burle de Politis, MD

Case History

A 44-year-old Caucasian man presented with slowly progressive visual loss in both eyes, felt over a period of 6 months, worsening on the right during the last 4 weeks. He lives in a small village, with difficult access to ophthalmological care. On the first examination (2016), corrected distance visual acuity (CDVA) was 2/10 on the right (RE) and 7/10 on the left (LE). Biomicroscopy and tonometry were normal. Fundoscopy revealed signs of peripapillary chorioretinal degeneration and macular pigmentary changes bilaterally. Jagged irregular reddish lines of variable caliber, resembling retinal vessels, were visible radiating from the optic disc, though subretinally located (under the true vessels). A hard exudate was noticed in the right macula, raising the suspicion of choroidal neovascularization (**Figure 1**).

Multimodal imaging investigation with fundus fluorescein angiography (FFA) and optical coherence tomography (OCT) was conducted. FFA revealed radial peripapillary angioid bands on both sides, of varying fluorescence, from hyper to hypofluorescent, depending on the status of the RPE and Bruch's membrane. There was also subfoveal leakage (hyperfluorescent lesion) indicative of choroidal neovascularization on the right eye. OCT revealed subfoveal hyper-reflectivity with fluid in the RE, corresponding to the "leaky" area on the FFA, confirming the diagnosis of choroidal neovascular membrane (CNVM). The bands appeared as a combination of RPE degeneration and hyper-reflective thickness, also depending on the status of the RPE and Bruch's membrane. (**Figures 2 and 3**). OCT angiography (OCT-A) was not conducted at the time, since it was not available.

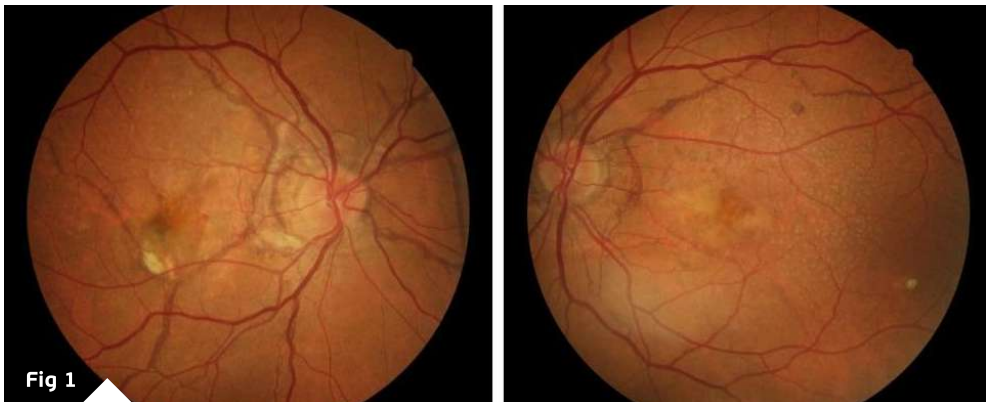

Figure 1: digital color fundus photographs showing posterior pole fundus degeneration with irregular, jagged, dark lines, radiating from the optic disc on both eyes, more pronounced on the right.

Figure 2: Late phase FFA showing peripapillary and macular bands of hyper- and hypofluorescence, consistent with a disruption in Bruch's membrane and the RPE. On the RE, there is a subfoveal hyperfluorescent lesion, indicative of leakage and corresponding to a CNVM.

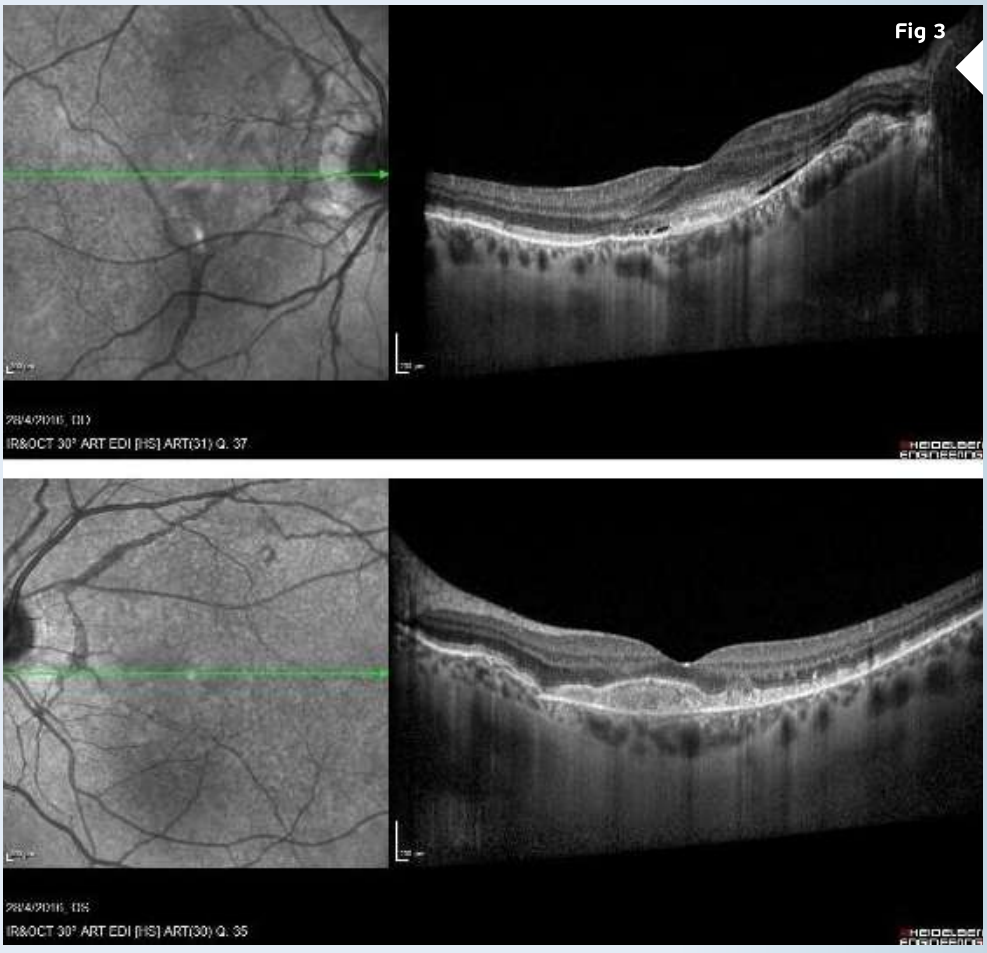

Figure 3: OCT shows peripapillary and subfoveal hyper-reflectivity on the RE, corresponding to the lesion, as well as macular subretinal fluid. Hyper-reflectivity is also observed on the LE, without the presence of fluid.

Based on the clinical and image findings, the diagnosis of angioid streaks with submacular choroidal neovascularization was established. Considering the ophthalmological status, the patient was started on intravitreal injection of anti-VEGF (bevacizumab) on the right eye only and scheduled for follow-up every 4 weeks. At 20 months of follow-up, with regular injections on the right, vision on the left eye decreased, too. Further multimodal imaging investigation with OCT and OCT-A (ultimately available) was conducted (**Figure 5 top row**), revealing CNVM also on the LE, so treatment was started on that eye as well.

Additional History

Even though phenotype was suggestive of acromegaly for both the patient and close family members, extensive clinical investigation was inconclusive for systemic diseases. The patient has been followed-up for 5 years now and treated with intravitreal injections of anti-VEGF every 2 to 3 months, depending on visual status and signs of subretinal fluid or active neovascularization. Visual acuity (CDVA) has fluctuated from 4/10 to 6/10 on the right eye and 2/10 to 7/10 on the left. Present CDVA is 4/10 (right eye) and 6/10 (left eye). Present OCT shows bilateral macular hyper-reflectivity (**Figure 4**). With the advent of OCT-A, choroidal neovascularization (CNV) could be better demonstrated. OCT-A images depict persistent, prominent and possibly growing neovascularization (**Figure 5**), granting the need for continuous follow-up and frequent treatment.

Figure 4: Recent OCT showing increased subfoveal reflectivity, partially due to scarring on the RE, with some possible intraretinal fluid. The picture on the LE remains stable with no fluid.

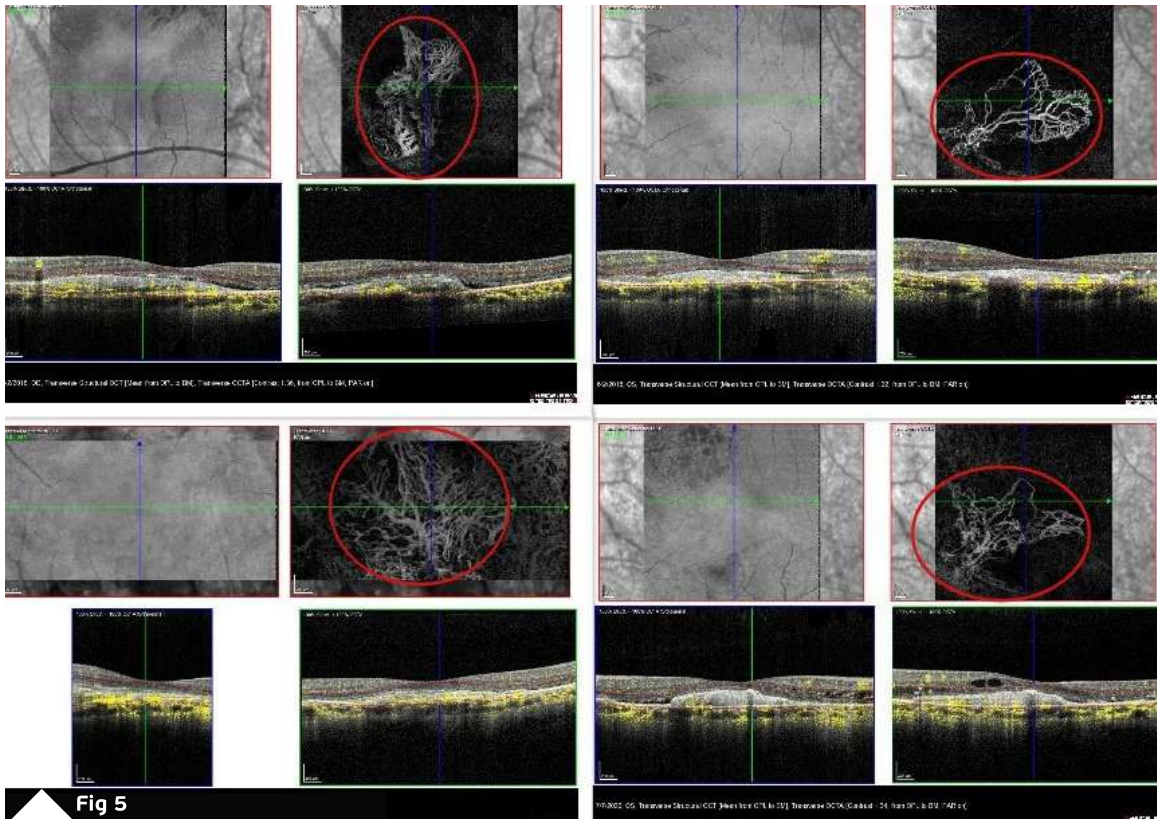

Figure 5:
Top row: RE and LE OCT-A in 2018, revealing the presence of subretinal neovascular membrane (SRNVM) on the RE and confirming the lesion also on the LE. **Bottom row**: RE and LE OCT-A in 2021. Notice the apparent expansion of the SRNVM, particularly on the RE, despite the relatively stable visual status.

Differential Diagnosis

- normal retinal vessels
- lacquer cracks (pathological myopia)
- reticular dystrophy of the RPE
- subretinal tracks (due to ophthalmomyiasis interna)
- subretinal bands (due to long-standing or operated retinal detachment)
- bilateral disciform scars in wAMD
- presumed ocular histoplasmosis syndrome

Pathologic and family history, ocular and/or systemic associations and multimodal imaging are necessary for the proper diagnosis and management of angioid streaks. Bilateral presentation (though with asymmetric fundus changes), location behind the equator, macular involvement and abrupt tapering of the vessel-like bands at their distal end (towards periphery) are characteristic of angioid streaks.

Discussion and Literature

Angioid streaks, also called Knapp's streaks or Knapp's striae, are crack-like dehiscences of a degenerated and calcified Bruch's membrane, typically forming around the optic disc and radiating from it. Aspect is usually linear or resembling blood vessels, hence the term angioid. Uncomplicated angioid streaks are asymptomatic. Number, width and length of the breaks may increase with age. Central visual impairment results from foveal involvement. Due to the fragility in Bruch's membrane, subretinal bleeding may occur even after trivial trauma, and choroidal neovascularization (CNV) is a major complication, occurring in up to 86% of cases, with bilateral involvement in up to 71%. The age of onset is variable, but the condition most commonly presents in the mid-fifties. Caucasian individuals are most frequently affected. There is no gender predilection.

Angioid streaks may be idiopathic (up to 50% of cases) or associated with systemic diseases, such as pseudoxanthoma elasticum (PXE), Ehlers-Danlos syndrome, acromegaly, Paget's disease of bone, hemoglobinopathies like Sickle cell anemia, different collagen disorders. The most important systemic association is PXE (Gronblad-Strandberg syndrome), an autosomal recessive disease featuring calcification and fragmentation of elastic tissues. Examination of family members may help find syndromic cases.

Multimodal retinal imaging is of primal importance in diagnosing, evaluating, and monitoring the disease. Subtle angioid streaks may be taken for regular vessels, especially in eyes with foggy media. Fundus fluorescein angiogram (FFA) shows window defects in the areas of angioid streaks and is very important to detect CNV. Angioid streaks may display hyperfluorescence, hypofluorescence or a mixed pattern. Optical coherence tomography (OCT) reveals the retinal/subretinal/sub-RPE changes of CNV and hyper-reflectivity at the Bruch's membrane level due to calcification. EDI (enhanced depth imaging) OCT of eyes with angioid streaks and CNV usually reveals a thinner choroid when compared to angioid streaks without CNV. OCT-angiography (OCT-A) outlines CNV related to the angioid streak. On indocyanine green angiography (ICGA), the streaks are usually better delineated as hyperfluorescent lesions.

In cases with subretinal hemorrhage and /or exudation, FFA should be performed to rule out CNV. If CNV is absent, the hemorrhage usually resolves on its own. If CNV is detected, intervention is mandatory. The management options have historically included laser photocoagulation, photodynamic therapy (PDT), transpupillary thermotherapy (TTT), and macular translocation surgery. Anti-vascular endothelial growth factor (anti-VEGF) agents (ranibizumab, aflibercept, bevacizumab) halt both macular and juxta-papillary CNV, rapidly improving retinal anatomy and increasing or stabilizing visual acuity, and are the mainstay of ocular treatment. However, recurrence is common and serial treatment is often necessary.

Keep in mind

- ✓ Angioid streaks are usually asymptomatic and do not need treatment, but prevention of any kind of ocular trauma is advised.
- ✓ Patients presenting with angioid streaks should be investigated for systemic associations.
- ✓ Follow-up for early detection of subretinal bleeding is required, since untreated choroidal neovascularization compromises visual prognosis.

References

1. Tripathy K & Quint JM. Angioid Streaks. [Updated 2021 Feb 14]. In: StatPearls [Internet]. Treasure Island (FL): StatPearls Publishing; 2021 Jan. https://www.ncbi.nlm.nih.gov/books/NBK538151
2. Chatziralli I, Saitakis G, Dimitriou E, Chatzirallis A, Stoungioti S, Theodossiadis G & Theodossiadis P (2019). ANGIOID STREAKS: A Comprehensive Review From Pathophysiology to Treatment. Retina (Philadelphia,Pa.),39(1),1–11. https://doi.org/10.1097/IAE.0000000000002327
3. Goel S, Gupta I, Mishra S, Garg B, Saurabh K & Roy R (2020). Multimodal imaging of angioid streaks. GMS ophthalmology cases, 10, Doc38. https://doi.org/10.3205/oc000165
4. Chapron T, Mimoun G, Miere A, Srour M, El Ameen A, Semoun O & Souied EH (2019). Optical coherence tomography angiography features of choroidal neovascularization secondary to angioid streaks. Eye (London, England), 33(3), 385–391. https://doi.org/10.1038/s41433-018-0213-1
5. Lekha T, Prasad HN, Sarwate RN, Patel M & Karthikeyan S (2017). Intravitreal Bevacizumab for Choroidal Neovascularization Associated with Angioid Streaks: Long-term Results. Middle East African journal of ophthalmology, 24(3), 136–142. https://doi.org/10.4103/meajo.MEAJO_17_17
6. Martinez-Serrano MG, Rodriguez-Reyes A, Guerrero-Naranjo JL, Salcedo-Villanueva G, Fromow-Guerra J, García-Aguirre G, Morales-Canton V & Velez-Montoya R (2016). Long-term follow-up of patients with choroidal neovascularization due to angioid streaks. Clinical ophthalmology (Auckland, N.Z.), 11, 23–30. https://doi.org/10.2147/OPTH.S118016
7. Katagiri S, Negishi Y, Mizobuchi K, Urashima M, Nakano T & Hayashi T (2017). ABCC6 Gene Analysis in 20 Japanese Patients with Angioid Streaks Revealing Four Frequent and Two Novel Variants and Pseudodominant Inheritance. Journal of ophthalmology, 2017, 1079687. https://doi.org/10.1155/2017/1079687

Case 8 - May 2021

OCULAR CICATRICIAL PEMPHIGOID

A 79-year-old woman presented with pain, redness and photophobia on the right eye.

Presented by
Presented by Dimitrios Sakellaris, MD

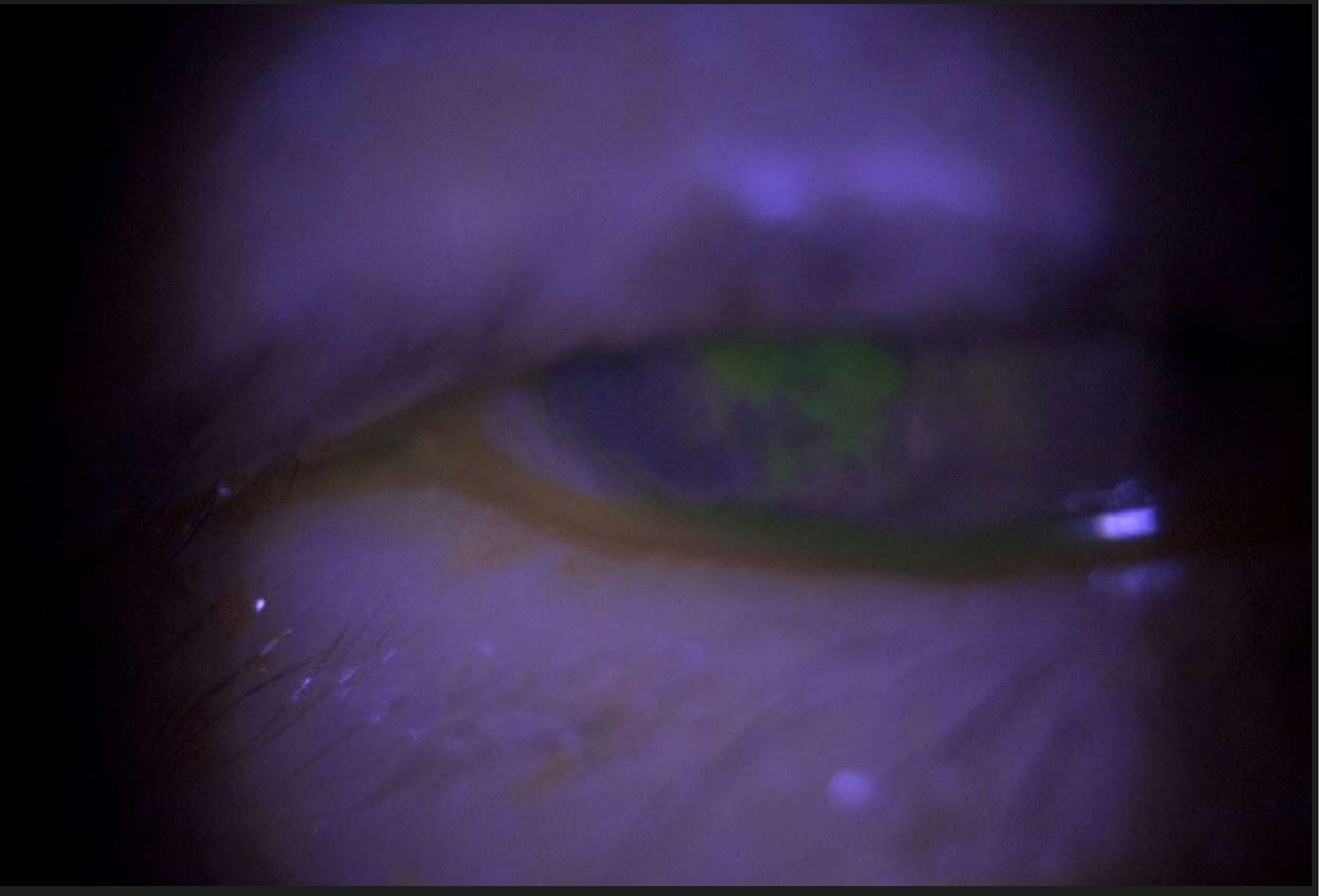

Edited by
Penelope Burle de Politis, MD

Case History

A 79-year-old Caucasian woman presented with pain, tearing, photophobia and redness on the right eye (RE) for about a month, worsening in the last couple of days. She had seen several ophthalmologists and tried different drug regimens without any significant improvement. The pain was intense, continuous, causing strong blepharospasm and requiring powerful analgesics. Upon emergency examination, a central corneal ulcer of 4 X 5 mm was detected, with an adjacent area of corneal thinning and neovessels. Anterior chamber reaction was graded as 2+ (**Figure 1**). The left eye (LE) was slightly red but displayed no other signs of active inflammation. She was started on topical ceftazidime, moxifloxacin and vancomycin for the RE, with significant improvement noticed after 3 days.

Long-term control of surface inflammation was achieved with sparse administration of high-dose corticosteroid drops and lubrication on the RE and low-dose corticosteroid drops on the LE. The patient underwent uneventful phacoemulsification for dense cataract on the RE, but vision remained low, due to age-related macular degeneration and corneal scarring (**Figure 2**). Best corrected distance visual acuity (BCDVA) achieved after surgery was finger count. BCDVA on the LE is 6/10 and the patient is scheduled for cataract surgery on that eye.

Figure 1: Biomicroscopy photograph of the right eye displaying a central corneal ulcer.

Figure 2: Biomicroscopy photograph of the right eye showing corneal scarring.

Additional History

The patient had a long history of relapsing ocular inflammation, with little or no response to topical lubricants and mild corticosteroid drops. Symblepharon was evident on the right, while on the left there was merely a shallow lower fornix (Figure 3). Based on history and clinical findings, a suspicion for ocular cicatricial pemphigoid (OCP) was raised. A conjunctival biopsy was performed on the right, at the site of more prominent fibrosis, rendering a negative result, coming out simply as “chronic unspecified conjunctivitis”. A second biopsy was conducted, the sample sent to another laboratory, this time with an affirmative histopathologic diagnosis of OCP.

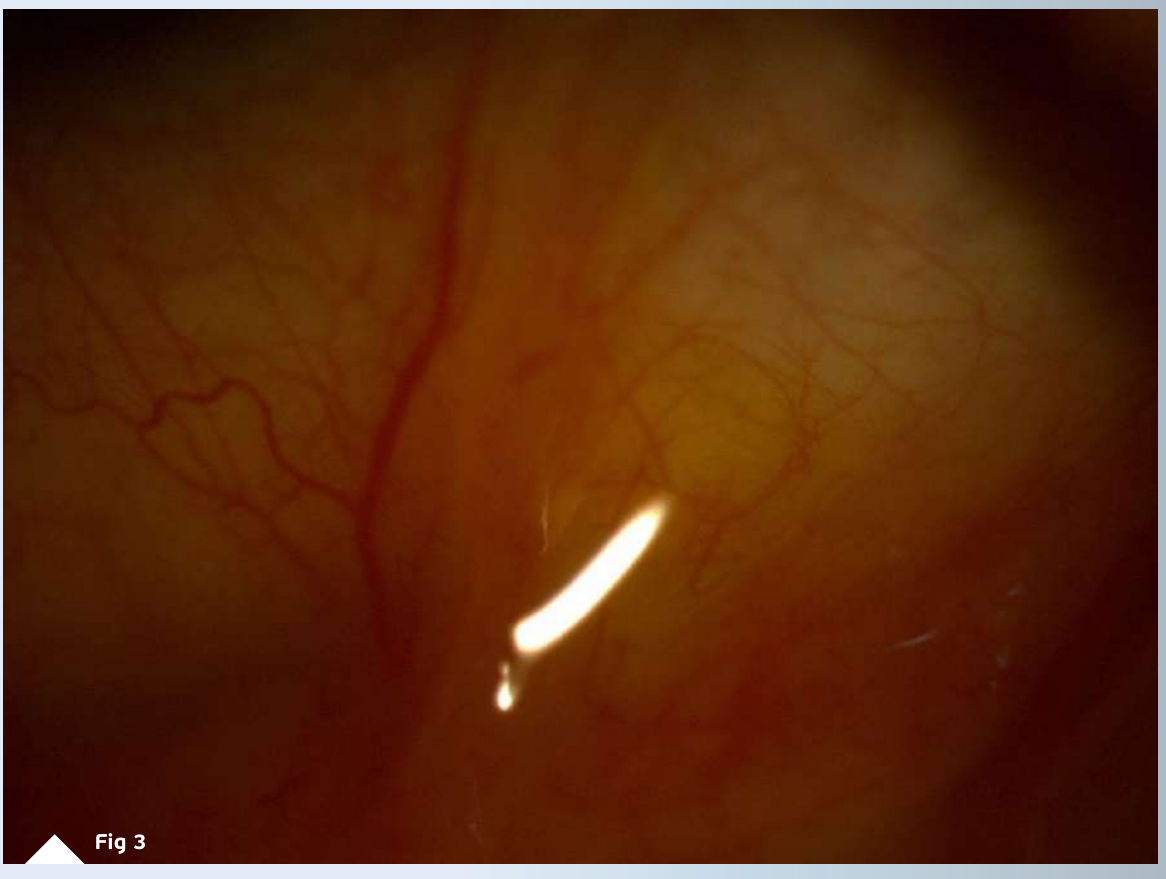

Figure 3: Biomicroscopy photograph of the right eye illustrating a symblepharon at the lower fornix.

Differential Diagnosis

- ocular cicatricial pemphigoid
- Stevens-Johnson syndrome
- dry eye syndrome
- history of adenoviral conjunctivitis
- atopic keratoconjunctivitis
- medicamentosa (from topical glaucoma and anti-herpetic medication)
- chemical burn
- trachoma
- radiation exposure
- toxic epidermal necrolysis
- graft-versus-host disease
- neoplasia

The differential diagnosis of OCP encompasses all forms of asymmetric bilateral chronic conjunctivitis with conjunctival scarring. A common confounder is medicamentosa, which induces pseudopemphigoid, a condition identical to OCP. A distinguishing feature is that symblepharons of OCP are progressive. Definite distinction is made by conjunctival biopsies showing linear staining of the basement membrane.

Discussion and Literature

Ocular cicatricial pemphigoid (OCP) is a form of mucous membrane pemphigoid (MMP) presenting as a chronic, relapsing-remitting, bilateral conjunctivitis, leading to conjunctival scarring. A heterogeneous group of autoimmune subepithelial blistering disorders, MMP primarily affects orificial mucous membranes (conjunctiva, nasal cavity, trachea, mouth, oropharynx, esophagus, genitalia and anus), causing erosions, blisters and strictures. In some cases, there is also skin involvement.

Ocular cicatricial pemphigoid is present in 60% to 70% of patients with MMP. Considered a rare disease, with an estimated incidence of 1 per 10,000 to 50,000, OCP affects predominantly females (2:1 over males). The age of onset is around 60 years of age or older, though in studies age ranges from 20 to 91 years. There is no racial predilection. When unresponsive or left untreated, OCP progresses to ocular surface failure, inflammatory and infectious complications, corneal opacification and permanent vision loss.

The pathophysiological mechanism of OCP is a type 2 hypersensitivity reaction to the basal epithelial membrane of the conjunctiva. Like most autoimmune diseases, environmental factors and genetic susceptibility are believed to play a role in initiating a loss of tolerance to one or more components of the basal membrane zone (BMZ).

Conjunctival biopsy with direct immunofluorescence (DIF) is the most reliable method and the gold standard to confirm diagnosis, though 20% to 40% of patients with clinically evident OCP may have a negative biopsy. When positive, there is a linear antibody deposition in the epithelial BMZ. Histological analysis can help differentiate from neoplasia if DIF is inconclusive. Hematoxylin-eosin (H&E) often displays an inflammatory stain pattern. Periodic acid–Schiff (PAS) stains show a decrease in goblet cells, while in Giemsa stains there is an increased mast cell population.

Management of OCP is aimed at controlling the immune-mediated inflammatory disease, preventing fibrosis, and managing ocular surface disruption. Early diagnosis and appropriate treatment are of paramount importance and require a high level of expertise as the condition can be extremely challenging, even for experienced specialists. Systemic immunosuppression is sometimes required to control inflammatory reaction and halt fibrosis, preventing progression to more advanced stages. Topical treatment is useful for managing surface inflammation and providing symptomatic relief.

Keep in mind

- ✓ OCP is a challenging surface disorder, both to diagnose and to treat.
- ✓ A thorough history and careful slit-lamp examination must be added to conjunctival biopsy for precise diagnosis. A second biopsy may be needed when history and ocular findings point to OCP and a first sample comes out negative.
- ✓ Management of OCP requires prompt and attentive intervention, in order to prevent surface scarring, severe lid changes and loss of vision.

References

1. Schonberg S & Stokkermans TJ. Ocular Pemphigoid. [Updated 2021 Feb 13]. In: StatPearls [Internet]. Treasure Island (FL): StatPearls Publishing; 2021 Jan-. Available from: https://www.ncbi.nlm.nih.gov/books/NBK526100/
2. Tolaymat L & Hall MR. Cicatricial Pemphigoid. [Updated 2020 Sep 12]. In: StatPearls [Internet]. Treasure Island (FL): StatPearls Publishing; 2021 Jan-. Available from: https://www.ncbi.nlm.nih.gov/books/NBK526120/
3. Vazirani J, Donthineni PR, Goel S, Sane SS, Mahuvakar S, Narang P, Shanbhag SS & Basu S (2020). Chronic cicatrizing conjunctivitis: A review of the differential diagnosis and an algorithmic approach to management. Indian journal of ophthalmology, 68(11), 2349–2355. https://doi.org/10.4103/ijo.IJO_604_20
4. Branisteanu DC, Stoleriu G, Branisteanu DE, Boda D, Branisteanu CI, Maranduca MA, Moraru A, Stanca HT, Zemba M & Balta F (2020). Ocular cicatricial pemphigoid (Review). Experimental and therapeutic medicine, 20(4), 3379–3382. https://doi.org/10.3892/etm.2020.8972
5. Stan C, Diaconu E, Hopirca L, Petra N, Rednic A & Stan C (2020). Ocular cicatricial pemphigoid. Romanian journal of ophthalmology, 64(2), 226–230. https://www.ncbi.nlm.nih.gov/pmc/articles/PMC7339695/
6. Georgoudis P, Sabatino F, Szentmary N, Palioura S, Fodor E, Hamada S, Scholl H & Gatzioufas Z (2019). Ocular Mucous Membrane Pemphigoid: Current State of Pathophysiology, Diagnostics and Treatment. Ophthalmology and therapy, 8(1), 5–17. https://doi.org/10.1007/s40123-019-0164-z
7. https://eyewiki.aao.org/Ocular_Cicatricial_Pemphigoid

Case 9 - August 2021

BIRDSHOT CHORIORETINOPATHY

A 53-year-old woman presented with gradual blurring of vision for 6 months.

Presented by
Paris Tranos, MD, PhD, ICOphth, FRCS

Edited by
Penelope Burle de Politis, MD

Case History

A 53-year-old Caucasian woman presented with a complaint of progressively blurred vision over the course of 6 months and persistent floaters for 3 years, predominantly in her right eye. Her past medical history was unremarkable and systemic examination was negative for joint, skin, chest or bowel involvement.

Upon ophthalmic examination, corrected distance visual acuity (CDVA) was 4/10 and 6/10 in the right eye (RE) and the left eye (LE) respectively. There were no signs of inflammatory cells in the anterior chamber but there was moderate vitritis in both eyes. Intraocular pressure was within normal limits bilaterally. Fundoscopy revealed bilateral, multiple, scattered, yellow-white choroidal lesions predominantly located around the optic disc and mild disc swelling more noticeable in the RE (**Figure 1**). Fluorescein angiography showed bilateral diffuse vasculitis and extensive stippled hyperfluorescence resulting from fluorescein leakage at the RPE level, in addition to bilateral "hot" disc and leakage at the macula (**Figure 2, top**). Indocyanine green (ICG) demonstrated bilateral, multiple hypofluorescent areas, corresponding to the yellow-white lesions noticed during fundoscopy (**Figure 2, bottom**). OCT showed bilateral accumulation of intraretinal and subretinal fluid at the macula (**Figure 3**).

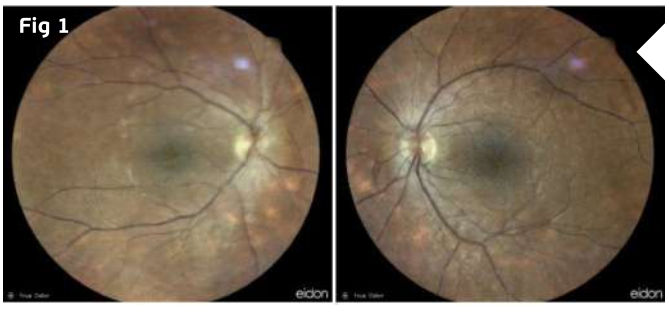

Figure 1: Biomicroscopy photograph of the right eye displaying a central corneal ulcer.

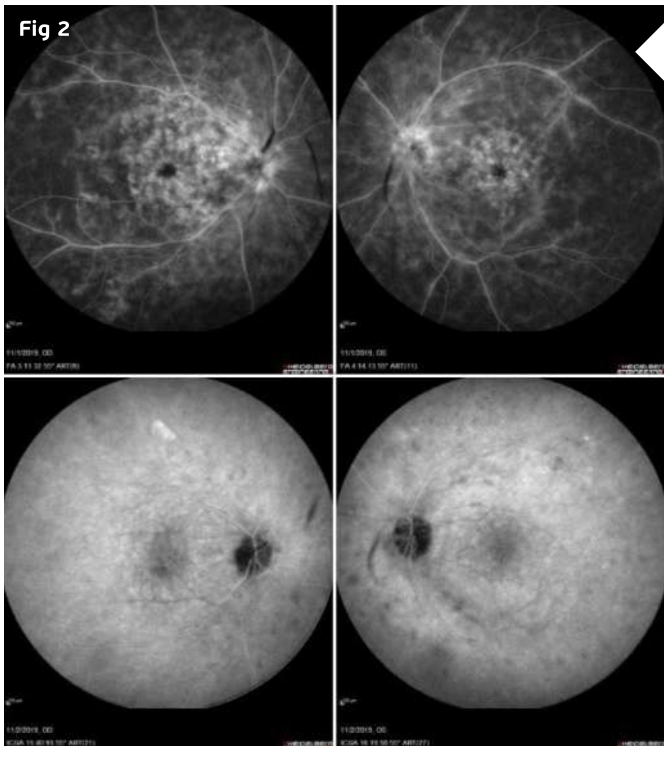

Figure 2: Fluorescein angiography images demonstrating bilateral diffuse vasculitis and extensive stippled hyperfluorescence, in addition to bilateral "hot" disc and fluorescein leakage at the macula (top). Indocyanine green showing bilateral, multiple hypofluorescence areas, corresponding to the yellow-white lesions noticed during fundoscopy (bottom).

Differential Diagnosis

- birdshot chorioretinopathy (BCR)
- acute posterior multifocal placoid pigment epitheliopathy (APMPPE)
- multiple evanescent white dot syndrome (MEWDS)
- multifocal choroiditis and panuveitis (MCP)
- punctate inner choroidopathy (PIC)
- tuberculosis
- syphilis
- primary ocular histoplasmosis syndrome (POHS)
- sarcoidosis
- Vogt-Koyanagi-Harada (VKH) syndrome
- intraocular lymphoma

Additional History

A complete laboratory workup was carried out, rendering a positive result for the HLA-A29 antigen, thus confirming the diagnosis of birdshot chorioretinopathy.

Baseline visual fields test (VFT) and 30 Hz flicker electroretinogram (ERG) were conducted and systemic therapy with methylprednisolone was initiated. Following 2 months of steroid treatment, despite functional and anatomical improvement, there was sustained vasculitis with residual macular edema in both eyes (Figure 3, 2nd line). Subcutaneous biweekly injections of adalimumab (monoclonal antibody which inactivates tumor necrosis factor-alpha) were added to the treatment regimen. One month later, there was complete resolution of the cystoid macular oedema (CMO) in the RE and presence of only minimal intraretinal fluid on the left (Figure 3, 3rd line).

Treatment with adalimumab was continued for 2 years, resulting in complete remission of inflammation and absence of CMO recurrence during the follow-up period. Patient's visual acuity improved to 7/10 and 9/10 in the right and the left eye respectively and repeat VFT and 30 Hz flicker ERG confirmed clinical stability, allowing for tapering of the monoclonal antibody to monthly injections.

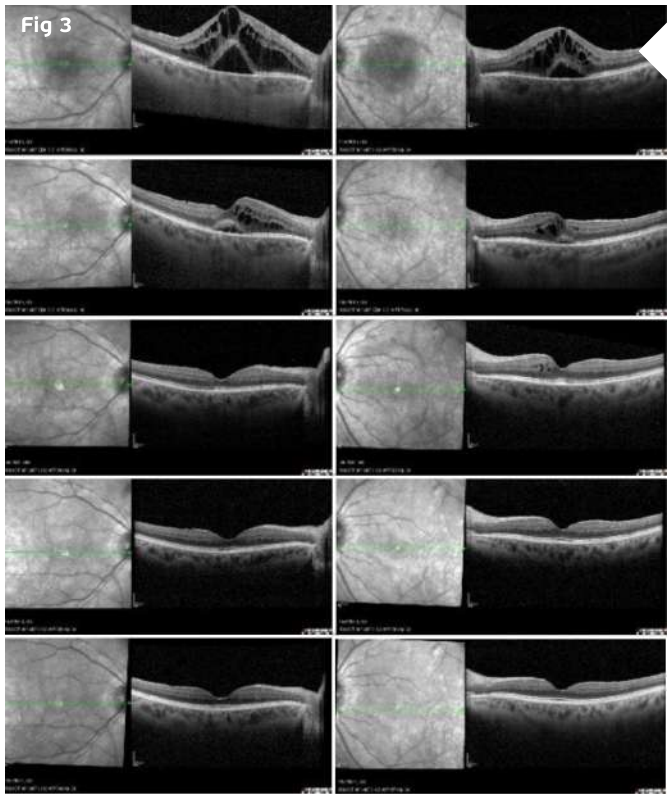

Figure 3: SD-OCT showing bilateral macular edema (RE on the right, LE on the left) at the time of diagnosis (top line), at 2 months following treatment with systemic steroids (2nd line), 1 month after initiation of adalimumab (3rd line), 1 year later (4th line) and 2 years later (bottom line).

Discussion and Literature

Birdshot chorioretinopathy (BCR) is one of the white dot syndromes, in which the common defining clinical feature is the presence of multiple white lesions located at the deeper levels of the retina and choroid. BCR is a rare (estimated 1 to 5 cases per 500,000) form of chronic, bilateral, probably autoimmune posterior uveitis with a distinguishing clinical phenotype and a strong association with HLA-A29. The disease predominantly affects middle-aged individuals (age 40 to 60 years), females more often than males, with an apparent predilection for those with Northern European Caucasian ancestry.

There is continuing debate as to whether BCR is primarily a disease of the choroid or the retina. BCR typically presents as a white, painless eye, with minimal anterior segment inflammation, but with vitritis, retinal vascular leakage, and cream-colored spots at the level of the retinal pigment epithelium (RPE) or deeper retinal layers. The indistinct appearance of the lesions, lack of associated RPE pigmentary changes, and the angiographic features of the lesions suggest that these lesions are located in the deep choroidal stroma and are associated with the choroidal veins. The retinal and choroidal changes are not necessarily concordant. Histological studies show massive infiltration of blood leukocytes, mostly T lymphocytes CD4 (“T helper” cells) and CD8 (“cytotoxic” T cells), at various levels of the choroid and retina layers, prelaminar optic nerve head, and surrounding retinal blood vessels, suggesting a primary disease of the choroid with secondary involvement of the retina.

Typically, the onset of visual symptoms involves one eye, but over time the other eye is also affected. Initial manifestations are mild, often resulting in delayed treatment and permanent ocular damage, particularly when visual acuity is not affected. Symptoms may be common to other white dot syndromes and include photopsia, floaters, decreased or blurred vision, in the early stages. Later symptoms include glare, photophobia, nyctalopia, metamorphopsia, dyschromatopsia, diminished contrast sensitivity, small scotomata, reduced peripheral vision, and decreased depth perception. Fundus examination reveals vitreous inflammation (in up to 83 % of cases) associated with multiple yellow-white, creamy, ovoid choroidal spots, initially observed inferior to the optic nerve head and radiating nasally. Lesions are usually 500 to 1500 micrometers in diameter, with a typical "birdshot" appearance and distribution: “cream-colored, irregular or elongated, with indistinct borders, the long axis of which is radial to the optic disk.” As the disease progresses, the lesions become more confluent and linear around the veins, eventually becoming more atrophic in appearance. There is no consistently associated systemic disease.

Multimodal imaging is cardinal not only for diagnosing but also for monitoring response to therapy and disease remission. Fluorescein angiography (FA) often reveals diffuse vasculitis and leaking from the optic nerve head and the macula. Indocyanine green angiography usually shows multiple hypofluorescent areas at the posterior pole and periphery, confirming choroidal stroma involvement. SD-OCT is useful in demonstrating macular edema, the leading cause of visual loss in patients with BCR. Enhanced depth imaging (EDI) OCT is a non-invasive imaging modality which provides detailed imaging of the choroid and allows accurate measurement of its thickness. Depending on the stage of the disease, choroidal thickness is either increased (in early disease) or decreased (in late, poorly controlled disease). Visual field assessment is a useful modality for monitoring disease activity and response to treatment in BCR, although extensive peripheral visual field deterioration may coexist with relatively well-preserved central visual acuity. Electroretinography is superior to visual field testing for evaluating disease activity and therapeutic response. Changes in the 30 Hz cone flicker implicit time are the most sensitive and consistently affected ERG parameter, making it an extremely valuable tool. Restoration of flickering implicit time is a common finding following disease improvement.

Over the years, a number of diagnostic criteria have been proposed for BCR. Essential criteria are (1) bilateral disease; (2) three or more characteristic birdshot lesions inferior or nasal to the disk in one eye; (3) low-grade anterior chamber inflammation (no more than 1+ cells in the anterior chamber on the SUN score); (4) low-grade vitreous inflammation (no more than 2+ on the NEI/SUN vitreous haze score).

Common causes of visual loss in BCR include those inherent to chorioretinopathy, such as refractory CME, choroidal neovascularization (CNV), epiretinal membrane (ERM) and macular scarring. Diffuse retinal dysfunction associated with the long duration of the disease is also recognized as a significant risk factor for vision loss.

Treatment usually consists of steroids, steroid-sparing immunomodulatory therapy, or a combination of both, aimed at suppressing ocular inflammation and managing complications, predominantly CMO. Cases that develop CNV require intravitreal anti-VEGF injections, while symptomatic epiretinal membranes are managed with pars plana vitrectomy and ERM peel.

Keep in mind

- ✓ Being a form of vision-threatening chorioretinopathy, BCR must be considered in the presence of bilateral, multiple white-dot lesions, with associated mild vitritis, especially in middle-aged women.
- ✓ There is strong association with the HLA-A29 histocompatibility antigen, which is positive in approximately 90% of patients with BCR.
- ✓ Early identification and aggressive management of BCR, usually with at least two immunomodulatory agents, are of paramount importance to prevent severe visual impairment.

References

1. Mount GR & Kaufman EJ (2021). White Dot Syndromes. In StatPearls. StatPearls Publishing. https://www.ncbi.nlm.nih.gov/books/NBK557854/
2. Takeuchi M, Mizuki N & Ohno S (2021). Pathogenesis of Non-Infectious Uveitis Elucidated by Recent Genetic Findings. Frontiers in immunology, 12, 640473. https://doi.org/10.3389/fimmu.2021.640473
3. Bergstrom R & Czyz CN (2020). Birdshot Retinopathy. In StatPearls. StatPearls Publishing. https://www.ncbi.nlm.nih.gov/books/NBK554416/
4. Kuiper J & Venema WJ (2020). HLA-A29 and Birdshot Uveitis: Further Down the Rabbit Hole. Frontiers in immunology, 11, 599558. https://doi.org/10.3389/fimmu.2020.599558
5. Sternes PR, Martin TM, Paley M, Diamond S, Asquith MJ, Brown MA & Rosenbaum JT (2020). HLA-A alleles including HLA-A29 affect the composition of the gut microbiome: a potential clue to the pathogenesis of birdshot retinochoroidopathy. Scientific reports, 10(1), 17636. https://doi.org/10.1038/s41598-020-74751-0
6. Minos E, Barry RJ, Southworth S, Folkard A, Murray PI, Duker JS, Keane PA & Denniston AK (2016). Birdshot chorioretinopathy: current knowledge and new concepts in pathophysiology, diagnosis, monitoring and treatment. Orphanet journal of rare diseases, 11(1), 61. https://doi.org/10.1186/s13023-016-0429-8
7. Kuiper J, Rothova A, de Boer J & Radstake T (2015). The immunopathogenesis of birdshot chorioretinopathy; a bird of many feathers. Progress in retinal and eye research, 44, 99–110. https://doi.org/10.1016/j.preteyeres.2014.11.003
8. Freitas-Neto, Clovis Arcoverde et al. Birdshot retinochoroidopathy review. Arquivos Brasileiros de Oftalmologia [online]. 2015, v. 78, n. 1, pp. 56-61. ISSN 1678-2925. https://www.scielo.br/j/abo/a/xc3F4b365W3hbCCkrvLpBvS/?lang=en.
9. Monnet D & Brézin AP (2006). Birdshot chorioretinopathy. Current opinion in ophthalmology, 17(6), 545–550. https://doi.org/10.1097/ICU.0b013e3280109479
10. Rothova A, Berendschot TT, Probst K, van Kooij B & Baarsma GS (2004). Birdshot chorioretinopathy: long-term manifestations and visual prognosis. Ophthalmology, 111(5), 954–959. https://doi.org/10.1016/j.ophtha.2003.09.031

Case 10 - September 2021

VITAMIN A DEFICIENCY

A 51-year-old man presented with night blindness for 3 months.

Presented by
Thanos Vakalis, MD
& Stavrenia Koukoula, MD, PhD

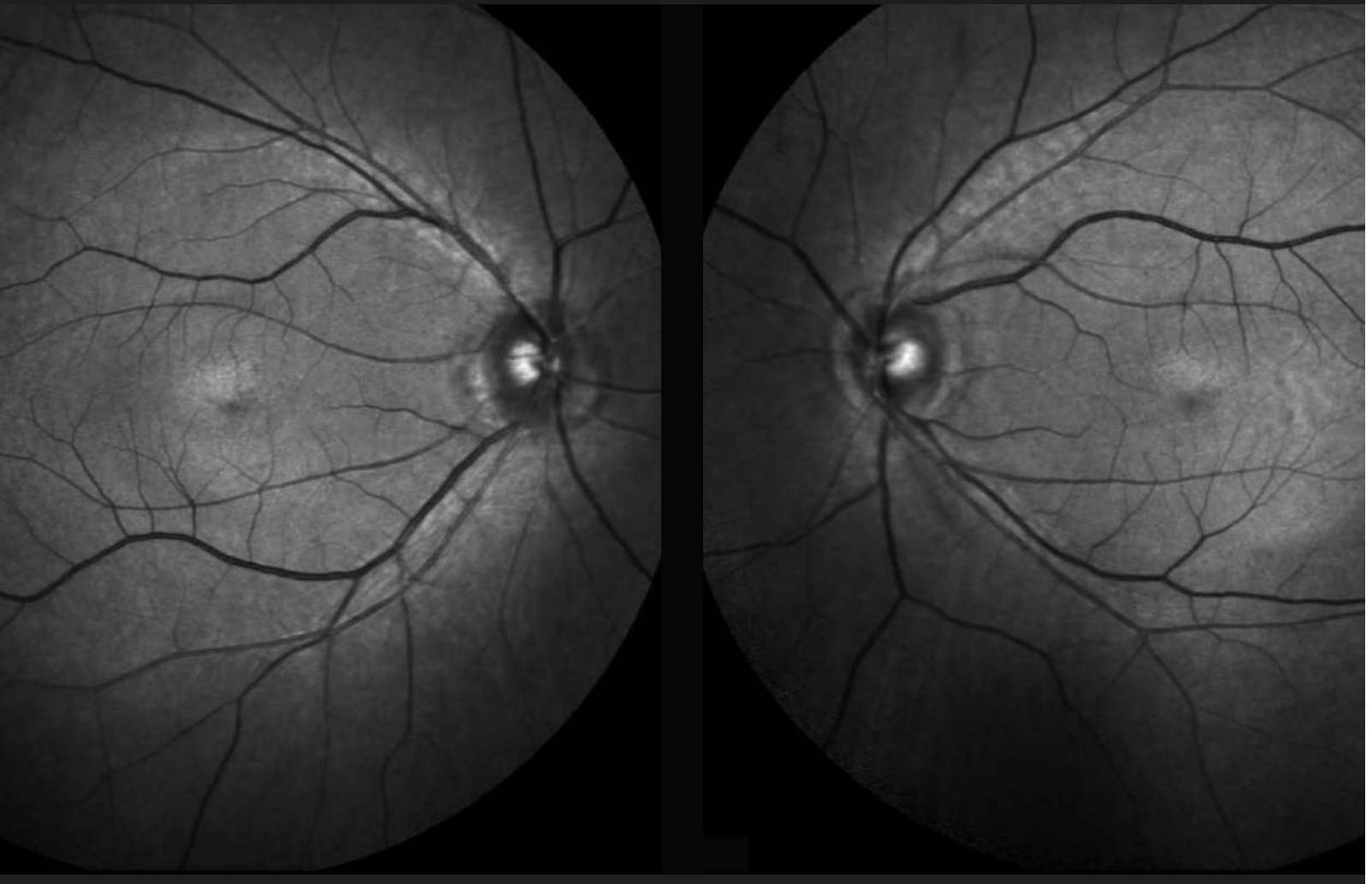

Edited by
Penelope Burle de Politis, MD

Case History

A 51-year-old Caucasian man with a 3-month complaint of nyctalopia was referred for retinal examination. He had been an emmetrope all his life, with excellent distance vision in both eyes, having started using reading glasses around 45 years of age. Remaining ophthalmological history was unremarkable. Family history was negative for severe ocular disorders. Upon examination, uncorrected distance visual acuity was 10/10 bilaterally. Both eyes were calm and intraocular pressure was within the physiological range. Direct fundoscopy was normal for the age, with nonspecific pigmentary changes. HD-OCT showed diffuse mottled hypo-autofluorescence on fundus autofluorescence imaging bilaterally and a macular drusen on the right (**Figures 1 & 2**). Spectral domain OCT (SD-OCT) confirmed the findings, without any other abnormalities (**Figure 3**).

Figure 1: Green filter HD-OCT (Spectralis®, Heidelberg Engineering) showing bilateral nonspecific retinal pigmentary changes.

Figure 2: Fundus autofluorescence scan revealing a macular drusen on the right eye.

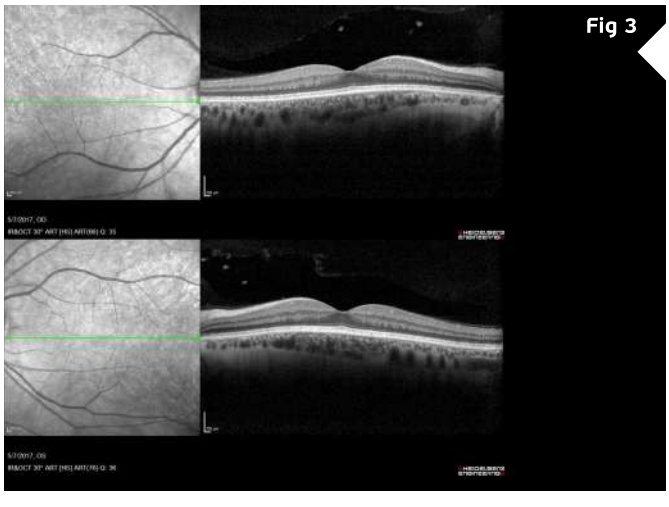

Figure 3: SD-OCT showing normal retinal structure in both eyes, except for a minute macular drusen on the right.

Additional History

The patient had undergone a Whipple procedure (pancreaticoduodenectomy) about a year before, for the resection of a malignant tumor, having suffered from chronic steatorrhea for the last 6 months. The only medication he was on were capsules of pancreatic enzymes. Due to the high probability of a malabsorption-related condition, an electrophysiological evaluation was ordered, whose results were consistent with hypovitaminosis A **(Figure 4**).

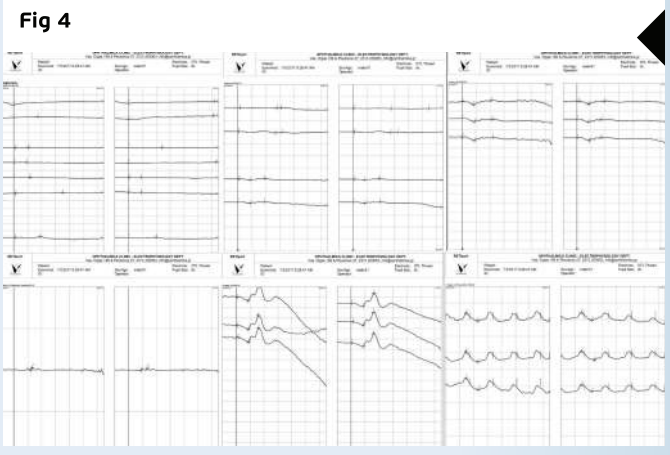

Figure 4: Electroretinography (ERG) showing reduced scotopic rod responses bilaterally. The maximal rod-cone ERG is bilaterally grossly abnormal, with substantially reduced a- and b-wave amplitudes. The Arden ratios are also substantially reduced for both eyes.

Oral supplementation of vitamin A was started, with a significant improvement of scotopic vision being reported after a week. New ERG was obtained at 2 months of vitamin A supplementation, with a clear change towards normality (Figure 5).

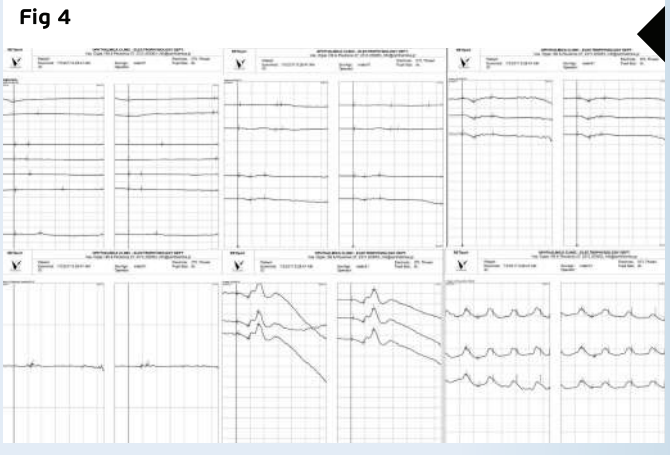

Figure 5: Full-field ERG after 2 months of therapy with vitamin A oral supplement, displaying rod function improvement.

Differential Diagnosis

- vitamin A deficiency
- choroideremia
- retinitis pigmentosa
- gyrate atrophy
- albinism
- uncorrected myopia
- cataracts
- glaucoma
- Oguchi Disease
- optic neuropathy
- siderosis
- zinc deficiency

The differential diagnosis of vitamin A deficiency encompasses all causes of nyctalopia. Since the symptom is subjective and may coexist with other ocular conditions, careful history obtention is of primary importance.

Discussion and Literature

Vitamin A is an essential fat-soluble vitamin important for the function of various body systems. In the eye, it is necessary for the synthesis of pigments in photoreceptors and plays an important role in corneal and conjunctival metabolism. Vitamin A deficiency is a rare condition in developed countries, but may follow intestinal or gastric bypasses and has gained increasing significance with the dissemination of bariatric procedures, with an incidence of 69% at 4 years after surgery.

The earliest and most common symptom of vitamin A deficiency is nyctalopia. Color perception may also be affected. Clinical signs that help identify chronic hypovitaminosis A are xerophthalmia and Bitot's spots, a 'foamy' appearing buildup of keratin located superficially on the nasal and temporal conjunctiva. Multiple retinal yellowish-white spots are a common fundus finding. Long-standing vitamin A deprivation may lead to conjunctival and corneal xerosis, keratomalacia or corneal ulceration. If left untreated, lesions can progress to cause permanent visual loss.

Early diagnosis is based on serum levels of vitamin A, OCT scanning and electrophysiology studies. Color sensitivity testing with the Ishihara chart may also be helpful. Visual fields may be altered, showing superior and inferior arcuate defects or concentric narrowing, but are not a constant finding in vitamin A deficiency.

OCT may be entirely normal and advanced scanning is more likely to show abnormalities. On SD-OCT, central macular thickness and ganglion cell layer thickness may be reduced. There may be partial ellipsoid zone disruption, appearing as hyperreflectivity spots that may correspond to an accumulation of shed outer segments of photoreceptor above the retinal pigmented epithelium, with localized lipofuscin loss. These spots are seen as hypo-autofluorescent mottling on FAF.

Reduced ganglion cell layer in patients with vitamin A deficiency reflects on oscillatory potentials on the ERG. Electroretinography may have focal or diffusely undetectable patterns, S-cone waves of reduced amplitude, reduction or electronegativity of whilst bright flash a-waves. Dim flash rod ERGs may be undetectable. Photopic 30 Hz flicker and single flash cone alterations may present severe generalized rod system dysfunction.

The vitamin A supplementation route depends on the severity of deficiency. Standard managing is with oral capsules, but severe cases may need intramuscular and even intravenous administration. Rapid recovery is possible with appropriate treatment, with total reversal of symptoms from as early as 3 days of vitamin supplementation, though electrophysiology may take up to 7 months to return to normal.

Vitamin A deficiency–related retinopathy after abdominal surgery may be an underreported complication. It is a preventable cause of blindness and must be considered even in apparently well-nourished individuals with a history of gastrointestinal procedures.

Keep in mind

- ✓ Vitamin A deficiency must always be considered in the investigation of night blindness, especially in the setting of abdominal surgery.
- ✓ Electrophysiology assessment is more sensitive than serum dosing for the detection of hypovitaminosis A in early or mild cases of nyctalopia.
- ✓ Vitamin A supplementation renders fast recovery from nyctalopia caused by prolonged malabsorption, preventing progression to extensive ocular damage.

References

1 Hansen BA, Mendoza-Santiesteban CE & Hedges TR 3rd (2018). REVERSIBLE NYCTALOPIA ASSOCIATED WITH VITAMIN A DEFICIENCY AFTER RESECTED MALIGNANT ILEAL CARCINOID AND PANCREATIC ADENOCARCINOMA. Retinal cases & brief reports, 12(2), 127–130. https://doi.org/10.1097/ICB.0000000000000441

2 Cheshire J & Kolli S (2017). Vitamin A deficiency due to chronic malabsorption: an ophthalmic manifestation of a systemic condition. BMJ case reports, 2017, bcr2017220024. https://doi.org/10.1136/bcr-2017-220024

3 Saenz-de-Viteri M & Sádaba LM (2016). Optical Coherence Tomography Assessment Before and After Vitamin Supplementation in a Patient With Vitamin A Deficiency: A Case Report and Literature Review. Medicine, 95(6), e2680. https://doi.org/10.1097/MD.0000000000002680

4 Kontos A, Kayhanian H, El-Khouly F & Gillmore R (2015). Night blindness due to vitamin A deficiency associated with resected adenocarcinoma of the pancreas. International journal of ophthalmology, 8(1), 206–207. https://doi.org/10.3980/j.issn.2222-3959.2015.01.36

5 Anastasakis A, Plainis S, Giannakopoulou T et al. (2013). Xerophthalmia and acquired night blindness in a patient with a history of gastrointestinal neoplasia and normal serum vitamin A levels. Documenta ophthalmologica. Advances in ophthalmology, 126(2), 159–162. https://doi.org/10.1007/s10633-012-9370-x

6 Aleman TS, Garrity ST & Brucker AJ (2013). Retinal structure in vitamin A deficiency as explored with multimodal imaging. Documenta ophthalmologica. Advances in ophthalmology, 127(3), 239–243. https://doi.org/10.1007/s10633-013-9403-0

7 Tiang S & Warne R (2010). Nyctalopia: the sequelae of hypovitaminosis A. BMJ case reports, 2010, bcr0520102965. https://doi.org/10.1136/bcr.05.2010.2965

8 Genead MA, Fishman GA & Lindeman M (2009). Fundus white spots and acquired night blindness due to vitamin A deficiency. Documenta ophthalmologica. Advances in ophthalmology, 119(3), 229–233. https://doi.org/10.1007/s10633-009-9200-y

9 Dolan FM, Sandinha T, Purdy A, Parks S & Keating D (2006). Vitamin A deficiency modifies the mfERG: a case study of rod influence on the mfERG. Documenta ophthalmologica. Advances in ophthalmology, 112(1), 31–34. https://doi.org/10.1007/s10633-006-0002-1

10 Perlman I, Barzilai D, Haim T & Schramek A (1983). Night vision in a case of vitamin A deficiency due to malabsorption. The British journal of ophthalmology, 67(1), 37–42. https://doi.org/10.1136/bjo.67.1.37

Case 11 - January 2022

RETINAL CAVERNOUS HEMANGIOMA

A 16-year-old boy was referred for further investigation of a right retinal lesion noticed during routine eye examination.

Presented by
Paris Tranos, MD, PhD, ICOphth, FRCS

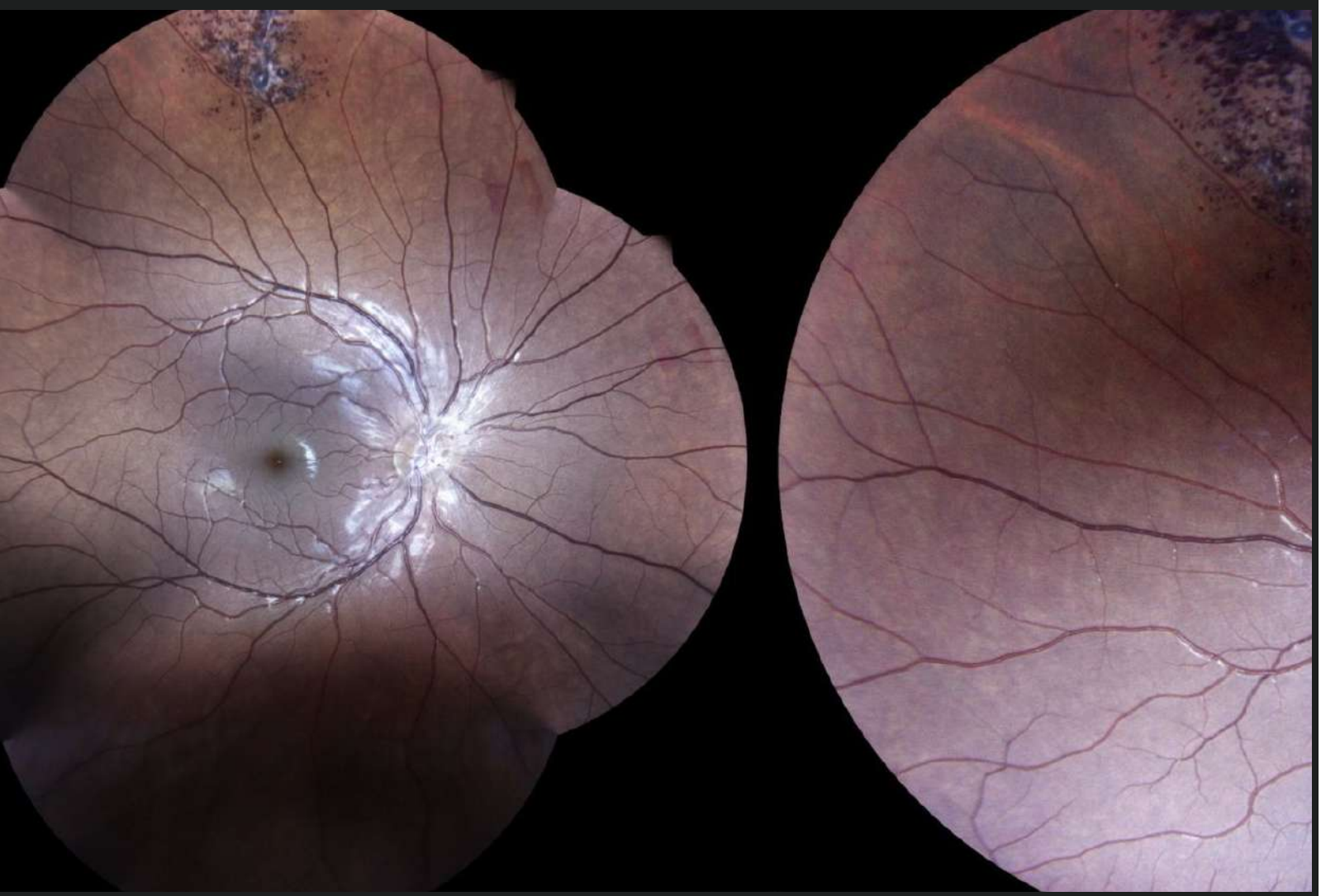

Edited by
Penelope Burle de Politis, MD

Case History

A 16-year-old Caucasian boy was referred for further investigation of a fundus lesion detected during routine ophthalmological examination. Previous ocular and systemic history were unremarkable. Family history was negative for severe ophthalmological disorders. Upon examination, uncorrected distance visual acuity was 10/10 in both eyes with emmetropia. Slit-lamp examination showed no abnormalities and intraocular pressure was within normal limits bilaterally. Fundoscopy revealed dark intraretinal aneurysms with a characteristic "cluster-of-grapes" appearance at the superior retinal periphery of the right eye (**Figure 1**), whereas retinal examination of the left eye was unremarkable.

Fundus fluorescein angiography (FA) showed early hypofluorescence, followed by slow filling of the saccular lesions during the venous phase, and subsequent progressive hyperfluorescence. Pooling of dye in the upper half of the saccules was noted in the late phase, giving it the appearance of a “fluorescein cap” (**Figure 2**).

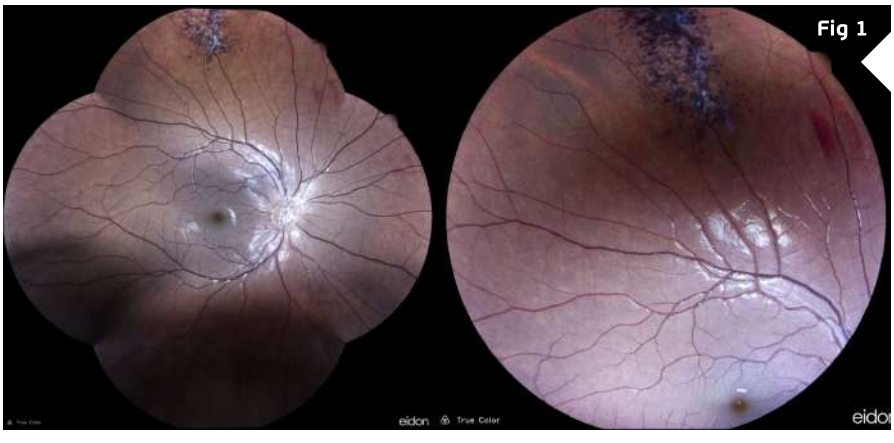

Figure 1: Wide-angle and close-up color fundus photographs showing a cluster of saccular lesions at the 12 o'clock position of retinal periphery in the right eye.

Further investigation with multimodal imaging — autofluorescence (AF), fundus fluorescein angiography (FFA), optical coherence tomography (OCT) and indocyanine green (ICG) angiography — was carried on (**Figures 2 and 3**).

Differential Diagnosis

- choroidal melanoma
- retinal capillary hemangioma
- retinal cavernous hemangioma
- retinal vasoproliferative tumor
- racemose hemangiomatosis
- extraophthalmic cancer metastatic to the choroid
- benign reactive lymphoid hyperplasia of the choroid
- leukemic choroidal infiltration

Clinical findings and multimodal imaging were consistent with the diagnosis of retinal cavernous hemangioma. The main differentiation of this benign lesion is with the other forms of fundus vascular tumors; however, lesions with potentially high morbidity and mortality such as choroidal melanoma must be excluded.

Figure 2: FA (Spectralis, Heidelberg Engineering) of the right eye, evidentiating the retinal lesion. Notice the progressively increasing fluorescence pattern through the early, venous and late phases of the angiogram.

Additional history

Further investigation with magnetic resonance imaging (MRI) of the brain and ultrasonography (USG) of the liver was recommended. Pediatric neurological and neurosurgical workup rendered the detection of multiple small encephalic and cerebellar hemangiomas. Due to the asymptomatic nature of the retinal lesion, no ocular intervention was undertaken, and the patient was scheduled for periodical examination.

Discussion and Literature

The vascular tumors of the retina and choroid comprise a diverse group of congenital and acquired lesions. The major vascular tumors of the retina include retinal capillary hemangioma, retinal cavernous hemangioma, retinal vasoproliferative tumor, and racemose hemangiomatosis or Wyburn-Mason syndrome. Choroidal vascular tumors are hemangiomas, classified into two subtypes, circumscribed and diffuse, based on the extent of choroidal involvement.

Chorioretinal vascular tumors can occur independently or in association with systemic diseases, present with ocular manifestations or be diagnosed by chance during routine ophthalmological examination. Any patient with an intraocular vascular lesion must be therefore evaluated for lesions in other locations and evidence of syndromic conditions (e.g., retinal hemangioblastoma in von Hippel Lindau disease, choroidal hemangioma in Sturge–Weber syndrome, retinal cavernous hemangioma in familial cerebral cavernomatosis).

Retinal cavernous hemangioma (RCH) is a rare benign vascular tumor, usually diagnosed in children and young adults. There is a clearly higher prevalence among white individuals, with even gender distribution. The vast majority of cases are isolated solitary lesions, but RCH may occur as a component of an autosomal dominantly inherited neuro-oculo-cutaneous syndrome featuring histologically similar central nervous system and cutaneous vascular malformations. Bilateral cases are strongly correlated with the hereditary form. Intracranial involvement occurs in about 15% of patients with RCH. Though a history of headache or visual disturbances is suggestive of intracranial involvement, most patients are asymptomatic.

Decision to treat any of the types of benign retinal vascular tumors should be based on the presence and extent of visual symptoms and potential for visual recovery. Treatment depends on tumor location, the presence of subretinal fluid, and the extent of symptoms. Periodic observation alone may be warranted for asymptomatic cases where tumors lack subretinal fluid threatening the macula. When vision impairment occurs, therapy is aimed at inducing tumor atrophy, with resolution of subretinal fluid and foveal distortion. Current treatment options include argon laser photocoagulation, proton beam radiotherapy, transpupillary thermotherapy (TTT), photodynamic therapy (PDT), and anti-vascular endothelial growth factor (VEGF) therapy.

Keep in mind

- ✓ Retinal cavernous hemangioma is a rare benign vascular tumor, commonly asymptomatic.
- ✓ Accurate differential diagnosis and detection of systemic associations is a crucial step in management of RCH.
- ✓ Ocular treatment of RCH is restricted to vision-threatening complications, since most lesions require observation only.

References

1 Turell ME & Singh AD (2010). Vascular tumors of the retina and choroid: diagnosis and treatment. Middle East African journal of ophthalmology, 17(3), 191–200. https://doi.org/10.4103/0974-9233.65486

2 Shanmugam PM & Ramanjulu R (2015). Vascular tumors of the choroid and retina. Indian journal of ophthalmology, 63(2), 133–140. https://doi.org/10.4103/0301-4738.154387

3 Shields JA & Shields CL. Vascular tumors of the retina and optic disc. In: Shields JA, Shields CL. Intraocular Tumors: An Atlas and Textbook.2nd ed. Philadelphia, PA: Lippincott Williams & Wilkins; 2008:382–389.

4 Wang W & Chen L (2017). CAVERNOUS HEMANGIOMA OF THE RETINA: A Comprehensive Review of the Literature (1934-2015). Retina (Philadelphia, Pa.), 37(4), 611–621. https://doi.org/10.1097/IAE.0000000000001374

5 Gass JD (1971). Cavernous hemangioma of the retina. A neuro-oculo-cutaneous syndrome. American journal of ophthalmology, 71(4), 799–814. https://doi.org/10.1016/0002-9394(71)90245-5

6 Heimann H, Jmor F & Damato B (2013). Imaging of retinal and choroidal vascular tumours. Eye (London, England), 27(2), 208–216. https://doi.org/10.1038/eye.2012.251

7 Dobyns WB, Michels VV, Groover RV, Mokri B, Trautmann JC, Forbes GS & Laws ER Jr (1987). Familial cavernous malformations of the central nervous system and retina. Annals of neurology, 21(6), 578–583. https://doi.org/10.1002/ana.410210609

8 Toll A, Parera E, Giménez-Arnau AM, Pou A, Lloreta J, Limaye N, Vikkula M & Pujol RM (2009). Cutaneous venous malformations in familial cerebral cavernomatosis caused by KRIT1 gene mutations. Dermatology (Basel, Switzerland), 218(4), 307–313. https://doi.org/10.1159/000199461

9 Sakano LY, Neufeld CR & Aihara T (2020). Medical monitoring of patient with cavernous hemangioma of the retina and intracranial involvement. American journal of ophthalmology case reports, 17, 100602. https://doi.org/10.1016/j.ajoc.2020.100602

Case 12 - February 2022

OPTIC NEURITIS POST-COVID-19 INFECTION

A 26-year-old woman presented with bilateral visual loss after a COVID-19 infection.

Presented by
Zachos Zachariadis, MD, DO

Edited by
Penelope Burle de Politis, MD

Case History

A 26-year-old Caucasian woman presented with bilateral blurry vision for 3 days. She was previously healthy, except for an infection with COVID-19 a week before, for which she was taking azithromycin, acetylcysteine, colchicine, vitamins C and D, zinc, an inhalable budesonide and formoterol combination, and enoxaparin 4,000 IU subcutaneously. Her family medical history was unremarkable. Upon examination, her corrected distance visual acuity (CDVA) was 6/10 in the right eye (RE) and 4/10 in the left eye (LE). Refractometry was -3.00 -0.75 @180° (RE) and -1.50 -0.75 @175°(LE). A relative afferent pupillary defect was apparent on the left. Color vision was impaired in both eyes, noticeably in the LE. Red desaturation testing was abnormal bilaterally. Extraocular movements, slit-lamp examination, tonometry and fundoscopy featured no abnormalities. Central visual field analysis revealed marked diffuse sensitivity reduction in both eyes, more pronounced on the left (**Figure 1**).

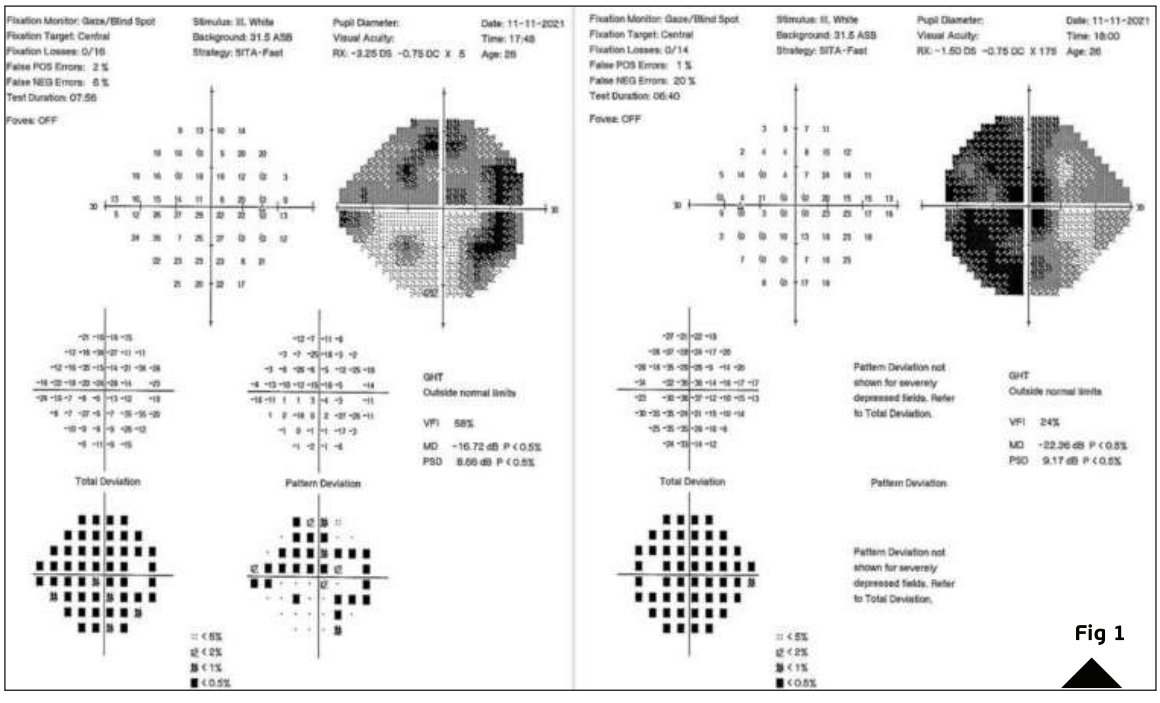

Figure 1: Humphrey automated perimetry showing marked diffuse visual field depression in both eyes, more pronounced on the left.

Additional History

The case was managed conjointly with a neuroophthalmology specialist. Neuroimaging (magnetic resonance) of the brain obtained 2 days after ocular examination was inconclusive. Based on history and clinical findings, a diagnosis of bilateral retrobulbar optic neuritis secondary to coronavirus disease was established. The Optic Neuritis Treatment Trial (ONTT) protocol was added to the drug regimen in use, with a favorable outcome. At 3 months of follow-up, there was total remission of the acute manifestations, with CDVA returning to 10/10 in both eyes and visual field analysis displaying significant improvement bilaterally (**Figure 2**). The patient was scheduled for review every 6 months, or earlier in case of relapse.

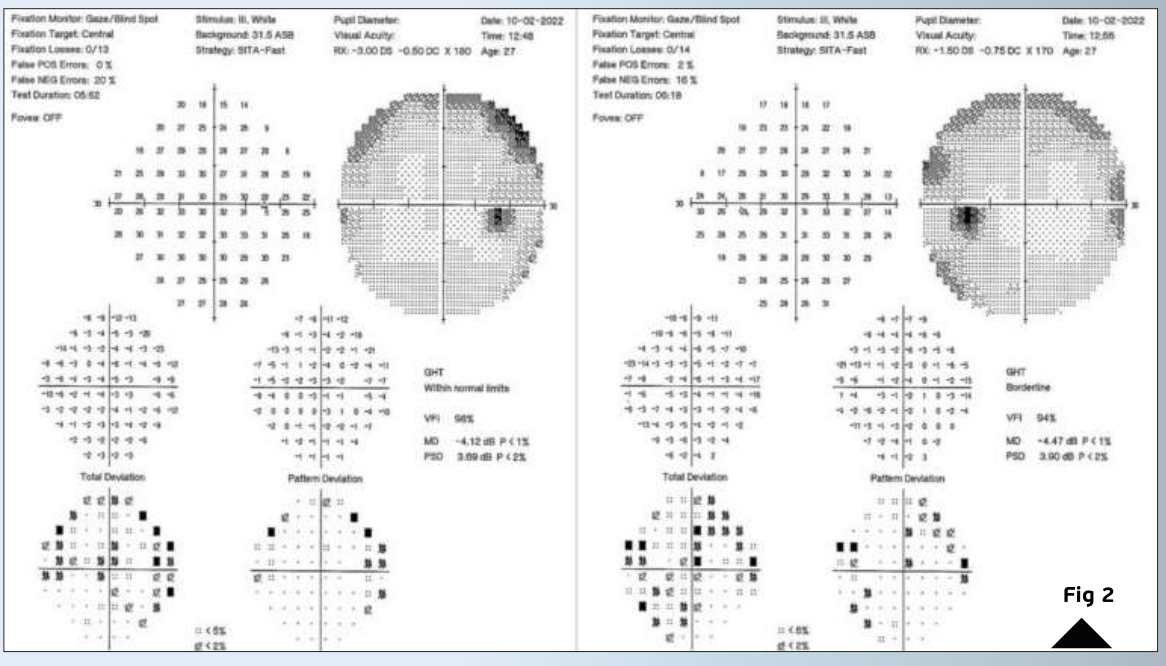

Figure 2: Central visual field analysis at 3-month follow-up showing significant improvement in both eyes.

Differential Diagnosis of Acute Binocular Loss of Vision

- toxic optic neuropathy
  (e.g. methanol, quinine, ethambutol, ergot alkaloids, salicylates)
- optic neuritis
- stroke
- seizures
- severe hypoperfusion, hypoxemia, hypoglycemia
- post-concussion
- migraine
- hysteria
- malingering

The etiological diagnosis of acute persistent bilateral visual loss lies mainly in the distinction between systemic and ocular disorders, a fundamental step in management.

Discussion and Literature

Acute bilateral vision loss can result from ocular and systemic conditions. The first crucial step in management is defining whether the visual deficit is transient (i.e., of less than 24-hour duration) or persistent (i.e., lasting at least 24 hours). Acute transient binocular visual loss is rarer than monocular and generally results from a cerebral dysfunction such as migraine, partial occipital lobe seizures, vertebrobasilar ischemia, or cranial hypertension.

Acute persistent binocular visual loss is usually related to systemic or visual pathway disorders. Visual pathway malfunction can be due to optic nerve, chiasmal, or retrochiasmal pathology. In cases where ocular examination is normal, a thorough history and neuroimaging may be necessary for an accurate diagnosis.

COVID-19 can affect almost every organ or system in the body, including the eye and vision. From the lid to the visual cortex, various ocular complications have been reported. Ophthalmic manifestations may be the presenting feature of the infection or develop several weeks after recovery. While follicular conjunctivitis is the most common COVID-19-related oculopathy, even some of the drugs used in infection management carry the risk of ocular toxicity. Neurologic complications have been documented in 36.4% of the cases of SARS-CoV-2, with central and/or peripheral involvement. Viral neurotropism has been proposed as one of the mechanisms responsible for the neurological (and neuro-ophthalmic) manifestations, which range from mild or moderate anosmia, headache, dizziness, and hypogeusia, to more severe outcomes such as ischemic stroke and Guillain-Barré syndrome.

Neuro-ophthalmic manifestations of COVID-19 infection have been described in patients from 6 to 71 years of age, independently of systemic comorbidity. The median gap to the onset of ophthalmic complaints is 5 days but can occur anytime between 0 and 42 days of the first COVID-19 symptoms. The spectrum of neuro-ophthalmic involvement comprises papillophlebitis, optic neuritis, Adie's tonic pupil, Miller Fisher syndrome with cranial nerve palsy, neurogenic ptosis, and cerebrovascular accident with vision loss. In cases of optic neuritis, patients typically present with painful vision loss, relative afferent pupillary defect in the more severely affected eye, visual field defects, and optic nerve enhancement on magnetic resonance imaging. The virus has not been isolated from the cerebrospinal fluid of affected patients, which suggests an immune-mediated rather than direct viral insult.

Optic neuritis in adults is usually unilateral and commonly linked to multiple sclerosis. Bilateral acute optic neuritis is a rare phenomenon occurring in individuals with known systemic inflammatory or autoimmune conditions. Post-COVID optic neuritis, either unilateral or bilateral, is no longer an uncommon complication of the infection. Of note, optic neuritis can ensue even after mild COVID-19 infection with no oxygen requirement or steroid use, i.e., with an otherwise uneventful recovery. Recent analyses have shown that females are more affected than males and the left eye is more liable to the drop in visual acuity, though there is no significant difference between right and left eyes in long-term vision loss. Some cases of COVID-19 induced optic neuritis test positive for myelin oligodendrocyte glycoprotein (MOG) and antibodies against AQP4 and present associated demyelination, which reinforces the importance of optic neuritis post-recovery follow-up.

Intravenous (methylprednisolone 1 g/day for 3 days) followed by oral steroids (prednisone 1 mg/kg/day for 11 days remain the choice of treatment for optic neuritis of this etiology. Most case reports showed full resolution of symptoms within 2 to 3 weeks after initiation of steroids. Delay in the diagnosis of neuro-ophthalmic manifestations of COVID-19 may lead to irreversible optic atrophy and permanent visual impairment. For this reason, it is important to increase awareness of ocular involvement by this new infective agent.

Keep in mind

- ✓ In general, acute persistent bilateral visual loss results from systemic or visual pathway disorders.
- ✓ COVID-19 can affect vision either by direct insult to different structures of the eye or through immune-mediated mechanisms.
- ✓ Optic neuritis is one of the possible complications of SARS-CoV-2 whose prompt diagnosis and treatment can preserve organ function.

References

1. Balmitgere T & Vighetto A (2009). Troubles visuels binoculaires transitoires: une approche diagnostique [Transient binocular visual loss: a diagnostic approach]. Journal francais d'ophtalmologie, 32(10), 770–774. https://doi.org/10.1016/j.jfo.2009.10.004
2. Garg RK (2020). Spectrum of Neurological Manifestations in Covid-19: A Review. Neurology India, 68(3), 560–572. https://doi.org/10.4103/0028-3886.289000
3. Selvaraj V, Sacchetti D, Finn A & Dapaah-Afriyie K (2020). Acute Vision Loss in a Patient with COVID-19. Rhode Island medical journal (2013), 103(6), 37–38. https://doi.org/10.1101/2020.06.03.20112540
4. Cyr DG, Vicidomini CM, Siu NY & Elmann SE (2020). Severe Bilateral Vision Loss in 2 Patients With Coronavirus Disease 2019. Journal of neuro-ophthalmology : the official journal of the North American Neuro-Ophthalmology Society, 40(3), 403–405. https://doi.org/10.1097/WNO.0000000000001039
5. Sawalha K, Adeodokun S & Kamoga GR (2020). COVID-19-Induced Acute Bilateral Optic Neuritis. Journal of investigative medicine high impact case reports, 8, 2324709620976018. https://doi.org/10.1177/2324709620976018
6. Deane K, Sarfraz A, Sarfraz Z, Valentine D, Idowu AR & Sanche V (2021). Unilateral Optic Neuritis Associated with SARS-CoV-2 Infection: A Rare Complication. The American journal of case reports, 22, e931665. https://doi.org/10.12659/AJCR.931665
7. Rodríguez-Rodríguez MS, Romero-Castro RM, Alvarado-de la Barrera C, González-Cannata MG, García-Morales AK & Ávila-Ríos S (2021). Optic neuritis following SARS-CoV-2 infection. Journal of neurovirology, 27(2), 359–363. https://doi.org/10.1007/s13365-021-00959-z
8. Sen M, Honavar SG, Sharma N & Sachdev MS (2021). COVID-19 and Eye: A Review of Ophthalmic Manifestations of COVID-19. Indian journal of ophthalmology, 69(3), 488–509. https://doi.org/10.4103/ijo.IJO_297_21
9. Azab MA, Hasaneen SF, Hanifa H & Azzam AY (2021). Optic neuritis post-COVID-19 infection. A case report with meta-analysis. Interdisciplinary neurosurgery : Advanced techniques and case management, 26, 101320. https://doi.org/10.1016/j.inat.2021.101320
10. Jossy A, Jacob N, Sarkar S, Gokhale T, Kaliaperumal S & Deb AK (2022). COVID-19-associated optic neuritis - A case series and review of literature. Indian journal of ophthalmology, 70(1), 310–316. https://doi.org/10.4103/ijo.IJO_2235_21

Case 13 - April 2022

ADULT-ONSET COATS' DISEASE

A 43-year-old woman presented with subacute painless visual loss in the left eye.

Presented by
Chrysa Koutsiouki, MD

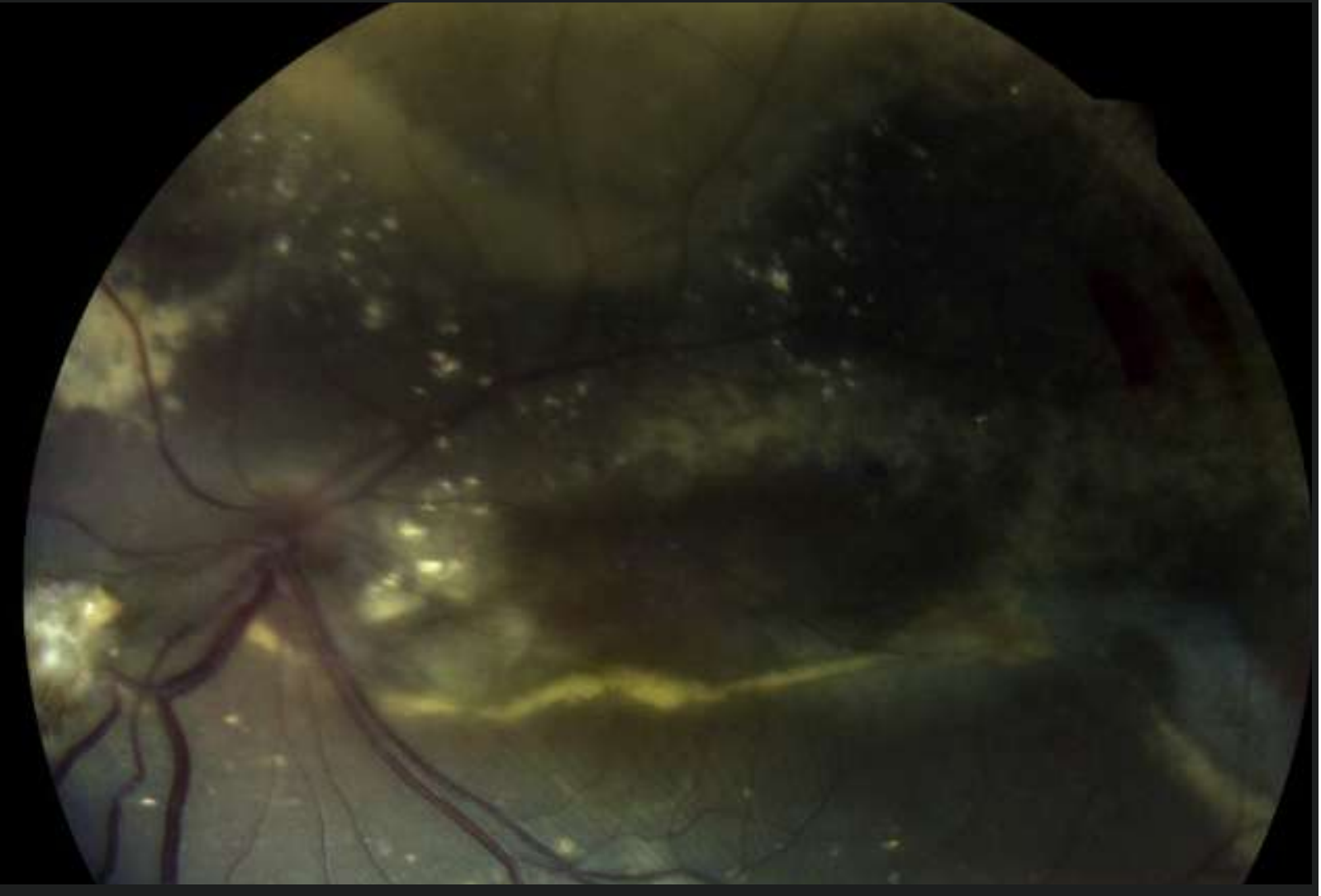

Edited by
Penelope Burle de Politis, MD

Case History

A 43-year-old Caucasian woman was referred for investigation of decreased vision in the left eye (LE) noticed by chance 1 week prior to the visit while self-occluding the right eye (RE). The patient suffered from mixed anxiety-depressive disorder (MADD) diagnosed 2 years before and was currently in use of venlafaxine and bromazepam. Her past ocular history was unremarkable. Her family medical history was negative for ophthalmic diseases. Her corrected distance visual acuity (CDVA) was 10/10 in the RE and limited to light perception (LP) in the LE. Refractometry without cycloplegia was -0.25 in the RE and plano in the LE. A relative afferent pupillary defect was present on the left with a relatively fixed pupil. Biomicroscopy revealed posterior synechiae in the LE — extending from 3 to 7 o'clock — with no evidence of anterior chamber reaction (cells, keratic precipitates, flare), nor iris nodules or transillumination defects. Intraocular pressure (IOP) was within the normal range in both eyes. Fundus examination of the LE showed massive exudation in all 4 quadrants, in the form of hard-exudate plaques and circinate deposits, exudative retinal detachment along the inferior arcade extending to the inferior quadrant, and dilation and angulation of the retinal veins (**Figure 1**). Findings in the RE were limited to mild macular retinal pigment epithelium (RPE) changes (**Figure 2**).

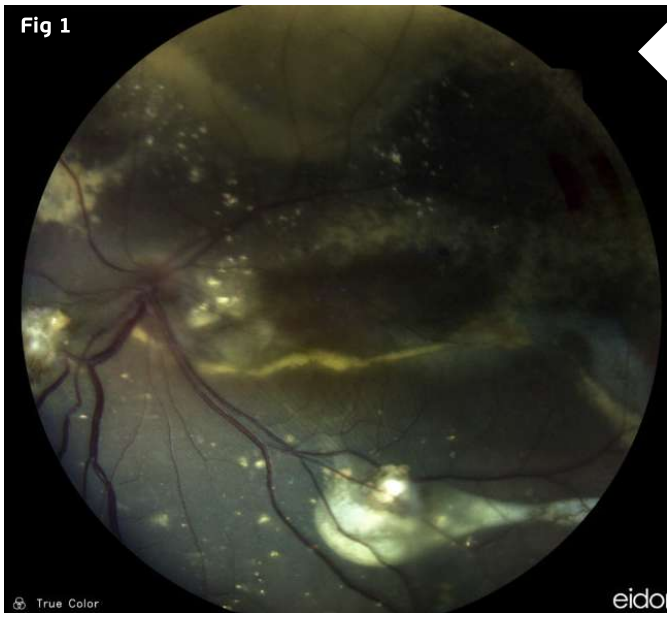

Figure 1: Color photograph of the left eye posterior pole showing macular edema, hard exudates in a circinate pattern and in plaques, and inferior retinal folds resulting from exudative retinal detachment, with anterior displacement of the retinal vessels.

Figure 2: Confocal high-resolution widefield imaging of the right eye (iCare EIDON®).

Spectral-domain optical coherence tomography (SD-OCT) displayed retinal thickening and extensive parafoveal neurosensory detachment inferior to the macula in the LE, secondary to exudative detachment (**Figure 3**). A small, shallow perifoveal pigment epithelium detachment (PED) was detected in the RE.

Fundus fluorescein angiography (FFA) was normal in the RE. In the LE there was early leakage at the macula and periphery resulting from the telangiectatic changes, followed by late diffuse leakage (**Figure 4**).

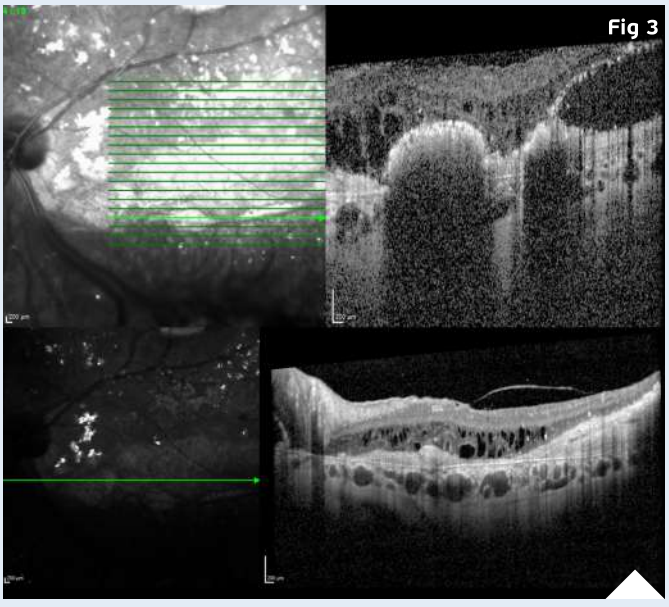

Figure 3: Spectralis SD-OCT (Heidelberg Engineering®) of the LE displaying the parafoveal neurosensory detachment extending to the optic disc. Diffuse retinal thickening, cystoid macular oedema (CMO), hyper-reflective material and outer retina atrophic changes are noticeable.

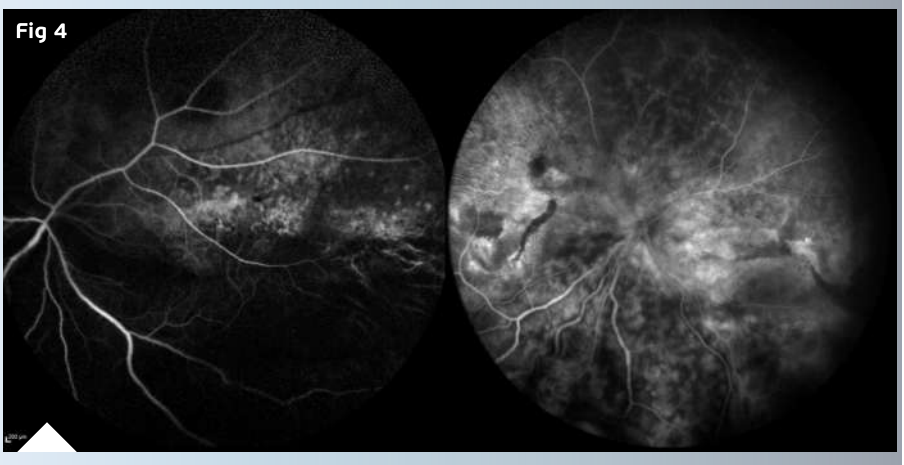

Figure 4: FFA of the LE (Heidelberg Engineering®). Early frame (right): inferior exudative detachment with the demarcation line noticed as hypofluorescence caused by the retinal fold masking. Late frame (left): diffuse leakage.

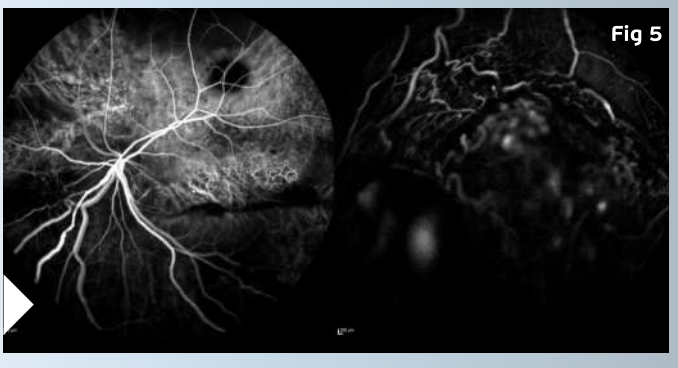

Figure 5: ICG-A of the LE (Heidelberg Engineering®). Early frame (right): evidence of telangiectatic changes. Late frame (left): telangiectatic vessels at the area of the exudative detachment.

Indocyanine-green angiography (ICG-A) was normal in the RE. In the LE, telangiectatic changes were noticed in the early frames, along the area of the inferiorly located exudative detachment (**Figure 5**).

Additional History

A full systemic laboratory workup aiming at inflammatory disorders was requested, and the therapy options were discussed with the patient. Intravitreal anti-VEGF and/or dexamethasone implant were proposed for the LE. Upon return 4 weeks later, all laboratory results were normal — full blood count (FBC), liver function test (LFT), urea and electrolytes (U&E) — or negative — antinuclear antibodies (ANA), antineutrophil cytoplasmic autoantibodies (ANCA), anti-DNA, QuantiFERON-TB (QFT), venereal disease research laboratory (VDRL) and fluorescent treponemal antibody absorption (FTA-ABS) test. The clinical picture was stable. Based on the ophthalmological findings, in the absence of correlated systemic conditions, a diagnosis of adult-onset Coats' disease with significant macular edema, exudative retinal detachment and posterior peripheral synechiae was established. The patient consented to the dexamethasone implant therapy (Ozurdex®) despite guarded prognosis given the longstanding macular edema. The intravitreal implant was injected, and the patient was given a follow-up visit in 2 weeks' time for IOP check and at 6 weeks for assessment of treatment response. IOP remained within normal limits and vision improved from LP to hand movement (HM), with reduction of retinal thickening on the follow-up SD-OCT (**Figure 6**).

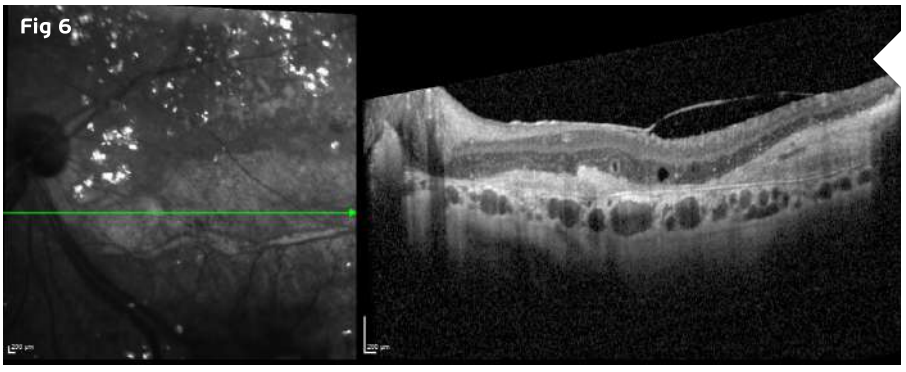

Figure 6: Spectralis SD-OCT (Heidelberg Engineering®) at 6 weeks post-Ozurdex® implantation, showing significant improvement with complete resolution of the cystoid macular edema. Hyper-reflective material corresponding to the hard-exudate plaque and evidence of retinal atrophy can be observed.

Differential Diagnosis of Adult-onset Coats' Disease

- IRVAN (idiopathic retinal vasculitis, aneurysms and neuroretinitis)
- sarcoidosis
- tuberculosis
- vasoproliferative tumors (e.g. retinal capillary hemangioma)
- Eales' disease
- sickle-cell retinopathy
- lipidemia retinalis (familial hypercholesterolemia)
- toxocariasis
- age-related macular degeneration
- diabetes
- hypertension
- retinoblastoma

Because adult-onset Coats' disease is a rare entity, diagnostic distinction must be made with more common conditions. The occurrence of retinal telangiectasis and exudation in adults, female patients, or bilaterally should prompt a search for non-Coats causes. Furthermore, a Coats'-like response may occur in patients with ocular inflammation, infection, retinal degeneration, and post radiation therapy. History and clinical presentation help differentiate such patients from the idiopathic form of retinal exudation with telangiectasia that characterizes Coats' disease.

Discussion and Literature

Coats' disease is an idiopathic, sporadic (non-hereditary) condition first described by Coats in 1908 as a retinal telangiectatic and aneurysmal disease associated with retinal exudation. Also referred to as idiopathic peripheral retinal telangiectasia (IPT), it typically presents in young male boys, usually younger than five years of age. More than 75% of patients are male, and 95% of cases are unilateral. There is no clear racial predilection.

The complete pathogenesis remains unclear but involves breaking of the blood-retinal barrier increasing vascular permeability and presence of abnormal pericytes leading to weakness of the vascular wall. There have been reports of localized mutations in proteins controlling retinal angiogenesis.

Coats' disease diagnosed in adulthood is an exudative retinopathy with different features from the childhood disorder. Vascular abnormalities are often present both peripherally and juxtamacular. Adults more commonly demonstrate localized lipid deposition and hemorrhage around macroaneurysms. Milder forms are more frequent, with slower disease progression, though loss of follow-up and lack of treatment may result in irreversible vision decline.

Clinical presentation in Coats' disease varies. Some patients may remain asymptomatic and be diagnosed by chance. Decreased vision is the most common presenting complaint. Some patients notice a defect in the visual field. Anterior segment signs such as those of uveitis may be present in advanced cases. Leukocoria is another possible finding and must push the differential diagnosis to diseases of higher morbimortality.

Coats' disease can be classified and staged using the Shields method (following the 2000 Proctor Lecture): Stage 1, retinal telangiectasia only; Stage 2, combined with retinal exudation (stage 2A, extrafoveal exudation; 3A2 foveal exudation); Stage 3, exudative retinal detachment (stage 3A, subtotal detachment; 3A1, extrafoveal only; 3A2 foveal detachment); stage 3B, total retinal detachment; Stage 4: total retinal detachment and glaucoma; Stage 5, advanced end-stage disease.

Vascular abnormalities in fellow eyes of patients with Coats' disease have been described, but may be asymptomatic and not necessarily progress over time. While observation is a reasonable initial management strategy, modern multimodal imaging allows the detection of even subtle vascular changes.

Due to the rarity of the diagnosis in adulthood, treatment protocols and clinical courses have not been clearly defined. The treatment regimen must be case-tailored, considering disease presentation, staging and outcomes. Combinations of intravitreal anti-VEGF, retinal photocoagulation and cryotherapy are the current mainstays. Intravitreal corticosteroids have been used to address macular edema and subretinal fluid. Epiretinal membrane and macular hole are possible long-term complications and must be managed accordingly.

Keep in mind

- ✓ Coats' disease is mainly a vascular retinopathy of young boys. Presentation in adulthood features less extensive involvement, more benign natural course, and more favorable treatment outcomes.
- ✓ Even in unilateral cases, the bilateral nature of Coats' disease reinforces the need for regular follow-up to detect a possible future involvement of the fellow eye.
- ✓ Management of adult-onset Coats' disease is case-based, considering the extension of involvement, disease staging, and response to treatment modalities.

References

1 Mandura RA & Alqahtani AS (2021). Coats' Disease Diagnosed During Adulthood. Cureus, 13(7), e16303. https://doi.org/10.7759/cureus.16303

2 Gawęcki M (2021). Idiopathic Peripheral Retinal Telangiectasia in Adults: A Case Series and Literature Review. Journal of clinical medicine, 10(8), 1767. https://doi.org/10.3390/jcm10081767

3 Ashkenazy N, Acon D, Kalavar M & Berrocal AM (2021). Optical coherence tomography angiography and multimodal imaging in the management of Coats' disease. American journal of ophthalmology case reports, 23, 101177. https://doi.org/10.1016/j.ajoc.2021.101177

4 Brockmann C, Löwen J, Schönfeld S, Rossel-Zemkouo M, Seibel I, Winterhalter S, Müller B & Joussen AM (2021). Vascular findings in primarily affected and fellow eyes of middle-aged patients with Coats' disease using multimodal imaging. The British journal of ophthalmology, 105(10), 1444–1453. https://doi.org/10.1136/bjophthalmol-2020-317101

5 Sen M, Shields CL, Honavar SG & Shields JA (2019). Coats disease: An overview of classification, management and outcomes. Indian journal of ophthalmology, 67(6), 763–771. https://doi.org/10.4103/ijo.IJO_841_19

6 Kumar K, Raj P, Chandnani N & Agarwal A (2019). Intravitreal dexamethasone implant with retinal photocoagulation for adult-onset Coats' disease. International ophthalmology, 39(2), 465–470. https://doi.org/10.1007/s10792-018-0827-0

7 Jeng-Miller KW, Soomro T, Scott NL, Rao P, Marlow E, Chang EY et al. (2019). Longitudinal Examination of Fellow-Eye Vascular Anomalies in Coats' Disease With Widefield Fluorescein Angiography: A Multicenter Study. Ophthalmic surgery, lasers & imaging retina, 50(4), 221–227. https://doi.org/10.3928/23258160-20190401-04

8 Sakurada Y, Freund KB & Yannuzzi LA (2018). Multimodal Imaging in Adult-Onset Coats' Disease. Ophthalmology, 125(4), 485. https://doi.org/10.1016/j.ophtha.2017.12.007

9 Li S, Deng G, Liu J, Ma Y & Lu H (2017). The effects of a treatment combination of anti-VEGF injections, laser coagulation and cryotherapy on patients with type 3 Coat's disease. BMC ophthalmology, 17(1), 76. https://doi.org/10.1186/s12886-017-0469-4

10 Kumar P & Kumar V (2017). Vitrectomy for epiretinal membrane in adult-onset Coats' disease. Indian journal of ophthalmology, 65(10), 1046–1048. https://doi.org/10.4103/ijo.IJO_322_17

11 Rishi E, Rishi P, Appukuttan B, Uparkar M, Sharma T & Gopal L (2016). Coats' disease of adult-onset in 48 eyes. Indian journal of ophthalmology, 64(7), 518–523. https://doi.org/10.4103/0301-4738.190141

12 Grosso A, Pellegrini M, Cereda MG, Panico C, Staurenghi G & Sigler EJ (2015). Pearls and pitfalls in diagnosis and management of Coats' disease. Retina (Philadelphia, Pa.), 35(4), 614–623. https://doi.org/10.1097/IAE.0000000000000485

13 Otani T, Yasuda K, Aizawa N, Sakai F, Nakazawa T & Shimura M (2011). Over 10 years follow-up of Coats' disease in adulthood. Clinical ophthalmology (Auckland, N.Z.), 5, 1729–1732. https://doi.org/10.2147/OPTH.S27938

Case 14 - June 2022

HERPETIC KERATITIS POST-COVID-19 INFECTION

A 31-year-old woman presented with corneal scarring after a SARS-CoV-2 infection.

Presented by
Miltos Balidis, MD, PhD, FEBOphth, ICOphth

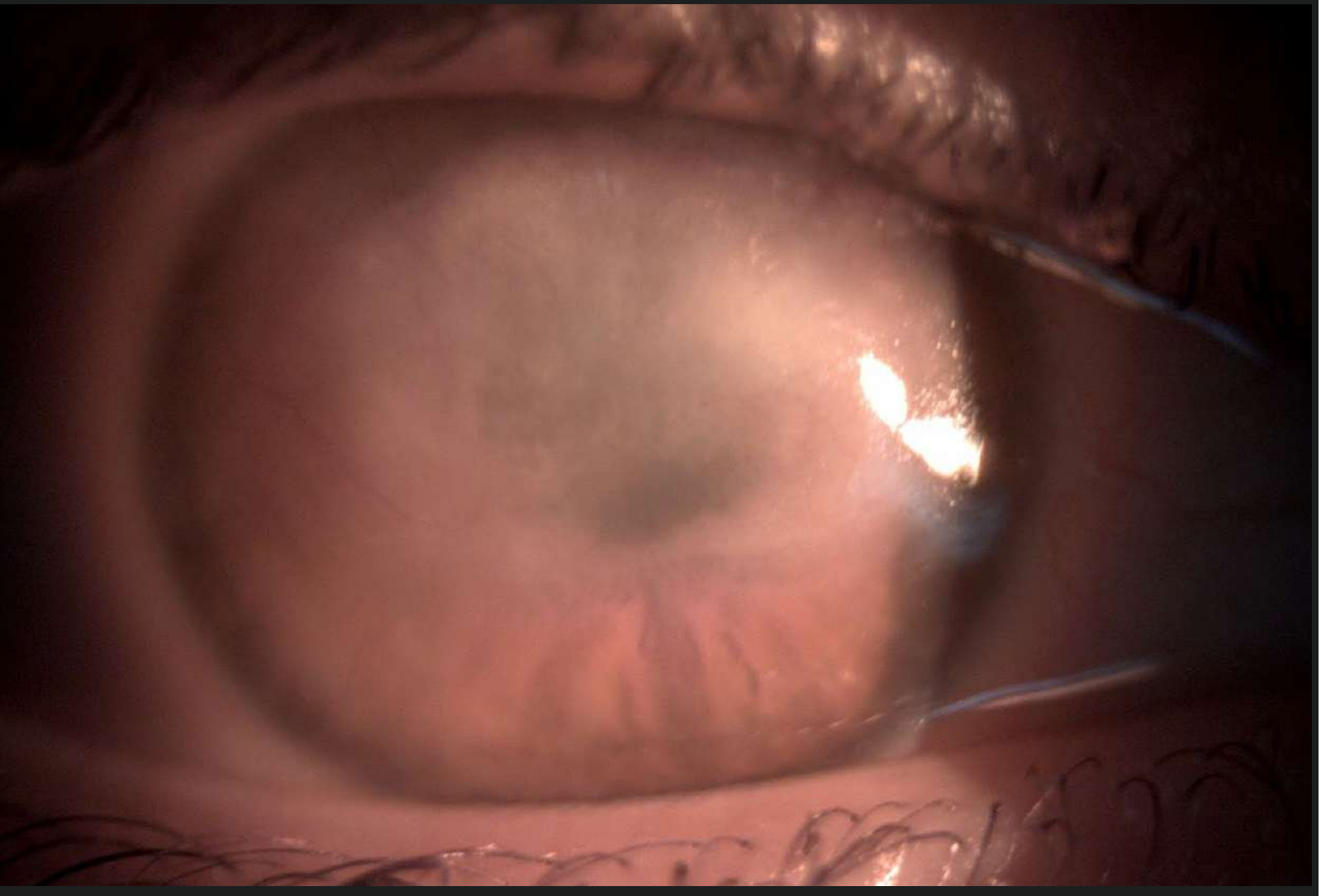

Edited by
Penelope Burle de Politis, MD

Case History

A 31-year-old Caucasian woman presented with extensive corneal scarring in the right eye (RE) after a 2-month permanence at an intensive care unit (ICU) for Severe Acute Respiratory Syndrome Coronavirus 2 (SARS-CoV-2). The patient had been treated with an eye drop combination of gentamicin and dexamethasone. She had no previous history of ocular diseases or visual deficiency. Her family history was unremarkable. Ophthalmological examination revealed a corrected distance visual acuity (CDVA) of finger count (FC) in the RE and 10/10 in the left eye (LE). Under biomicroscopy, the RE featured extensive stromal fibrosis involving the upper ⅔ of the cornea, measuring 10 x 4 mm in the largest axes (**Figure 1**), compromising the pupillary area, with residual stromal infiltrates and neovascularization at 180° of the corneal circumference (**Figure 2**). Intraocular pressure was 17 mmHg in the RE and 15 mmHg in the LE. Fundoscopy was unfeasible in the RE but normal in the LE.

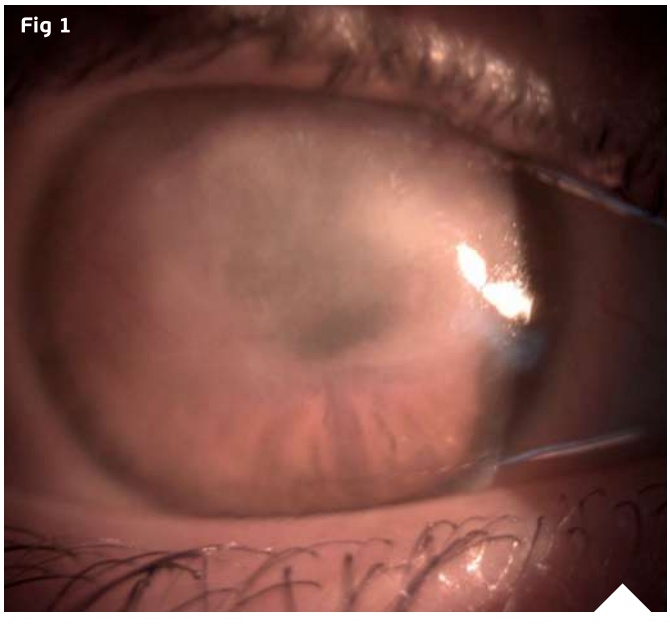

Figure 1: Wide beam slit lamp photography of the right eye displaying diffuse scarring of the corneal upper two thirds.

Figure 2: Slit lamp photography with a higher magnification showing sparse stromal infiltrates at the mid-periphery of the cornea and prominent neovascularization over the area of corneal scarring.

Anterior segment spectral domain optical coherence tomography (anterior SD-OCT) showed diffuse reduction of corneal pachymetry (Figure 3), indicating that the scar had developed over a ground of previous tissue loss, probably corneal melting.

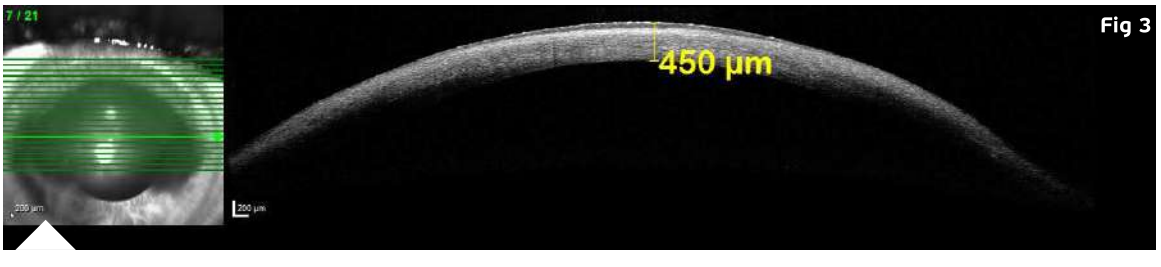

Figure 3: Anterior SD-OCT (Heidelberg Engineering®) of the RE showing the change in corneal architecture with extensive thinning (central pachymetry of 450 µm).

The patient was put on dexamethasone drops for the RE every 4 hours and scheduled for review in 8 weeks. Upon return, UCVA had improved to 0.3/10. Corneal pachymetry remained stable, and the infiltrates were no longer noticeable; therefore, a slow tapering of the corticotherapy was started.

However, on a second follow-up visit 3 weeks later, the patient presented with a hyperemic RE of a week duration, and the biomicroscopic examination revealed new corneal infiltrates (**Figure 4**).

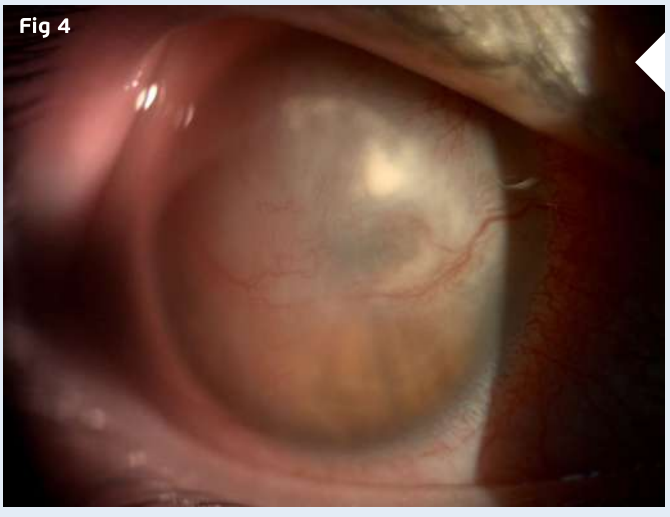

Figure 4: Slit lamp photography of the RE showing a broad stromal infiltrate involving the whole superior nasal quadrant of the cornea, with diffuse conjunctival injection and exacerbation of the neovessels in the area of corneal scarring.

Additional History

The patient had a history of labial herpes. Even though the lesion was not typical of an intermediate herpetic keratitis, the absence of other risk factors such as trauma or contact lens wear, added to the corneal change with diffuse thinning, scarring and neovessels, led to the suspicion of a herpetic etiology. For this reason, the dexamethasone drops were restarted and valacyclovir p.o. (1g b.i.d.) was added to the drug regimen.

A week later, the infiltrates had subsided, vision was stable and there was no evidence of further corneal thinning on the OCT. Due to the temporal correlation with the ICU admission for SARS-CoV-2 treatment and considering the numerous reports on increased susceptibility and reactivation of latent infection by the entire herpesviridae family in COVID-19 patients, the diagnosis of severe herpetic keratitis induced by SARS-CoV-2 was established.

Medication was sustained according to the current protocols for intermediate herpetic keratitis, and the patient will be checked-up closely for the regression of the acute corneal picture, so that a plan can be drawn in the future in order to improve her visual acuity in the affected eye.

Differential Diagnosis of Corneal Scarring

- trauma
- chemical injuries
- infections (viral, fungal, bacterial, protozoal)
- surgeries
- dystrophies
- keratoconus
- ocular surface disorders (e.g., severe dry eye)
- ocular cicatricial pemphigoid

The differentiation among the possible causes of corneal scarring is crucial in determining an accurate diagnosis and proper management. Knowledge of the pathophysiological basis of tissue scarring, a thorough history (present and past, ocular and systemic), and careful corneal examination including high-resolution methods may be extremely useful in guiding the ophthalmologist towards the right etiology.

Discussion and Literature

Injuries to the cornea produce varying amounts of corneal scarring depending on the magnitude of cellular and molecular responses to injury. The pathophysiological process that leads to corneal scarring can be attributable to corneal fibroblast and/or myofibroblast generation, with or without neovascularization (as triggered by hypoxia, inflammation, and/or infection), typically following trauma, chemical burns, infections, surgeries, and corneal or ocular surface disorders.

One of the most prevalent infectious causes of corneal scarring is herpes simplex. The virus can manifest at any of the corneal layers, leading to more or less severe complications depending on the depth and extension of corneal involvement. Stromal herpetic keratitis is a leading cause of corneal scarring, with the consequent loss of corneal transparency and visual acuity.

COVID-19 and anti-COVID-19 vaccines have been proved to affect the eye in several different ways, ranging from mild conjunctivitis to corneal graft rejection. Among COVID-19 patients, the prevalence of ophthalmic manifestations ranges from 2-32%. The mechanism involved in each ocular manifestation can be of inflammatory and/or immunological basis. It has been shown that corneal and conjunctival cells show co-expression of the TMPRSS2 and ACE2 genes involved in COVID-19 infection, though at a lower concentration than in other tissues such as the nasal cavity or lung parenchyma. Acute-onset bilateral interstitial keratitis induced by COVID-19 has been reported.

Recent findings have pointed to a clear association between COVID-19 and an increased incidence of cases involving the entire herpesviridae family (i.e., Epstein-Barr virus, cytomegalovirus, varicella-zoster virus, herpes simplex virus, human-herpes viruses, Kaposi's sarcoma virus), especially in critically ill patients. It is possible that the use of corticosteroids in the management of COVID-19 infection facilitates the emergence of herpes as an opportunistic manifestation. Moreover, it has been demonstrated that some of the new antiviral drugs used to treat SARS-CoV-2 infection can induce reactivation of some of the herpesviridae viruses. Reactivation of herpes viruses has also been reported following anti-COVID-19 vaccination.

Though presently limited to a few case reports, the induction of corneal herpes is a potential COVID-19-associated condition, which may present either during the acute or in the convalescent phase of the illness. In mild cases, COVID-19-induced herpetic keratitis can be restricted to the epithelium and subside leaving no scarring or visual loss. However, in patients staying in ICUs due to SARS-CoV-2, the possibility of deeper corneal involvement must always be considered in order to ensure prompt management, thus avoiding or minimizing vision-threatening corneal opacification. Differential diagnosis with other infectious etiologies facilitated by SARS-CoV-2 must be made, notably fungus and atypical opportunistic microorganisms. Polymerase chain reaction (PCR) tests and even biopsy may be necessary in doubtful or refractory cases.

Keep in mind

- ✓ Herpetic keratitis is one the most common causes of corneal scarring.
- ✓ COVID-19 increases susceptibility to infection and reactivation of latent viruses of the entire herpesviridae family, including herpes simplex in the eye.
- ✓ COVID-19 and its related vaccines must now be considered among the possible etiologies of acute ocular manifestations of obscure causes.

References

1 Wilson SE, Sampaio LP, Shiju TM, Hilgert G & de Oliveira RC (2022). Corneal Opacity: Cell Biological Determinants of the Transition From Transparency to Transient Haze to Scarring Fibrosis, and Resolution, After Injury. Investigative ophthalmology & visual science, 63(1), 22. https://doi.org/10.1167/iovs.63.1.22

2 Sen M, Honavar SG, Sharma N & Sachdev MS (2021). COVID-19 and Eye: A Review of Ophthalmic Manifestations of COVID-19. Indian journal of ophthalmology, 69(3), 488–509. https://doi.org/10.4103/ijo.IJO_297_21

3 Balidis M, Mikropoulos D, Gatzioufas Z, de Politis PB, Sidiropoulos G & Vassiliadis V (2021). Acute corneal graft rejection after anti-severe acute respiratory syndrome-coronavirus-2 vaccination: A report of four cases. European journal of ophthalmology, 11206721211064033. Advance online publication. https://doi.org/10.1177/11206721211064033

4 Schnichels S, Rohrbach JM, Bayyoud T, Thaler S, Ziemssen F & Hurs J (2021). Can SARS-CoV-2 infect the eye? An overview of the receptor status in ocular tissue. Kann SARS-CoV-2 das Auge infizieren? – Ein Überblick über den Rezeptorstatus in okularem Gewebe. English version. Der Ophthalmologe : Zeitschrift der Deutschen Ophthalmologischen Gesellschaft, 118(Suppl 1), 81–84. https://doi.org/10.1007/s00347-020-01281-5

5 Cano-Ortiz A, Leiva-Gea I, Ventosa ÁS, González-Cruces T, Sánchez-González JM, Morales P & Villarrubia A (2022). Stromal interstitial keratitis in a patient with COVID-19. Journal français d'ophtalmologie, 45(4), e175–e177. https://doi.org/10.1016/j.jfo.2021.11.004

6 Le Balc'h P, Pinceaux K, Pronier C, Seguin P, Tadié JM & Reizine F (2020). Herpes simplex virus and cytomegalovirus reactivations among severe COVID-19 patients. Critical care (London, England), 24(1), 530. https://doi.org/10.1186/s13054-020-03252-3

7 Honore PM, Barreto Gutierrez L, Kugener L, Redant S, Attou R, Gallerani A & De Bels D (2020). SARS-CoV-2 infection as a risk factor for herpesviridae reactivation: consider the potential influence of corticosteroid therapy. Critical care (London, England), 24(1), 623. https://doi.org/10.1186/s13054-020-03349-9

8 Simonnet A, Engelmann I, Moreau AS, Garcia B, Six S, El Kalioubie A, Robriquet L, Hober D & Jourdain M (2021). High incidence of Epstein-Barr virus, cytomegalovirus, and human-herpes virus-6 reactivations in critically ill patients with COVID-19. Infectious diseases now, 51(3), 296–299. https://doi.org/10.1016/j.idnow.2021.01.005

9 Im JH, Nahm CH, Je YS, Lee JS, Baek JH, Kwon HY, Chung MH, Jang JH, Kim JS, Lim JH & Park MH (2022). The effect of Epstein-Barr virus viremia on the progression to severe COVID-19. Medicine, 101(18), e29027. https://doi.org/10.1097/MD.0000000000029027

10 Chen J, Dai L, Barrett L, James J, Plaisance-Bonstaff K, Post SR & Qin Z (2021). SARS-CoV-2 proteins and anti-COVID-19 drugs induce lytic reactivation of an oncogenic virus. Communications biology, 4(1), 682. https://doi.org/10.1038/s42003-021-02220-z

11 Fathy R A, McMahon D E, Lee C, Chamberlin GC, Rosenbach M, Lipoff JB, Tyagi A, Desai SR, French LE, Lim HW, Thiers BH, Hruza GJ, Fassett M, Fox LP, Greenberg HL, Blumenthal K & Freeman EE (2022). Varicella-zoster and herpes simplex virus reactivation post-COVID-19 vaccination: a review of 40 cases in an International Dermatology Registry. Journal of the European Academy of Dermatology and Venereology : JEADV, 36(1), e6–e9. https://doi.org/10.1111/jdv.17646

12 Majtanova N, Kriskova P, Keri P, Fellner Z, Majtan J & Kolar P (2021). Herpes Simplex Keratitis in Patients with SARS-CoV-2 Infection: A Series of Five Cases. Medicina (Kaunas, Lithuania), 57(5), 412. https://doi.org/10.3390/medicina57050412

13 Das N, Das J & Pal D (2022). Stromal and endothelial herpes simplex virus keratitis reactivation in the convalescent period of COVID-19 - A case report. Indian journal of ophthalmology, 70(4), 1410–1412. https://doi.org/10.4103/ijo.IJO_2838_21

14 You IC, Ahn M & Cho NC (2022). A Case Report of Herpes Zoster Ophthalmicus and Meningitis After COVID-19 Vaccination. Journal of Korean medical science, 37(20), e165. https://doi.org/10.3346/jkms.2022.37.e165

15 Roy A, Chaurasia S, Ramappa M, Joseph J & Mishra DK (2022). Clinical profile of keratitis treated within 3 months of acute COVID-19 illness at a tertiary care eye center. International ophthalmology, 1–9. Advance online publication. https://doi.org/10.1007/s10792-022-02288-4

Case 15 - August 2022

UVEITIS-GLAUCOMA-HYPHEMA SYNDROME

A 72-year-old man was referred for intermittent unilateral blurry vision for several months.

Presented by
Paris Tranos, MD, PhD, ICOphth, FRCS

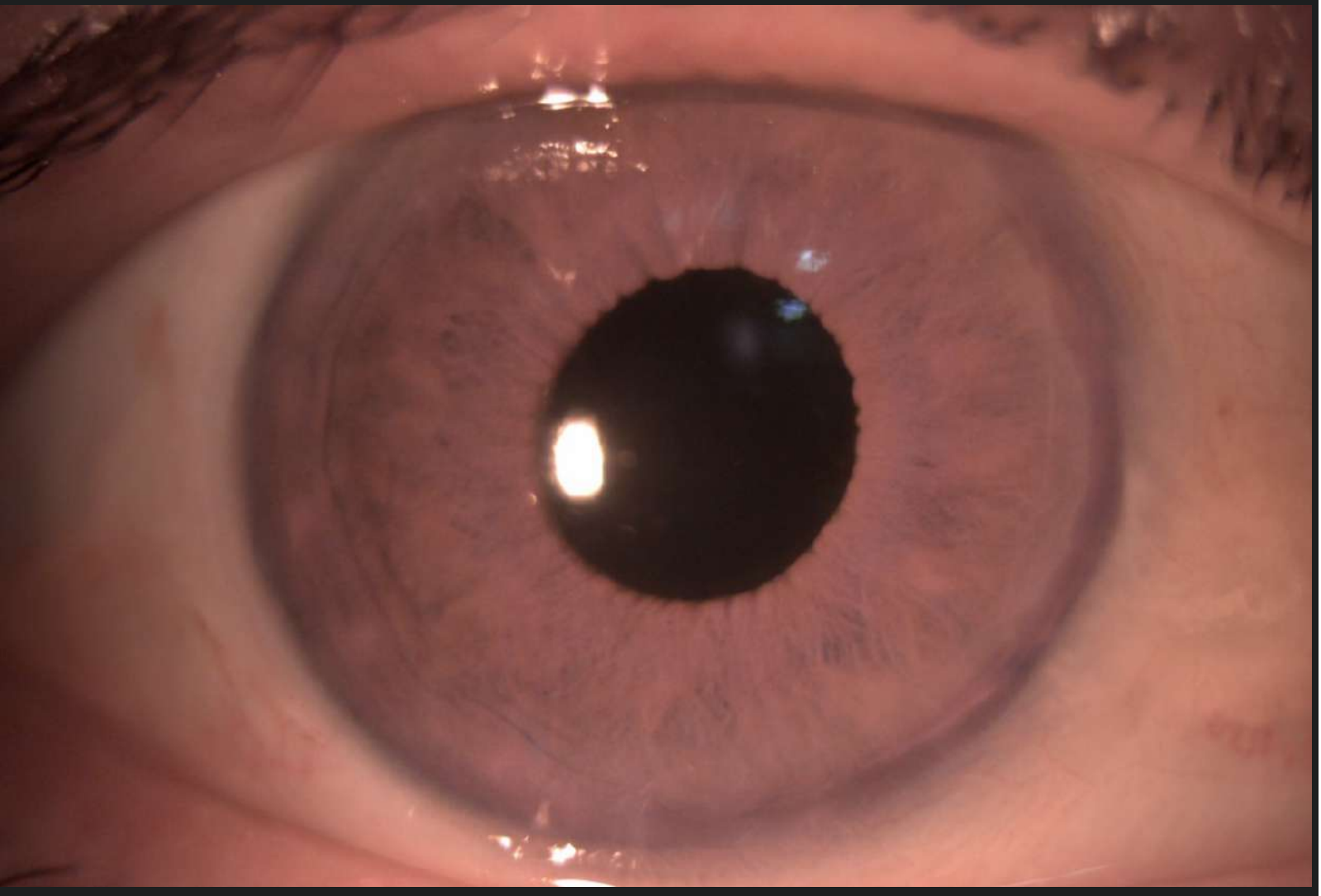

Edited by
Penelope Burle de Politis, MD

Case History

A 72-year-old Caucasian man was referred for intermittent blurred vision in the right eye (RE) over the course of several months, as well as long-standing floaters with periods of exacerbation. His clinical picture had been attributed to a recurrent hypertensive anterior uveitis of unknown cause which was being managed with the use of topical dexamethasone, tropicamide and a combination of timolol and dorzolamide.

The patient had undergone phacoemulsification with intraocular lens (IOL) implantation in the right eye 5 years before. His family history was unremarkable. On examination, his corrected distance visual acuity (CDVA) was 7/10 in both eyes (BE). Biomicroscopy revealed pseudophakia with a discrete irregularity of the pupillary roundness in the RE (**Figure 1**) and a moderate nuclear cataract in the left eye (LE). Both eyes had signs of pseudoexfoliation syndrome (PXE) and a moderate inflammatory anterior chamber reaction (cells+) was detected in the RE. There was no evidence of iris transillumination defects, nodules or keratic precipitates. Intraocular pressure was within normal limits in BE. Fundoscopy revealed bilateral cellophane epiretinal membrane and a vitreous hemorrhage with an atypical location at the superotemporal quadrant of the RE (**Figure 2**).

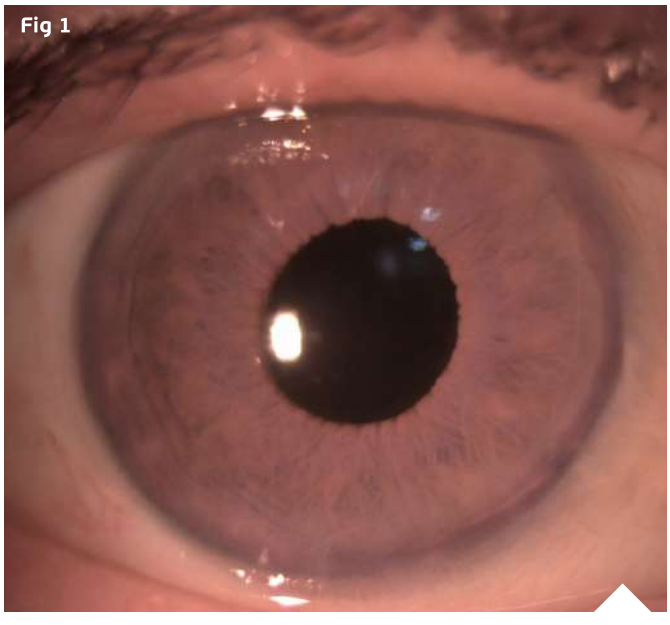

Figure 1: Color slit-lamp photograph of the right eye displaying pseudophakia and a slightly irregular pupil.

Figure 2: Color fundus photograph of the right eye (EIDON true-color confocal scanner®) showing a mild vitreous hemorrhage at the superotemporal retinal periphery.

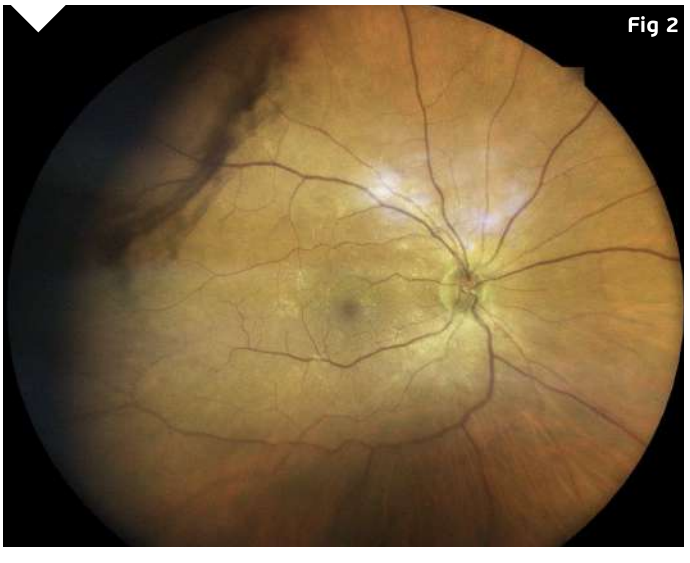

Fundus fluorescein angiography (FFA) showed a “hot disc” in the RE, with mild fluorescein leakage at the macula but without retinal vasculitis. (**Figure 3**).

Figure 3: FFA of the RE (Heidelberg Engineering®) demonstrating a "hot disc" and a focal leakage at the macula.

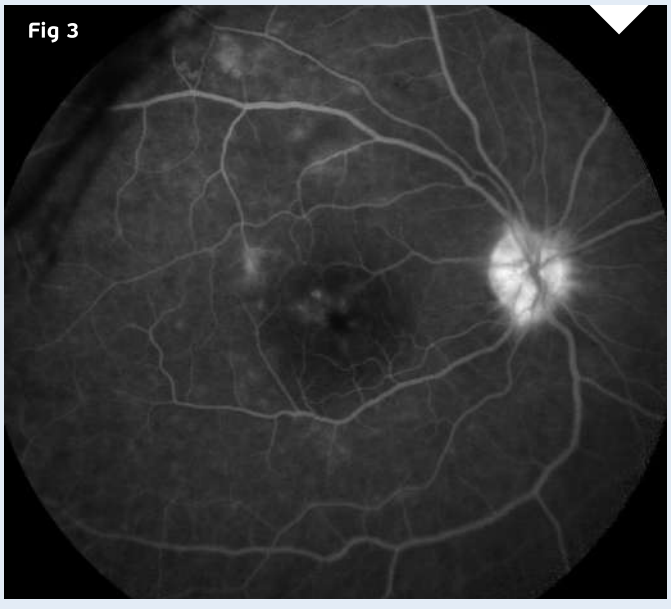

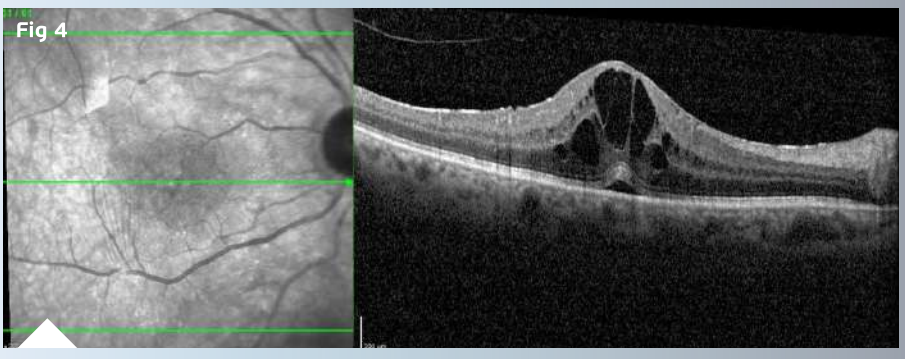

Figure 4: SD-OCT of the RE showing the presence of intraretinal fluid and cysts at the macula.

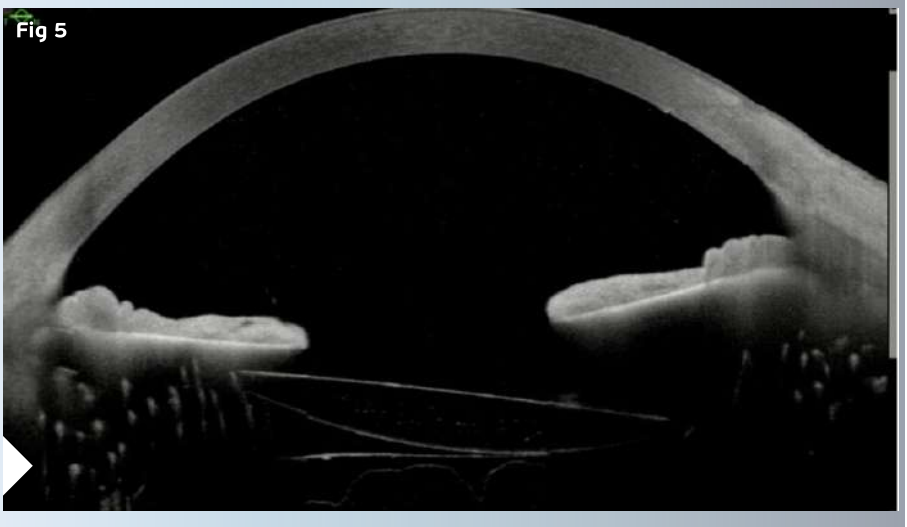

Figure 5: SD-OCT of the RE showing the presence of intraretinal fluid and cysts at the macula.

Spectral domain optical coherence tomography (SD-OCT) confirmed the presence of cystoid macular edema (CME) in the RE (**Figure 4**).

An anterior segment OCT (AS-OCT) was obtained, revealing a significant tilt of the IOL in relation to the pupillary plane, resulting in posterior iris touch and friction during normal iris excursion (**Figure 5**).

Differential Diagnosis

- trauma (e.g. blunt)
- hypertensive uveitis (e.g. herpetic)
- IOL subluxation due to underlying PXE syndrome
- proliferative retinal vascular occlusions (e.g. retinal vein occlusion, diabetic retinopathy, sickle cell disease)
- coagulation disorders
- uveitis-glaucoma-hyphema (UGH) Syndrome

The presence of iris chafing by the tilted IOL, in conjunction with hypertensive anterior uveitis and vitreous hemorrhage is consistent with the diagnosis of UGH syndrome.

Additional History

A full blood and imaging investigation was performed to exclude underlying infections and systemic inflammatory conditions, rendering negative results. Based on the clinical presentation and imaging findings, with a tilted IOL chafing the iris, along with a hypertensive anterior uveitis and vitreous hemorrhage, the diagnosis of uveitis-glaucoma-hyphema (UGH) Syndrome was established.

The patient was treated with topical steroid and non-steroid anti-inflammatory agents and topical antiglaucoma medication. Topical cyclopentolate was added to the drug regimen to reduce iris rubbing by the IOL.

Two months later, the CME and vitreous hemorrhage had resolved, IOP was within normal limits and there was no evidence of anterior chamber reaction. Tapering of dexamethasone and nepafenac was initiated. The antiglaucoma drops were discontinued but cyclopentolate was maintained.

The patient remains stable and there are no longer signs of active ocular inflammation. Due to the favorable outcome, no surgical intervention for IOL exchange has been planned for the moment.

Discussion and Literature

Uveitis glaucoma hyphema (UGH) or Ellingson syndrome is a relatively rare condition characterized by chronic inflammation, pigment dispersion, raised IOP, and intraocular hemorrhage in an eye that has undergone cataract surgery with IOL implantation. It is a late postoperative complication where the cause of inflammation is mechanical irritation to the iris and other intraocular structures due to chafing by the implants. It was first described in 1978 as related to rigid anterior chamber intraocular lens (ACIOL), but almost all anterior segment implants may be associated with UGH syndrome, including iris-sutured IOL, retropupillary iris-claw IOL, cosmetic iris implants, capsular tension rings, glaucoma filtration devices, scleral fixated lenses, IOL placed in the sulcus, and even the most modern single-piece posterior chamber IOL (PCIOL) placed in the bag.

IOL quality plays a significant role in the pathophysiology of UGH syndrome. Poor finishing of the edges (serrated, sharpened, or uneven), warped footplates, and imperfect polishing of injection-molded IOLs may all lead to recurrent mechanical excoriation of the iris, anterior chamber angle or ciliary body, hence disrupting the blood-aqueous barrier and leading to uveitis. Mechanical trauma to the iris by IOL optics or haptics induces the inflammatory cascade through complement and fibrin activation. Bacteria, leukocytes and red blood cells (RBCs) may adhere to the IOL surface, causing lens discoloration. A thick membrane of inflammatory debris (“cocoon”) may develop, totally or partially covering the optic, haptic or footplate of the IOL.

Patients with PXE have a higher risk of developing UGH syndrome, either by pseudophacodonesis due to the zonular laxity (resulting in chafing of the posterior iris surface), or by focal capsular fibrosis around the haptic causing iris touch. The rise in IOP may be caused by various factors, including hyphema, uveitis, pigment dispersion, direct damage to the anterior chamber angle, and steroid response to therapy. A high IOP at the first hemorrhage increases the risk for needing subsequent IOP-lowering therapy.

UGH syndrome may occur after uneventful ocular surgery or after an ocular surgery with intraoperative complications resulting in malposition of the implant. Patients usually present with multiple acute episodes of blurred vision weeks to months after surgery, in an intermittent white-out of vision or intermittent decreased vision fashion.

Gonioscopy can be valuable in the workup of UGH syndrome because it may disclose blood in the trabecular meshwork between attacks. However, the gold standard diagnostic modality for the condition is anterior segment imaging. It helps document the disease, monitor the response to therapy and counsel the patient. Anterior segment OCT and/or ultrasound biomicroscopy (UBM) may confirm the position of haptics and optics and their proximity to uveal tissue. B-Scan ultrasound is helpful in the diagnosis of cases presenting with vitreous hemorrhage. OCT of the macula can be used to detect CME. FFA helps to rule out the other causes of vitreous hemorrhage or iris new vessels. All the other causes of uveitis need to be ruled out. A coagulation profile and a history of anticoagulant medications should be sought in cases with recurrent hyphema.

The management of UGH Syndrome must be case-tailored, depending upon the cause. Antiglaucoma medications (topical and systemic if necessary) and corticosteroids are used to lower intraocular pressure and control anterior segment inflammation. Adjuvant therapy in the form of non-steroidal anti-inflammatory drugs and cycloplegics is also helpful in relieving pain due to ciliary and iris sphincter spasm, bringing symptomatic relief to the patient and preventing IOL-iris friction. Miotics (including pilocarpine) should be avoided as they increase the mechanical chafing of the iris.

UGH syndrome is one of the most common indications (around 12%) of IOL exchange. IOL exchange is the definitive treatment but may not guarantee the resolution of UGH syndrome. IOL exchange, explant, repositioning, or amputation of IOL haptic should be performed if the inflammation is not controlled medically and the vision is reduced.

Keep in mind

- ✓ UGH syndrome must be considered in the differential diagnosis of recurrent uveitis in every eye submitted to cataract surgery with IOL implantation.
- ✓ Accurate diagnosis and prompt intervention in UGH episodes is essential to prevent long-term vision-threatening complications.
- ✓ Removal of the causative device is required in severe cases when unresponsive to clinical treatment.

References

1 Sen S, Tripathy K. Uveitis Glaucoma Hyphema Syndrome. [Updated 2022 Mar 1]. In: StatPearls [Internet]. Treasure Island (FL): StatPearls Publishing; 2022 Jan-. Available from: https://www.ncbi.nlm.nih.gov/books/NBK580530/

2 Accorinti M, Saturno MC, Paroli MP, De Geronimo D & Gilardi M (2021). Uveitis-Glaucoma-Hyphema Syndrome: Clinical Features and Differential Diagnosis. Ocular immunology and inflammation, 1–6. Advance online publication. https://doi.org/10.1080/09273948.2021.1881563

3 Zemba M & Camburu G (2017). Uveitis-Glaucoma-Hyphaema Syndrome. General review. Romanian journal of ophthalmology, 61(1), 11–17. https://doi.org/10.22336/rjo.2017.3

4 Armonaite L & Behndig A (2021). Seventy-one cases of uveitis-glaucoma-hyphaema syndrome. Acta ophthalmologica, 99(1), 69–74. https://doi.org/10.1111/aos.14477

5 Badakere SV, Senthil S, Turaga K & Garg P (2016). Uveitis-glaucoma-hyphaema syndrome with in-the-bag placement of intraocular lens. BMJ case reports, 2016, bcr2015213745. https://doi.org/10.1136/bcr-2015-213745

6 Lippera M, Nicolosi C, Vannozzi L, Bacherini D, Vicini G, Rizzo S, Virgili G & Giansanti F (2022). The role of anterior segment optical coherence tomography in uveitis-glaucoma-hyphema syndrome. European journal of ophthalmology, 32(4), 2211–2218. https://doi.org/10.1177/11206721211063738

7 Alfaro-Juárez A Vital-Berral C, Sánchez-Vicente JL, Alfaro-Juárez A & Muñoz-Morales A (2015). Uveitis-glaucoma-hyphema syndrome associated with recurrent vitreous hemorrhage. Archivos de la Sociedad Espanola de Oftalmologia, 90(8), 392–394. https://doi.org/10.1016/j.oftal.2014.11.007

8 Zhang L, Hood CT, Vrabec JP, Cullen AL, Parrish EA & Moroi SE (2014). Mechanisms for in-the-bag uveitis-glaucoma-hyphema syndrome. Journal of cataract and refractive surgery, 40(3), 490–492. https://doi.org/10.1016/j.jcrs.2013.12.002

9 Rajak SN, Bahra A, Aburn NS, Warden NJ & Mossman SS (2007). Recurrent anterior chamber hemorrhage from an intraocular lens simulating amaurosis fugax. Journal of cataract and refractive surgery, 33(8), 1492–1493. https://doi.org/10.1016/j.jcrs.2007.04.018

10 Cates CA & Newman DK (1998). Transient monocular visual loss due to uveitis-glaucoma-hyphaema (UGH) syndrome. Journal of neurology, neurosurgery, and psychiatry, 65(1), 131–132. https://doi.org/10.1136/jnnp.65.1.131

11 Asaria RH, Salmon JF, Skinner AR, Ferguson DJ & McDonald B (1997). Electron microscopy findings on an intraocular lens in the uveitis, glaucoma, hyphaema syndrome. Eye (London, England), 11 (Pt 6), 827–829. https://doi.org/10.1038/eye.1997.213

12 Van Liefferinge T, Van Oye R & Kestelyn P (1994). Uveitis-glaucoma-hyphema syndrome: a late complication of posterior chamber lenses. Bulletin de la Société belge d'ophtalmologie, 252, 61–66.

Case 16 - October 2022

NEUROFIBROMATOSIS TYPE 2

A 9-year-old boy with monocular vision presented with reduction of visual acuity in his previously normal eye.

Presented by
Lambros Lambrogiannis, MD, MSc, PhD, FEBO
Solon Asteriades, MD, FRCS
& Zachos Zacharidis, MD, DO

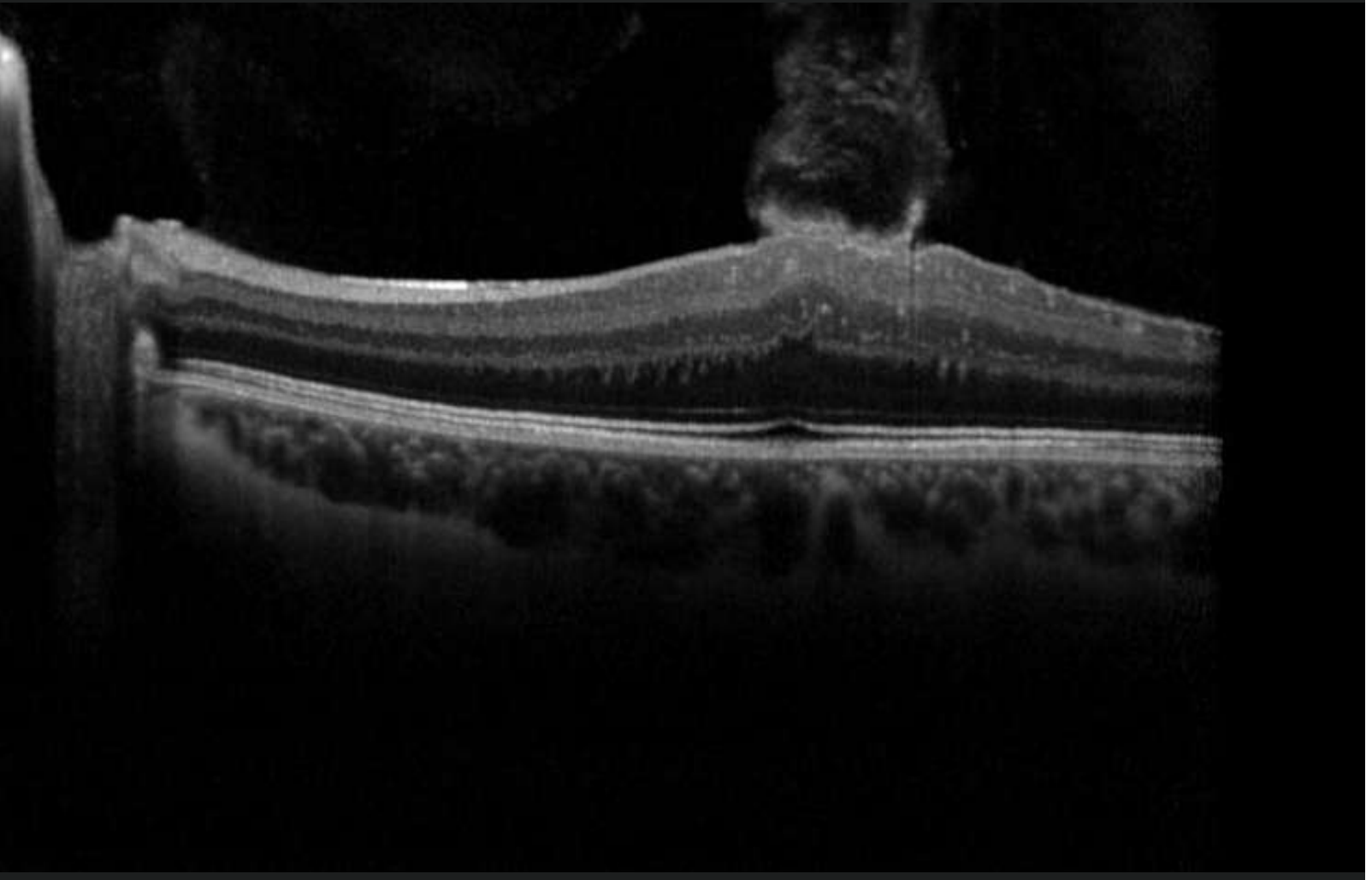

Edited by
Penelope Burle de Politis, MD

Case History

A 9-year-old Caucasian boy was diagnosed with an optic nerve meningioma in the right eye (RE) 4 years ago. Further investigation had revealed a second neural tumor elsewhere, leading to the diagnosis of neurofibromatosis type II. At the time of diagnosis, the patient underwent a decompressive procedure for the optic neural tumor – fenestration – but the condition ultimately progressed to optic nerve atrophy in that eye.

Upon referral for ophthalmologic examination, best-corrected visual acuity (BCVA) in the left eye (LE) was 7/10. Spectral-domain optical coherence tomography (SD-OCT) of the LE displayed a flame-shaped macular tuft of epiretinal tissue projecting into the vitreous chamber (**Figure 1**). An identical lesion as found in the RE (**Figure 2**), aside from an atrophic optic papilla (**Figure 3**).

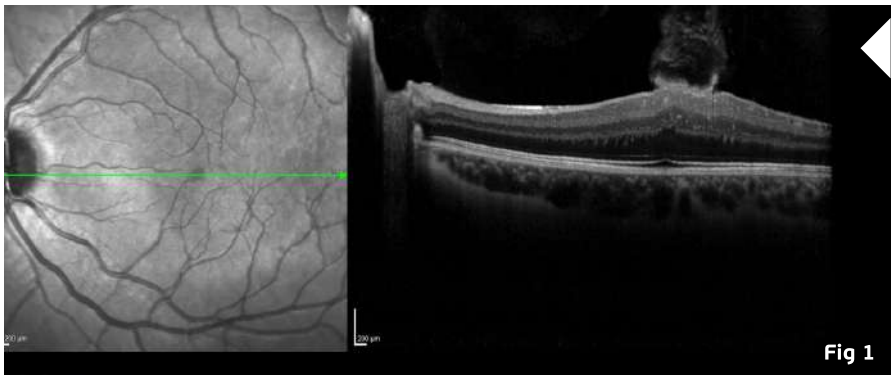

Figure 1: Spectralis SD-OCT (Heidelberg Engineering®) of the left eye featuring a macular tuft and loss of foveal contour.

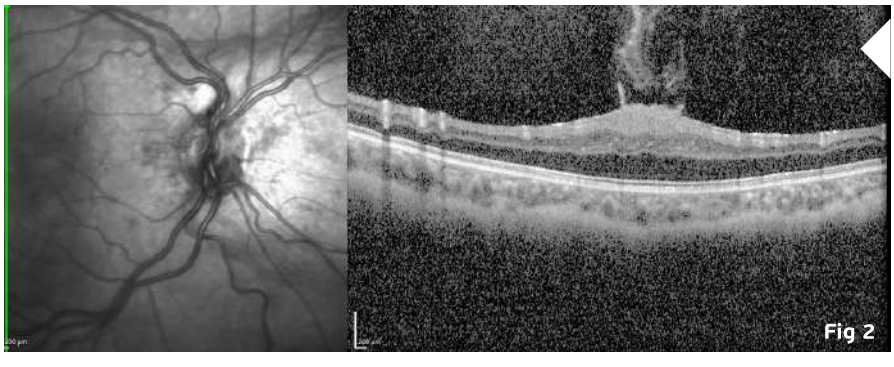

Figure 2: SD-OCT of the RE displaying an atrophic optic papilla and a macular tuft of epiretinal tissue projecting into the vitreous chamber. Notice the loss of foveal depression, increased retinal thickness, absence of cystoid spaces or retinal pigment epithelium (RPE) disruption, and preservation of the inner segment-outer segment junction.

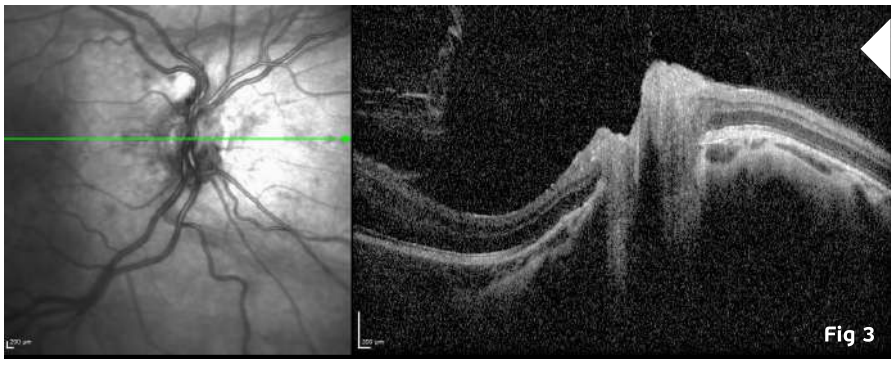

Figure 3: SD-OCT of the RE showing distortion of the optic papilla and peripapillary atrophy.

Differential Diagnosis

- combined hamartoma of the retina and RPE
- proliferative vitreoretinopathy
- tractional retinal detachment
- familial exudative vitreoretinopathy
- non-specific epiretinal membrane (e.g., idiopathic, traumatic, uveitic)

The characteristic aspect of the epiretinal membrane, in a flame-shaped disposition directed towards the vitreous center, is considered specific and diagnostic of neurofibromatosis type 2.

Additional History

A careful assessment of the pediatric and developmental status of the patient was conducted. Considering the child's stable general health condition and absence of significant behavioral distress, a conservative approach was discussed and decided along with his parents. Close interdisciplinary monitoring for disease progression and eventual necessary interventions will be kept for the moment.

Discussion and Literature

Neurofibromatosis type 2 (NF2) is an autosomal dominant, single-gene disorder, caused by either sporadic (more frequent) or inherited pathogenic variants of the NF2 gene on chromosome 22. The incidence of NF2 is reported to be as high as 1 in 25,000 individuals in 2 large population studies — in Finland and in England. NF2 is characterized by the development of schwannomas — especially vestibular —, meningiomas, and ependymomas. The classical phenotype of NF2 also includes ocular features such as cataracts, retinal abnormalities — retinal hamartomas with or without RPE involvement —, epiretinal membranes (ERMs), paralytic strabismus, optic disk gliomas, and optic nerve sheath meningiomas.

Symptoms and signs relating to vestibular schwannomas are not always the presenting feature in NF2, even less so in children, who more commonly manifest eye, skin, or neurological problems. The detection of ocular features can aid in the clinical diagnosis of NF2 and prompt early genetic testing. The recent identification of numerous retinal abnormalities by SD-OCT suggests that the retinal features of NF2 may be more common than previously thought. They are also more common in more severe NF2 genotypes, as captured by the UK NF2 Genetic Severity Score — 1. tissue mosaic; 2A. mild classic; 2B moderate classic; 3. severe.

SD-OCT imaging-based studies have been able to characterize retinal findings in patients with NF2 in greater detail than previously possible and to identify novel retinal abnormalities such as retinal tufts specific to NF2. These are projections of tissue extending from the inner retina into the vitreous and occur far more commonly than typical ERMs in these patients.

Often resembling horns or flames, they are thought to be either focal ERMs or small elevations of retinal tissue, termed subclinical hamartomas due to their small size, with similar histopathologic origin — from glial cells. Increased central macular thickness is another feature of the ocular abnormalities associated with NF2, apparently less prominent when optic atrophy is present.

Potentially treatable sources of damage to vision must be identified early and treated effectively to retain useful vision throughout life. There are no standard guidelines for treating NF2 patients with ERMs. Observation and surgical intervention are the current treatment choices. Macular tufts can be peeled through microincision vitrectomy surgery (MIVS) but may pose a challenge when deeply integrated into the retina as retinal damage or tears may ensue. Even with complete removal of the ERM, the abnormally thickened macula may remain unchanged even after years postoperatively. Postoperative visual outcomes have been reported for only 3 cases so far. Although surgery can improve retinal sensitivity and visual acuity, the potential surgical risks related to vitreoretinal surgery in pediatric eyes require careful consideration on a case-by-case basis. A significant decrease in quality of life, as impairment for regular activities or performance at school, may justify the decision for a surgical intervention.

Insights into the molecular biology of NF2 have shed light on the etiology and variable severity of the disease and suggested numerous putative molecular targets for therapeutic intervention. Chromosome 22q12.1, whose mutation is involved in the pathogenesis of NF2, encodes for a protein called merlin or schwannomin, in the merlin pathway. Multiple additional pathways have been identified, and pre-clinical and clinical investigation of novel therapeutic agents including FAK, EGFR, cMET, PD-1/PD-L1, and VEGFR inhibitors is underway. Biological treatment strategies aimed at multiple tumor regression or arrest of progression — employing Lapatinib, Erlotinib, Everolimus, Picropodophyllin, OSU.03012, Imatinib, Sorafenib, and Bevacizumab — are under research.

Keep in mind

- ✓ Initial manifestations of NF2 differ between children and adults. NF2-specific ophthalmological findings can be diagnostic for the disease.
- ✓ Early-onset NF2 is associated with higher severity and marked disease progression, especially in the presence of characteristic ocular abnormalities.
- ✓ Young patients with NF2 must be carefully monitored for timely detection of treatable manifestations and preservation of visual function throughout life.

References

1 Emmanouil B, Wasik M, Charbel Issa P, Halliday D, Parry A & Sharma SM (2022). Structural Abnormalities of the Central Retina in Neurofibromatosis Type 2. Ophthalmic research, 65(1), 77–85. https://doi.org/10.1159/000519143

2 Waisberg V, Rodrigues LO, Nehemy MB, Frasson M & de Miranda DM (2016). Spectral-Domain Optical Coherence Tomography Findings in Neurofibromatosis Type 2. Investigative ophthalmology & visual science, 57(9), OCT262–OCT267. https://doi.org/10.1167/iovs.15-18919

3 Sisk RA, Berrocal AM, Schefler AC, Dubovy SR & Bauer MS (2010). Epiretinal membranes indicate a severe phenotype of neurofibromatosis type 2. Retina (Philadelphia, Pa.), 30(4 Suppl), S51–S58. https://doi.org/10.1097/IAE.0b013e3181dc58bf

4 Bosch MM, Boltshauser E, Harpes P & Landau K (2006). Ophthalmologic findings and long-term course in patients with neurofibromatosis type 2. American journal of ophthalmology, 141(6), 1068–1077. https://doi.org/10.1016/j.ajo.2005.12.042

5 Kunikata H, Nishiguchi KM, Watanabe M & Nakazawa T (2022). Surgical outcome and pathological findings in macular epiretinal membrane caused by neurofibromatosis type 2. Digital journal of ophthalmology: DJO, 28(1), 12–16. https://doi.org/10.5693/djo.02.2021.06.001

6 Ruggieri M, Iannetti P, Polizzi A, La Mantia I, Spalice A, Giliberto O, Platania N, Gabriele AL, Albanese V & Pavone L (2005). Earliest clinical manifestations and natural history of neurofibromatosis type 2 (NF2) in childhood: a study of 24 patients. Neuropediatrics, 36(1), 21–34. https://doi.org/10.1055/s-2005-837581

7 Coy S, Rashid R, Stemmer-Rachamimov A & Santagata S (2020). An update on the CNS manifestations of neurofibromatosis type 2. Acta neuropathologica, 139(4), 643–665. https://doi.org/10.1007/s00401-019-02029-5

8 Ruggieri M, Praticò AD & Evans DG (2015). Diagnosis, Management, and New Therapeutic Options in Childhood Neurofibromatosis Type 2 and Related Forms. Seminars in pediatric neurology, 22(4), 240–258. https://doi.org/10.1016/j.spen.2015.10.008

9 Waisberg V, Rodrigues L, Nehemy MB, Bastos-Rodrigues L & de Miranda DM (2019). Ocular alterations, molecular findings, and three novel pathological mutations in a series of NF2 patients. Graefe's archive for clinical and experimental ophthalmology = Albrecht von Graefes Archiv fur klinische und experimentelle Ophthalmologie, 257(7), 1453–1458. https://doi.org/10.1007/s00417-019-04348-5

10 Painter SL, Sipkova Z, Emmanouil B, Halliday D, Parry A & Elston JS (2019). Neurofibromatosis Type 2-Related Eye Disease Correlated With Genetic Severity Type. Journal of neuro-ophthalmology : the official journal of the North American Neuro-Ophthalmology Society, 39(1), 44–49. https://doi.org/10.1097/WNO.0000000000000675

Case 17 - December 2022

METASTATIC RENAL CELL ORBITAL CARCINOMA

A 76-year-old man presented with rapid-onset exophthalmos and lacrimation on the left.

Presented by
Evaggelos Lokovitis, MD, FEBOphth

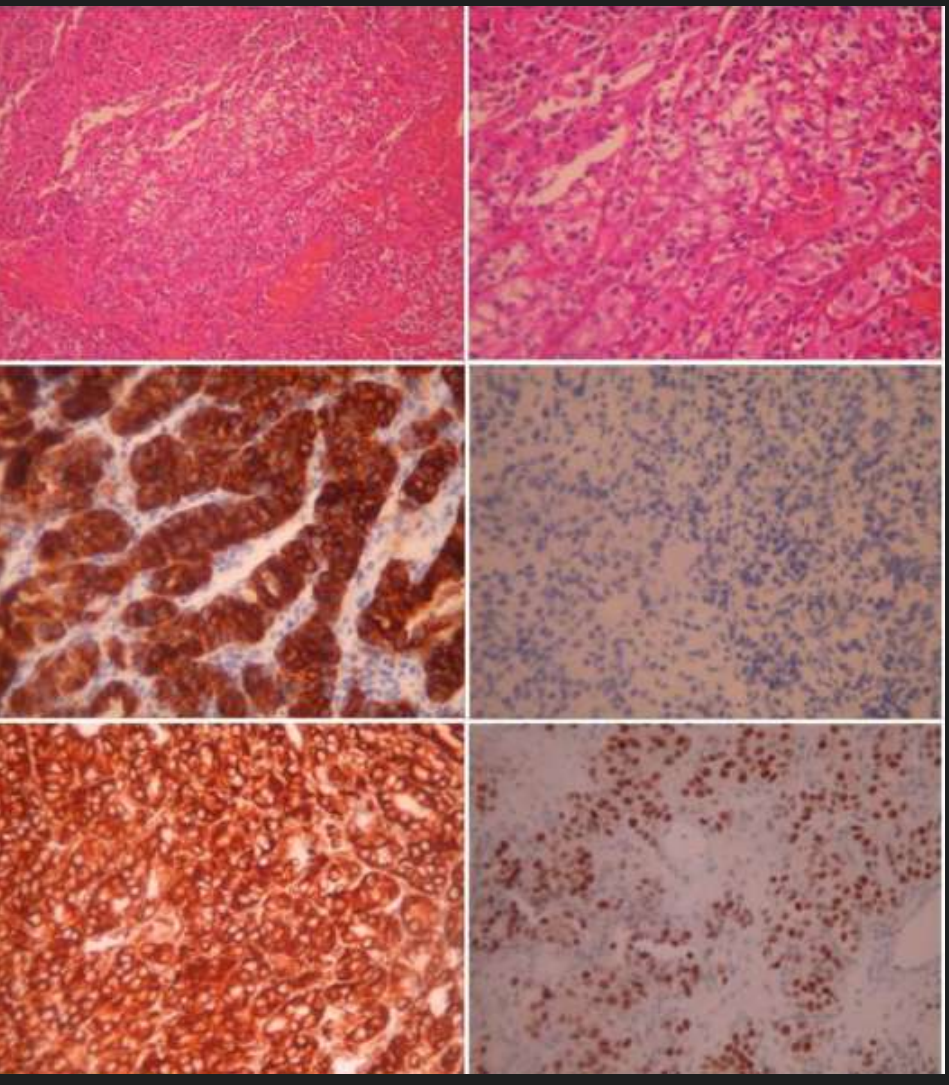

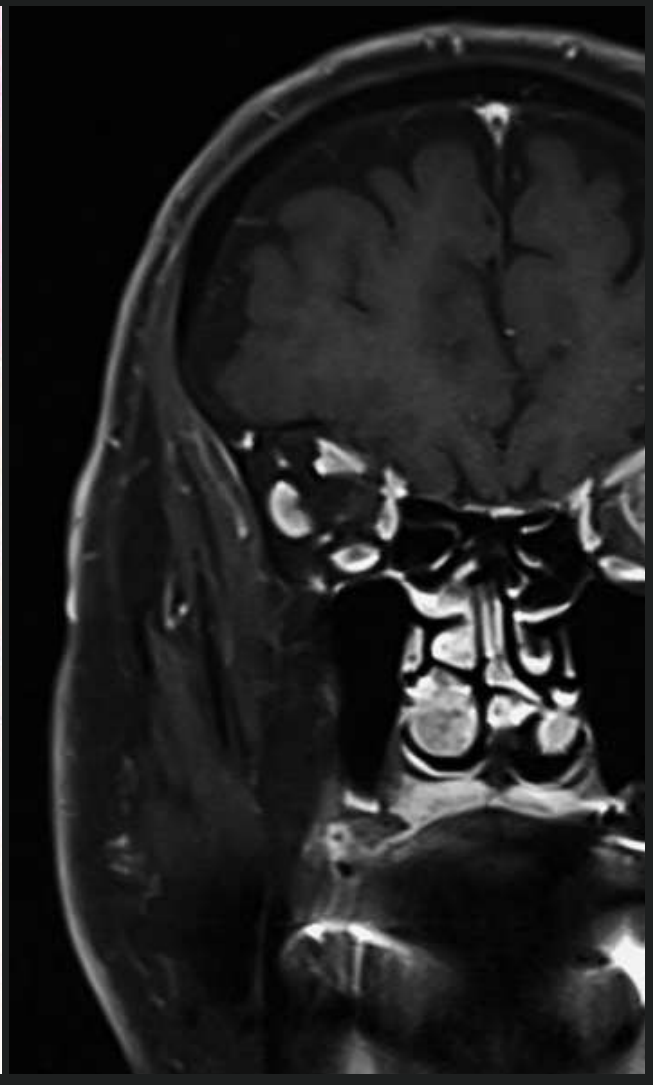

Edited by
Penelope Burle de Politis, MD

Case History

A 76-year-old Caucasian man presented with a complaint of tearing from his left eye (LE) for about 3 months. Ectoscopically, a slight elevation of the left upper lid crease was noticeable, without accompanying lid retraction (**Figure 2, top**). Uncorrected distance visual acuity (UDVA) was 10/10 bilaterally. Biomicroscopy was unremarkable, fundoscopy was indicative of mild hypertensive retinopathy, and intraocular pressure was within the normal range in both eyes. The LE had a discrete proptosis of 1mm (**Figure 2, bottom**), with no identifiable impairment of extraocular muscle function or blepharoptosis. There was neither a relative afferent pupillary defect nor a visual field defect. No mass could be detected on palpation. There was mild resistance to retropulsion of the globe, without pain, pulse or bruit.

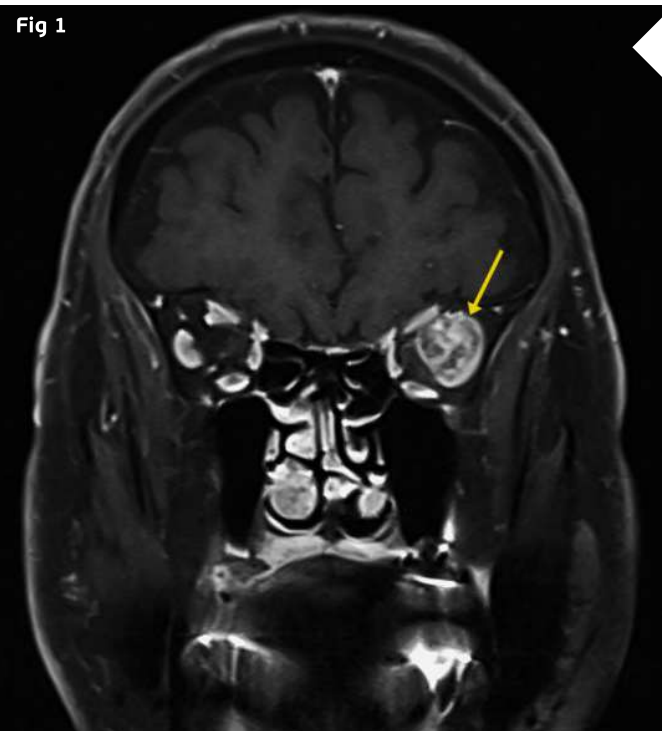

Figure 1: Coronal magnetic resonance T1-weighted imaging (T1-MRI) of the skull showing a roundish mass at the temporal aspect of the left orbit (arrow), with a highly heterogeneous intensity pattern, without apparent disruption of the orbital walls.

Figure 2: A slight elevation of the left upper lid crease is noticeable (top), with no lid retraction. A discrete proptosis is present on the left (bottom), without manifest ocular deviation.

Investigation proceeded with radiological imaging, rendering the detection of an irregular mass at the temporal aspect of the left orbit (**Figure 1**). Under magnetic resonance imaging, the tumor presented a fusiform disposition, following the lateral rectus muscle configuration (**Figure 3**). Following contrast injection, the mass displayed a characteristic enhancement pattern, with no clear delimitation from the muscle bundles.

A surgical approach was indicated, and a total excisional biopsy was performed through a superolateral orbitotomy. A yellowish mass was found at the belly of the lateral rectus muscle, intricately mingled with the muscle fibers. Despite the friable, non-encapsulated nature of the tumor, careful dissection allowed for a complete resection, without impairment of muscle contractility, damage to adjacent conal structures, or external disfiguration.

The surgical specimen was sent to an experienced pathologist for histological analysis. Microscopic examination of the neoplasm revealed bundles of large cells with clear or eosinophilic cytoplasm (**Figure 4)**. The tumor cells exhibited strong positivity for the anti-cytokeratin monoclonal antibodies AE1 and AE3 (CKAE1/AE3) and the protein vimentin. The cells were also negative for CK7, and many showed nuclear positivity for paired-box gene 8 (PAX8). The histological morphology of the neoplasm, in combination with its immunophenotype, was consistent with the diagnosis of metastatic clear-cell renal carcinoma.

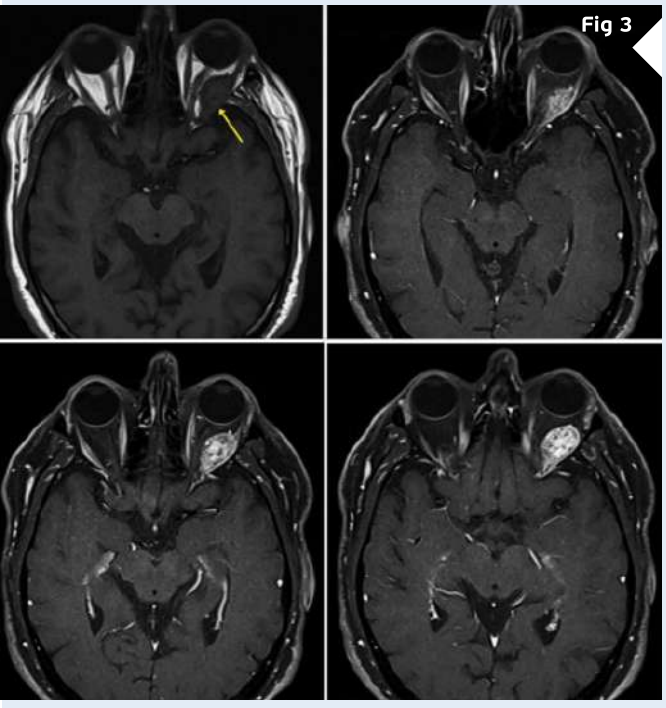

Figure 3: Axial MRI of the orbits with contrast-enhanced images (**left top & bottom**) showing the high signal intensity pattern of the fusiform mass. Though initially the tumor seems to be encapsulated (**top right & left**), lower cuts reveal the intimate imbrication with the muscular tissue (**bottom right & left**).

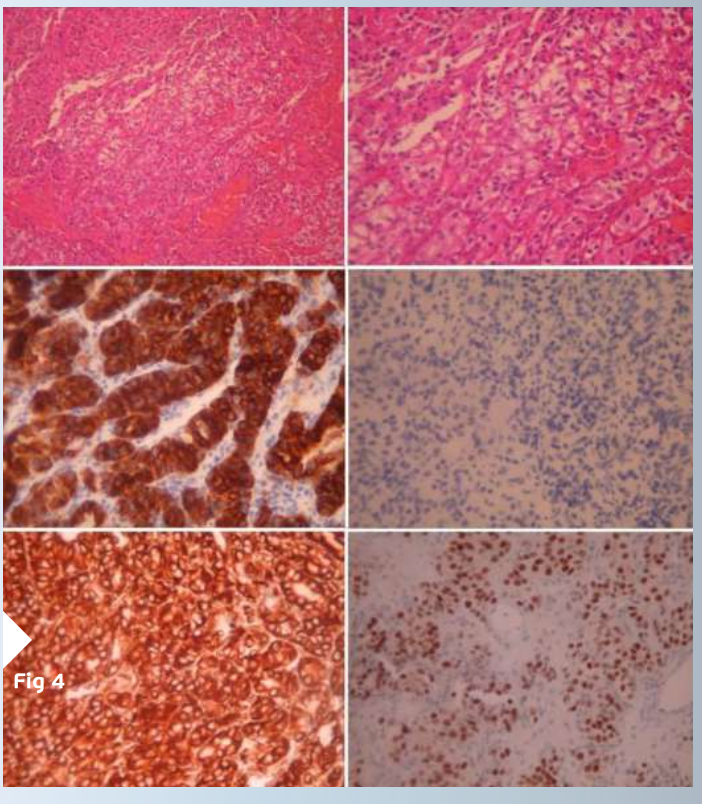

Figure 4: Microscopic photographs (histopathology) of the neoplasm, with the typical features of clear-cell renal carcinoma. Top left: hematoxylin-eosin stain (H+E) at 100X magnification (X 100) displaying large tumor cells with clear or eosinophilic cytoplasm. Top right: the same area in higher magnification (X 200). Middle left: Immunohistochemistry (IHC) X 200 showing the strong positivity of the tumor cells for CKAE1/AE3. Middle right: negative IHC for CK7 (X 200). Bottom left: strong positivity of the tumor cells for vimentin (IHC X 200). Bottom right: many tumor cells showing nuclear positivity for PAX8 (X 200).

Investigation proceeded with radiological imaging, rendering the detection of an irregular mass at the temporal aspect of the left orbit (**Figure 1**). Under magnetic resonance imaging, the tumor presented a fusiform disposition, following the lateral rectus muscle configuration (**Figure 3**). Following contrast injection, the mass displayed a characteristic enhancement pattern, with no clear delimitation from the muscle bundles.

A surgical approach was indicated, and a total excisional biopsy was performed through a superolateral orbitotomy. A yellowish mass was found at the belly of the lateral rectus muscle, intricately mingled with the muscle fibers. Despite the friable, non-encapsulated nature of the tumor, careful dissection allowed for a complete resection, without impairment of muscle contractility, damage to adjacent conal structures, or external disfiguration.

Additional History

The patient had undergone a right nephrectomy due to renal carcinoma five years before. He also had a history of atrial fibrillation, an aortic aneurysm, and a surgical correction of inguinal hernia 6 months earlier. He was currently in use of sotalol, olmesartan, furosemide, rosuvastatin, and rivaroxaban (Xarelto®).

Differential Diagnosis of Metastatic Orbital Carcinoma

- lymphoma
- cavernous hemangioma
- tumors of the lacrimal gland
- orbital schwannoma
- meningioma
- neurofibroma
- lymphangioma

The definitive diagnosis of an orbital tumor is obtained through biopsy. It is nearly impossible to differentiate these lesions based solely on clinical exams. Cellular architecture exhibiting disorganized arrangements with variable degrees of necrosis, hemorrhage, cystic degeneration and calcifications is suggestive of a malignant neoplasm.

Discussion and Literature

The improved survival of cancer patients, together with the longer aging of the population, has led to a higher incidence of patients living with metastatic disease in unusual sites such as the orbit and ocular adnexa. Besides, vigilant surveillance and advances in diagnostic techniques have increased the detection of orbital metastases (OM), even before disclosure of the primary site.

Metastatic orbital lesions have been estimated to account for 1 to 13% of all orbital tumors. Between 2 and 5% of patients with systemic cancer are reported to have an orbital metastasis. Breast carcinoma accounts for most metastatic lesions of the orbit and ocular adnexa (48 to 53%). The other 2 most common primary cancers with OM are lung and prostate. Less usual sites include kidney, thyroid, stomach, skin (melanoma), and pancreas. Most OM are carcinomas. The most common symptoms are proptosis (52.3%) and relative afferent pupillary defect (38.7%) – due to direct compression of the optic nerve, usually at the orbital apex. Other clinical presentations include diplopia (48%), pain (19%), decreased vision (16%), ptosis (10%), and palpable mass.

The mean age of patients with OM is 60 years. The mean time of presentation after diagnosis of the primary cancer has been found to be 52 months; however, orbital metastasis can occur at any time after the initial cancer diagnosis. In more than 25% of cases, OM are the first manifestation of a primary tumor of unknown origin. In contrast to uveal metastases, OM are much more often unilateral than bilateral.

Some metastases are very vascular (e.g., renal cell carcinoma) and biopsy can result in significant morbidity. Because the eye has no lymphatic channels, OM are secondary to hematogenous spread of the primary tumor. Therefore, the lungs are likely to be involved and must be investigated in these patients.

Considering an orbital mass in a patient with a cancer history, the anamnesis, physical examination, and imaging characteristics can usually determine if the tumor must be suspected to be a metastasis. Due to the small space of the orbit and the relatively rapid growth of most metastatic lesions, the presence of symptoms is suggestive of a metastatic orbital mass. Although any space-occupying mass – benign or malignant – may result in axial displacement of the globe, most metastases will produce a motility deficit, pain, or a decrease in vision. Benign lesions are usually asymptomatic, or symptoms may progress very slowly on the order of years. In the absence of previous cancer history, nonspecific signs involving other systems may guide the physician to a possible primary lesion; for example, hematuria may lead to the suspicion of the kidneys being the site of origin.

Renal cell carcinomas (RCCs) are classified in several histological subtypes, clear-cell renal cell carcinoma (ccRCC) being by far the most common (70 to 75% of all RCCs). Clear-cell RCC usually affects patients over 50 years of age, and most cases (95%) are sporadic. Macroscopically, ccRCC is a solid, yellowish lesion with variable degrees of internal necrosis, hemorrhage, cystic degeneration and calcifications. Histologically, such lesions present clear cells because of their lipid- and glycogen-rich cytoplasmic content. Imaging findings are compatible with such histopathological features, denoting hypervascularized, heterogeneous lesions. Hematogenous metastases are relatively common in ccRCC, affecting mostly the lungs, bones, lymph nodes, and liver.

Carcinoma is the most common malignancy of the kidney, but only rarely does it metastasize to the orbit. Metastases to the head and neck have been found in 15% of RCC patients, most frequently involving the nose, paranasal sinuses, and oral cavity. Ocular metastases from kidney cancer usually involve the iris, ciliary body, and choroids, although eyelid and lacrimal sac involvement have also been described. Because these tumors can be confused with other amelanotic or vascular tumors, a high index of suspicion is required for early detection and management of the primary tumor, as this can affect the patient's overall survival.

The clinical features of OM from kidney cancer are non-specific, therefore imaging is crucial to orient the diagnosis and to identify the ideal site for tissue biopsy or surgical approach. Imaging features are also helpful in determining whether a mass can be a metastasis or not. Metastatic lesions are more common at the anterior rather than posterior orbit. Well-encapsulated, discrete, and focal intraconal masses are unlikely to be metastases, while masses involving the extraocular muscles or causing bone erosion are much more likely to be metastases. No area of the orbit is immune to metastasis, with cases having been reported to every anatomic structure of the orbit, including the subperiosteal space. Tumor patterns can vary from diffuse infiltrative to a focal mass. Metastases from carcinoid, renal cell carcinoma, and melanoma tend to be circumscribed. All OM should show some enhancement with contrast injection on MRI.

Incisional biopsy with histopathological evaluation may be crucial for diagnosis and appropriate therapy. Situations in which biopsy may be necessary include a solitary metastasis to the orbit with no other metastatic disease. To provide an accurate, specific, and sufficiently comprehensive diagnosis, to optimize clinical management and estimate prognosis, pathological examination of a tissue biopsy is essential. Diagnostic orbital tissue biopsy is obtained through a minimally invasive orbitotomy procedure or, in selected cases, fine needle aspiration. The outcome of successful biopsy, however, is centered on its representativeness, processing, and interpretation. Owing to the often-small volume of the orbital biopsies, artifacts in the specimens should be limited by careful per-operatory tissue handling, fixation, processing, and storage.

Orbital metastases often lead to functional impairment. A recent review of the literature showed that most metastases have a diffuse location within the orbit (19%), with preferential infiltration of orbital soft tissues (40.2%), while in 5.4% tumors extended intracranially. Incisional biopsy (63.7%) is generally preferred over fine-needle aspiration (10.2%). Excisional biopsy has the advantage of removing the whole mass, thus providing an adequate specimen for histopathological diagnosis. It is also used as a therapeutic excision, in cases such as malignant lesions. Post-treatment symptom improvement is significantly higher after surgical resection when compared to biopsy only ($p = 0.005$).

Mortality rate for metastatic RCC decreased significantly since 2012. Advances in diagnostic modalities and targeted therapies over the last 15 years have allowed significant improvement in survival of patients with metastatic RCC, including those with orbital metastasis, leading to better quality of life and preservation of ocular function. Multidisciplinary management is related to increased survival outcomes. Therapeutic options include surgical biopsy, debulking or excision, hormonal therapy, chemotherapy, radiation therapy, and immunotherapy using biological agents.

Keep in mind

- ✓ A rapid-onset unilateral orbital mass should always raise suspicion to a malignant lesion, possibly metastatic.
- ✓ Although rare, metastatic renal carcinoma must be included in the differential diagnosis of an orbital mass in a patient with a history of kidney cancer.
- ✓ Better survival rates for metastatic orbital carcinoma depend on timely diagnosis and comprehensive treatment.

References

1 Ahmad SM & Esmaeli B (2007). Metastatic tumors of the orbit and ocular adnexa. Current opinion in ophthalmology, 18(5), 405–413. https://doi.org/10.1097/ICU.0b013e3282c5077c

2 Allen RC (2018). Orbital Metastases: When to Suspect? When to biopsy?. Middle East African journal of ophthalmology, 25(2), 60–64. https://doi.org/10.4103/meajo.MEAJO_93_18

3 Palmisciano P, Ferini G, Ogasawara C, Wahood W, Bin Alamer O, Gupta AD, Scalia G, Larsen AMG, Yu K, Umana GE, Cohen-Gadol AA, El Ahmadieh TY & Haider AS (2021). Orbital Metastases: A Systematic Review of Clinical Characteristics, Management Strategies, and Treatment Outcomes. Cancers, 14(1), 94. https://doi.org/10.3390/cancers14010094

4 Muglia VF & Prando A (2015). Renal cell carcinoma: histological classification and correlation with imaging findings. Radiologia brasileira, 48(3), 166–174. https://doi.org/10.1590/0100-3984.2013.1927

5 Tan SY, Bastion MC & Mohd Khialdin S (2021). Orbital Tumor As First Manifestation of Metastatic Renal Cell Carcinoma. Cureus, 13(7), e16275. https://doi.org/10.7759/cureus.16275

6 Vogele D, Sollmann N, Beck A, Haggenmüller B, Schmidt SA, Schmitz B, Kapapa T, Ozpeynirci Y, Beer M & Kloth C (2022). Orbital Tumors-Clinical, Radiologic and Histopathologic Correlation. Diagnostics (Basel, Switzerland), 12(10), 2376. https://doi.org/10.3390/diagnostics12102376

7 Alkatan HM, Alyousef NA, Alshabib NS & Aljasser IHJ (2021). A comprehensive review of biopsy techniques for oculoplastic and orbital surgeons from ophthalmic pathologists' perspective. Saudi Journal of Ophthalmology: Official Journal of the Saudi Ophthalmological Society. 2021 Jul-Sep;35(3):174-178. https://europepmc.org/article/med/35601859

8 Mombaerts I, Ramberg I, Coupland SE & Heegaard S (2019). Diagnosis of orbital mass lesions: clinical, radiological, and pathological recommendations. Survey of ophthalmology, 64(6), 741–756. https://doi.org/10.1016/j.survophthal.2019.06.006

9 Schick U, Lermen O & Hassler W (2006). Management of orbital metastases. Zentralblatt fur Neurochirurgie, 67(1), 1–7. https://doi.org/10.1055/s-2005-836922

10 Coloma-González I, Ceriotto A, Amezquita-García E, Flores-Preciado J & Salcedo-Casillas G (2014). Orbital pulsatile metastasis as initial presenting sign of metastatic clear cell renal carcinoma. Archivos de la Sociedad Espanola de Oftalmologia, 89(12), 500–503. https://doi.org/10.1016/j.oftal.2013.11.012

11 Magan T, Pradeep T, Tuluc M, Bilyk JR & Milman T (2022). Ocular adnexal metastases from renal cell carcinoma: An update and comprehensive literature review. Saudi journal of ophthalmology: official journal of the Saudi Ophthalmological Society, 35(3), 209–216. https://doi.org/10.4103/SJOPT.SJOPT_96_21

12 Shome D, Honavar SG, Gupta P, Vemuganti GK & Reddy PV (2007). Metastasis to the eye and orbit from renal cell carcinoma--a report of three cases and review of literature. Survey of ophthalmology, 52(2), 213–223. https://doi.org/10.1016/j.survophthal.2006.12.004

13 Mudiyanselage SY, Prabhakaran VC, Davis GJ & Selva D (2008). Metastatic renal cell carcinoma presenting as a circumscribed orbital mass. European journal of ophthalmology, 18(3), 483–485. https://doi.org/10.1177/112067210801800332

14 Ho CC, Krishna KK, Praveen S, Goh EH, Lee BC & Zulkifli MZ (2010). Proptosis: a rare presentation of metastatic renal cell carcinoma. The Medical journal of Malaysia, 65(3), 229–230. http://www.e-mjm.org/2010/v65n3/Proptosis.pdf

15 El-Hadad C, Koka K, Dong W, Do T, Haider M, Ursua JD, Ning J, Debnam JM & Esmaeli B (2021). Multidisciplinary Management of Orbital Metastasis and Survival Outcomes. Ophthalmic plastic and reconstructive surgery, 37(6), 541–545. https://doi.org/10.1097/IOP.0000000000001939

Case 18 - February 2023

GRANULAR CORNEAL DYSTROPHY TYPE 2

A 26-year-old woman presented with longstanding, slowly progressive bilateral low visual acuity and recurrent ocular irritation and foreign body sensation.

Presented by
Dimitrios Sakellaris, MD

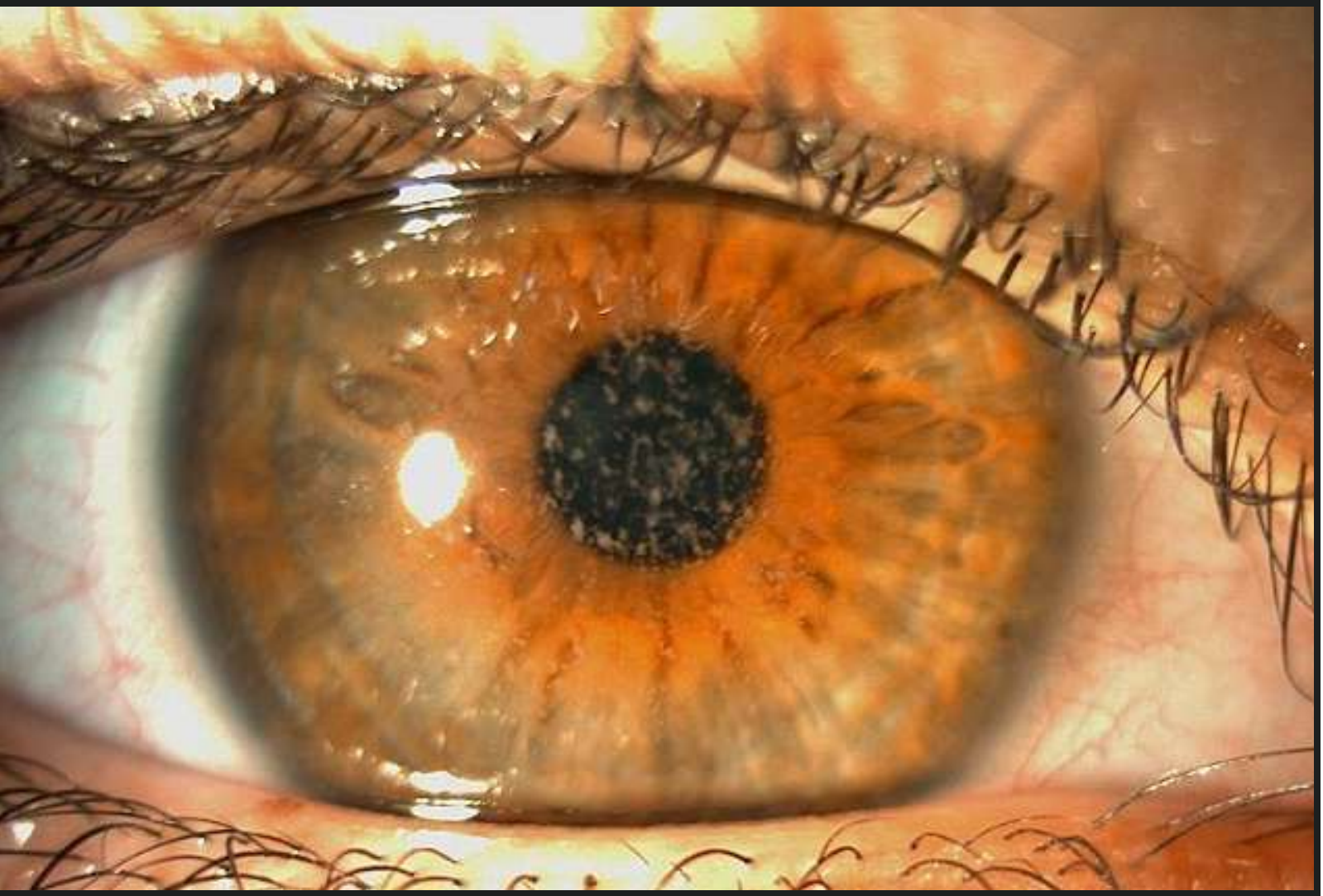

Edited by
Penelope Burle de Politis, MD

Case History

A 26-year-old Caucasian woman presented with a history of slowly progressively low visual acuity and frequent ocular surface irritation and foreign body sensation in both eyes since childhood. She had been wearing glasses for 20 years and would like to know if her eyes were suitable for laser correction. She denied any previous contact lens usage and was not on any medication. Upon ophthalmological examination, autorefractometer measurements were -0.50@165° in the right eye (RE) and -1.00 -1.00@10° in the left eye (LE), with a distance corrected visual acuity (DCVA) of 5/10-2 bilaterally. Fundoscopy was unremarkable and intraocular pressure (IOP) was 13 mmHg in both eyes. Pupils were normally reactive to light and there were no extraocular muscle imbalances. Biomicroscopy revealed heterogeneous anterior stromal corneal deposits permeated with areas of normal corneal stroma in both eyes (**Figure 1**).

Preservative-free artificial tears were prescribed and started on a regular basis. Symptomatic relief was achieved after a few days of treatment, with a slight subjective improvement in vision as well. Surgical treatment options were discussed but put on hold, given the current clinical presentation and their risks and benefits.

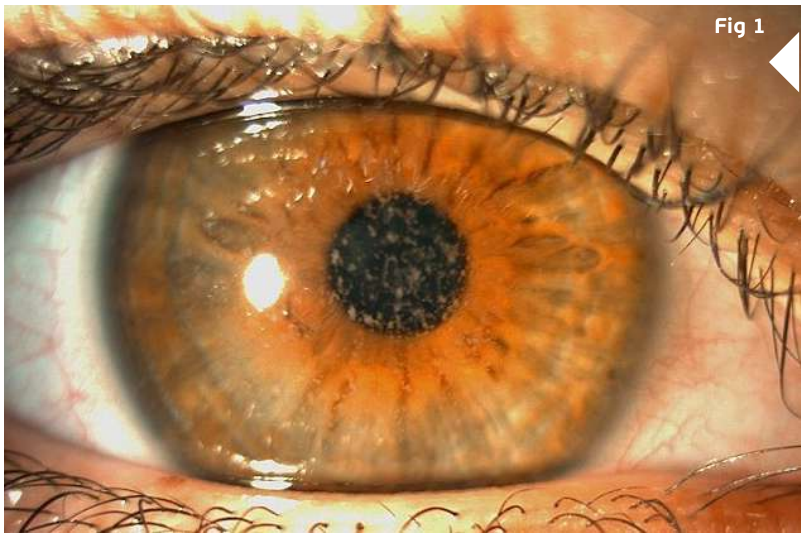

Figure 1: Slit-lamp photograph of the right eye displaying heterogeneous stromal deposits interspersed by areas of normal corneal stroma.

Additional History

The patient's father had a history of some sort of keratopathy and cataract in his RE, having undergone a scraping procedure for diagnosis a few years before. He had also been told he could need eye drops for ocular hypertension, which he actually never used. He was 58 years-old and presented a refraction error of +3.00 -0.50@15° in the LE, with a DCVA of 8/10+2. In the RE, refractometry was hardly feasible and the best achievable DCVA was 4/10 with a correction of +2.00 -2.50@180°. IOP was 21 and 18 in the RE and LE respectively, and there were no fundus abnormalities. Under biomicroscopic examination, he was found to have a mild nuclear sclerosis and a corneal aspect identical to his daughter's, more pronounced in his RE (**Figure 2**).

The ocular history and clinical findings, added to the spontaneous occurrence in direct family members, led to the diagnosis of a corneal dystrophy. The mixed nature of the stromal deposits, both granular and lattice in appearance, were characteristic of Granular Corneal Dystrophy Type 2 (GCD2 or Avellino type).

Figure 2: Slit-lamp photograph of the father's right eye displaying anterior stromal deposits in a coarser pattern but similar to that seen in his daughter's cornea.

The ocular history and clinical findings, added to the spontaneous occurrence in direct family members, led to the diagnosis of a corneal dystrophy. The mixed nature of the stromal deposits, both granular and lattice in appearance, were characteristic of Granular Corneal Dystrophy Type 2 (GCD2 or Avellino type).

Differential Diagnosis of Granular Corneal Dystrophy Type 2 (GCD2)

- cystinosis
- recurrent corneal erosion
- keratoconjunctivitis sicca
- adenoviral keratitis
- monoclonal gammopathy

The main differential diagnosis of GCD2 is with other forms of corneal dystrophies. Aside from careful slit-lamp examination, biochemical analysis of scraped-off deposits and genetic testing can help in diagnosis.

Discussion and Literature

Corneal dystrophies (CD) are a heterogenous group of bilateral, genetically determined, non-inflammatory diseases restricted to the cornea. Clinically, CD can be divided into three groups based on the sole or predominant anatomical location of the abnormalities. Some affect primarily the corneal epithelium and its basement membrane, or Bowman's layer and the anterior corneal stroma (anterior CD), others the mid and posterior corneal stroma (stromal CD), or Descemet's membrane and the corneal endothelium (posterior CD).

Most CD present with variably shaped corneal opacities in a clear or cloudy cornea and affect visual acuity to different degrees. The inheritance of CD may be autosomal dominant, autosomal recessive or X-linked recessive. The available molecular tests for their precise diagnosis are based on the knowledge of the genetic mutation responsible for each corneal dystrophy. A corneal dystrophy should be suspected when corneal transparency is lost or when corneal opacities occur spontaneously, particularly in both corneas, and especially in the presence of a positive family history or in the offspring of consanguineous parents.

Granular corneal dystrophies (GCD) belong to the stromal CD. Subtle differences in the clinical appearance of the corneal opacities characterize two types of GCD: GCD type I (GCD1, Groenouw type) and GCD type II (GCD2, Avellino type). GCD2 tends to have fewer corneal deposits than GCD1, and the corneal deposits in GCD2 sometimes resemble a combination of GCD and lattice CD, featuring both granular and amyloid deposits. GCD1 seems to be most prevalent in Europe, while GCD2 is more common in Japan, Korea and the USA. The ancestry of some families with GCD2 have been traced to the Avellino district of Italy - hence the synonym Avellino corneal dystrophy.

GCD2 is an autosomal dominant disorder and results from the mutation p.Arg124His (arginine to histidine substitution at codon 124) in the transforming growth factor ß-induced (TGFBI) gene, also referred to as TGFBI p.R124H. Patients with GCD2 have different ages of onset and progression rates, depending on whether the p.R124H variant is heterozygous or homozygous. In patients with the homozygous p.R124H variant, corneal deposits appear as early as 3 years of age, and visual loss begins in childhood. On the other hand, heterozygous patients have a highly variable phenotype due to incomplete penetrance even in the same family. They are usually diagnosed as teenagers or young adults and progress slowly.

The severity of opacity in CD might not always correlate to visual function. Recent technologies such as anterior segment optical coherence tomography (AS-OCT) and wavefront-based aberrometry has allowed for better understanding of how CD affect vision. It has been demonstrated that the stromal opacities of CD induce not only scatter but also morphometric changes in the anterior and posterior corneal surfaces that can cause high-order aberrations (coma, trefoil, spherical aberration etc.). In GCD2, those are lesser than in other forms of CD such as lattice and macular, having different repercussions on patients' visual acuity.

To treat the opacities in GCD2, phototherapeutic keratectomy (PTK), lamellar keratoplasty, deep lamellar keratoplasty, and penetrating keratoplasty (PKP) have been used. However, recurrence is still an unsolved problem, because corneal trauma activates TGFBI, the main component of the corneal opacities. In fact, several studies have reported an exacerbation of GCD2 after corneal refractive surgery such as photorefractive keratectomy (PRK), laser in situ keratomileusis (LASIK), and laser epithelial keratomileusis (LASEK). For this reason, TGFBI gene screening is advisable for candidates with a family history of corneal disease or granular opacities in corneal stroma before refractive surgery.

The pathogenesis of GCD2 lies in lysosomal dysfunction and autophagy of corneal fibroblasts. In GCD2 corneal fibroblasts, mutant-TGFBIp accumulates in the lysosomal compartments due to defective autophagy.

Transcription factor EB (TFEB) plays an essential role in cellular homeostasis, modulating lysosomal function and autophagy. New research sheds light on TFEB as a potential therapeutic target for maintaining the physiological function of corneal fibroblasts. Apparently, exogenous TFEB expression improves mutant-TGFBIp clearance and lysosomal abnormalities in GCD2 cells. Preclinical studies to evaluate the possible consequences of TFEB overexpression or activation are still pending.

Keep in mind

- ✓ A corneal dystrophy should always be suspected when corneal opacities occur spontaneously, particularly if bilaterally, and especially in the presence of a positive family history.
- ✓ GCD2 phenotypes may vary widely, even in the same family, depending on heterozygosity or homozygosity and on complete or incomplete penetrance of the mutant gene.
- ✓ Pros and cons of therapeutic procedures for GCD2 must be weighed against the visual deficit presented by each patient and its effects on their quality of life.

References

1. Klintworth GK (2009). Corneal dystrophies. Orphanet journal of rare diseases, 4, 7. https://doi.org/10.1186/1750-1172-4-7
2. Park JE, Yun SA, Roh EY, Yoon JH, Shin S & Ki CS (2021). Prevalence of granular corneal dystrophy type 2-related TGFBI p.R124H variant in a South Korean population. Molecular vision, 27, 283–287. https://www.ncbi.nlm.nih.gov/pmc/articles/PMC8116257/
3. Han KE, Kim TI, Chung WS, Choi SI, Kim BY & Kim EK (2010). Clinical findings and treatments of granular corneal dystrophy type 2 (avellino corneal dystrophy): a review of the literature. Eye & contact lens, 36(5), 296–299. https://doi.org/10.1097/ICL.0b013e3181ef0da0
4. Han KE, Choi SI, Chung WS, Jung SH, Katsanis N, Kim TI & Kim EK (2012). Extremely varied phenotypes in granular corneal dystrophy type 2 heterozygotes. Molecular vision, 18, 1755–1762. https://www.ncbi.nlm.nih.gov/pmc/articles/PMC3398492/
5. Abazi Z, Magarasevic L, Grubisa I & Risovic D (2013). Individual phenotypic variances in a family with Avellino corneal dystrophy. BMC ophthalmology, 13, 30. https://doi.org/10.1186/1471-2415-13-30
6. Yagi-Yaguchi Y, Yamaguchi T, Okuyama Y, Satake Y, Tsubota K & Shimazaki J (2016). Corneal Higher Order Aberrations in Granular, Lattice and Macular Corneal Dystrophies. PloS one, 11(8), e0161075. https://doi.org/10.1371/journal.pone.0161075
7. Abe Y, Omoto T, Kitamoto K, Toyono T, Yoshida J, Asaoka R, Yamagami S, Miyai T & Usui T (2022). Corneal irregularity and visual function using anterior segment optical coherence tomography in TGFBI corneal dystrophy. Scientific reports, 12(1), 13759. https://doi.org/10.1038/s41598-022-17738-3

8 Rana RS, Bajracharya L & Gurung R (2021). Recurrence of Avellino Corneal Dystrophy Following Penetrating Keratoplasty: A Case Report. JNMA; journal of the Nepal Medical Association, 59(236), 406–408. https://doi.org/10.31729/jnma.5726

9 Jiang X & Zhang H (2021). Deterioration of Avellino corneal dystrophy in a Chinese family after LASIK. International journal of ophthalmology, 14(6), 795–799. https://doi.org/10.18240/ijo.2021.06.02

10 Choi SI, Woo JH & Kim EK (2020). Lysosomal dysfunction of corneal fibroblasts underlies the pathogenesis of Granular Corneal Dystrophy Type 2 and can be rescued by TFEB. Journal of cellular and molecular medicine, 24(18), 10343–10355. https://doi.org/10.1111/jcmm.15646

Case 19 - April 2023

HIV-RELATED SYPHILITIC UVEITIS

A 41-year-old man was referred for severe recurrent bilateral anterior uveitis poorly responsive to topical treatment.

Presented by
Chrysa Koutsiouki, MD

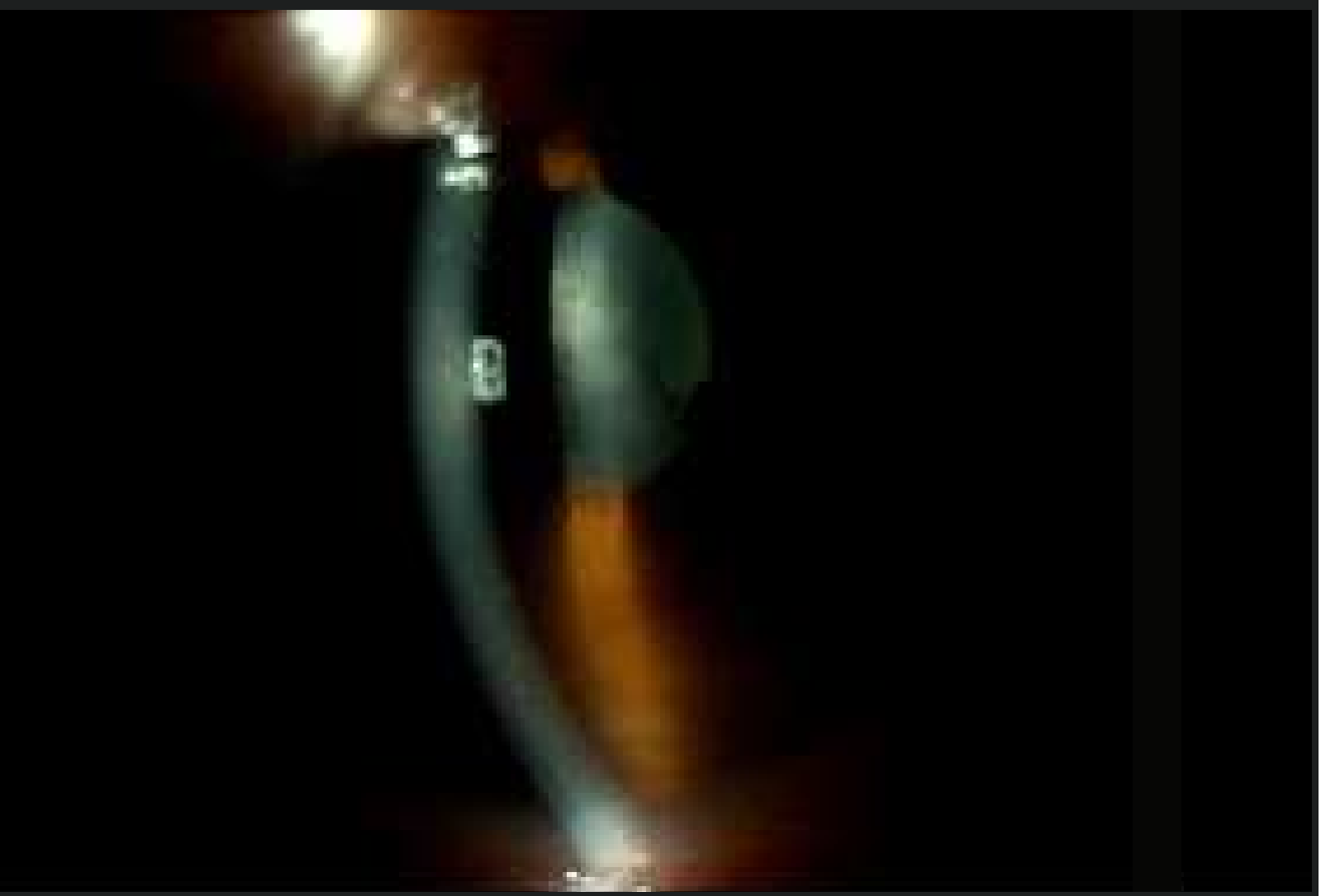

Edited by
Penelope Burle de Politis, MD

Case History

A 41-year-old Caucasian man of Greek descent was referred for investigation of severe recurrent bilateral anterior uveitis for 3 months (**Figure 1**). He had been on treatment with topical dexamethasone 0.1%, with some response only while instillation was under 2-hourly. He reported nonspecific joint soreness and a few skin rashes on his face, but no back pain, oral or genital ulcers, nor genitourinary or gastrointestinal issues. There was no history of cough or shortness of breath, weight loss, night sweats, pins and needles' sensation, nor contact with tuberculosis.

Distance corrected visual acuity (DCVA) was 10/10 bilaterally, with respectively -4.50 and -5.00 spherical diopters in the right eye (RE) and left eye (LE). IOP was 20 mmHg in both eyes (BE). At biomicroscopic examination, there were pigmented keratic precipitates (KP), anterior chamber cell reaction of 2+ and flare of 1+ bilaterally. There were posterior synechiae from 4 to 8 hours of the iris border in the RE and a ground-glass appearance of both crystalline lenses. Fundus findings in BE were a mild vitritis, a hyperemic optic disc (more evident in the RE), yellowish preretinal dots at the inferior quadrant, and discrete vascular sheathing suggestive of periphlebitis (**Figure 2**).

Figure 1: Slit-lamp photograph displaying bilateral keratic and lenticular precipitates, as well as posterior synechiae in the right eye.

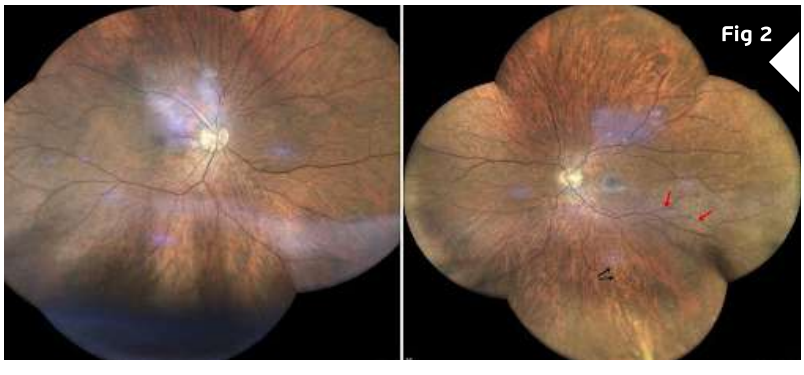

Figure 2: Mosaic display of confocal high-resolution widefield imaging (iCare EIDON®) showing a "hot" disk and pale yellowish perivascular preretinal dots at the end of the inferior temporal arcade and mid-periphery (black arrows), and mild sheathing of temporal vessels (red arrows) in both eyes.

Spectral-domain optical coherence tomography (SD-OCT) evidentiated bilateral subclinical macular edema, more pronounced in the RE (Figure 3, top images). The retinal nerve fiber layer (RNFL) was normal in BE.

While the retinal changes accompanying the anterior inflammation were still subtle, the impression drawn was of a bilateral subacute panuveitis in an exacerbation phase. Instillation of the dexamethasone drops was increased to hourly and tropicamide b.i.d. was added to the regimen. A systemic workup was requested, and the patient was scheduled for a review 10 days later.

Additional History

The patient had been diagnosed HIV-positive for about a year and was in use of darunavir/ritonavir and dolutegravir with regular follow-up by the specific clinic. He had a recent CD4+ count of 400 cells/mm3 and a viral load of 20 copies/mL. Systemic workup results showed a slight megaloblastic anemia as pointed out by the RBC (3.94 mi/mm3), MCH (34.5 pg) and MCV (103.8 fL) indexes. Erythrocyte sedimentation rate (ESR) was 60 mm/h. QuantiFERON™-TB, angiotensin-converting enzyme (ACE) and HLA-B27 were negative, and the thorax CT was normal. The venereal disease research laboratory (VDRL) test was negative. However, both fluorescent treponemal antibody absorption (FTA-ABS) IgM and IgG were positive (respectively 1/10 and 1/40). C-reactive protein (CRP) was at 0.83 mg/dL (N<0.5 mg/dL).

Upon review, inflammatory signs were partially resolved, with pigmentation of the KP in the RE and reduction of the anterior chamber cell reaction to 1+ in the LE. However, in the face of the laboratory results, the diagnosis was updated to syphilitic bilateral uveitis associated with HIV infection, thus requiring referral to a sexual health / genitourinary medicine (SHC or GUM) clinic for treatment and monitoring.

The patient was started on IM penicillin – route of patient's choice – and presented for a review 2 weeks later with worsening of the inflammation in the LE, noticed as newer KP and increased anterior chamber cell reaction to 2+. Fundus findings were unchanged, but OCT revealed a slight increase in the macular edema in that eye. Considering the signs of imminent deterioration, therapy was discussed with the GUM Clinic staff, who agreed to the initiation of oral prednisone starting at 40 mg/day and weekly tapering. Omeprazole was prescribed as well. Dexamethasone drops were taken back to every 2 hours.

Two weeks later and after the 5th penicillin injection, there was subjective improvement in vision, and the joint soreness and skin rashes had subsided. There were no longer signs of anterior uveitis in either eye, pigmented KP had resolved almost entirely and the iris in the RE was 360° free. OCT findings were improving as well (Figure 3). The patient was examined again 4 weeks later and remains stable.

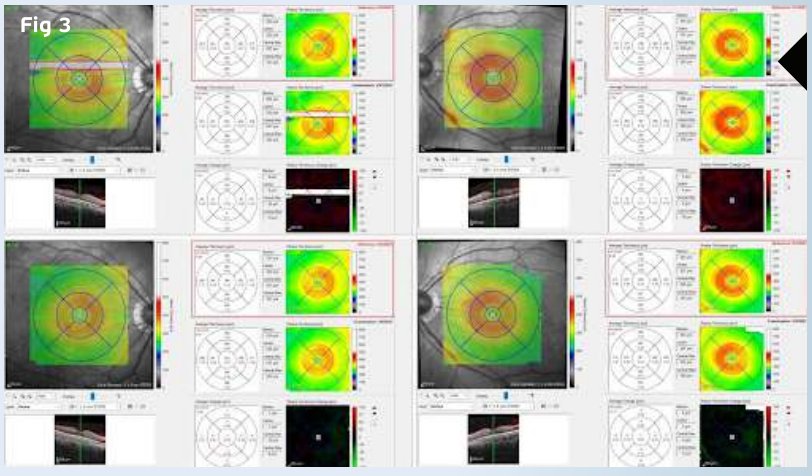

Figure 3: Spectralis SD-OCT (Heidelberg Engineering®) thickness map illustrating bilateral subclinical macular edema, with more increased thickness in the RE (average reaching 400 µm in the nasal quadrant before treatment – **top right**). **Bottom right**: RE after treatment (average thickness in the nasal quadrant dropping to 359 µm). Left: LE before treatment (**top**), average thickness reaching 393 µm in the nasal quadrant and dropping to 374 µm after treatment (**bottom**).

Differential Diagnosis of Recurrent Uveitis in Adults

- sarcoidosis
- infections (syphilis, tuberculosis, toxoplasmosis, toxocariasis, bartonellosis, brucellosis, herpes simplex virus, varicella zoster virus, cytomegalovirus)
- HLA-B27-associated diseases (ankylosing spondylitis, reactive arthritis, psoriatic arthritis, inflammatory bowel disease)

Identification of the predominantly involved location can narrow the differential. Posterior uveitis is more commonly associated with an infectious cause. Syphilis and tuberculosis should be excluded in all uveitis cases. Immunodepression can be associated with any form of uveitis. In immunocompromised patients, an infectious etiology is much more likely than in immunocompetent ones.

Discussion and Literature

Syphilis is a common worldwide sexually transmitted infection transmitted via oral, anal and vaginal intercourse. Congenital syphilis refers to vertical transmission of the etiological agent, the spirochete Treponema pallidum, from mother to fetus transplacentally during pregnancy. Syphilis can infect any organ, with complex and variable manifestations that can mimic many other inflammatory, infectious or autoimmune diseases, thus being called “the great impostor”, "the great masquerader" or the “great imitator”.

Since the use of penicillin in the mid-20th century, the spread of syphilis has been largely controlled, although efforts to eradicate it entirely have been unsuccessful. The disease has increased exponentially in the United Kingdom, Europe, United States, and Asia over the past decade and poses a significant public health problem. Demographic data vary among studies according to social and cultural factors and the stigma around sexually transmitted diseases, which makes under-reporting a possibility. Diagnosis in the early stages is key, since the condition is treatable and, if left untreated, can result in permanent sequelae.

Typically, syphilis presents in the waxing and waning phases of the disease and, when untreated, can progress through four defined stages: primary, secondary, latent, and tertiary syphilis. Primary syphilis is characterized by a chancre at the site of inoculation. Secondary syphilis classically presents as a macular rash with generalized lymphadenopathy as a result of hematogenous dissemination. Tertiary syphilis can affect virtually any system of the body and is often devastating to the patient. T. pallidum disseminates to the central nervous system within days after exposure. While the majority of cases are treated before they progress to late stages, studies suggest rates of neurosyphilis are as high as 3.5%.

Ocular syphilis refers to the group of inflammatory eye diseases that result from infection of the ocular tissues with T. pallidum and affects about 1% of those with early syphilis. Ocular manifestations can occur at any stage of the disease and may involve any

ocular structure, from the anterior segment, lens, uveal tract, retina and retinal vasculature, to the optic nerve, cranial nerves and pupillomotor pathways. Primary ocular syphilis can manifest as chancres on the eyelid or conjunctiva. Reported ocular signs of secondary syphilis include scleritis, keratitis, anterior uveitis, posterior uveitis, panuveitis, vitritis, chorioretinitis, and necrotizing retinitis. Inflammation is bilateral in most patients. The most frequently reported ocular manifestation of tertiary syphilis is bilateral diffuse periostitis.

Syphilis may lead to any type of intraocular inflammation. Uveitis accounts for most cases of ocular syphilis, but diverse forms of anterior, intermediate, posterior and panuveitis have been described. The most frequent form of intraocular inflammation in syphilis is panuveitis, the posterior segment being inflamed in 90% of eyes. The most frequent posterior manifestations are vitritis (85%), followed by retinal involvement (76%) and optic disc abnormalities (63.5%). Isolated anterior uveitis is rare and 96% of patients presenting with isolated anterior uveitis are HIV-positive. Optic nerve involvement occurs in 78% of patients, most commonly as inflammatory disc oedema, a more frequent finding in HIV-positive patients comparatively to HIV-negative, apparently with a preference for the left eye though the cause is unknown.

Syphilitic uveitis is rising in incidence in tandem with the continuing overall rise of early syphilis in Europe, with peaks in 2005 and between 2010 and 2014, the highest index in 7 decades. Epidemiology has been influenced by factors that include high-risk sexual practices and global travel, immunomodulatory impacts of infection with HIV and highly active antiretroviral therapy (HAART), and changes in antibiotic sensitivity of T. pallidum. Almost all patients are men, more frequently middle-aged, and most are men who have sex with men (MSM). A high level of vigilance in undertaking relevant history-taking for associated risk factors and symptoms is important, since early diagnosis and treatment usually leads to a good visual outcome.

The clinical findings of syphilitic uveitis are highly diverse and nonspecific. Characteristic presentations include acute syphilitic posterior placoid chorioretinitis (ASPPC) and syphilitic punctate inner retinitis. Preretinal pale yellowish dots located in the vitreous-retina transition, mainly overlying vasculature and in the periphery are considered characteristic and highly suggestive of ocular syphilis. However, due to the lack of pathognomonic signs and to the fact that uveitis may be the first (and even sole) manifestation of the disease, a high index of suspicion is essential for a definite diagnosis. A triad of headache, red eye or eye pain, and elevated ESR should raise clinical suspicion for ocular syphilis, yet syphilis tests should be routinely performed in all patients with uveitis, retinitis, optic neuritis, or optic atrophy.

The VA at presentation of ocular syphilis can vary and reflects the presence or absence of direct macular involvement or the severity of panuveitis. Visual improvement or complete recovery is possible in most cases with early antimicrobial treatment. Factors associated with final visual acuity ≤ 1.0 despite therapy are worse initial VA, delayed treatment, longer duration of symptoms, higher VDRL titers, presence of HIV coinfection, concomitant neurosyphilis, and inadvertent use of systemic corticosteroids prior to the definite diagnosis. Structural damage to the optic nerve and retina is the main cause of permanent visual loss. It is important to notice that patients may go a long way with low or even falsely negative VDRL titers in up to 30% of cases. FTA-ABS or MHA-TP are more sensitive and specific but provide no indication of disease activity.

Syphilis is an important facilitator of HIV transmission with currently reported co-infection rates of 50-70%, not related to immune deficiency but rather to the same route of infection. The presence of HIV may alter the presentation of syphilis, with possibly a more rapid progression to neurosyphilis. People living with HIV (PLWH) have a 77 to 86 times higher chance of being co-infected with syphilis than HIV-negative individuals. Ocular syphilis remains one of the common causes of bacterial infection in HIV-positive patients.

Ocular complications occur in up to 70-80% of untreated HIV-infected patients, and more than half of these are associated with intraocular inflammation or uveitis. The specific immune condition of patients infected with HIV makes diagnosing HIV-related uveitis difficult. Uveitis is one of the most common ocular complications in PLWH and can be classified into HIV-induced uveitis, co-infection related uveitis, drug-induced uveitis, and immune recovery uveitis (CMV-related). The introduction of antiretroviral therapy (ART) has considerably changed the incidence, diagnosis, and treatment of different types of HIV-related uveitis. Paradoxically, the incidence of ocular syphilis has continuously increased since the combined antiretroviral therapy (cART) era.

As with all patients with uveitis, the approach to the HIV-positive patient with intraocular inflammation should start with a complete history and review of systems. This should include the duration of HIV disease, recent measurements of CD4+ cell count and HIV load, current medications, and any history of other sexually transmitted infections or AIDS-defining illnesses or complications. An immunocompromised state has been found in 13% of uveitis patients, 23% of which are HIV-related. Syphilis infection in HIV-infected men has been associated with a significant increase in the HIV viral load and a significant decrease in the CD4 cell count. However, syphilitic uveitis can occur with any CD4 counts and in virtually any stage of syphilis (primary, secondary, or latent), although it is more commonly seen in secondary syphilis.

Given that the eye is an extension of the central nervous system, ocular syphilis is best regarded as neurosyphilis, with possible associated central nervous system involvement. In fact, the presence of uveitis is one of the criteria of early neurosyphilis in the clinicopathological classification of neurosyphilis symptoms, defined by symptoms of decreased vision, eye pain or photophobia, with diagnosis confirmed by slit-lamp examination. The 2010 Centers for Disease Control and Prevention guidelines recommend that ocular syphilis be treated as neurosyphilis, regardless of the stage of clinical presentation or of lumbar puncture results, with intravenous (IV) crystalline penicillin G, 24 million international units per day, for 10-14 days or longer depending on the patient's status. In case of penicillin allergy, doxycycline or erythromycin can be used as an alternative, not as effective treatment. The Jarisch-Herxheimer reaction, a transient phenomenon resembling bacterial sepsis, usually starting 6 to 8 hours after the initial anti-spirochete treatment, can present as worsening of ocular signs.

There are no controlled studies proving the benefits of adjunctive systemic corticosteroid treatment for syphilitic uveitis. However, timely administration of oral corticosteroids has been shown to be effective in controlling posterior inflammation in ocular syphilis. Alternatively, it can be added if the initial IV penicillin treatment is not followed by an improvement in ocular signs and/or visual function. Periocular dexamethasone injections and methylprednisolone pulses are not indicated as they negatively affect the outcomes. Oral methotrexate (MTX) has also been reported to be beneficial as an

adjunctive therapy for ocular syphilis in resolving residual intraocular inflammation and cystic macular edema (CME). HAART does not prevent the occurrence of ocular syphilis but can help early resolution along with definitive anti-syphilitic treatment.

Keep in mind

- ✓ Syphilis is on the rise, especially, but not only, in people living with HIV. All uveitis patients (HIV-positive included) must be tested for syphilis.
- ✓ Syphilitic uveitis must be regarded as neurosyphilis, since it is often accompanied by retinitis and ocular nerve involvement, both of which are risk factors for adverse outcomes.
- ✓ Early diagnosis and treatment of ocular syphilis with parenteral penicillin are crucial for rapid recovery and prevention of permanent visual loss.

References

1 Mathew RG, Goh BT & Westcott MC (2014). British Ocular Syphilis Study (BOSS): 2-year national surveillance study of intraocular inflammation secondary to ocular syphilis. Investigative ophthalmology & visual science, 55(8), 5394–5400. https://doi.org/10.1167/iovs.14-14559

2 Wells J, Wood C, Sukthankar A & Jones NP (2018). Ocular syphilis: the re-establishment of an old disease. Eye (London, England), 32(1), 99–103. https://doi.org/10.1038/eye.2017.155

3 Lee MI, Lee AW, Sumsion SM & Gorchynski JA (2016). Don't Forget What You Can't See: A Case of Ocular Syphilis. The western journal of emergency medicine, 17(4), 473–476. https://doi.org/10.5811/westjem.2016.5.28933

4 Rothova A, Hajjaj A, de Hoog J, Thiadens AAHJ & Dalm VASH (2019). Uveitis causes according to immune status of patients. Acta ophthalmologica, 97(1), 53–59. https://doi.org/10.1111/aos.13877

5 Furtado JM, Arantes TE, Nascimento H et al. (2018). Clinical Manifestations and Ophthalmic Outcomes of Ocular Syphilis at a Time of Re-Emergence of the Systemic Infection. Scientific reports, 8(1), 12071. https://doi.org/10.1038/s41598-018-30559-7

6 Klein A, Fischer N, Goldstein M, Shulman S & Habot-Wilner Z (2019). The great imitator on the rise: ocular and optic nerve manifestations in patients with newly diagnosed syphilis. Acta ophthalmologica, 97(4), e641–e647. https://doi.org/10.1111/aos.13963

7 Queiroz RP, Inês DV, Diligenti FT et al. (2019). The ghost of the great imitator: prognostic factors for poor outcome in syphilitic uveitis. Journal of ophthalmic inflammation and infection, 9(1), 2. https://doi.org/10.1186/s12348-019-0169-8

8 Yang M, Kamoi K, Zong Y, Zhang J & Ohno-Matsui K (2023). Human Immunodeficiency Virus and Uveitis. Viruses, 15(2), 444. https://doi.org/10.3390/v15020444

9 Cunningham ET Jr (2000). Uveitis in HIV positive patients. The British journal of ophthalmology, 84(3), 233–235. https://doi.org/10.1136/bjo.84.3.233

10 Joyce PW, Haye KR & Ellis ME (1989). Syphilitic retinitis in a homosexual man with concurrent HIV infection: case report. Genitourinary medicine, 65(4), 244–247. https://doi.org/10.1136/sti.65.4.244

11 Lee SY, Cheng V, Rodger D & Rao N (2015). Clinical and laboratory characteristics of ocular syphilis: a new face in the era of HIV co-infection. Journal of ophthalmic inflammation and infection, 5(1), 56. https://doi.org/10.1186/s12348-015-0056-x

12 Sudharshan S, Nair N, Curi A, Banker A & Kempen JH (2020). Human immunodeficiency virus and intraocular inflammation in the era of highly active antiretroviral therapy - An update. Indian journal of ophthalmology, 68(9), 1787–1798. https://doi.org/10.4103/ijo.IJO_1248_20

13 Buscho SE, Ishihara R, Gupta PK & Mopuru R (2022). Secondary Syphilis Presenting as Bilateral Simultaneous Papillitis in an Immunocompetent Individual. Cureus, 14(8), e28465. https://doi.org/10.7759/cureus.28465

14 Mohd Fadzil NI, Abd Hamid A, Muhammed J & Hashim H (2022). Ocular Syphilis: Our Experience in Selayang Hospital, Malaysia. Cureus, 14(7), e26655. https://doi.org/10.7759/cureus.26655

15 Sahin O & Ziaei A (2015). Clinical and laboratory characteristics of ocular syphilis, co-infection, and therapy response. Clinical ophthalmology (Auckland, N.Z.), 10, 13–28. https://doi.org/10.2147/OPTH.S94376

16 Sittivarakul W, Aramrungroj S & Seepongphun U (2022). Clinical features and incidence of visual improvement following systemic antibiotic treatment in patients with syphilitic uveitis. Scientific reports, 12(1), 12553. https://doi.org/10.1038/s41598-022-16780-5

17 Sun CB, Liu GH, Wu R & Liu Z (2022). Demographic, Clinical and Laboratory Characteristics of Ocular Syphilis: 6-Years Case Series Study From an Eye Center in East-China. Frontiers in immunology, 13, 910337. https://doi.org/10.3389/fimmu.2022.910337

18 Balamurugan S, Gurnani B & Kaur K (2020). Commentry: Ocular coinfections in human immunodeficiency virus infection – What is so different? Indian journal of ophthalmology, 68(9), 1997–1998. https://doi.org/10.4103/ijo.IJO_680_20

19 Bollemeijer JG, Wieringa WG, Missotten TO et al. (2016). Clinical Manifestations and Outcome of Syphilitic Uveitis. Investigative ophthalmology & visual science, 57(2), 404–411. https://doi.org/10.1167/iovs.15-17906

20 Rodrigues RA, Nascimento HM & Muccioli C (2014). Yellowish dots in the retina: a finding of ocular syphilis?. Arquivos brasileiros de oftalmologia, 77(5), 324–326. https://doi.org/10.5935/0004-2749.20140081

21 Gu X, Gao Y, Yan Y et al. (2020). The importance of proper and prompt treatment of ocular syphilis: a lesson from permanent vision loss in 52 eyes. Journal of the European Academy of Dermatology and Venereology : JEADV, 34(7), 1569–1578. https://doi.org/10.1111/jdv.16347

22 Daey Ouwens IM, Ott A, Fiolet A et al. (2019). Clinical Presentation of Laboratory Confirmed Neurosyphilis in a Recent Cases Series. Clinical neuropsychiatry, 16(1), 17–24. https://www.ncbi.nlm.nih.gov/pmc/articles/PMC8650203/

Case 20 - June 2023

PRE-DESCEMET CORNEAL DYSTROPHY

A 59-year-old man was referred for investigation of bilateral diffuse corneal opacities.

Presented by
Miltos Balidis, MD, PhD, FEBOphth, ICOphth

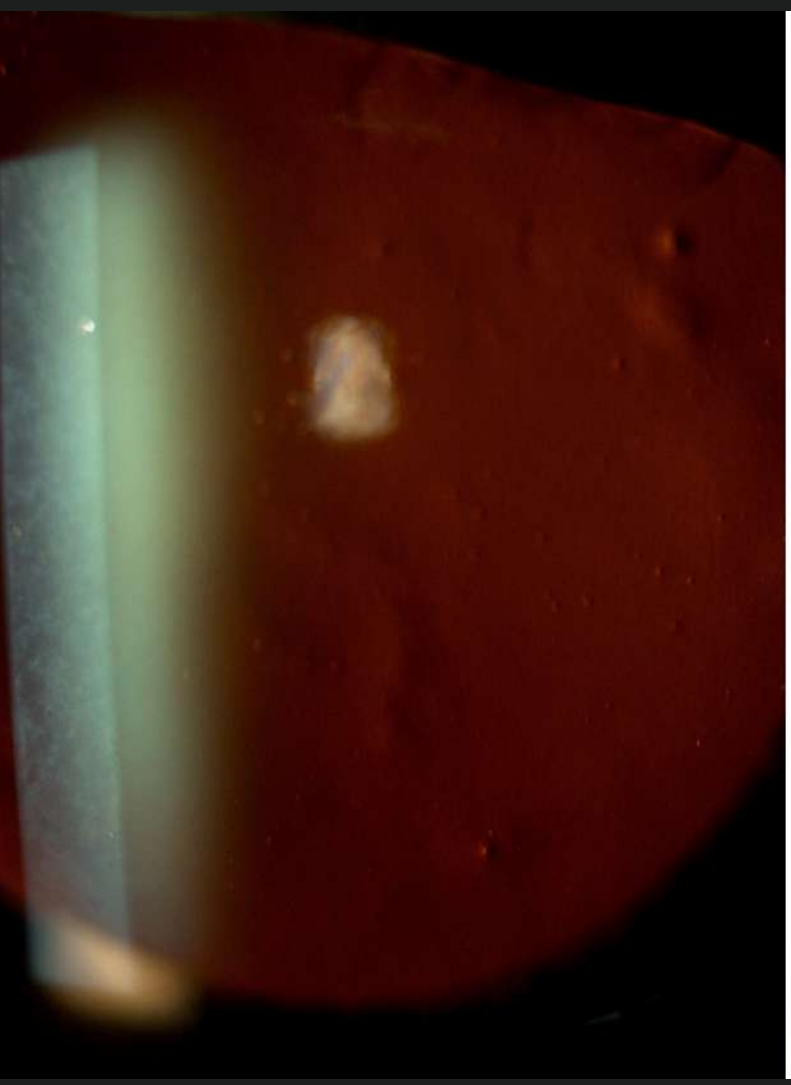

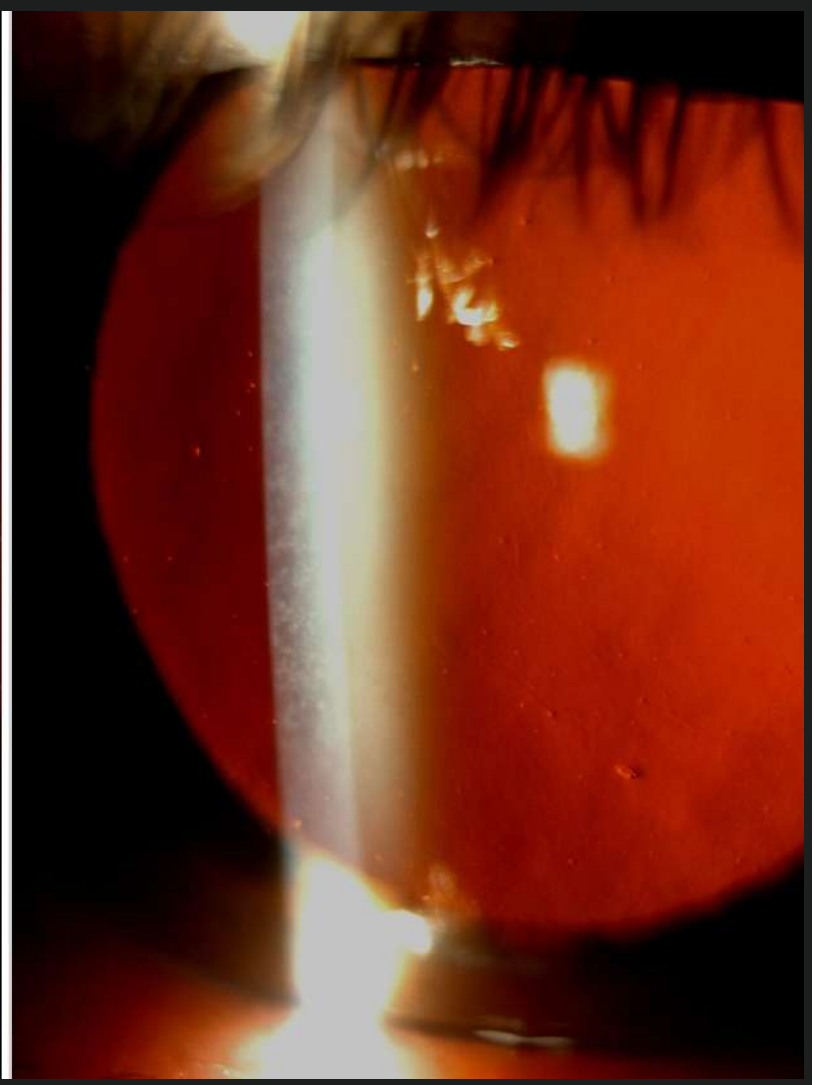

Edited by
Penelope Burle de Politis, MD

Case History

A 59-year-old Caucasian man was referred for diagnosis and management of diffuse corneal opacities of unknown duration in both eyes (BE). He had no previous records of ocular or systemic diseases. His family history was unremarkable. Upon ophthalmological examination, his corrected distance visual acuity (CDVA) was 10/10 in the right eye (RE) and 8/10 in the left eye (LE). Refractometry was -2.00 -0.75@75° in the RE and -2.00 -0.50@45° in the LE, and intraocular pressure was respectively 11 and 12 mmHg. Fundoscopy was bilaterally normal. Under biomicroscopy, BE featured a deep net of thin, confluent corneal opacities with intervening clear cornea, extending to 360° of the corneal radius, with relative sparing of the corneal periphery (**Figure 1**). Higher magnification revealed that the opacities varied in shape from dendritic to filiform and laid along the posterior stroma (**Figure 2**). The eyes were calm, and a grade 1-2 nuclear cataract was detected in the LE.

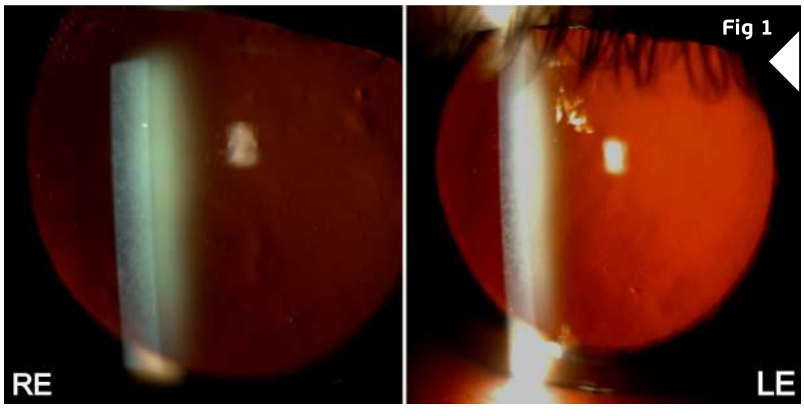

Figure 1: Low-magnification slit-lamp photograph showing a symmetrical dust-like appearance of both corneas, predominantly in the center and mid-periphery.

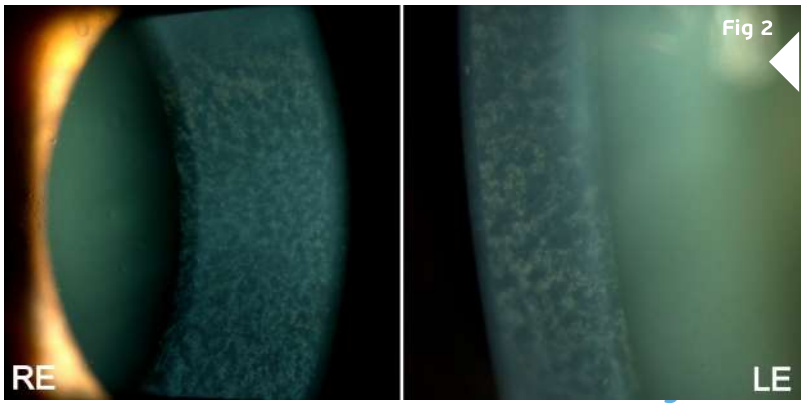

Figure 2: High-magnification slit-lamp photograph showing a normally-appearing anterior corneal stroma in both eyes, while the posterior stroma is diffusely taken by fine, pleomorphic grayish deposits. A moderately mature nuclear cataract is also noticeable in the LE.

Anterior segment spectral domain optical coherence tomography (anterior SD-OCT) revealed a dense hyperreflective band in the pre-Descemet corneal stroma, evenly extending from limbus to limbus, as well as scattered hyperreflective bodies throughout the corneal stroma in BE. Corneal pachymetry was within the normal range bilaterally (**Figure 3**).

Corneal tomography displayed a slightly irregular astigmatism (**Fig. 4**) and Scheimpflug Corneal Densitometry was consistent with a hyperdense pre-Descemet stroma in BE (**Figure 5**). Keratometric values were unremarkable and the epithelial maps obtained with the Anterion® platform showed no significant changes in either eye.

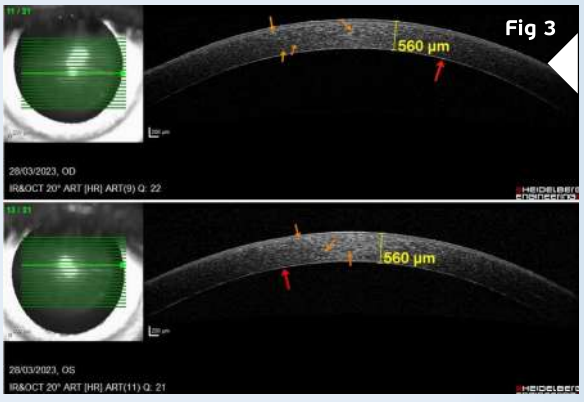

Figure 3: Anterior SD-OCT (Heidelberg Engineering®) displaying bilateral punctate hyperreflective particles at different depths of the cornea (orange arrows) and forming a dense band in the posterior stroma immediately anterior to the Descemet's membrane (red arrows). There are no signs of corneal edema (central pachymetry of 560 µm in BE).

Figure 4: Refractive Display of the Pentacam® corneal tomography showing slight topographic irregularity in BE. Kmax is 42.9 D in the RE and 42.9 D in the LE.

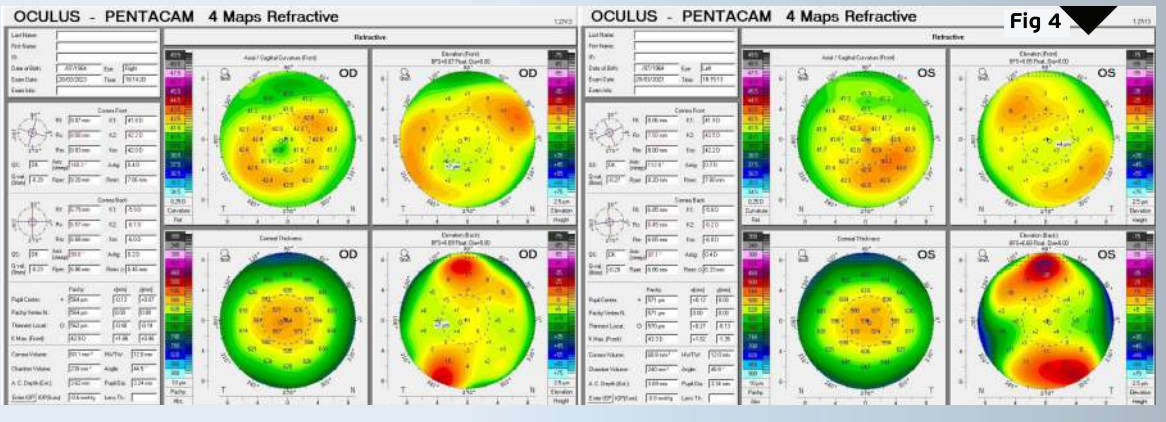

Figure 5: Corneal Optical Densitometry display (Pentacam®) demonstrating areas of increased density in all depths (anterior, center and posterior) and all circumferences (from 0-2 to 10-12 mm) of both corneas.

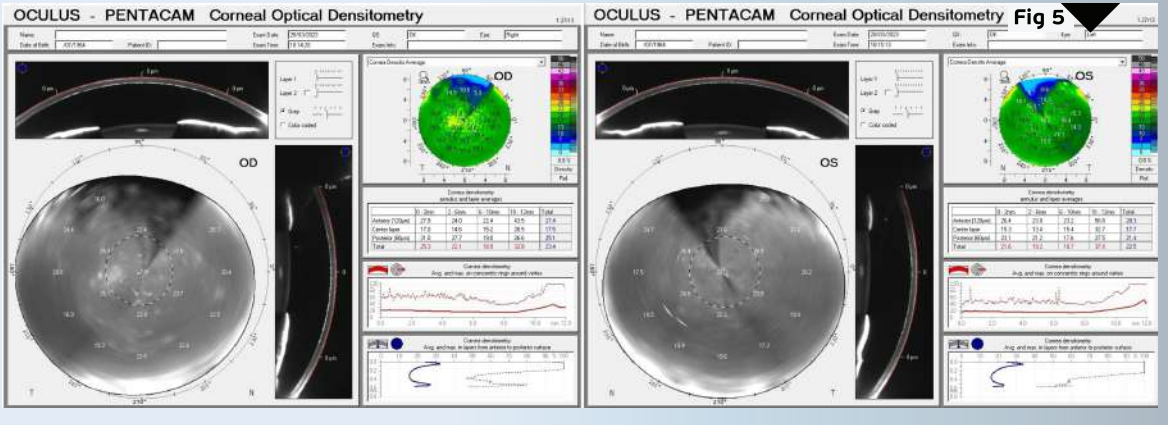

Figure 6: Scheimpflug Images (Pentacam®) revealing a bimodal peak light scattering in both corneas with a posterior peak (in gray scale units — GSU) of 50.6 in the RE and of 40.8 in the LE. Increased nuclear lens density in the LE is evident as well.

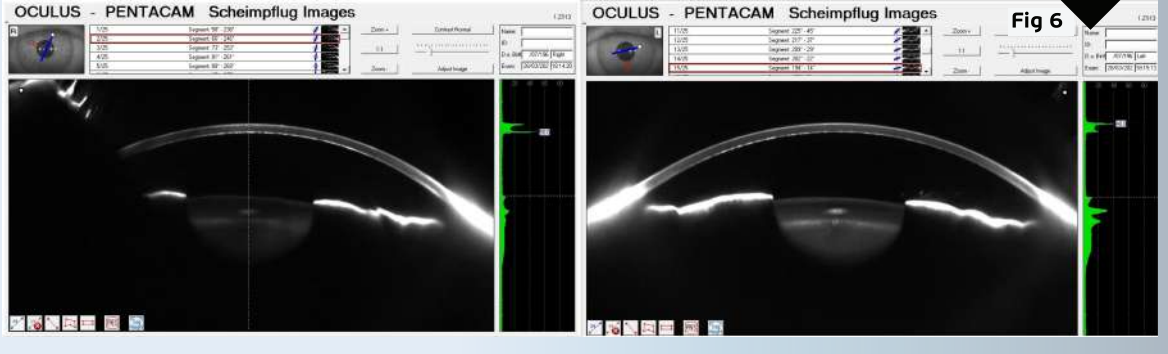

Additional History

Based on the clinical and multimodal image findings, the diagnosis of pre-Descemet corneal dystrophy was established.

Considering the lack of complaints and good visual acuity in BE, conservative follow-up was the management of choice for the moment.

Differential Diagnosis of Pre-Descemet Corneal Dystrophy

- cornea farinata
- long-term contact lens use
- Fleck corneal dystrophy
- corneal epithelial basement membrane dystrophy
- Fuchs corneal endothelial dystrophy
- crystalline keratopathy related to monoclonal gammopathy

The differentiation among the different types of posterior corneal dystrophy is based on their morphology and distribution of abnormal material within the corneal tissue. While histopathologic study remains the gold standard for diagnosis, attentive corneal examination complemented by high-resolution methods are the definite tool for accurate identification and proper management of each disorder.

Discussion and Literature

Corneal dystrophies (CDs) are a collection of hereditary non-inflammatory disorders that affect corneal transparency and refraction due to abnormal deposition of substances in the cornea. According to the International Classification of Corneal Dystrophies (IC3D — 2015), CDs are subclassified in epithelial/subepithelial, epithelial-stromal, stromal, and endothelial dystrophies, depending on their location. Patients with CD can be asymptomatic or present with bilateral visual acuity loss, typically in the form of irregular astigmatism. Symptoms can begin at various ages and treatment can range from conservative measures to corneal transplantation.

Pre-Descemet is a rarer form of CD, first described in 1947. It has been referred to as cornea farinata, posterior filiform dystrophy or posterior punctiform dystrophy, and described as the accumulation of gray-white-bluish dust-like opacities made of lipids that are characteristically located at the pre-Descemet area of the cornea. These deposits are well demarcated and can be better visualized under biomicroscopic retroillumination. Their shape can vary from circular to linear, dendritic, filiform, comma- or "boomerang"-shaped. They can be confined to the axial area of the cornea alone (axial type), be located 1 to 2 mm within the limbus, sparing both the peripheral and axial cornea (annular type), or be diffusely distributed throughout the cornea (diffuse type).

The diagnosis of PDCD is based mainly on the slit-lamp findings of fine, polymorphic opacities just anterior to Descemet's membrane. Nonetheless, the latest high-resolution anterior segment imaging technologies allow for non-invasive assessment of corneal structure and histology. Both spectral domain optical coherence tomography (SD-OCT) and in vivo confocal microscopy (IVCM) have been used to corroborate the diagnosis of PDCD and for a better understanding of its pathophysiology. Other propaedeutic methods such as corneal tomography can be useful in discarding other corneal abnormalities that may occur simultaneously with the condition, such as keratoconus. No biological tests for PDCD are available at the moment.

Due to its asymptomatic nature, pre-Descemet CD (PDCD) may go undiagnosed for long. The disorder is found more often in females and usually presents later in life (third to fourth decade). The condition can be asymmetric but is always bilateral. The lesions may confluence and form clumps. Because neither the endothelium nor the epithelium is involved, there is no corneal edema, photophobia, pain, or surface changes. Corneal sensitivity is not affected.

Even though patients with pure PDCD are asymptomatic, the condition has been found in conjunction with other CDs and systemic disorders such as ichthyosis. Isolated PDCD is often sporadic; however, a genetic form of the disease, probably with autosomal dominant inheritance and unknown gene location, has been described. A genetic basis has been identified in the subtype punctiform and polychromatic pre-Descemet corneal dystrophy (PPPCD), which also features increased corneal stiffness.

Although classically described as pre-Descemet, PDCD may involve the entire cornea. Both transmission electron microscopy and IVCM have evidentiated enlarged hyperreflective posterior stromal keratocytes with either hyperreflective or hyporeflective intracellular dots corresponding to intracytoplasmic inclusions of electron-dense, lipofuscin-like lipoprotein. This degenerative change in posterior stromal keratocytes is likely to be the origin of the slit-lamp presentation of PDCD. On the other hand, IVCM allows for a layer-by-layer analysis and demonstrates that the pathology is more extensive, with signs not only in the corneal stroma, but also in the endothelium and sub-basal nerves, whilst without functional compromise.

The current trend is that PDCD may be a variant of different corneal diseases sharing the same pathophysiological pathway. Latest evidence suggests that sporadic PDCD belongs in the spectrum of degenerative corneal disorders. Similar histological findings have been described in other conditions such as long-term contact lens wear. Recently, an identical corneal disorder was described in dogs, both through OCT and IVCM, with signs that support the degenerative theory.

For the moment, PDCD is neither a contraindication for laser corneal ablation nor an indication for phototherapeutic corneal procedures, as uneventful outcomes of PRK have been reported with no alteration of the corneal deposits. Conservative follow-up remains the management of choice for isolated cases. Genetic counseling is advised in cases where a genetic form can be traced back in the family tree.

Keep in mind

- ✓ Unlike other forms of posterior corneal dystrophies, PDCD is predominantly located at the pre-Descemet stroma, thus its absence of symptoms and lack of visual impairment.
- ✓ Even though the diagnosis of PDCD is typically obtained through biomicroscopy, other non-invasive imaging methods can be used to confirm it, exclude other corneal disorders, and help understand its physiopathology.
- ✓ Due to its benign clinical course, PDCD does not require any intervention. However, until the condition is fully elucidated, regular follow-up is advised.

References

1 Moshirfar M, Bennett P & Ronquillo Y (2022). Corneal Dystrophy. In StatPearls. StatPearls Publishing.

2 Vemuganti GK, Rathi VM & Murthy SI (2011). Histological landmarks in corneal dystrophy: pathology of corneal dystrophies. Developments in ophthalmology, 48, 24–50. https://doi.org/10.1159/000324261

3 Grayson M & Wilbrandt H (1967). Pre-Descemet dystrophy. American journal of ophthalmology, 64(2), 276–282. https://doi.org/10.1016/0002-9394(67)92524-x

4 Curran RE, Kenyon KR & Green WR (1974). Pre-Descemet's membrane corneal dystrophy. American journal of ophthalmology, 77(5), 711–716. https://doi.org/10.1016/0002-9394(74)90536-4

5 Boere PM, Bonnet C, Frausto RF, Fung SSM & Aldave AJ (2020). Multimodal Imaging of Pre-Descemet Corneal Dystrophy Associated With X-Linked Ichthyosis and Deletion of the STS Gene. Cornea, 39(11), 1442–1445. https://doi.org/10.1097/ICO.0000000000002382

6 Alió Del Barrio JL, Chung DD, Al-Shymali O, Barrington A, Jatavallabhula K, Swamy VS, Yébana P, Angélica Henríquez-Recine M, Boto-de-Los-Bueis A, Alió JL & Aldave AJ (2020). Punctiform and Polychromatic Pre-Descemet Corneal Dystrophy: Clinical Evaluation and Identification of the Genetic Basis. American journal of ophthalmology, 212, 88–97. https://doi.org/10.1016/j.ajo.2019.11.024

7 Alafaleq M, Georgeon C, Grieve K & Borderie VM (2020). Multimodal imaging of pre-Descemet corneal dystrophy. European journal of ophthalmology, 30(5), 908–916. https://doi.org/10.1177/1120672119862505

8 Malhotra C, Jain AK, Dwivedi S, Chakma P, Rohilla V & Sachdeva K (2015). Characteristics of Pre-Descemet Membrane Corneal Dystrophy by Three Different Imaging Modalities-In Vivo Confocal Microscopy, Anterior Segment Optical Coherence Tomography, and Scheimpflug Corneal Densitometry Analysis. Cornea, 34(7), 829–832. https://doi.org/10.1097/ICO.0000000000000454

9 Park S, Sebbag L, Moore BA, Casanova MI, Leonard BC, Daley NL, Steele KA, Li JY, Murphy CJ & Thomasy SM (2022). Multimodal ocular imaging of known and novel corneal stromal disorders in dogs. BMC veterinary research, 18(1), 117. https://doi.org/10.1186/s12917-022-03214-7

10 Kontadakis GA, Kymionis GD, Kankariya VP, Papadiamantis AG & Pallikaris AI (2014). Corneal confocal microscopy findings in sporadic cases of pre-descemet corneal dystrophy. Eye & contact lens, 40(2), e8–e12. https://doi.org/10.1097/ICL.0b013e318273be9f

Case 21 - July 2023

MORNING GLORY SYNDROME

A 12-year-old boy was referred for investigation of peripapillary atrophy in one eye.

Presented by
Paris Tranos, MD, PhD, ICOphth, FRC
& Jenny Papastergiopoulou, MD

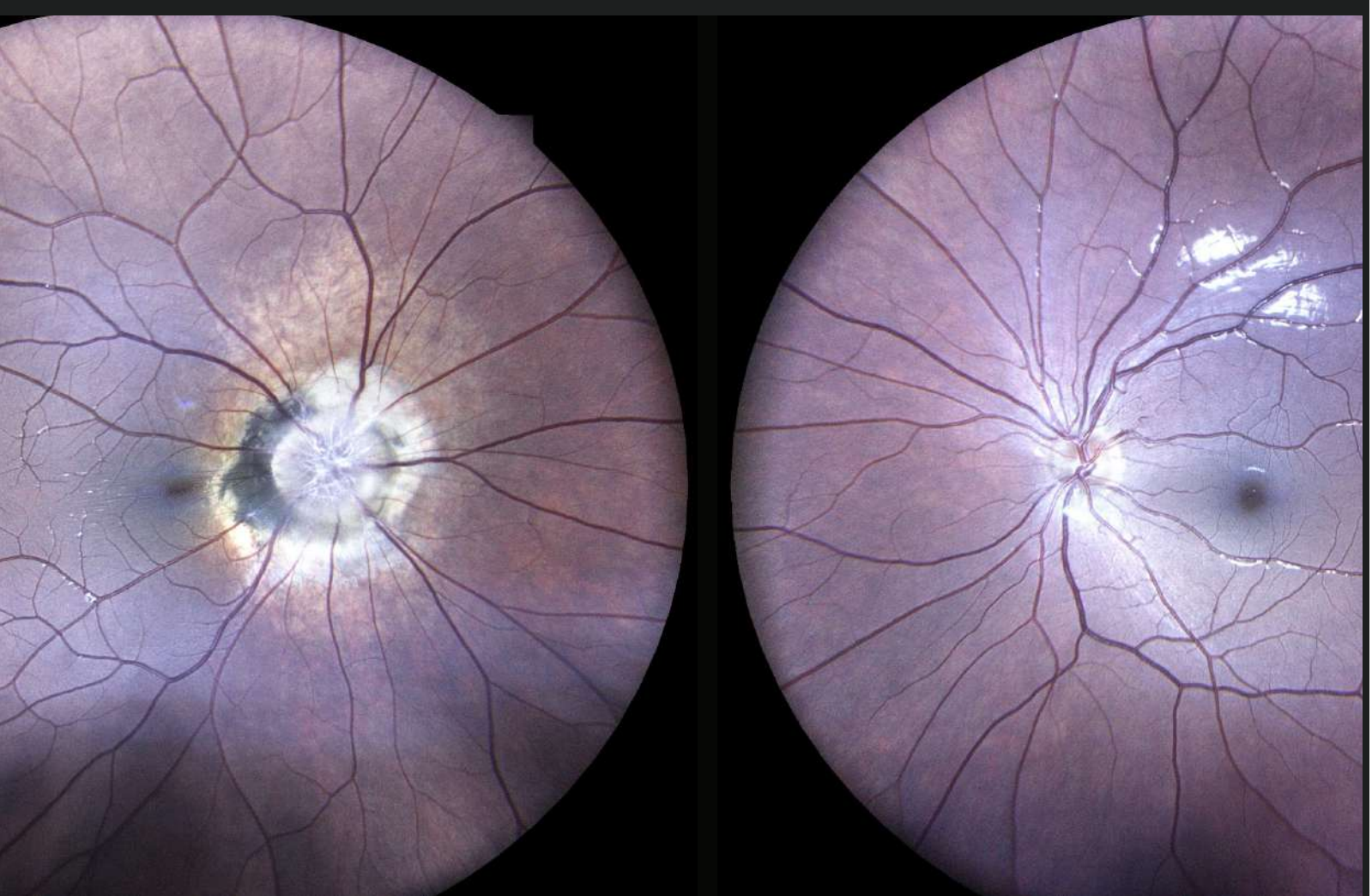

Edited by
Penelope Burle de Politis, MD

Case History

A 12-year-old Caucasian boy was referred for investigation of an accidentally found optic disc lesion in the right eye (RE). When questioned, he stated that his vision in the RE was somewhat worse than in the left eye (LE). There were no previous records of ocular disorders. He was a cystic fibrosis carrier. His family history was unremarkable. Upon ophthalmological examination, his corrected distance visual acuity (CDVA) was 10/10-1 in the RE and 10/10 in the LE. Refractometry was -0.75@40° in the RE and plano in the LE, and intraocular pressure was respectively 12 and 13 mmHg. There were no abnormalities under anterior segment biomicroscopy. At fundoscopy, LE was normal, while RE presented extensive peripapillary atrophy with pigmentary changes and abnormally rectified vessels. (**Figure 1**). There was no relative afferent pupillary defect (RAPD).

Fundus autofluorescence imaging of the RE displayed reduced autofluorescence at the peripapillary area (**Figure 2**).

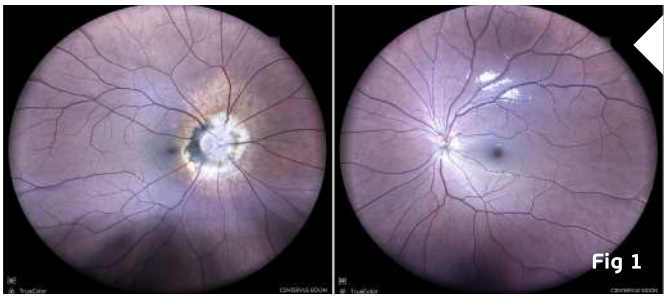

Figure 1: Color fundus photograph (EIDON true-color confocal scanner®) showing peripapillary atrophy and pigmentary changes in the right eye.

Figure 2: Fundus autofluorescence photograph of the RE (Heidelberg Engineering®) illustrating the extension of peripapillary atrophy and the vascular rectification.

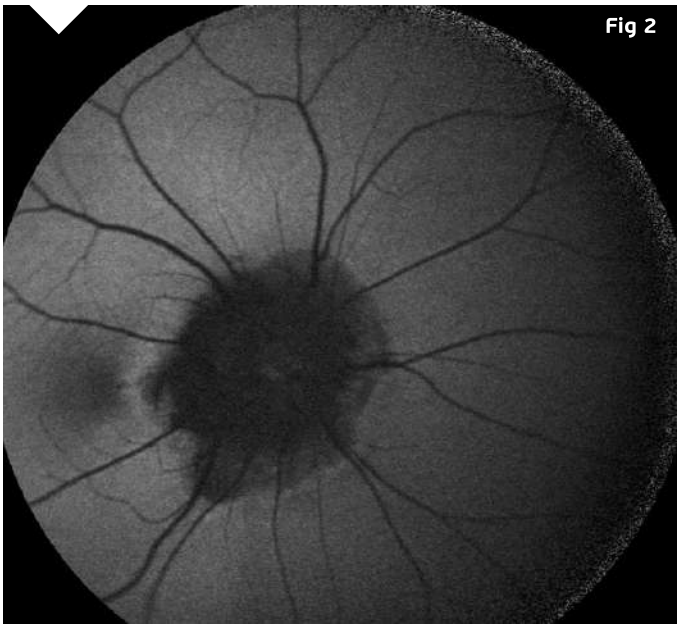

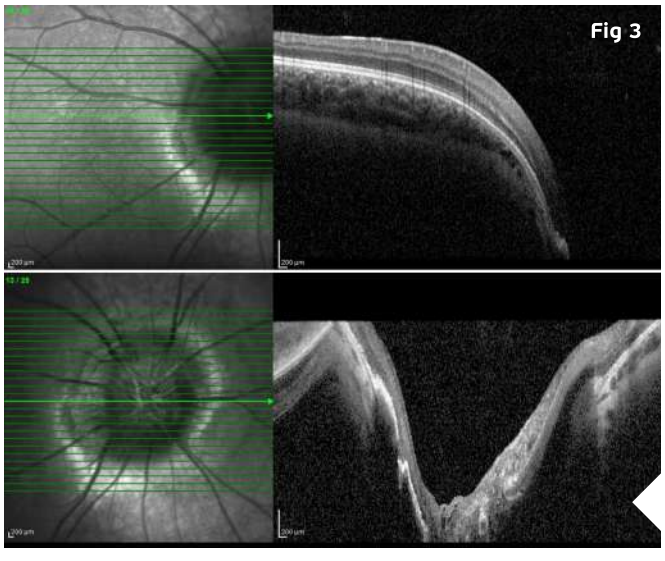

Figure 3: Spectral domain optical coherence tomography (SD-OCT, Heidelberg Engineering®) of the RE demonstrating a deep central pitting of the optic nerve head.

Spectral domain optical coherence tomography (SD-OCT) of the RE evidentiated a deep central slope at the optic nerve head (**Figure 3**).

B-scan did not reveal any evidence of optic disc calcification (**Figure 4**).

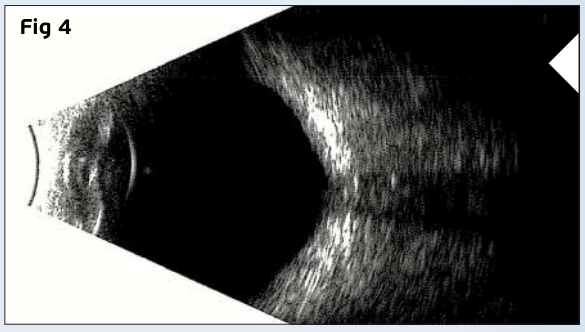

Figure 4: B-mode ultrasonography of the RE showing no evidence of calcification at the optic papilla.

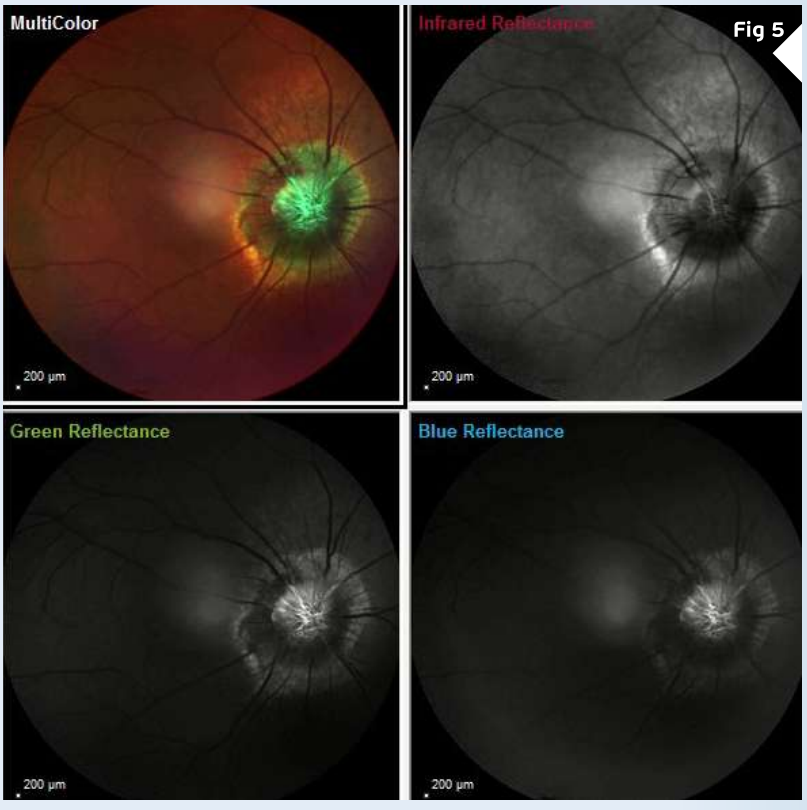

Figure 5: Infrared, blue, green, and multicolor reflectance photographs (Heidelberg Engineering®) of the RE featuring a characteristic flower-shaped pitting of the optic papilla. Notice the elevated rim outlining the optic nerve slope.

Fundus reflectance imaging using different color filters showed a characteristic aspect of the optic nerve pitting, resembling the shape of the morning glory flower (**Figure 5**).

Additional History

Based on the clinical and multimodal image findings, the diagnosis of morning glory syndrome was established.

Brain imaging with magnetic resonance (MRI, MRA – magnetic resonance angiography) and/or computed tomography (CT, CTA – computed tomography angiography) was requested in order to rule out central nervous system (CNS) involvement, including basal encephalocele, Moyamoya syndrome (abnormal narrowing of cerebral arteries causing cerebral ischemia), and other structural or vascular abnormalities.

Considering the good visual acuity and absence of high-risk predisposing retinal lesions, conservative follow-up was the management of choice for the moment.

Differential Diagnosis of Morning Glory Syndrome

- optic disc coloboma
- CHARGE syndrome
- optic nerve head avulsion
- optic nerve aplasia
- optic disc pit
- advanced glaucomatous optic neuropathy
- combined retinal RPE hamartoma
- choroidal osteoma
- circumscribed choroidal hemangioma
- amelanotic choroidal nevus

The differentiation among the different types of optic papillary abnormalities is based on their morphological, histological, and vascular features. Attentive fundus examination supplemented with multimodal imaging methods is key for accurate diagnosing and management.

Discussion and Literature

Morning glory syndrome (MGS) or morning glory disc anomaly (MGDA) is a rare sporadic disorder characterized by a funnel-shaped optic nerve head. It was first described by Handmann in 1929, then by Kindler in 1970, who called it morning glory disc anomaly because of its resemblance to the morning glory flower. It is a primary mesenchymal and neuroectodermal malformation in which abnormal differentiation results in faulty closure of the posterior sclera and herniation of the retina and optic nerve head. The developmental disruption most likely occurs at 4-5 weeks of embryonic growth.

The reported prevalence of MGS is 2.6 to 3.6 per 100,000. A preference of 2:1 for the female gender has been reported and according to USA statistics it is less common in black people. It is mostly unilateral (85% of cases). Most of the cases present in early childhood with decreased vision – visual acuity usually ranging from 20/200 to counting fingers –, strabismus – esotropia or exotropia –, or leukocoria – less frequently. Bilateral cases normally present with nystagmus as well. Affected eyes are typically myopic and astigmatic. An afferent pupillary defect is usually present in unilateral cases.

Fundus evaluation of MGDA reveals an enlarged, orange or pink disc, within an excavated area. The peripapillary area is elevated, with an annular zone of pigmentary changes. The junction between the disc and the peripapillary area is often obscured. A whitish, fluffy, glial tissue is present in the center of the optic disc slope. The retinal blood vessels arise from the periphery of the excavation in a radial spoke, wheel-like pattern-disc and course radially towards the retinal periphery. They are abnormally straight and branch at acute angles. It is often difficult to differentiate an artery from a vein. Vascular sheathing may be present. The macula may be incorporated in the funnel-shaped excavated area, a finding known as macular capture. Retinoschisis may be present.

Some cases of MGDA have systemic associations such as Moyamoya syndrome, facial or central nervous system abnormalities, or renal coloboma syndrome. Magnetic resonance imaging of the skull and abdominal ultrasonography should be performed to discard involvement of other organs. Computerized tomography (CT) of the orbits and brain can reveal intraocular calcifications and other abnormalities. Early diagnosis is crucial to avoid complications, mainly retinal detachment (RD), either tractional — due to subretinal neovascularization —, rhegmatogenous or serous (with or without retinal breaks). It is hypothesized that small breaks can form due to the contractile nature of the glial tissue, allowing for the accumulation of subretinal fluid. Eco- and tomographic findings point to the existence of an abnormal communication between the subretinal and subarachnoid or vitreous compartments, another explanation for the physiopathology of RD in MGS.

The severity of MGDA and comorbidities in an individual patient may not be revealed through routine ophthalmological examination, which calls for attention to associated risks. This is especially important as most patients are diagnosed at an age where intervention still can be highly meaningful. Refractive errors should be corrected when present to improve visual acuity and prevent amblyopia. Juxtapapillary laser photocoagulation can be used both prophylactically or supplementarily to vitrectomy in the prevention and management of MGS-associated RD. Recurrence and complications of the surgical interventions must be taken into consideration. Ecographic parameters such as cavitary depth, size of excavation and axial length can be used to assess the risk of RD and poor vision.

Keep in mind

- ✓ Morning glory syndrome is a rare, usually unilateral malformation of the optic papilla, and sometimes of other organs and systems. Neuroimaging is recommended to rule out CNS involvement.
- ✓ Morning glory disc anomaly classically presents during childhood, with decreased vision in the affected eye and strabismus.
- ✓ The most frequent complication of MGDA is RD; therefore, extensive search for predisposing lesions is crucial to prevent vision loss.

References

1 Gupta A, Singh P & Tripathy K (2023). Morning Glory Syndrome. In StatPearls. StatPearls Publishing.

2 Kindler P (1970). Morning glory syndrome: unusual congenital optic disk anomaly. American journal of ophthalmology, 69(3), 376–384. https://doi.org/10.1016/0002-9394(70)92269-5

3 Pollock S (1987). The morning glory disc anomaly: contractile movement, classification, and embryogenesis. Documenta ophthalmologica. Advances in ophthalmology, 65(4), 439–460. https://doi.org/10.1007/BF00143047

4 Dedhia CJ, Gogri PY & Rani PK (2016). Rare bilateral presentation of morning glory disc anomaly. BMJ case reports, 2016, bcr2016215846. https://doi.org/10.1136/bcr-2016-215846

5 Ceynowa DJ, Wickström R, Olsson M, Ek U, Eriksson U, Wiberg MK & Fahnehjelm KT (2015). Morning glory disc anomaly in childhood - a population-based study. Acta ophthalmologica, 93(7), 626–634. https://doi.org/10.1111/aos.12778

6 Zou Y, She K, Hu Y, Ren J, Fei P, Xu Y, Peng J & Zhao P (2022). Clinical and Echographic Features of Morning Glory Disc Anomaly in Children: A Retrospective Study of 249 Chinese Patients. Frontiers in medicine, 8, 800623. https://doi.org/10.3389/fmed.2021.800623

7 Cennamo G, de Crecchio G, Iaccarino G, Forte R & Cennamo G (2010). Evaluation of morning glory syndrome with spectral optical coherence tomography and echography. Ophthalmology, 117(6), 1269–1273. https://doi.org/10.1016/j.ophtha.2009.10.045

8 Harasymowycz P, Chevrette L, Décarie JC, Hanna N, Aroichane M, Jacob JL, Milot J, & Homsy M (2005). Morning glory syndrome: clinical, computerized tomographic, and ultrasonographic findings. Journal of pediatric ophthalmology and strabismus, 42(5), 290–295. https://doi.org/10.3928/0191-3913-20050901-11

9 Zou YH, She KQ, Ren JN, Liang TY, Fei P, Xu Y, Li J, Zhang X, Peng J & Zhao PQ (2022). Prophylactic juxtapapillary laser photocoagulation in pediatric morning glory syndrome. International journal of ophthalmology, 15(5), 766–772. https://doi.org/10.18240/ijo.2022.05.12

10 Etheridge T, Oake Z & Altaweel MM (2021). Management of Retinal Detachment Associated with Morning Glory Disc Syndrome. Case reports in ophthalmology, 12(2), 457–463. https://doi.org/10.1159/000516205

Case 22 - October 2023

ORBITAL CAVERNOUS HEMANGIOMA

A 50-year-old man was referred for management of a slowly progressive proptosis on the right.

Presented by
Evaggelos Lokovitis, MD, FEBOphth

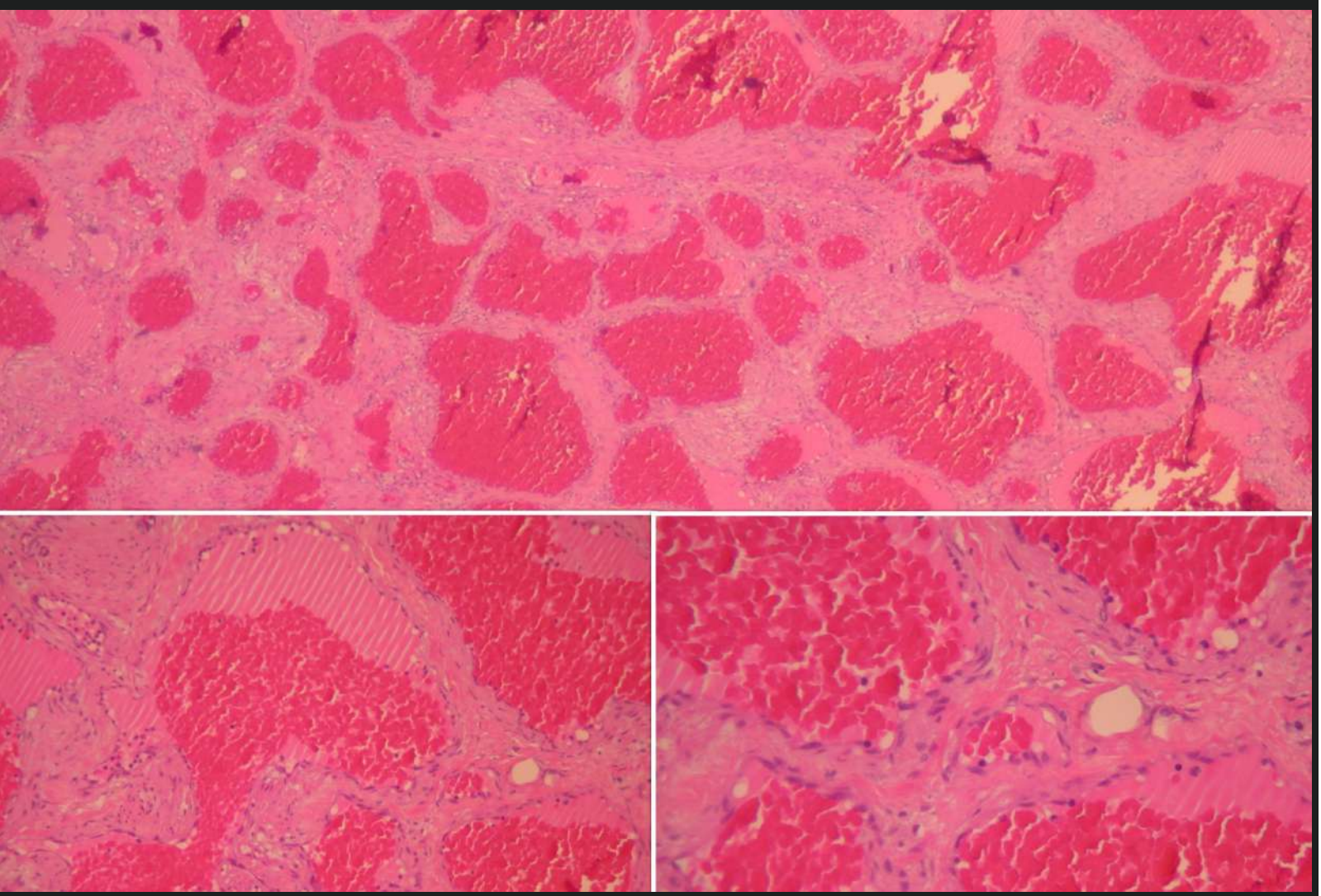

Edited by
Penelope Burle de Politis, MD

Case History

A 50-year-old Caucasian woman was referred for diagnosis and treatment of a progressive, painless proptosis of his right eye (RE) over the course of 6 months. He had no complaints of pain, diplopia, or vision loss. There were no records of trauma. His general health and family history were unremarkable. On examination, uncorrected visual acuity (UCVA) was 10/10 in both eyes. The right lid crease was slightly larger than the left, with no lid retraction (**Figure 1**). There were neither signs of ocular surface inflammation, nor ulcers or scars. Fundoscopy and intraocular pressure were bilaterally normal. There was neither limitation of the ocular movements nor relative afferent pupillary defect. Exophthalmometry on the right was 25/20/3.5. Palpation of the globe offered some resistance to retropulsion, but no external mass was detectable. No pulse or bruit could be felt.

The magnetic resonance imaging (MRI) of the skull ordered by the referring doctor and brought by the patient displayed an intraconal orbital mass of heterogeneous hyperintensity, in close contact with the optic nerve, with no apparent disruption of the nerve sheath. Visual field testing rendered normal results.

Surgical exploration for excisional biopsy was indicated. Through a transpalpebral superolateral orbitotomy (**Figure 2**), the mass was completely isolated and excised. Macroscopically, the tumor consisted of a lobulated, well-circumscribed, violaceous tissue growth, completely involved by a brilliant, smooth, translucid, highly vascularized capsule. The lesion measured 2.9 X 1.9 cm. The gross appearance was that of a vascular neoplasia, with no signs of necrosis or bleeding (**Figure 3**).

Figure 1: Photographs in orthostatic (top) and supine (bottom) positions illustrating the axial proptosis of the right eye, without relevant ocular deviation.

Figure 2: Surgical approach through a transpalpebral superolateral orbitotomy, allowing from direct visualization and total excision of the tumor.

The ectoscopic changes receded in the immediate postoperative period, with noticeable return of the ocular globe to its physiological position, with no functional or aesthetic sequelae.

Additional History

The excised lesion was sent to histopathological examination. Under microscopic examination, the neoplasm consisted of multiple vascular channels and abundant stroma. The vascular structures are filled with blood and variable degrees of thrombosis, confirming the main diagnostic hypothesis of orbital cavernous hemangioma (**Figure 4**).

Figure 3: Macroscopic aspect of the resected tumor, a roundish, lobulated mass of violaceous tissue of soft texture, measuring 2.9 cm in its longest axis.

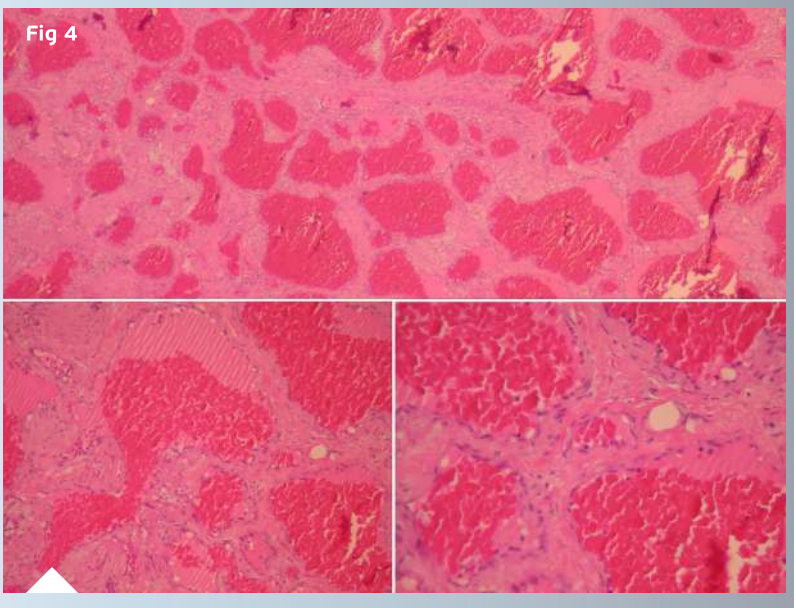

Figure 4: Microscopic photographs (histopathological images) of the mass, with the characteristic features of cavernous hemangioma. Top: hematoxylin-eosin stain (H+E) at 25X magnification displaying thin-walled, abnormally dilated and hyperemic vessels in fibrotic stroma. Bottom left: the same area in higher magnification (100X). Bottom right: 200X magnification showing that the inner surface of the vessels is covered by flat endothelial cells without atypia.

Considering the benign nature of the tumor, the thorough surgical excision, and the restoration of the orbital normality, the patient was scheduled for regular follow-up, without further interventions.

Differential Diagnosis of Orbital Cavernous Hemangioma

- lymphoma
- lymphangioma
- hemangiopericytoma
- orbital inflammatory syndrome (orbital pseudotumor)
- Grave's disease
- meningioma
- dermoid cyst
- fibrous histiocytoma
- neurofibroma
- orbital schwannoma
- orbital metastasis

Definitive diagnosis of any orbital neoplasm requires biopsy. It is nearly impossible to differentiate between these tumors based on clinical exam alone. An encapsulated tumor formed of an intricate net of slow-flow vascular structures is typical of orbital cavernous hemangiomas.

Discussion and Literature

Cavernous hemangioma (CH) is the most common primary orbital lesion of adults. Recently considered a type 3 low-flow arterial-venous malformation, orbital CH (OCH) occurs more often in women and typically presents in the fourth and fifth decades of life. It is a benign vascular growth characterized by a well-defined capsule and numerous large vascular channels. The most common sign of OCH is progressive axial proptosis from the preferential involvement of the intraconal orbital space. Optic nerve damage and other signs of orbital pathology may be present, with a variable degree of visual impairment.

There is no side predilection, but OCH are generally located at the temporal quadrant. Multifocal and bilateral occurrence has been described, sometimes associated with syndromes predisposing to hemangiomas. The progression rate is extremely variable. Symptoms may last for weeks to years and are nonspecific in the beginning. Pain is not common, but some patients may complain of frontal headache. Most of the cases present proptosis and orbital enlargement. Bruits or pulsations are rarely seen. Disc edema and choroidal folds are possible findings, but optic atrophy is rare. Diplopia and corneal compromise are uncommon. Intraocular tension is usually not affected.

B-Scan, computed tomography and magnetic resonance are the main imaging methods for the diagnosis of OCH. Surgical removal is recommended, at least in cases with constant growth tendency, marked bulbar protrusion or significant optic nerve compression. Imaging is paramount not only for differential diagnosis but also in planning the surgical approach. The majority of lesions are found within the muscle cone. In most cases, it is possible to dissect the cavernomas from the surrounding tissues since they are well encapsulated and occur as a single mass. Unlike the rarer intracranial cavernomas, OCHs have no tendency to bleed.

Micromorphologically, OCHs are benign vascular growths characterized by multiple large vascular channels covered by endothelial cells and abundant stroma. The vascular lumen is filled with blood and variable regions of intralesional thrombosis, reflecting vascular stasis/extremely slow flow. Unlike for subcutaneous and hepatic lesions, a well-defined and compact capsule is a typical feature of OCHs. Recent studies using immunohistochemistry, and the iteration for the classification of vascular lesions proposed by the International Society for the Study of Vascular Anomalies (ISSVA – 2018) suggest that these growths be classified as vascular malformations instead of neoplasia.

Possible complications of OCHs are acquired hyperopia of the affected eye, neurogenic or muscularly limited ductions (commonest in elevation), reduction of visual acuity, and visual field deficit due to direct compression of the optic nerve or its blood supply. Nevertheless, the prognosis of OCHs is usually good. The potential for malignization is virtually null. Smaller lesions without significant anatomical and functional distress can be safely kept under conservative follow-up. Recurrence has not been observed even for incomplete resection of masses located deep in the orbit.

Keep in mind

- ✓ In any unilateral, progressive proptosis, the possibility of an orbital tumor must be excluded.
- ✓ Orbital tumors may be benign or malignant. Prompt diagnosis allows for earlier resolution of symptoms and better prognosis.
- ✓ Large cavernous hemangiomas of the orbit may have aesthetic and/or functional implications, but surgical excision can be curative in most cases.

References

1. Herter T, Bennefeld H & Brandt M (1988). Orbital cavernous hemangiomas. Neurosurgical review, 11(2), 143–147. https://doi.org/10.1007/BF01794679
2. Calandriello L, Grimaldi G, Petrone G, Rigante M, Petroni S, Riso M & Savino G (2017). Cavernous venous malformation (cavernous hemangioma) of the orbit: Current concepts and a review of the literature. Survey of ophthalmology, 62(4), 393–403. https://doi.org/10.1016/j.survophthal.2017.01.004
3. Sullivan TJ (2018). Vascular Anomalies of the Orbit--A Reappraisal. Asia-Pacific journal of ophthalmology (Philadelphia, Pa.), 7(5), 356–363. https://doi.org/10.22608/APO.2017151
4. Tawfik HA & Dutton JJ (2022). Orbital Vascular Anomalies: A Nomenclatorial, Etiological, and Nosologic Conundrum. Ophthalmic plastic and reconstructive surgery, 38(2), 108–121. https://doi.org/10.1097/IOP.0000000000002029
5. Ansari SA & Mafee MF (2005). Orbital cavernous hemangioma: role of imaging. Neuroimaging clinics of North America, 15(1), 137–158. https://doi.org/10.1016/j.nic.2005.02.009
6. Zhang L, Li X, Tang F, Gan L & Wei X (2020). Diagnostic Imaging Methods and Comparative Analysis of Orbital Cavernous Hemangioma. Frontiers in oncology, 10, 577452. https://doi.org/10.3389/fonc.2020.577452
7. Bonavolontà G, Strianese D, Grassi P, Comune C, Tranfa F, Uccello G & Iuliano A (2013). An analysis of 2,480 space-occupying lesions of the orbit from 1976 to 2011. Ophthalmic plastic and reconstructive surgery, 29(2), 79–86. https://doi.org/10.1097/IOP.0b013e31827a7622
8. Mueller SK & Bleier BS (2022). Endoscopic surgery for intraconal orbital tumors. Endoskopische Chirurgie bei intrakonalen Orbitatumoren. HNO, 70(5), 345–351. https://doi.org/10.1007/s00106-022-01156-y
9. Scheuerle AF, Steiner HH, Kolling G, Kunze S & Aschoff A (2004). Treatment and long-term outcome of patients with orbital cavernomas. American journal of ophthalmology, 138(2), 237–244. https://doi.org/10.1016/j.ajo.2004.03.011

Case 23 - December 2023

SCLEROCHOROIDAL CALCIFICATION

A 66-year-old woman was referred for investigation of yellowish-white fundus lesions in the right eye.

Presented by
Paris Tranos, MD, PhD, ICOphth, FRCS

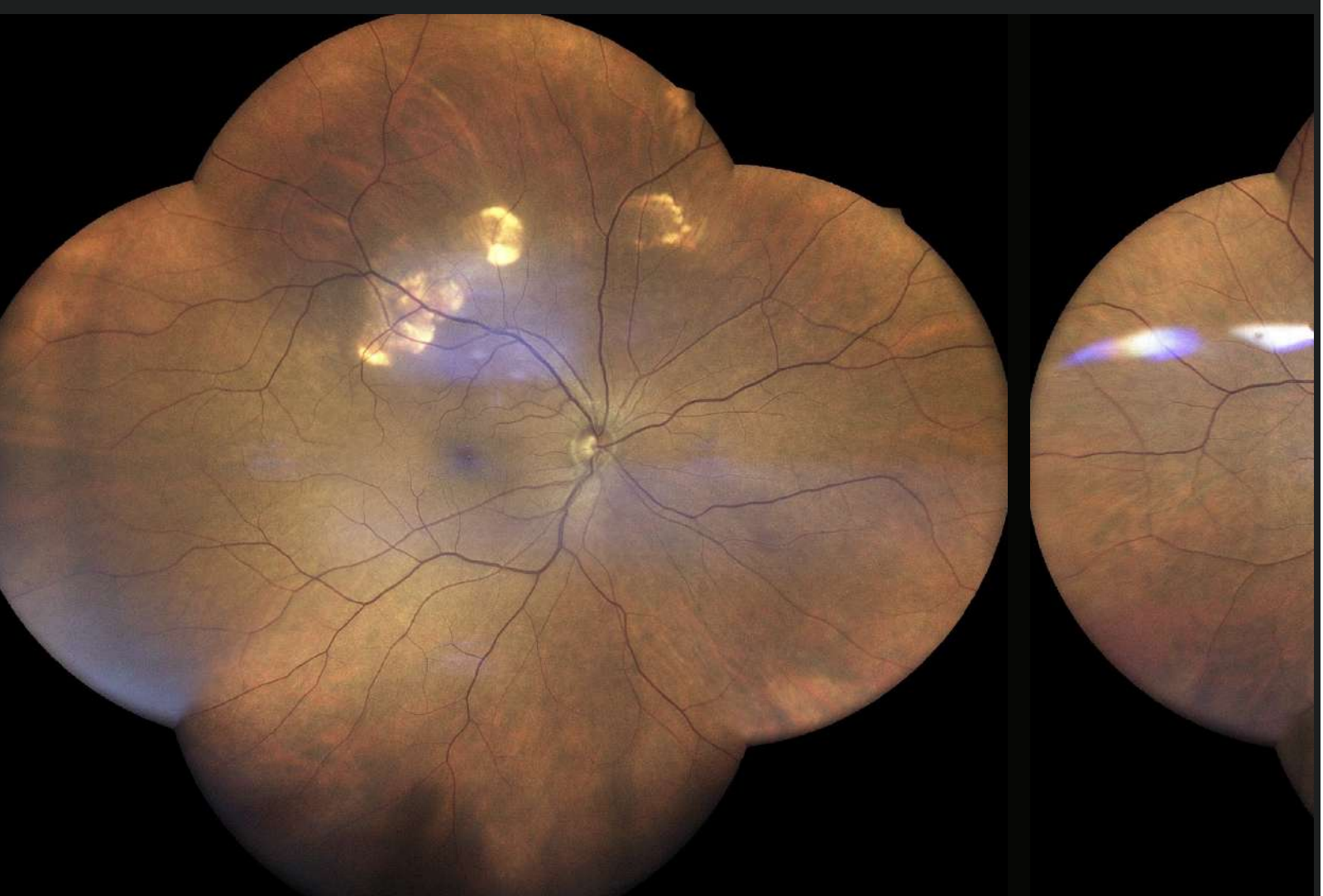

Edited by
Penelope Burle de Politis, MD

Case History

A 66-year-old Caucasian woman was referred for investigation of posterior pole lesions in the right eye (RE) noticed by chance during routine ophthalmological check-up. Her previous ocular history was unremarkable. Her past medical history included hypercholesterolaemia, rheumatoid arthritis, and hypothyroidism secondary to Hahimoto's disease. There was no relevant family history. Upon examination, her corrected distance visual acuity (CDVA) was 8/10 in the RE and 10/10- in the LE. Refractometry was -1.50-1.25@110° in the RE and +2.25-1.00@105° in the LE, and intraocular pressure was within normal limits bilaterally. Anterior segment biomicroscopy revealed bilateral moderate nuclear cataract, denser in the RE. At fundoscopy, both eyes (BE) presented yellowish-white longitudinal deep lesions at the superior midperiphery and along the superotemporal vascular arcades, more pronounced in the RE (**Figure 1**). There were no cells nor sheets in the vitreous.

Spectral domain optical coherence tomography (SD-OCT) evidenced a characteristic rocky configuration of the lesions, with undulations of the retinal pigment epithelium (RPE), dilation of Haller's layer in the choroid, and scleral thickening with focal compression of the choroid (**Figure 2**).

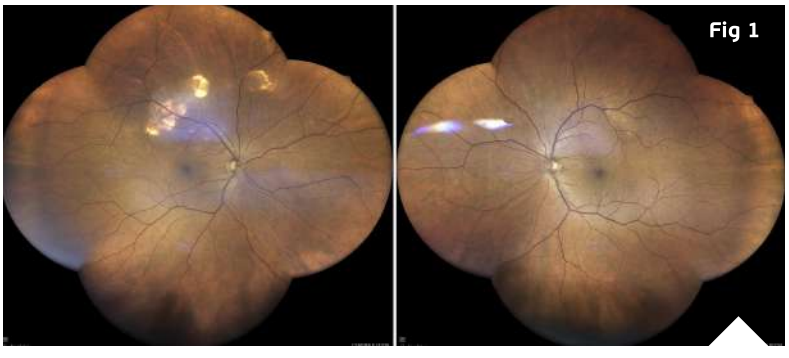

Figure 1: Color fundus photograph (EIDON true-color confocal scanner®) displaying temporal-superior yellowish-white lesions in both eyes, more evident in the right eye.

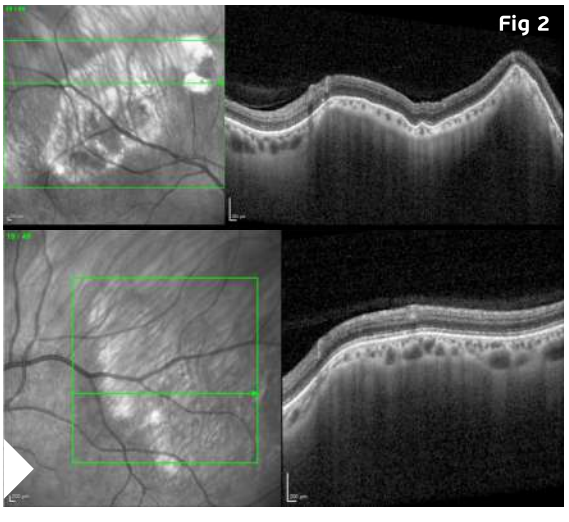

Figure 2: nfrared reflectance (IR) and enhanced depth imaging optical coherence tomography (EDI-OCT, Heidelberg Engineering®) demonstrating clusters of hyperdense lesions at the posterior pole (**left top and bottom**) and multiple elevations in both eyes, more numerous and exuberant in the right eye (**top images**).

Blue-light fundus autofluorescence (BAF) imaging displayed multiple hypoautofluorescent spots surrounded by hyperautofluorescent areas in the RE (**Figure 3**).

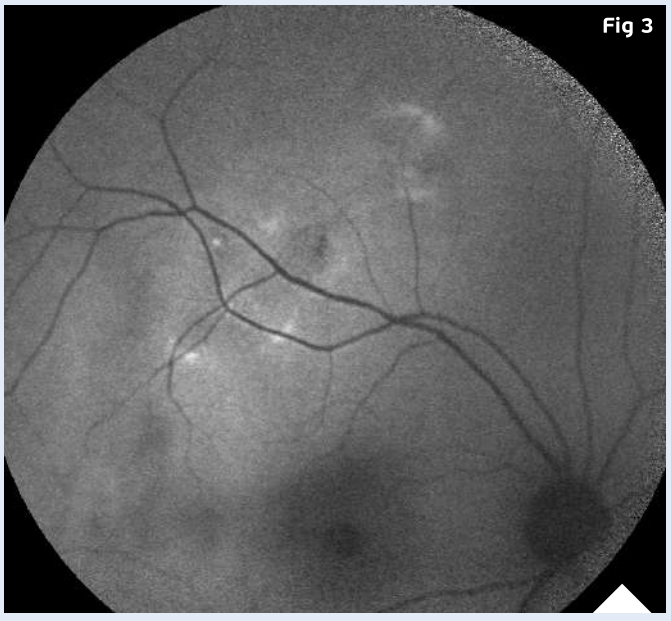

Figure 3: Blue-light fundus autofluorescence (BAF) photograph of the right eye (Heidelberg Engineering®) illustrating the hypoautofluorescent aspect of the lesions among hyperautofluorescent haloes.

Figure 4: Fundus Fluorescein Angiography (FFA, Heidelberg Engineering®) exhibiting late hyperfluorescence of the lesions in the right eye.

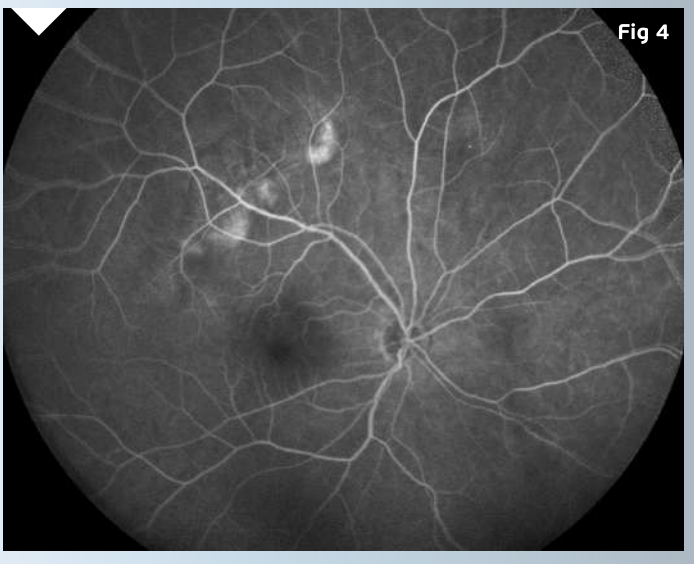

Indocyanine green angiography (ICGA) showed sustained hypocyanescence of the lesions throughout the exam (**Figure 5**).

Figure 5: Indocyanine green angiography (ICGA, Heidelberg Engineering®) featuring hypocyanescence of the lesions from early to late phases (progressively left to right) in both eyes (top: right eye; bottom: left eye).

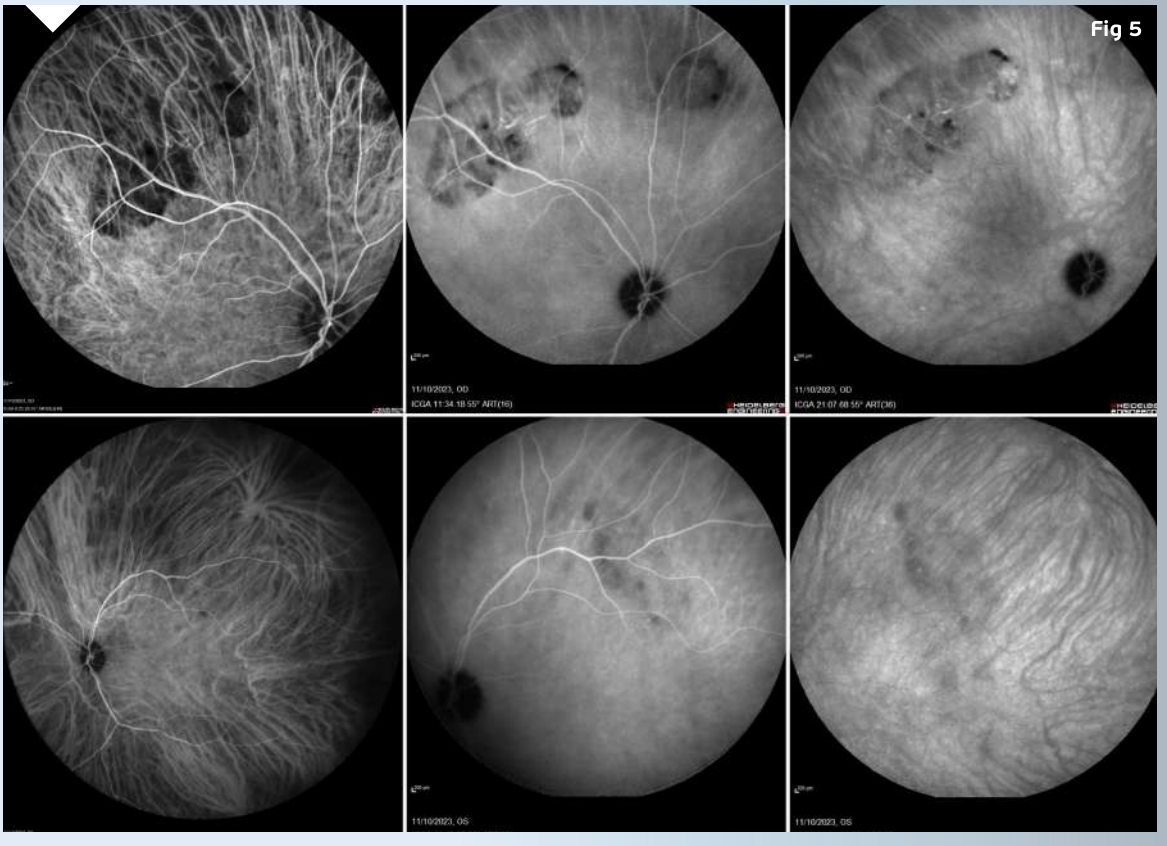

Discussion and Literature

Sclerochoroidal calcification (SCC) is a rare degenerative disorder characterized by calcium deposition in the sclera and/or choroid. SCC lesions characteristically appear as clear, uncircumscribed, yellowish-white, flat or minimally elevated placoid masses. Their typical localization is mid-peripheral, between the arcades and the equator, most frequently at the superotemporal quadrant, at the sites of insertions of the oblique extraocular muscles.

Idiopathic sclerochoroidal calcification may be easily overlooked or misdiagnosed. In the 1960s and 1970s, there were a few reports on the histopathology of ocular calcification in patients with parathyroid abnormalities. In 1982, fundus features of calcium deposition, labeled as "metastatic calcification," were reported in a patient with hyperparathyroidism. The term idiopathic sclerochoroidal calcification was first mentioned in 1989, in a case report of bilateral multiple calcific choroidal foci with no hypercalcemia or any other ocular abnormalities.

SCC is usually seen in elderly patients. There seems to be no gender predilection, though a slight female predominance has been noted. Most reported patients are Caucasians. SCC is usually found as an asymptomatic incidental finding. Lesions may be unilateral or bilateral, unifocal or multifocal. There is frequently a halo of retinal pigment epithelium (RPE) atrophy surrounding the lesion. Visual acuity is usually not affected unless there is CNV, subretinal fluid, or macular involvement.

SCC manifests as an acoustically solid mass with posterior shadowing on B-mode USG and displays calcification on CT. On FA, SCC shows early venous onset of fluorescence and late hyperfluorescence. On OCT, the lesion has either a smooth or jutted appearance with scleral hyperreflectivity, and posterior shadowing consistent with calcium content. On OCT-angiography (OCT-A), SCC displays hyporeflectivity in the outer retina and choriocapillaris from posterior shadowing. Associated CNV and retinochoroidal anastomosis may occur and can be demonstrated by OCT-A.

Systemic work-up is important in patients with SCC. Although most cases are idiopathic, renal, endocrinologic, and skeletal pathologies leading to abnormal calcium and phosphorus metabolism should be excluded in all patients. While idiopathic cases tend to be seen in elderly patients, SCC associated with a systemic disorder is usually seen at younger ages. Both idiopathic SCC and cases associated with systemic disorders usually appear as bilateral and multiple lesions. Early detection of systemic diseases altering calcium metabolism are crucial to prevent or reduce ocular and systemic morbidity.
In general, SCC is a benign condition and remains stable. In a minority of cases, it may demonstrate slow progression and enlargement on long-term follow-up. CNV is the most common cause of vision loss associated with SCC and thought to be related to choroidal compression by the calcified masses, with reduction of oxygen supply to the choroid. CNV in SCC is associated with subretinal fluid, subretinal hemorrhages, exudates, and hemorrhagic RPE detachments. There is no treatment available to ameliorate the degenerative effects of SCC on the sclera and choroid. However, since most cases are asymptomatic, SCC generally does not require treatment unless it is complicated. Secondary CNV can be observed or treated with laser photocoagulation, PDT, and/or intravitreal anti-VEGF injections if vision is affected. If CNV is far from the macula, close follow-up remains as the conservative option.

Keep in mind

- ✓ Sclerochoroidal calcification usually manifests as multiple yellow-whitish placoid lesions in the superotemporal midperiphery of asymptomatic older white individuals.
- ✓ Most cases of SCC are idiopathic, but all patients should be tested for systemic disorders involving abnormal calcium metabolism or renal function.
- ✓ Multimodal imaging is essential for accurate diagnosis of SCC and early detection of possible complications.

References

1 Schachat AP, Robertson DM, Mieler WF, Schwartz D, Augsburger JJ, Schatz H & Gass JD (1992). Sclerochoroidal calcification. Archives of ophthalmology (Chicago, Ill. : 1960), 110(2), 196–199.

2 Gündüz AK & Tetik D (2023). Diagnosis and Management Strategies in Sclerochoroidal Calcification: A Systematic Review. Clinical ophthalmology (Auckland, N.Z.), 17, 2665–2686. https://doi.org/10.2147/OPTH.S399058

3 Shields CL, Hasanreisoglu M, Saktanasate J, Shields PW, Seibel I & Shields JA (2015). Sclerochoroidal calcification: clinical features, outcomes, and relationship with hypercalcemia and parathyroid adenoma in 179 eyes. Retina (Philadelphia, Pa.), 35(3), 547–554. https://doi.org/10.1097/IAE.0000000000000450

4 Cooke CA, McAvoy C & Best R (2003). Idiopathic sclerochoroidal calcification. The British journal of ophthalmology, 87(2), 245–246. https://doi.org/10.1136/bjo.87.2.245

5 Mitamura M, Kase S & Ishida S (2020). Multimodal imaging in sclerochoroidal calcification: a case report and literature review. BMC ophthalmology, 20(1), 248. https://doi.org/10.1186/s12886-020-01520-y

6 Brahma VL, Shah SP, Chaudhry NA & Prenner JL (2017). Bilateral Idiopathic Sclerochoroidal Calcifications. The open ophthalmology journal, 11, 76–79. https://doi.org/10.2174/1874364101711010076

7 Honavar SG, Shields CL, Demirci H & Shields JA (2001). Sclerochoroidal calcification: clinical manifestations and systemic associations. Archives of ophthalmology (Chicago, Ill. : 1960), 119(6), 833–840. https://-doi.org/10.1001/archopht.119.6.833

8 Lindstedt EW, van den Born LI, Veckeneer M & Baarsma GS (2007). Sclerochoroidal calcification: idiopathic or associated with systemic disease?. Retinal cases & brief reports, 1(3), 141–144. https://doi.org/10.1097/01.ICB.0000279643.99324.93

9 Sugarman JA, Douglass AM, Say EA & Shields CL (2017). Stones, bones, groans, thrones, and psychiatric overtones: Systemic associations of sclerochoroidal calcification. Oman journal of ophthalmology, 10(1), 47–49. https://www.ncbi.nlm.nih.gov/pmc/articles/PMC5338055/

10 Abouzaid M, Al-Sharefi A, Artham S, Masri I, Kotagiri A & Joshi A (2019). A rare ophthalmic condition associated with primary hyperparathyroidism (PHPT): sclerochoroidal calcification (SC). Endocrinology, diabetes & metabolism case reports, 2019(1), 19-0003. https://doi.org/10.1530/EDM-19-0003

B-scan ultrasonography displayed hyperechogenic images with acoustic shadowing indicating calcified lesions in BE, more marked in the RE (**Figure 6**).

Figure 6: B-mode ultrasonography (respectively right and left eyes) showing characteristic hyper-echoic elevations with posterior shadowing at the posterior wall of both eyes, more pronounced in the right eye.

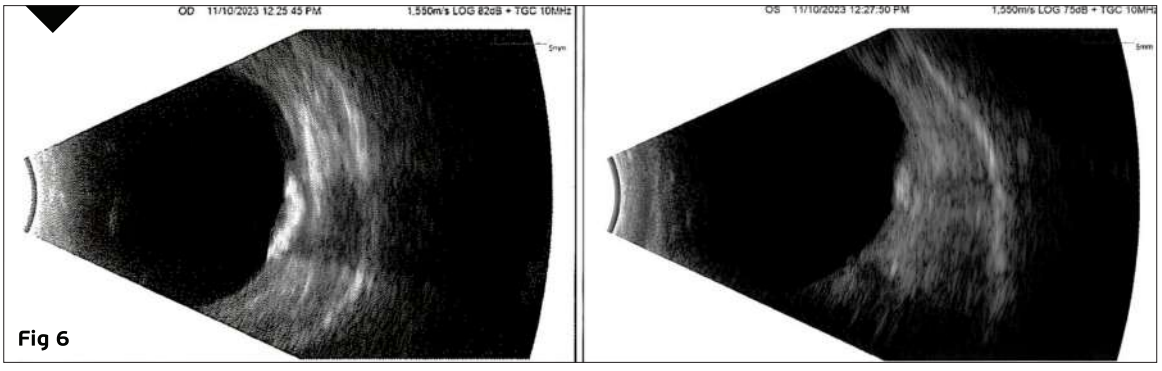

Additional History

Based on the clinical and multimodal image findings, the diagnosis of sclerochoroidal calcification was established.

Considering the benign nature of the lesions and lack of correlated visual compromise, the case was managed with conservative ophthalmological follow-up.

Further screening for underlying renal and/or parathyroid disease was advised.

Differential Diagnosis of Sclerochoroidal Calcification

- choroidal osteoma
- choroidal metastasis
- choroidal melanoma
- choroidal lymphoma
- amelanotic choroidal nevus
- choroidal granuloma
- choroidal hemangioma
- chorioretinitis
- regressed retinoblastoma
- retinal astrocytic hamartoma

The differential diagnosis between sclerochoroidal calcification and other fundus lesions is based on their distinct clinical presentation, fundus findings and multimodal imaging characteristics.

Case 24 - February 2024

CONE-ROD DYSTROPHY

A 16-year-old boy presented with a history of progressive bilateral visual loss since the age of 6.

Presented by
Stavrenia Koukoula, MD, PhD
& Theoni Panagiotoglou, MD, PhD

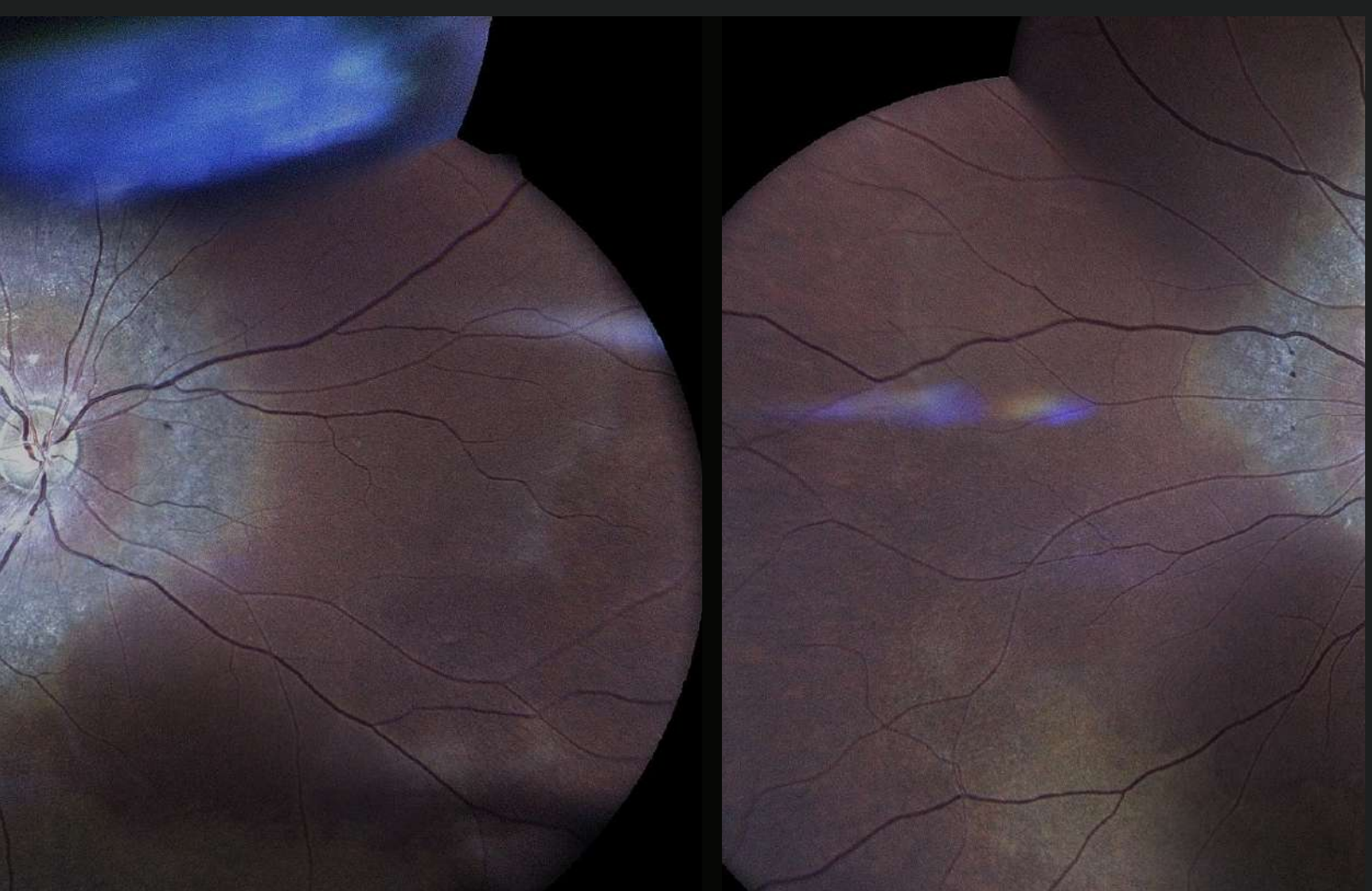

Edited by
Penelope Burle de Politis, MD

Case History

A 16-year-old boy of Albanian descent presented with a history of progressive bilateral visual loss since the age of 6. The patient referred to intermittent right exophoria and complained of photophobia. Due to his vision deficit, he had recently dropped school. He was born full-term and had no systemic diseases except for chronic otitis. His family history was negative for ocular disorders or blindness, but his parents were distant consanguineous relatives. Under ophthalmological examination, his corrected distance visual acuity (CDVA) was 1/10 in the right eye (RE) and 2/10 in the left eye (LE). Total bilateral color blindness could be verified. Refractometry was -0.50@75° in the RE and -0.50@55° in the LE, and intraocular pressure was 14mmHg bilaterally. Anterior segment biomicroscopy was normal in both eyes (BE). Neither tropias nor relative afferent pupillary defect (RAPD) were present. Fundoscopy revealed pale discoloration of both macular regions, relatively pale optic discs, mild attenuation of the retinal vessels, and mid-peripheral bone spicule-like intraretinal pigmentation in BE (**Figure 1**).

Spectral domain optical coherence tomography (SD-OCT) evidenced a general macular atrophy, with foveal thinning with loss of photoreceptors, of ellipsoid zone (EZ line), of outer nuclear layer, and of RPE in BE (**Figure 2**).

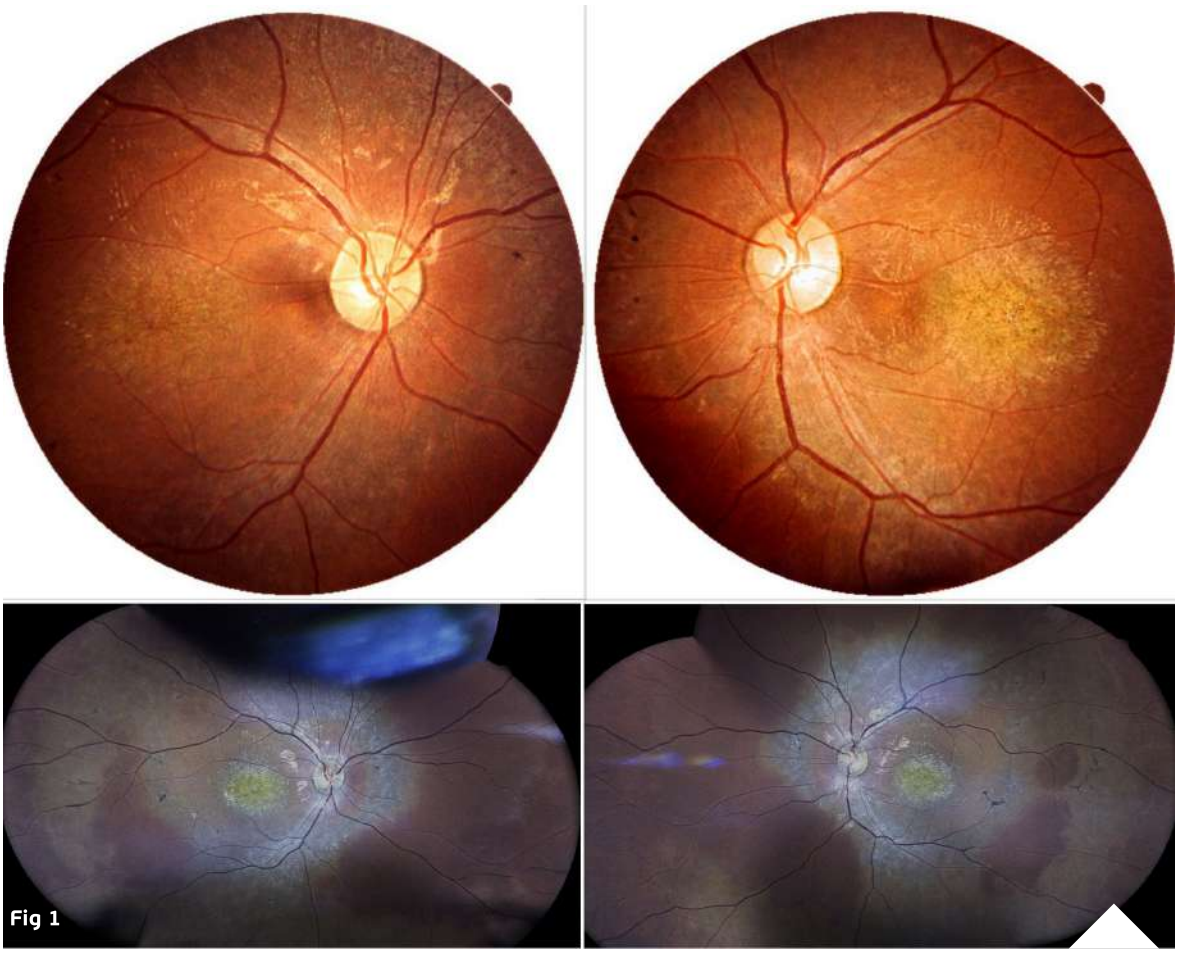

Figure 1: Color fundus photographs (**top**: REVO FC 80 Optopol Technology® retinal scan, courtesy of T. Panagiotoglou; **bottom**: iCare EIDON® widefield TrueColor confocal retinal mosaic scan) displaying retinal pigment deposits predominantly located at the macular region of both eyes.

Figure 2: Posterior pole scans demonstrating foveal thinning and attenuation of the inner segment ellipsoid zone in both foveas. **Top images**, respectively RE and LE: infrared reflectance (IR) and spectral domain optical coherence tomography (SD-OCT, Heidelberg Engineering®). **Bottom images**, respectively RE and LE: SD-OCT (REVO FC 80 Optopol Technology®), courtesy of T. Panagiotoglou.

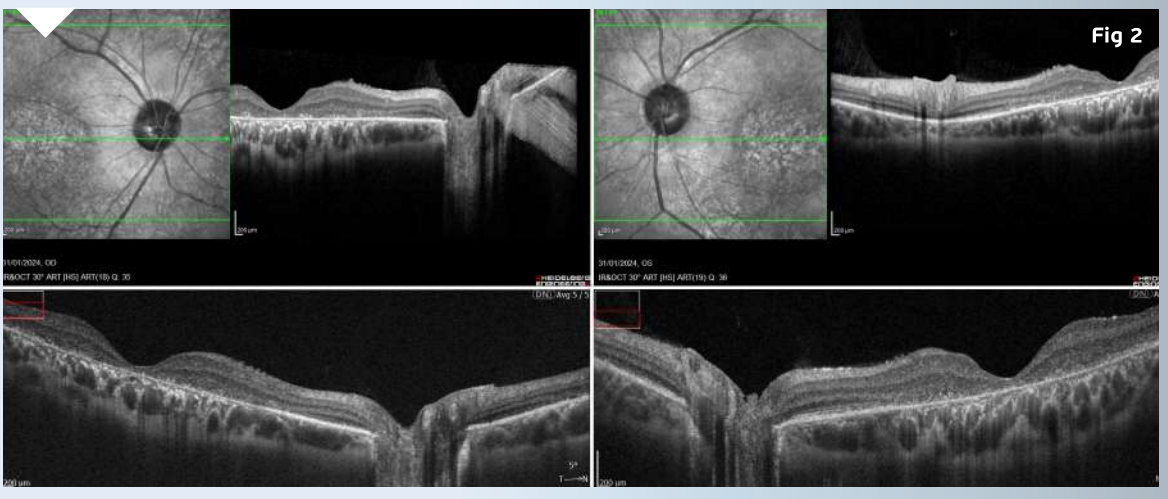

Blue-light fundus autofluorescence (BAF) imaging displayed various degrees of retinal atrophy (alternating areas of hypoautofluorescence and hyperautofluorescence; the more the atrophy of the retinal pigment epithelium (RPE), the more evident the hypoautofluorescence (**Figure 3**).

Figure 3: Blue-light fundus autofluorescence (BAF) photographs (Heidelberg Engineering®) illustrating a highly hypofluorescent macula and areas of RPE changes with speckled mid-peripheral hypoautofluorescence bilaterally (**upper row**: OD; **lower row**: OS; respectively at front, side, up and down gaze).

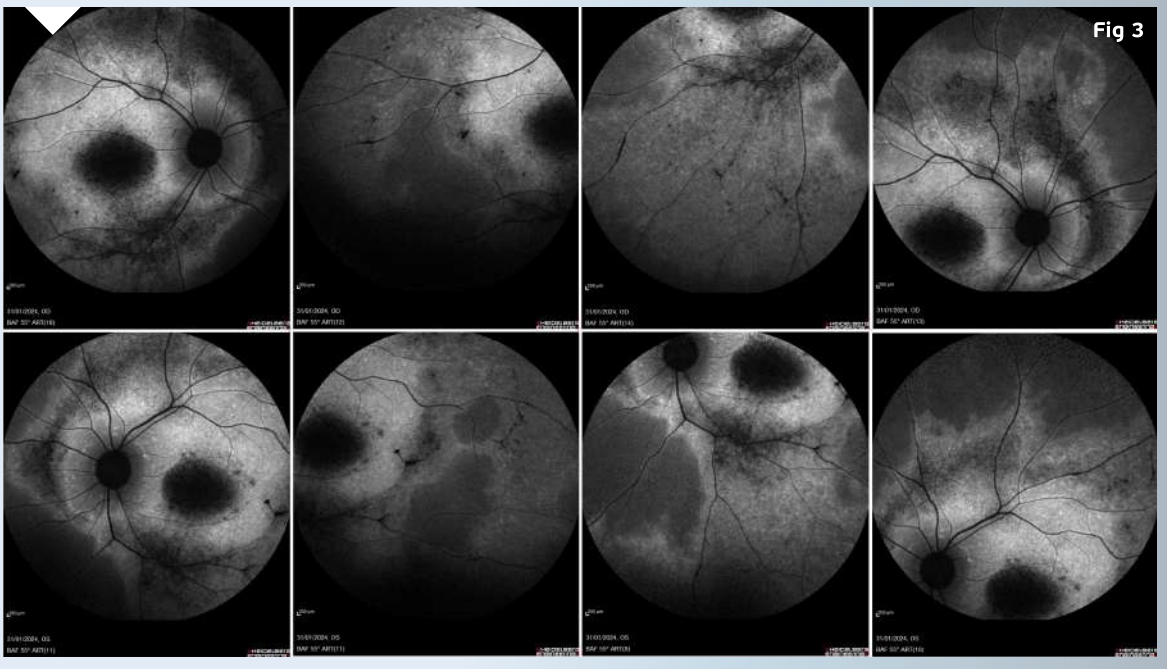

Additional History

Given the ocular history and fundus findings, the diagnostic hypothesis of cone-rod dystrophy was considered, hence the patient was referred for electrophysiological study of the retina. The electroretinogram (ERG) was consistent with generalized retinal dysfunction at the level of photoreceptors, both cones and rods, with macular involvement in BE (**Figure 4**).

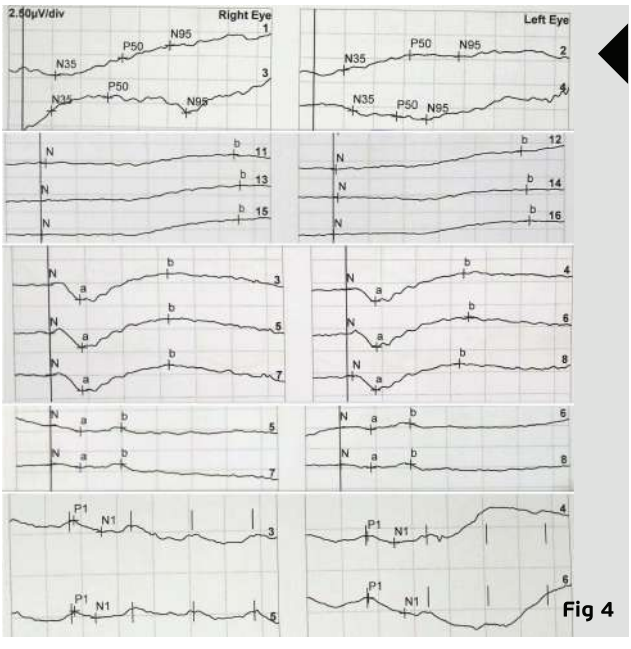

Figure 4: ERG records, respectively of RE and LE. **From top to bottom**: Pattern ERG (PERG): P50 undetectable to both standard and large field stimulus in BE. Full-field ERG (ffERG) protocols: rod-specific dark-adapted (DA 0,01) with b-wave amplitudes of 90µV on the RE and 80µV on the LE; bright flash dark-adapted (DA 10) with a- and b- wave peak times bilaterally subnormal and amplitudes of 50% the normal values; photopic light-adapted single flash (LA 3.0) with abnormal peak time bilaterally and a- and b- wave amplitudes respectively of 7µV and 15µV on the RE and 6µV and 13µV on the LE; 30Hz flicker (LA 3-30) peak times of 35-37ms (severely delayed), with amplitudes of 20-30µV (30% of normal) in BE.

Based on the ophthalmological examination, the multimodal image findings and the electrophysiological profile, the diagnosis of cone-rod dystrophy was confirmed.

Genetic counseling was given to the family and a multidisciplinary educational approach was advised.

Differential Diagnosis of Cone-Rod Dystrophy

- retinitis pigmentosa
- Stargardt's disease
- Leber congenital amaurosis
- pure cone dystrophy
- isolated achromatopsia
- rubella retinopathy
- drug-induced retinopathy (e.g. antimalarials)

The differential diagnosis between cone-rod dystrophies and other retinal disorders is based on disease course, fundoscopic aspects and electrophysiological features. Accurate differentiation from overlapping photoreceptor dysfunctions is crucial for proper management.

Discussion and Literature

Cone-rod dystrophies (CRDs or CORDs) are inherited dystrophies belonging to the group of pigmentary retinopathies. The reported prevalence of CRDs is 1:40,000 (ten times less frequent than retinitis pigmentosa (RP or rod-cone dystrophy). In contrast to rod-cone dystrophies (RCDs), CRDs typically present primary cone involvement or, sometimes, concomitant loss of cones and rods. As a result, CRDs present first as macular disease, or diffuse retinopathy with predominant macular involvement. The classical symptoms of CRDs are decreased visual acuity, color vision deficits, photoaversion and decreased central visual field sensitivity, later followed by progressive peripheral vision loss and night blindness. The clinical course of CRDs is generally more severe and rapid than that of RCDs, leading to earlier legal blindness and disability.

CRDs are most frequently non-syndromic but may be part of syndromes such as Bardet Biedl, Spinocerebellar Ataxia Type 7 (SCA7), ectodermal diseases, and dysmorphic syndromes. Non-syndromic CRDs are genetically heterogeneous and all three patterns of mendelian inheritance are seen. The autosomal recessive (AR) pattern is the commonest (60–70%), followed by autosomal dominant (AD, 20–30%) and X-linked recessive (XL, 5%). Mutations in about 30 genes are involved in the pathogenesis of CRDs (about 20 are responsible for AR CRD and 10 for AD CRD). For AR CRD, the major implicated genes are ABCA4 (which causes Stargardt's disease and 30 to 60% of AR CRD), CNGB3, KCNV2, and PDE6C. Dominant CRD is caused by a mutation in the GUCY2D and CRX genes. For X-linked cases, the affected gene is RPGR (which also causes about 2/3 of X-linked RP). There is some association between X-linked CRD and high myopia.

Two stages can be identified in the course of CRDs. In the first, the main symptom is decreased visual acuity, usually discovered at school, during the first decade of life. Patients often have a deviated gaze to project images on parafoveal less damaged regions. There is intense photophobia and a variable degree of dyschromatopsia. Night blindness is less prominent. Visual field testing shows central scotomas with peripheral sparing; hence patients have no difficulties moving. Fundus examination shows pigment deposits and various degrees of macular atrophy. Retinal vessels are normal or moderately attenuated. The optic disc is pale, particularly on the temporal side (macular fiber bundle). In the second stage, night blindness becomes more evident and peripheral visual loss progresses, compromising autonomous moving. Visual acuity continues to decrease to a level where reading is no longer possible. Nystagmus is often present. At this stage, patients are legally blind (visual acuity <1/20).

The diagnosis of CRDs is based on clinical history, fundus findings and electroretinogram. On the OCT of eyes with CRD, the IS/OS (ellipsoid) line is absent at the fovea. Fluorescein angiography and fundus autofluorescence show that the peripheral retina is also involved with heterogeneous fluorescence, but to a lesser extent than the macula. Since photoreceptors are distributed throughout the entire retina, imaging should not be limited to the posterior pole. Quantitative fundus AF (qAF) analysis (an indirect measure of lipofuscin within the RPE cell layer) may facilitate differential phenotypic diagnostics of CRDs. Characteristic electroretinogram (ERG) features are: implicit time (between a- and b-wave peaks) shift at the 30-Hz flicker cone responses; a- and b-wave single flash photopic response delayed (early), or with reduced amplitude (later); predominant involvement of photopic (cones) over scotopic (rods) responses. Molecular diagnosis can be made for certain genes but is not largely applied. Targeted next-generation sequencing (NGS) has been used to study the genotype-phenotype correlations in CRDs.

Visual prognosis is poor as CRDs lead to legal blindness in the majority of patients. Presently, there is no therapy to halt disease progression or restore vision. Management aims at slowing down the degenerative process (light protection, vitamin therapy), treating complications (cataract, macular edema, inflammation), and helping patients cope with the social and psychological impact of blindness. Filtrating spectacles can be used to minimize photophobia and low vision aids to improve functioning. Education must be adapted and carried out by a multiprofessional team. Genetic counseling is always advised. Ongoing research focuses on mechanisms of cone and rod cell death in these diseases so that their pathways can be better understood and potentially targeted for therapeutic intervention. Gene-based approaches are currently under study.

Keep in mind

- ✓ Cone-rod dystrophies are genetically heterogeneous pigmentary retinopathies that generally lead to legal blindness before adulthood.
- ✓ Low central visual acuity, photoaversion and poor color vision are the hallmarks of cone-rod dystrophy, nyctalopia being a later phase symptom.
- ✓ A precise diagnosis of cone-rod dystrophy requires electrophysiological study of the retina for adequate counseling and early rehabilitation.

References

1 Hamel CP (2007). Cone rod dystrophies. Orphanet journal of rare diseases, 2, 7. https://doi.org/10.1186/1750-1172-2-7

2 Thiadens AA, Phan TM, Zekveld-Vroon RC, Leroy BP, van den Born LI, Hoyng CB, Klaver CC, Writing Committee for the Cone Disorders Study Group Consortium, Roosing S, Pott JW, van Schooneveld MJ et al. (2012). Clinical course, genetic etiology, and visual outcome in cone and cone-rod dystrophy. Ophthalmology, 119(4), 819–826. https://www.sciencedirect.com/science/article/abs/pii/S0161642011009584

3 Tsang SH & Sharma T (2018). Progressive Cone Dystrophy and Cone-Rod Dystrophy (XL, AD, and AR). Advances in experimental medicine and biology, 1085, 53–60. https://doi.org/10.1007/978-3-319-95046-4_12

4 Georgiou M, Robson AG, Fujinami K, de Guimarães TAC, Fujinami-Yokokawa Y, Daich Varela M, Pontikos N, Kalitzeos A, Mahroo OA, Webster AR & Michaelides M (2024). Phenotyping and genotyping inherited retinal diseases: Molecular genetics, clinical and imaging features, and therapeutics of macular dystrophies, cone and cone-rod dystrophies, rod-cone dystrophies, leber congenital amaurosis, and cone dysfunction syndromes. Progress in retinal and eye research, 101244. Advance online publication. https://doi.org/10.1016/j.preteyeres.2024.101244

5 Oishi A, Oishi M, Ogino K, Morooka S & Yoshimura N (2016). Wide-Field Fundus Autofluorescence for Retinitis Pigmentosa and Cone/Cone-Rod Dystrophy. Advances in experimental medicine and biology, 854, 307–313. https://doi.org/10.1007/978-3-319-17121-0_41

6 Gliem M, Müller PL, Birtel J, Herrmann P, McGuinness MB, Holz FG & Charbel Issa P (2020). Quantitative Fundus Autofluorescence and Genetic Associations in Macular, Cone, and Cone-Rod Dystrophies. Ophthalmology. Retina, 4(7), 737–749. https://doi.org/10.1016/j.oret.2020.02.009

7 Yokochi M, Li D, Horiguchi M & Kishi S (2012). Inverse pattern of photoreceptor abnormalities in retinitis pigmentosa and cone-rod dystrophy. Documenta ophthalmologica. Advances in ophthalmology, 125(3), 211–218. https://doi.org/10.1007/s10633-012-9348-8

8 Birtel J, Eisenberger T, Gliem M, Müller PL, Herrmann P, Betz C, Zahnleiter D, Neuhaus C, Lenzner S, Holz FG, Mangold E, Bolz HJ & Charbel Issa P (2018). Clinical and genetic characteristics of 251 consecutive patients with macular and cone/cone-rod dystrophy. Scientific reports, 8(1), 4824. https://doi.org/10.1038/s41598-018-22096-0

9 Garafalo AV, Sheplock R, Sumaroka A, Roman AJ, Cideciyan AV & Jacobson SG (2021). Childhood-onset genetic cone-rod photoreceptor diseases and underlying pathobiology. EBioMedicine, 63, 103200. https://-doi.org/10.1016/j.ebiom.2020.103200

10 Gill JS, Georgiou M, Kalitzeos A, Moore AT & Michaelides M (2019). Progressive cone and cone-rod dystrophies: clinical features, molecular genetics and prospects for therapy. The British journal of ophthalmology, 103(5), 711–720. Advance online publication. https://doi.org/10.1136/bjophthalmol-2018-313278

Case 25 - April 2024

COMBINED HAMARTOMA OF THE RETINA AND RETINAL PIGMENT EPITHELIUM

A 30-year-old myope woman presented with floaters and progressive visual loss in the left eye over the course of 3 months.

Presented by
by Chrysa Koutsiouki, MD

Edited by
Penelope Burle de Politis, MD

Case History

A 30-year-old Caucasian woman presented with progressively decreased vision and floaters in the left eye (LE) noticed three months earlier. She had 3.00D myopia in both eyes (BE). Her past medical history was limited to well-controlled hypothyroidism from Hashimoto's disease. Her family medical history was negative for ophthalmic diseases. Upon examination, her corrected distance visual acuity (CDVA) was 10/10 in the right eye (RE) and hand movement (HM) in the LE. The anterior ocular segment was normal in BE. Intraocular pressure (IOP) was within the normal range bilaterally. Fundus examination of the LE showed a poorly defined central yellowish-white lesion, with macular involvement and significant retinal folds. There were no abnormalities in the RE (**Figure 1**). Further investigation using multimodal imaging revealed intraretinal lesions in the macular area of the LE, with accompanying edema and neovascularization (**Figures 2 to 6**).

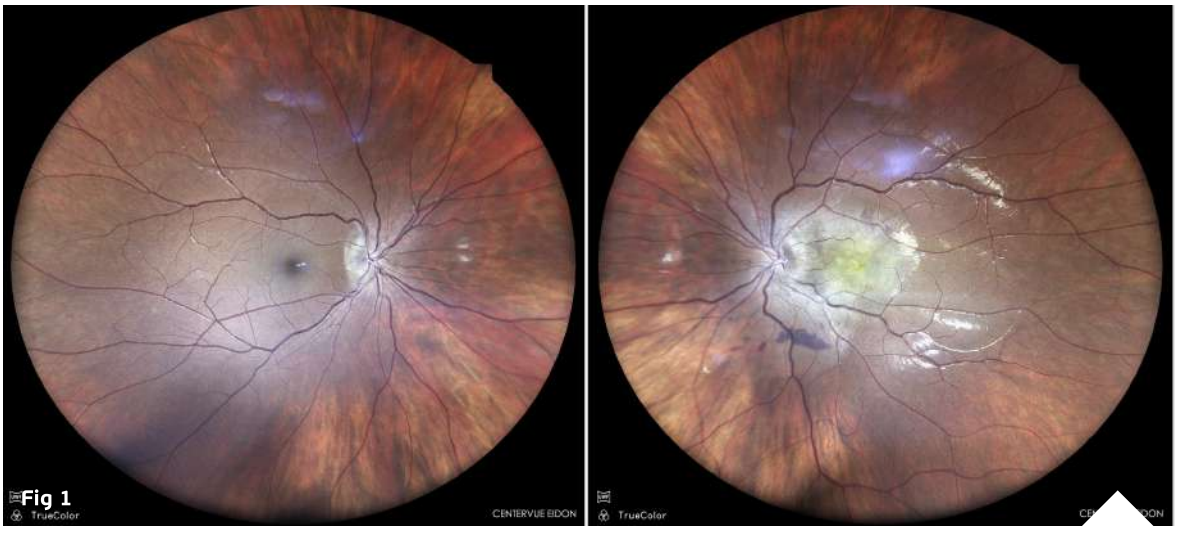

Figure 1: Fundus color photograph (iCare confocal high-resolution ultra-widefield Truecolor Centervue EIDON®) showing a yellowish-white lesion at the posterior pole of the left eye involving the macula.

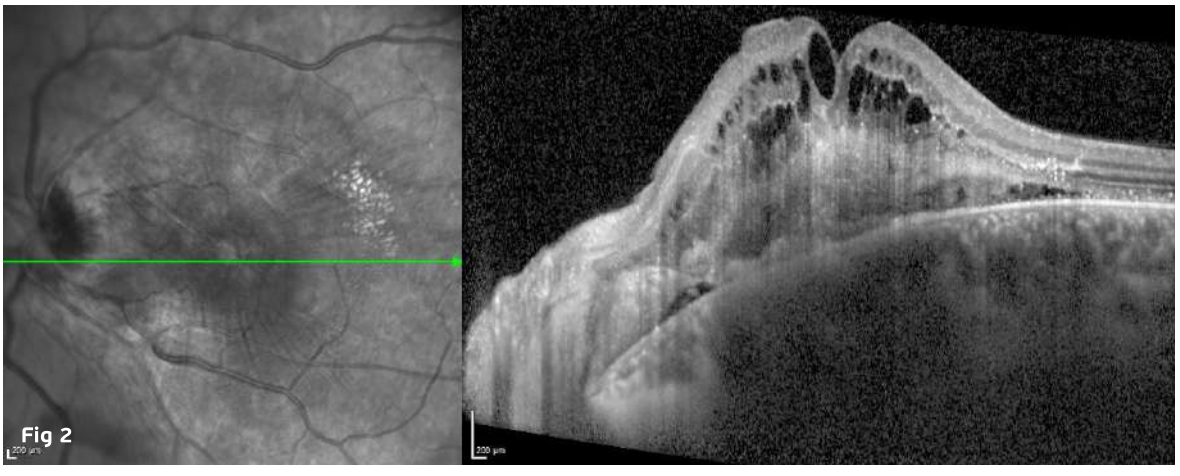

Figure 2: Enhanced depth mode of spectral-domain optical coherence tomography (EDI SD-OCT) of the LE (Spectralis, Heidelberg Engineering®) displaying increased retinal thickness, a hyperreflective material in the inner retina with loss of retinal architecture, and cystoid macular edema (CMO).

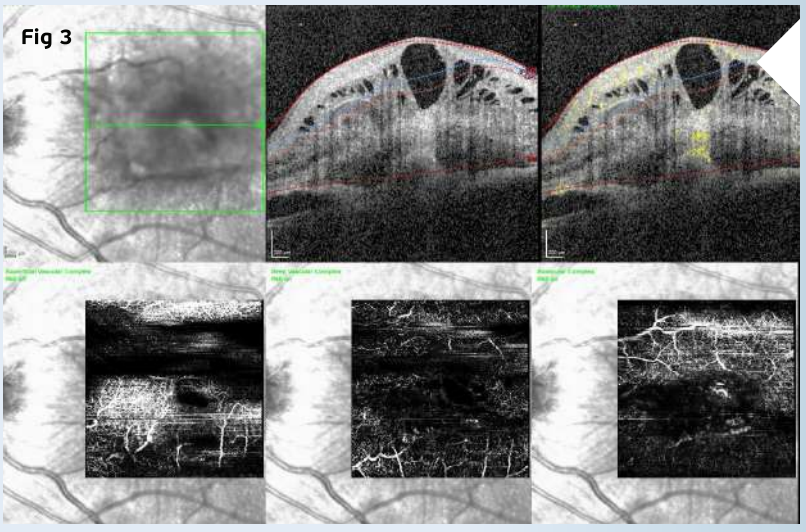

Figure 3: Optical coherence tomography angiography (OCT-A) of the LE (Spectralis, Heidelberg Engineering®) showing abnormal retinal vessels in the superficial (SCP) and deep retinal capillary plexuses (DCP), with evidence of flow.

Figure 4: Fundus fluorescein angiography (FFA) of the LE (Spectralis, Heidelberg Engineering®). Early frame (**right**): hypofluorescence from retinal fold masking, dilated perifoveal capillaries, progressively increasing leakage. Late frame (**left**): cystoid macular edema.

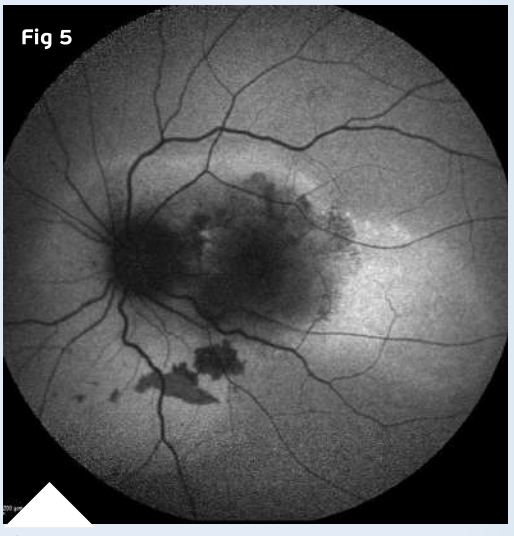

Figure 5: Blue-light fundus autofluorescence (BAF) of the LE (Spectralis, Heidelberg Engineering®) showing the hypoauto-fluorescence of the lesions with mild hyperautofluorescence in the nasal area.

Figure 6: Indocyanine-green angiography (ICG-A) of the LE (Spectralis, Heidelberg Engineering®). Early frame (**right**): hypofluorescence, along with retinal vessels crossing the foveal area. Late frame (**left**): hyperfluorescence of the abnormal vessels.

Additional History

Based on the clinical and image findings, the diagnosis of combined hamartoma of the retina and retinal pigment epithelium was established. Considering the acute-onset blurred vision and the presence of intraretinal fluid and neovascularization, intravitreal anti-VEGF was indicated. The prognostic perspectives were discussed with the patient and the injection was carried out. Follow-up imaging showed regression of the exudative component and improvement of retinal thickening (**Figure 7**), though no improvement in visual acuity could be noticed.

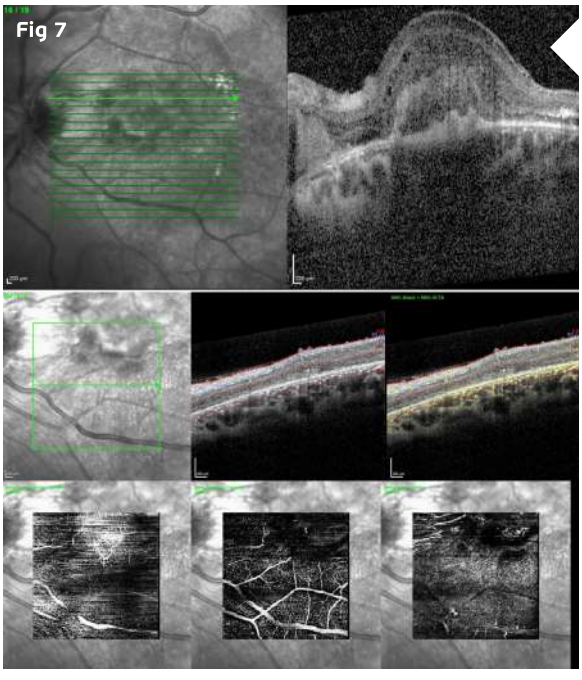

Figure 7: EDI SD-OCT (**top**) and OCT-A (**bottom**) of the LE at 6 weeks post-Avastin® (bevacizumab) injection, showing significant resolution of the cystoid macular edema, although with persistence of the hyper-reflective material.

Differential Diagnosis of Combined Hamartoma of the Retina and RPE

- choroidal melanoma
- choroidal nevus
- primary or secondary retinal gliosis
- adenoma or adenocarcinoma of RPE
- melanocytoma
- morning glory anomaly
- retinoblastoma
- toxocariasis
- astrocytoma
- hemangioma

Because combined hamartoma of the retina and retinal pigment epithelium can resemble other posterior pole lesions, accurate diagnosis using multimodal imaging technology is of ultimate importance for decision-making in case management.

Discussion and Literature

The term hamartoma derives from the Greek “hamartia,” meaning error. Hamartomas are benign, slow overgrowths that result from the abnormal proliferation of cells in regions where they are normally found. They occur in different parts of the body and most cases are asymptomatic and detected incidentally. Hamartomas can occur isolatedly or in association with a genetic syndrome. The retinal and optic disc hamartomas types are: astrocytic hamartoma, congenital hypertrophy of the retinal pigment epithelium (CHRPE), congenital simple hamartoma of the retinal pigment epithelium (CSHRPE), combined hamartoma of the retina and retinal pigment epithelium (CHR-RPE), retinal hemangioblastoma (retinal capillary hemangioma), and retinal cavernous hemangioma. For CHR-RPE, the possible systemic associations include neurofibromatosis types 1 and 2, Gorlin-Goltz syndrome, Poland anomaly, branchio-oculo-facial syndrome, brachio-oto-renal syndrome, and juvenile nasopharyngeal angiofibroma.

CHR-RPE is a rare lesion, usually presenting between the ages of 1 and 74 years (mean age 23 years). It is generally congenital and nonhereditary, and its etiology is uncertain. Males and females were equally affected. Caucasian race appears to predominate. The lesion is generally unilateral and most cases are sporadic. Bilateral lesions should raise suspicion of neurofibromatosis. Histologically, CHR-RPE is composed of a mixture of pigment epithelial cells, proliferating blood vessels, and glial tissue, located mostly in the sensory retina or optic disc tissue. It is believed to originate from the inner retina and progress towards the outer retina over time.

Visual acuity is variable, depending on lesion size and location and amount of retinal traction. Most patients with CHR-RPE that come to clinical attention are young children found to have poor vision on school examinations. The patients commonly present with a painless decrease in VA, strabismus, or with nonspecific ocular irritation. Less common presenting symptoms include floaters, ocular pain, and leukocoria. Tumors located in the macular area can lead to strabismus and amblyopia. Foveal ectopia secondary to traction by a peripheral lesion can also be a cause of amblyopia.

The CHR-RPE lesion has characteristic but variable clinical features. The most typical finding is an ill-defined retinal mass with tortuous or straightened retinal blood vessels. The tumor can be dusky brown, green, yellow, gray, or orange. The classic location is on or adjacent to the optic disc but other areas of the fundus may be involved. It can vary widely in size, ranging from a small 1-mm to a mass lesion larger than 10 mm in diameter. While young patients exhibit mainly inner retinal involvement, full-thickness retinal involvement is often seen in older patients. An increase in retinal thickness is more common in macular lesions than in other locations. Peripheral lesions can cause a “dragged disc” appearance due to retinal traction.

CHR-RPE was generally classified into three groups according to location: peripapillary, macular, and peripheral. However, a recent classification system has been proposed, based on tumor's location (posterior, mid-periphery, or far periphery), characteristics (presence of traction, retinoschisis, or retinal detachment), and OCT findings (epiretinal, partial retinal, or full-thickness retina/RPE involvement). According to the stage, management options can range from complete ophthalmologic evaluation at least every 6 months to surgical intervention.

On OCT, CHR-RPE exhibits an irregular lesion with vitreoretinal traction into a "sawtooth" or "folded" pattern that replaces full-thickness retinal tissue (mini-peak) and "omega sign" (maxi-peak). OCT-A demonstrates retinal vascular alterations and a "filigree" pattern in the intratumoral vessels. On FFA, the lesion is hyperfluorescent with early hypoflourescence, and there are markedly abnormal vessels in the mass, with gradual late staining of the lesion. Peripapillary pigmented lesions exhibit hyperautofluorescence on FAF. Indocyanine green angiography shows mild patchy hyperfluorescence in the late phase. Ultrasonography may help rule out other conditions with similar appearance. The usual ultrasonographic aspect is a plaque-like, slightly raised, acoustically solid lesion with moderate to high internal reflectivity and no extrascleral extension. If neurofibromatosis type II is suspected, further work-up is warranted.

Patients with CHR-RPE can suffer from progressive visual loss due to tumor growth or complications associated with the tumor, which include amblyopia, formation of ERM, retinal holes, retinoschisis, CNV, retinal neovascularization, vitreous hemorrhage, and retinal detachment. There is no highly effective method for treating CHR-RPE. When CHR-RPE presents at a young age, amblyopia prevention is paramount. Surgery for associated ERMs is still a subject of debate since visual acuity may not improve despite membrane removal. Also, it may not be possible to remove the whole ERM without damaging the retina and is not feasible if the lesion involves full thickness of the retina. Laser photocoagulation can be employed for neovascular membranes. Intravitreal anti-VEGF injection can be used to treat choroidal neovascularization.

Keep in mind

- ✓ CHR-RPE usually presents early in life and is found incidentally at any age.
- ✓ Posterior location of CHR-RPE is associated with lower visual acuity but complications can occur in peripheral lesions as well.
- ✓ Management of CHR-RPE is case-based and aimed at preserving visual acuity.

References

1 Shields JA & Shields CL (2017). Tumors and Related Lesions of the Pigmented Epithelium. Asia-Pacific journal of ophthalmology (Philadelphia, Pa.), 6(2), 215–223. https://doi.org/10.22608/APO.201705

2 Mirzayev I & Gündüz AK (2022). Hamartomas of the Retina and Optic Disc. Turkish journal of ophthalmology, 52(6), 421–431. https://doi.org/10.4274/tjo.galenos.2022.25979

3 Schachat AP, Shields JA, Fine SL, Sanborn GE, Weingeist TA, Valenzuela RE & Brucker AJ (1984). Combined hamartomas of the retina and retinal pigment epithelium. Ophthalmology, 91(12), 1609–1615. https://doi.org/10.1016/s0161-6420(84)34094-5

4 Dedania VS, Ozgonul C, Zacks DN & Besirli CG (2018). NOVEL CLASSIFICATION SYSTEM FOR COMBINED HAMARTOMA OF THE RETINA AND RETINAL PIGMENT EPITHELIUM. Retina (Philadelphia, Pa.), 38(1), 12–19. https://doi.org/10.1097/IAE.0000000000001499

5 Ren Q, Han N, Zhang R, Chen RF & Yu P (2023). Combined hamartoma of the retina and retinal pigment epithelium: A case report. World journal of clinical cases, 11(8), 1788–1793. https://doi.org/10.12998/wjcc.v11.i8.1788

6 Ledesma-Gil G, Essilfie J, Gupta R, Fung AT, Lupidi M, Pappuru RR, Nayak S, Sahoo NK, Kaliki S, Yannuzzi LA, Reid K, Lim L, Sacconi R, Dave V, Singh SR, Ayachit A, Gabrielle PH, Cai S, Lima LH, Querques G et al. (2021). Presumed Natural History of Combined Hamartoma of the Retina and Retinal Pigment Epithelium. Ophthalmology. Retina, 5(11), 1156–1163. https://doi.org/10.1016/j.oret.2021.01.011

7 Gupta R, Fung AT, Lupidi M, Pappuru RR, Nayak S, Sahoo NK, Kaliki S, Yannuzzi L, Reid K, Lim L, Sacconi R, Dave V, Singh SR, Ayachit A, Gabrielle PH, Cai S, Lima LH, Querques G, Arevalo JF, Freund KB et al. (2019). Peripapillary Versus Macular Combined Hamartoma of the Retina and Retinal Pigment Epithelium: Imaging Characteristics. American journal of ophthalmology, 200, 263–269. https://doi.org/10.1016/j.ajo.2019.01.016

8 Kaprinis K, Bobat H & De Salvo G (2018). MultiColorTM imaging in combined hamartoma of the retina and retinal pigment epithelium. Eye (London, England), 32(9), 1478–1482. https://doi.org/10.1038/s41433-018-0123-2

9 Shields CL, Thangappan A, Hartzell K, Valente P, Pirondini C & Shields JA (2008). Combined hamartoma of the retina and retinal pigment epithelium in 77 consecutive patients visual outcome based on macular versus extramacular tumor location. Ophthalmology, 115(12), 2246–2252.e3. https://doi.org/10.1016/j.ophtha.2008.08.008

10 Inoue M, Noda K, Ishida S, Yamaguchi T, Nagai N, Shinoda K, Shinoda H & Oguchi Y (2004). Successful treatment of subfoveal choroidal neovascularization associated with combined hamartoma of the retina and retinal pigment epithelium. American journal of ophthalmology, 138(1), 155–156. https://doi.org/10.1016/j.ajo.2004.02.020

Medical Team of Ophthalmica Institute:

Solon Asteriades,
MD, FRCS

Asteriadis

Miltos Balidis,
MD, PhD, FEBOphth, ICOphth

MBalidis

Chrysa Koutsiouki,
MD

Koutsiouki

Lambros Lambrogiannis,
MD, MSc, PhD, FEBO

Lamprogiannis

Evaggelos Lokovitis,
MD, FEBOphth

Lokovitis

Dimitrios Sakellaris,
MD

Sakellaris

Thanos Sousouras,
MD, DO

Sousouras

Paris Tranos,
MD, PhD, ICOphth, FRCS

ptranos

Thanos Vakalis,
MD

Vakalis

Zachos Zachariadis,
MD, DO

Zachariadis

Special Thanks To:

Stavrenia Koukoula, MD, PhD

Theoni Panagiotoglou, MD, PhD

Jenny Papastergiopoulou, MD

Giorgos Sidiropoulos, MD, FEBOphth

ophthalmica
Seeing is believing

www.ophthalmica.gr

INSTITUTE OF OPHTHALMOLOGY
AND MICROSURGERY

ophthalmica
Seeing is believing

ISBN 978-618-85557-2-3